Weathering effects on the carbon cycle in an Earth System Model

a PhD thesis
by
Greg Colbourn

School of Environmental Sciences
University of East Anglia
Norwich NR4 7TJ, UK

g.colbourn@uea.ac.uk
gcolbourn@hotmail.com

June 3, 2011

Abstract

Long after new terrestrial and ocean equilibria are reached in the carbon cycle, carbonate and silicate weathering will act to remove remaining fossil carbon from the atmosphere by indirect interaction with ocean sediments. A spatially explicit model of carbonate and silicate rock weathering was incorporated in modular form into GENIE, an Earth System Model of Intermediate Complexity, in order to explore carbon cycling over long timescales (kyr to Myr). The main dependencies of weathering - runoff, temperature and productivity - are taken from other parts of the model (an energy-moisture balance atmosphere and a parameterised terrestrial scheme); on comparison with real world datasets these fare well with their global averages, but less so with their spatial distributions. Despite this, a number of different model parameters were tested for long-term projections (up to 1Myr) of scenarios of 1000 and 5000GtC fossil fuel emissions (set against control runs of no emissions). Parameters that had a significant effect on timescales for the draw-down of CO_2 included: the silicate weathering feedback switch; where weathering was spatially explicit, the distribution of lithologies; and climate sensitivity. Parameters that had less of an effect were the formulation of runoff and productivity weathering feedbacks (whether explicit, or implicitly dependent on other variables); and the (literature-constrained) constants used in the formulation of temperature and runoff weathering feedbacks. Parameters that did not have a significant effect were the river-routing scheme used, and whether or not the atmosphere was "short-circuited" in the carbon cycle. Using a best estimate parameter set most inclusive of processes, and fitting the output to a series of exponentials, e-folding timescales for carbonate and silicate weathering processes were found to be ~8kyr, and ~110kyr respectively. The former validates, and the latter is significantly less than, earlier quantifications using box models.

Acknowledgements

I thank Tim Lenton, UEA and the Natural Environment Research Council (NERC) for taking me on for a PhD. Tim has provided indispensable guidance, supervision and feedback, and has kept me aware of the big picture. Andy Ridgwell (University of Bristol) has also been indispensable, providing copious help with both scientific and technical matters to do with the modelling. The Earth System Modelling Group, GENIE team (in particular Gethin Williams), and various office mates have also provided useful feedback, discussion and help with computing matters. I thank the people who run the UEA e-Science Cluster(s) - especially Chris Collins; they have been invaluable in helping with the (sometimes frustrating) task of running hundreds of million year simulations of the Earth System (several hundred years of CPU-time were used in the production of this thesis). I thank Bob Marsh and Andy Watson for thoroughly examining the thesis, and having faith in me being able to complete corrections in a "minor" time-span. I'm loathe to admit that I'm still not 100% happy with the final product (a couple of niggling issues still need ironing out); but 95% will do, and peer reviewed publications will hopefully provide better versions of the work.

It wouldn't have been quite so much fun (and maybe even have been finished a bit quicker), were it not for the large amounts of time spent in the Coffee Room/Grad Bar/Alex/Stores/Delaney's/Havana with Jim, Dave, Matt, Lee, Liz, Jenny, Monkey, Rich and the rest of the Grad Bar/ENV Happy Hour regulars, old and new. Thanks also to the NHS and the N&N A&E staff who were there to pick up the pieces not once, but twice (rest assured I'm now in my 30s and those days are behind me). I'm thankful for the fine city of Norwich, the nice campus at UEA, decent houses and housemates, and friends both near (Norwich) and far (London, Southampton and it's diaspora) for allowing pleasant living and working conditions, and welcome days/nights/weekends/weeks out. Being part of the environmental scene - Permaculture, Transition Norwich, Climate Camp, direct actions - was fun and meaningful in an altogether different way to doing the science (even if "direct action" sometimes meant that that other some-times emergency service were less than helpful). Ending this extra-curricular paragraph, I acknowledge the Internet for providing constant ~~distraction~~ intellectual stimulation; I may have spent a fair bit of time procrastinating whilst doing the PhD, but I'd like to think I also learnt a lot about interesting/useful stuff in addition to "weathering effects on the carbon cycle" (from global threats such as climate change, peak oil and unfriendly AI, to opportunities such as veganism, open source hardware, 3D printing, rationality, cryonics, and Giving What We Can). Nevertheless, I do hereby acknowledge Procrastination, and the Planning Fallacy.

Last not least, I thank my family - Mum, Dad, Tim, Chrissie - for providing much-needed support and motivation (even if at times it felt like nagging!) to get this finished. Special mention for my twin brother Tim, who with his own scientific career currently seems to be the monozygote with the most, constantly putting me to (self-imposed) shame; and who also funded the second half of my 4^{th} year. Becoming a father has not been nearly as hard as I might have thought, and has provided a focus to my life: Theo is a wonderful kid. Thanks to Ruth for being a great mother to him. I hope that the light of this scientific age only brightens as Theo grows up.

Greg Colbourn
UEA, June 2011

Contents

List of Figures

List of Tables

List of Abbreviations

0D	–	zero spatial dimensions
2D	–	two spatial dimensions
3D	–	three spatial dimensions
acid	–	Acid Volcanic (lithology)
ALK	–	Alkalinity
BioGeM	–	Bio-Geochemistry Model
BLAG	–	Berner, Lasaga and Garrels (1983 paper and model)
$CaCO_3$	–	calcium carbonate
carb	–	Carbonate (lithology)
$CaSiO_3$	–	calcium silicate
CCD	–	Carbonate Compensation Depth
COPSE	–	Carbon-Oxygen-Phosphorus-Sulfur-Evolution model
DIC	–	Disolved Inorganic Carbon
EMBM	–	Energy (and) Moisture Balance Model
EMIC	–	Earth system Model of Intermediate Complexity
ENTS	–	Efficient Numerical Terrestrial Scheme (land component of GENIE)
ESM	–	Earth System Model
f_Ca	–	carbonate weathering feedback
f_Si	–	silicate weathering feedback
GEM-CO2	–	Global Erosion Model for CO_2 fluxes
GENIE	–	Grid ENabled Earth System Model
GENIE-1	–	fast version of GENIE with simple 2D EMBM atmosphere
GEOCARB	–	Series of models (I, II and III) developed by Berner
GKWM	–	Gibbs and Kump Weathering Model
Globavg	–	Global Average (0D) version of RokGeM
GOLDSTEIN	–	Global Ocean Linear Drag Salt and Temperature Equation INtegrator
GPU	–	Graphics Processor Unit
GPGPU	–	General Purpose Graphics Processor Unit (cf. CPU)
GtC	–	10^9 tonnes of carbon (=PgC)
kyr	–	thousand years
lakh	–	10^5 (has common usage in Indian subcontinent)
MPM	–	McGill Paleoclimate Model
Myr	–	million years
p	–	precipitation
P	–	productivity
PETM	–	Paleocene-Eocene Thermal Maximum
R	–	runoff
R^2	–	measure of linear statistical correlation
RokGeM	–	Rock Geochemistry Model
sand	–	Sands and Sandstones (lithology)
SedGeM	–	Sediment Geochemistry Model
STN	–	Simulated Topological Network
T	–	temperature
UVic	–	University of Victoria (ESM)
WHAK	–	Walker, Hays and Kasting (1981 paper and model)

1 Introduction

The legacy of human disruptions to the carbon cycle will be a long one (Archer, 2005). The burning of fossil fuels, deforestation (and to a lesser extent cement production) have led to atmospheric concentrations of CO_2 increasing from a pre-industrial level of 280ppm to today's 388ppm and counting (Tans, 2010). This excess atmospheric carbon (and the climatic changes wrought by it) will persist until it is sequestered either by natural or anthropogenic means. Leaving aside potential further anthropogenic interference in the form of geo-engineering, I consider the natural carbon sinks. Broadly speaking, these involve short term (years to centuries) terrestrial processes, medium term (decades to millennia) oceanic processes, and long term (10^3-10^5 years) geologic processes. The latter, involving carbonate and silicate weathering of rocks, are what are modelled in this study. Firstly though, a brief summary of the other processes.

1.1 Natural carbon sequestration: from the present to lakhs (10^5) of years hence

The terrestrial biosphere absorbs carbon through the "CO_2 fertilisation" effect, as well as (humans permitting) forest regrowth. The input of carbon is partly transferred to the soil. These processes operate on timescales of years (plants) to centuries (soil). The ocean removes excess atmospheric CO_2 first by CO_2 dissolving in and reacting with surface waters (over the course of years), and then via carbonate chemistry buffering (over decades) and ocean mixing (over decades to centuries).

When deep water undersaturated in CO_2 reaches the surface, it allows more CO_2 to be drawn from the atmosphere. Dissolved CO_2 forms carbonic acid (Equation 1), which quickly dissociates into bicarbonate (2) and carbonate (3) ions, allowing more CO_2 to enter the ocean from the atmosphere.

$$CO_{2(aq)} + H_2O_{(l)} \longrightarrow H_2CO_{3(aq)} \tag{1}$$

$$H_2CO_{3(aq)} \longrightarrow HCO^-_{3(aq)} + H^+_{(aq)} \tag{2}$$

$$HCO^-_{3(aq)} \longrightarrow CO^{2-}_{3(aq)} + H^+_{(aq)} \tag{3}$$

This buffering allows approximately a factor of 10 more carbon to be absorbed by the ocean than would otherwise be the case were it to remain undifferentiated like oxygen (Revelle and Suiss, 1957). When including all anthropogenic disruptions to the carbon cycle (cement production, and deforestation as well as fossil fuel burning), both the land and ocean carbon sinks are thought to currently absorb approximately 30% each of the excess atmospheric CO_2, although the land sink is more variable on a multi-year timescale (Le Quere et al., 2009). However, as more CO_2 enters the atmosphere, we are approaching the point where the immediate terrestrial and oceanic sinks start to become saturated and so are less able to absorb excess atmospheric CO_2 (Canadell et al., 2007; Le Quéré et al., 2007). The airborne fraction of CO_2 (remaining over emitted, per annum) has increased from 40% to 45% in recent decades (Le Quere et al., 2009). Results from the Coupled Carbon Cycle Climate Model Intercomparison Project (C^4MIP), show a lessening of land and oceanic carbon uptake relative to emissions throughout the 21st century (Friedlingstein et al., 2006), although there is significant uncertainty over the magnitude of this reduction, given the spread between models. It should be noted however, that any apparent century scale "saturation" of the ocean sink is a transitory phenomena, awaiting disruption through long-term (10^2-10^3 year) ocean mixing.

The addition of CO_2 to the ocean causes acidification through the release of protons during the dissociation of carbonic acid into bicarbonate and carbonate (Equations (2) and (3)). Once the ocean is mixed down to depth this acidification causes the Carbonate Compensation Depth (CCD; the border between water over-saturated and water under-saturated in calcium carbonate, $CaCO_3$) to move upward. This leads to the dissolution of $CaCO_3$ sediments (4) on parts of the ocean floor now lying below the CCD. This is analogous to a mountain range where the snow line (CCD) moves upward, melting the snow ($CaCO_3$) from the slopes.

$$CaCO_{3(s)} \longrightarrow Ca^{2+}_{(aq)} + CO^{2-}_{3(aq)} \tag{4}$$

Further sequestration of atmospheric CO_2 occurs through the weathering of terrestrial (calcium- or magnesium-) carbonate rocks; chemically, this involves the same reactions as those occurring between DIC and sedimentary $CaCO_3$ in the ocean, but uni-directionally toward replenishing bicarbonate. Carbon dioxide dissolves in rain water to form a weak carbonic acid that breaks down the rocks, producing calcium and bicarbonate ions (Equation 5; here given for calcium, but could equally be for magnesium). Through riverine transport, this

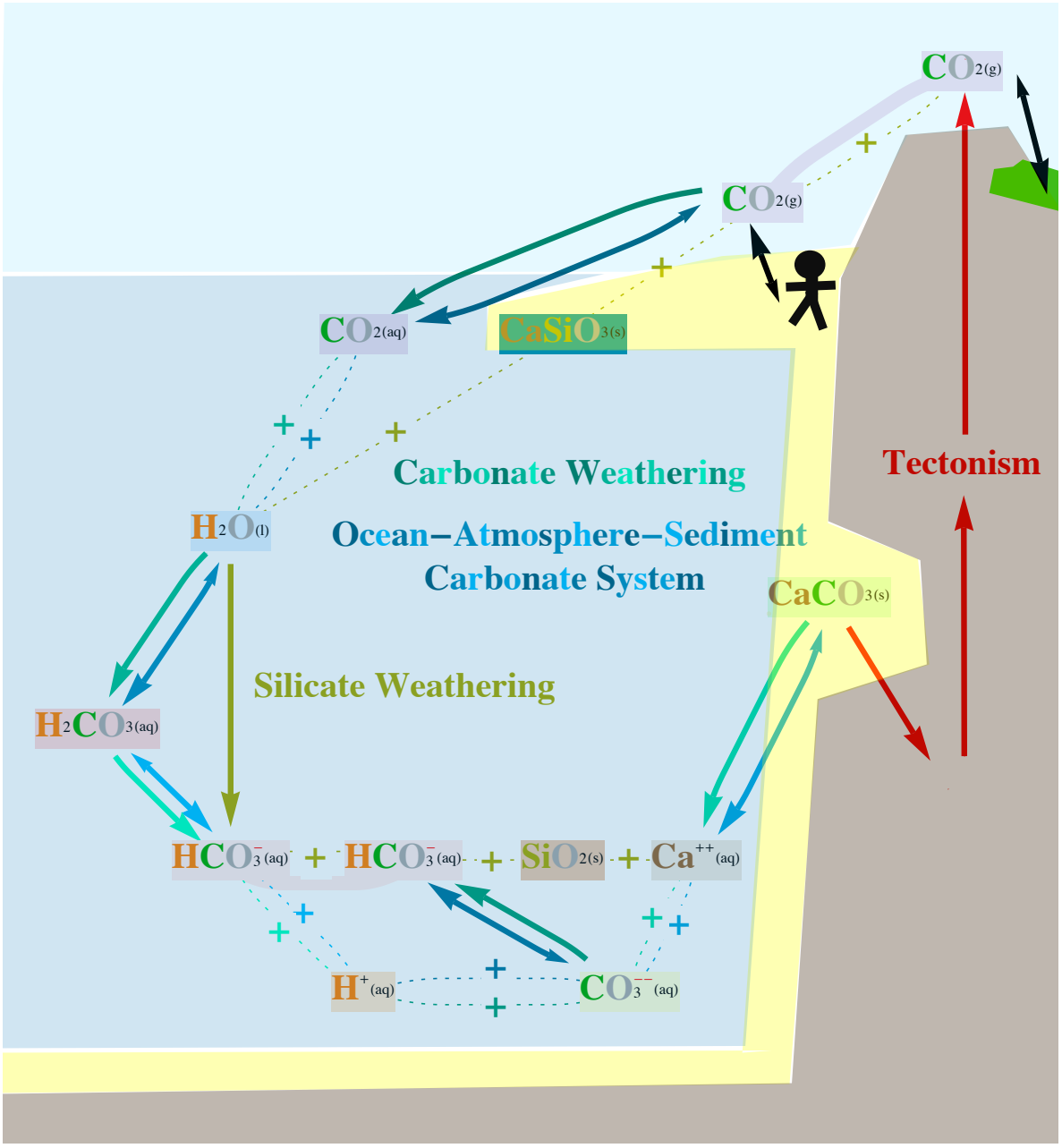

Figure 1: Chemistry of the long-term carbon cycle. Elements, molecules, chemical equations and processes/systems are colour coded. For weathering, the blue shaded area represents land surface water, and the yellow shaded area exposed rock; for the ocean-atmosphere sediment carbonate system, the blue represents ocean, and the yellow, ocean sediment. Chemical equations are drawn in straight lines where possible (of the 11 equations illustrated, only 2 are not in straight lines: the silicate weathering pseudo-formula, and the dissociation/recombination of bicarbonate). The red and black arrows denote flows of carbon between reservoirs (geologic, anthropogenic and biomass) rather than direct molecular chemical transformation. In the reversible transformations, bigger arrowheads mark the direction of current dominant flows, and smaller arrowheads lesser and future flows.

bicarbonate reaches the ocean. This process is known as "terrestrial neutralisation" (Ridgwell and Edwards, 2007).

$$CO_{2(aq)} + H_2O_{(l)} + CaCO_{3(s)} \longrightarrow Ca^{2+}_{(aq)} + 2HCO^-_{3(aq)} \tag{5}$$

The partitioning of carbon between the atmosphere, ocean and sediments allows for the fraction of initial emissions remaining in the atmosphere to be as little as 6% after equilibrium is reached on a timescale of around 100kyr (Goodwin and Ridgwell, 2010). The remaining fraction of anthropogenic carbon is removed from the atmosphere by the process of silicate weathering, whereby two moles of carbon are consumed for every

one that is available for subsequent transfer back to the atmosphere from the ocean-sediment system (Equation 6; compare with Equation 5):

$$2CO_{2(aq)} + H_2O_{(l)} + CaSiO_{3(s)} \longrightarrow Ca^{2+}_{(aq)} + 2HCO^{-}_{3(aq)} + SiO_{2(aq)} \tag{6}$$

Eq. (6) is a simplification of the common naturally occurring reaction, the weathering of the tectosilicate plagioclase feldspar endmember Anorthite:

$$2CO_{2(aq)} + 3H_2O_{(l)} + CaAl_2Si_2O_{8(s)} \longrightarrow Ca^{2+}_{(aq)} + 2HCO^{-}_{3(aq)} + Al_2Si_2O_5(OH)_{4(s)} \tag{7}$$

The chemistry of the long-term carbon cycle (Equations 1-6) is illustrated schematically in Figure 1.

Although both have a significant effect on the long-term carbon cycle, and hence long-term climate, carbonate and silicate weathering involve fundamentally different processes. Carbonate weathering involves carbonation and congruent dissolution, whereby all products are dissolved and (through the hydrological cycle) removed from the weathering site. Silicate weathering, on the other hand, involves hydrolysis and the precipitation of secondary clay minerals; an incongruent dissolution, the products of which contribute to soil formation.

1.2 The silicate weathering feedback

Silicate weathering is *the* fundamental geological thermostat operating on Earth: increased atmospheric CO_2 begets a warmer, wetter climate, which causes increased weathering, which draws down atmospheric CO_2 and thus begets a cooler, dryer climate, which causes less weathering (Walker et al., 1981). Throughout Earth history, the climate has been stable over geological epochs largely because of this mechanism, with silicate-weathering drawing down atmospheric CO_2 at a rate in equilibrium with volcanic outgassing (Berner and Caldeira, 1997). Epochal shifts in climate are ultimately stabilised by shifts in silicate weathering over the order of hundreds of thousands of years. If nature is left to take it's course, the same will be true of the Anthropocene. A million years hence, the only evidence of the human interference in the Earth System will be a slightly more weathered continental surface and a thick layer of sedimentary carbonate at the bottom of the ocean (Ridgwell and Edwards, 2007).

The chemical weathering of silicate minerals is both physically and biologically mediated, in addition to being subject to rate kinetics. Physically, erosion of mineral surfaces increases the surface area available for chemical reaction. At low levels of erosion, weathering is "transport limited" (West et al., 2005); soils accumulate in areas of low erosion, leaving less material available for weathering. Here, weathering is directly proportional to the rate of supply of new material from erosion. This is also known as "supply limited weathering" (Riebe et al., 2004). At higher rates of erosion (or denudation), there is plenty of material (regolith) for chemical weathering to proceed with only "kinetic limitation" (this is also known somewhat eponymously as "weathering limited" weathering (Tipper et al., 2006)). Here, weathering is dependent on variables that directly control the reactions: temperature and runoff and to a lesser extent, erosion. A summary of weathering dependence (adapted from West et al. (2005) and Gibbs et al. (1999)) is given in Equation 8:

$$w_{\mathrm{Si}} = \sum_i f_i \begin{cases} W_i \tau_i \epsilon_i & \text{for } \epsilon < \epsilon_t\,(T,R) \quad \text{transport/supply limitation} \\ k_i \left(\frac{\epsilon_i}{\epsilon_0}\right)^{\alpha_i} \left(\frac{R}{R_0}\right)^{\beta_i} e^{-\frac{E_a}{R}\left(\frac{1}{T}-\frac{1}{T_0}\right)} & \text{for } \epsilon > \epsilon_t\,(T,R) \quad \text{kinetic/weathering limitation} \end{cases} \tag{8}$$

Where w_{Si} is the silicate weathering rate (typical units: Mmol km^{-2} yr^{-1}); i is the rock type, which contains silicate minerals covering f_i fraction of the land surface; W the kinetic rate of mineral dissolution (yr^{-1}); τ the time available for reaction (yr); ϵ the rate of erosion (Mmol km^{-2} yr^{-1}); ϵ_t the threshold value of erosion between different regimes of weathering rate limitation; R runoff (mm yr^{-1}; T temperature (°K); E_a the activation energy for the weathering reaction (kJ mol^{-1}) and R the molar gas constant. The constant k is a normalisation factor dependent on the base values taken for erosion, runoff and temperature (T_0, R_0, ϵ_0) and the specific lithology (i). The exponents α and β are determined empirically. Fitting of field data gives values of the runoff dependence exponent β of 0.68-0.75 (range covers differing lithologies i (Bluth and Kump, 1994)) and 0.80±0.32 (a bulk value not differentiating between lithologies; error from least-squared fitting (West et al., 2005)). From the latter least squares fitting, α was determined to be 0.42±0.15. From work dividing the globe into different lithological classes, values of $k(\epsilon_0/\epsilon)^{\alpha} {R_0}^{\beta}$ range from 0.724 (sands and sandstones) to 8.318 (shales) (Bluth and Kump, 1994) for a varying β, or 0.152 to 0.627 for $\beta = 1$ (Amiotte-Suchet et al., 2003).

Temperature and runoff are both amenable to being included as dependencies in a weathering model incorporated into an Earth system Model of Intermediate Complexity (EMIC), however, erosion is less so, as it is

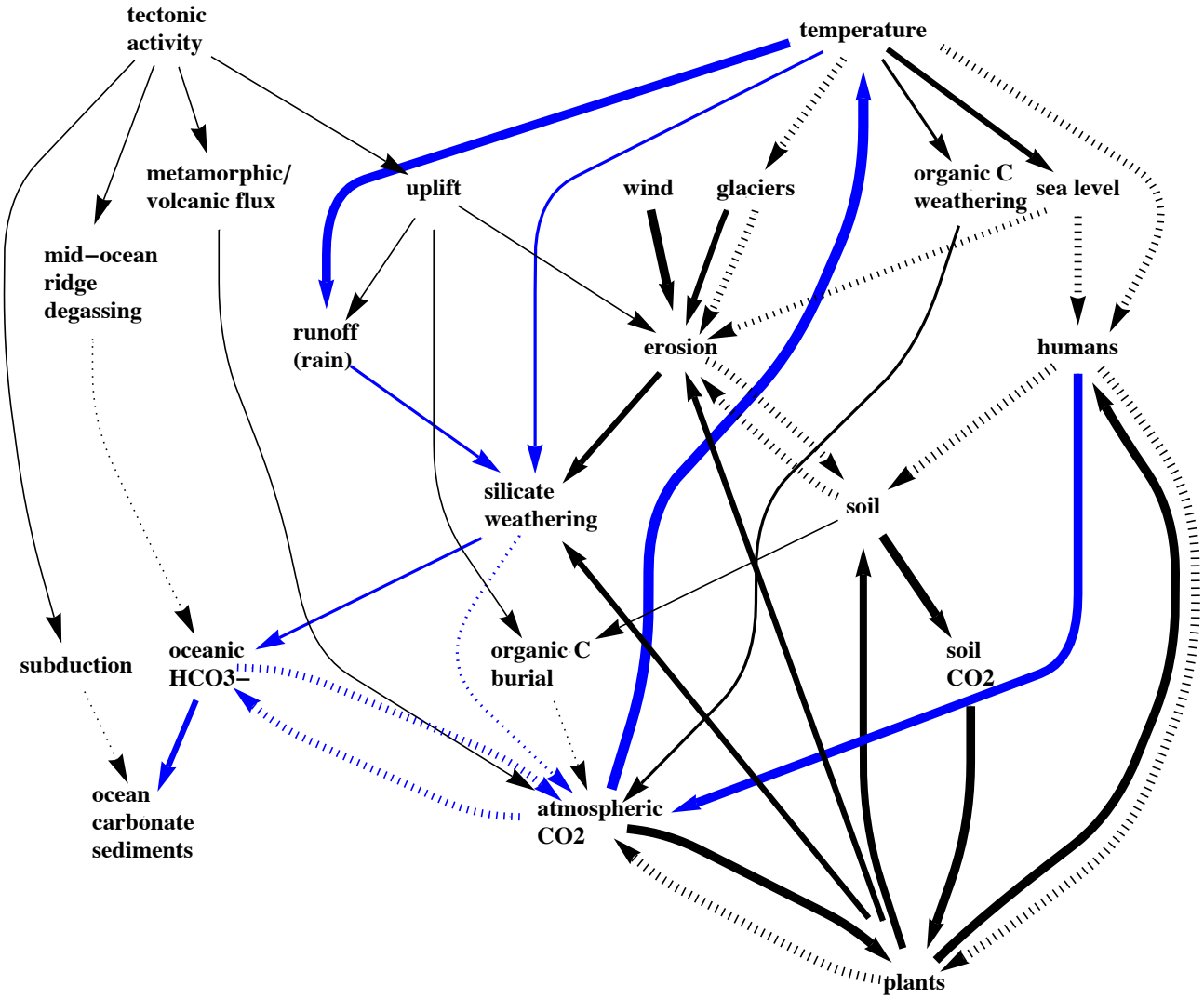

Figure 2: Feedbacks related to weathering and the long-term carbon cycle. Solid arrows represent positive couplings between system components (increase in component causes increase in connected component) and dashed arrows negative couplings (increase causes decrease). Complete loops with an odd number of negative couplings represent negative feedback loops; Loops with an even number of dashed arrows are positive feedback loops. The width of each arrow denotes the approximate speed of the coupling on a logarithmic scale: arrow widths are the thinnest for 10^6 year timescales, and thickest for 10^0 year timescales. Couplings included in the model described in this thesis are highlighted in blue. See §5.2.1 for discussion relating to the processes not included. Fig. 1 of Kump et al. (2000) is used as a basis for this figure.

not included in even state of the art land surface schemes, on account of their design for short (sub-millennial) integration times. For this reason, the model developed for this thesis contains no erosion dependence, and no differentiation of weathering into transport and kinetic limitation regimes. In recent work (Hilley and Porder, 2008), weathering zone thickness (where kinetically limited weathering occurs in shallow weathering zones and transport limited weathering in deep weathering zones), and dust transport have been explicitly included in calculations predicting silicate weathering flux. These too, are factors complicating the picture that are not readily amenable to modelling, on account of their variability on spatial scales far smaller than the resolution of today's EMICs.

Both chemical and mechanical weathering of carbonate and silicate rock are in long-term feedback with climate. The more important of these is perhaps mechanical weathering, with concentrations of suspended inorganic material (SIM) in rivers varying more with temperature and rainfall (Gislason et al., 2006). However, concentrations of SIM are greatly affected by glacial cover, rock age and the presence of dams, and their effects on erosion (Gislason et al., 2008). Direct evidence of feedback between climate and weathering - an increase in weathering rates in response to climate change - is provided by decades of data from Icelandic river catchments (Gislason et al., 2008, 2009). Correlations are stronger for temperature than they are for runoff. This is in part

due to the fact that temperature and runoff are themselves rarely statistically significantly correlated at the annual or catchment level (see §3.4).

Biospheric productivity affects the rate of weathering of rocks by both physical and chemical means. Physically, plant root systems put rocks under mechanical stress, leading to cracking and greater exposed surface areas available for weathering (Cochran and Berner, 1996). Chemically, through the decay of carbon containing litter, plants increase the concentration of acids in water in contact with rocks, which increases the weathering rate. (Berner, 1992) Plants also directly produce biogenic minerals, by way of building up soils. Soils are effective at trapping CO_2, which increases weathering through increased concentration of carbonic acid. However, soils can also inhibit chemical weathering by covering bedrock with a protective layer of clay. On balance however, the simple fact that plants do not cycle nutrients with perfect efficiency, requires that rock decomposition is a factor in their continued existence (Berner, 1992). Indirectly, plants alter hydrology at both local and regional scales, which alters runoff. (Kelly et al., 1998). Eq. 8 factors in productivity implicitly through it's grounding in observational and empirical study of the natural world. However, attempts have been made in modelling studies to explicitly account for productivity (Schwartzman and Volk, 1989; Lenton and von Bloh, 2001; Bergman et al., 2004; Lenton and Britton, 2006) (see §1.4).

With the accumulation of river chemistry data (Meybeck, 1987; Berner and Berner, 1987) came a debate as to whether weathering was most influenced by tectonic uplift, or climate (temperature and the hydrological cycle). Tectonic uplift was said to affect weathering (Raymo et al., 1988) by: increasing the breakdown of rocks and thus physical weathering; increasing the volume of exposed (easily weatherable) sedimentary rocks; and increasing runoff through the orographic influence on precipitation. Note that the last of these was included as an important factor by those on the other side of the debate, thus finely illustrating the complex nature of silicate weathering feedback.

A schematic of the processes and feedbacks related to weathering and the long term carbon cycle is shown in Figure 2 (see caption for details). It serves to illustrate the complexity of weathering and it's effect on the carbon cycle.

1.3 Global rates of CO_2 consumption by weathering

Compilations of river dissolved load data have been used to estimate global rates of CO_2 consumption by silicate and carbonate weathering. Early work, using data from small unpolluted monolithological watersheds in France, and scaling to global proportions for each rock type, estimated the totals of CO_2 consumed to be 12 and 12.6Tmol/yr for carbonate and silicate weathering respectively (Meybeck, 1987). Adding in the spatial distribution of rock types, and a linear dependence (differing by lithology) of weathering fluxes on runoff, a result of 21.7Tmol/yr total CO_2 consumption (by carbonates and silicates) was obtained (Amiotte Suchet and Probst, 1995). This latter data assimilation model, GEM-CO2 (Global Erosion Model for CO_2 fluxes), is incorporated into the model developed for this thesis (see §3.7.1). A similar study, but this time taking data from rivers in the United States, Puerto Rico and Iceland, suggested a fractional power for the runoff dependencies (Bluth and Kump, 1994). This model, referred to as the Gibbs and Kump Weathering Model (GKWM; also used in this thesis - see section §3.7.2), gives global CO_2 consumption fluxes of 8.9 and 17.9Tmol/yr for carbonate and silicate weathering respectively (Gibbs et al., 1999), using a slightly different lithological map. Later work, applying GEM-CO2 to runoff data for the world's 40 largest river basins, gave estimates of global CO_2 consumption rates of 8.6Tmol/yr for carbonate weathering and 12.9Tmol/yr for silicate weathering (Amiotte-Suchet et al., 2003). Lithological classes, in order of decreasing contribution to global rates of CO_2 consumption by weathering, are: carbonates, shales, granites, basalts and sandstones.

In a more direct approach, a meta-analysis of dissolved load data from the worlds 60 largest rivers was performed (Gaillardet et al., 1999). The contributions of different lithological classes (including evaporites - rock salts) were separated out by looking at ratios of various dissolved species: the ratios of Ca, Mg and HCO_3^- to Na are different for different rock types. Atmospheric (rain) and human inputs were separated out by looking at the Cl/Na ratio. The global silicate weathering flux was determined by solving a series of mass budget equations using these ratios and the mixing proportions of Na for the different input sources (silicate, carbonate, evaporite, rainwater and also human activities). A figure of 8.7Tmol/yr was arrived at, 5Tmol/yr of which coming from calcium- and magnesium- silicates. A further 3Tmol/yr was estimated to come from the weathering of volcanic rocks on oceanic islands and volcanic arcs. Carbonate weathering was estimated at 12.3Tmol/yr. In a follow-up study (Dessert et al., 2003), the weathering of basaltic volcanic arc islands (not included in the meta-analysis of large watersheds), was estimated to add ~1.6Tmol/yr (out of a total of 4.08Tmol/yr for basalt weathering) to CO_2 consumption rates. This latter study underlines the importance of basalt weathering - and specifically that from volcanic arc islands - as a subclass of silicate weathering; in the earlier studies involving GEM-CO2 and GKWM, island arc sources are not included.

Table 1: Estimates of global weathering rates (Tmol/yr of atmospheric CO_2 consumed)

Reference	Carbonate weathering	Silicate weathering	Total
Meybeck (1987)	12.0	12.6	24.6
Amiotte Suchet and Probst (1995)	-	-	21.7
Gibbs et al. (1999)	8.9	17.9	26.8
Gaillardet et al. (1999)	12.3	11.7	24.0
Amiotte-Suchet et al. (2003)	8.6	12.9	21.5

Table 1 shows a summary of estimated global carbonate and silicate weathering rates. Converted into GtC/yr (billion tonnes of carbon per year), estimates for global CO_2 consumption cover the ranges 0.11-0.14GtC/yr for carbonate weathering, and 0.10-0.21GtC/yr for silicate weathering. These rates of consumption are small in comparison to the ~8GtC/yr currently being produced and emitted to the atmosphere by human activities, but they will win out in the end: weathering processes will continue to remove anthropogenic CO_2 from the atmosphere long after humans have stopped supplying it.

The work done in elucidating these estimates, as well as the weathering dependencies described above (§1.2), can be thought of as data assimilation, in that detailed river discharge and sample data are aggregated into an "offline" model, which is then populated with lithological data, climate data and GCM output. Interactive ("online") models of global carbon cycling including weathering processes are now looked at.

1.4 Early modelling: the carbon cycle over Earth history

Early work using box (not spatially resolved) models now known as WHAK (Walker et al., 1981), BLAG (Berner et al., 1983) and GEOCARB (Berner, 1990; Berner, 1991) demonstrated the essential role weathering plays in the regulation of climate over geological timescales. In WHAK, the global rate of silicate weathering is given a dependence on atmospheric pCO_2 (CO_2 partial pressure) and temperature. The draw-down of atmospheric CO_2 through silicate weathering, and the positive relationship between temperature and pCO2, creates the now commonly known silicate weathering feedback loop. WHAK is a basic model, relying on results from early global climate models (GCMs), but it is the archetype for models linking global silicate weathering and climate.

Following WHAK, it was suggested that the abiological model be amended to include biology, noting that pCO_2 in soil is enhanced to levels much (10-40 times) higher than atmospheric levels due to the presence of terrestrial life (Lovelock and Whitfield, 1982; Lovelock and Watson, 1982). This gives the geological silicate weathering feedback a geophysiological (or Gaian) flavour; it is argued that this is necessary to keep pCO_2 and hence temperature low enough for continued functioning of the biosphere over the eons. It was later calculated, using a model based on WHAK, but including an (estimated) biological amplification factor of 100 to 1000, that an abiotic Earth would be between 30 or 45°C warmer (Schwartzman and Volk, 1989). The biological amplification factor included the raising of soil pCO_2 as well as: the stabilisation of soil; the production of organic acids (a soil matrix has high surface area, which stores water, containing the acids produced in solution which weather the minerals in contact with them); and enhanced physical weathering through the fracturing (roots) and microfracturing (microbes) of rocks and mineral grains. Further work (Schwartzman and Volk, 1991) demonstrated the plausibility of a biologically enhanced silicate weathering feedback being a mechanism for planetary homeostasis over the full range of Earth history. Indeed, applying a similar model eons into the future, the remaining lifespan of the biosphere was calculated to be 0.9-1.5Gyr (Caldeira and Kasting, 1992). Later modelling (Lenton and von Bloh, 2001), including a direct (hyperbolic) dependence of weathering on (biological) productivity, showed that biotic and abiotic states of the Earth system were bistable; with a large enough perturbation (the size of which diminishes with increasing solar luminosity), the system can flip from the biotic to abiotic state.

BLAG put the silicate weathering mediated geological carbon cycle into a late Phanerozoic (last 100Myr) context. Weathering processes were, as with WHAK, abiological, but precipitation of carbonate in the ocean was included, which is biological in origin. Also included were the tectonic processes of metamorphic decarbonation and CO_2 outgassing. The model involves a series of non-linear mass balance equations for determining fluxes into and out of land and ocean mineralogical reservoirs, and the atmospheric CO_2 reservoir. BLAG was the basis for the more extensive GEOCARB model, which was constructed to model atmospheric pCO_2 over the complete Phanerozoic eon. GEOCARB simplified the maths of BLAG by aggregating carbonate minerals and combining the ocean and atmosphere into a single reservoir. The soil-biological enhancement of weathering was included as a parameterisation. Other factors controlling weathering rates in GEOCARB are continental land area, mean elevation and runoff. Results of the model show that both geological and biological effects are important in the regulation of CO_2 over geologic time. Successive versions, GEOCARB II (Berner, 1994) and GEOCARB III (Berner and Kothavala, 2001) have refined the model by constraining and detailing its parameterisations with

new scientific observations and (for climate variables) GCM output. A larger Phanerozoic geochemical cycling model that includes other elements than carbon, COPSE (Bergman et al., 2004), expands on the weathering feedbacks of GEOCARB with an interactive biota that is co-evolutionary with CO_2.

In contrast to the "steady state" maintained by the silicate weathering feedback in the GEOCARB model (CO_2 removal equilibrates to match tectonic outgassing), the "uplift hypothesis" (Raymo and Ruddiman, 1992) suggest that CO_2 levels are drawn down out of equilibrium during eras of tectonic uplift, such as the current late Cenozoic era (the past 40Myr). However, such uplift cannot be an overriding mechanism controlling CO_2 levels over geological era without breaking the mass balance of the system (Berner and Caldeira, 1997).

Moving from the geological, to mere glacial-interglacial timescales, an attempt was made (Munhoven, 2002) to account for the oscillations in atmospheric CO_2 recorded in the Vostok ice cores by applying GKWM and GEM-CO2 (see 1.3 above) to GCM output of runoff from the PMIP (Paleo Model Intercomparison Project). It was found that pCO_2 concentrations were drawn down by a small (4.4-13.8ppm), but non-negligible fraction of the glacial-interglacial variation (~75ppm). However, recent work is ambiguous as to whether there have been significant variation of weathering on glacial-interglacial timescales (Foster and Vance, 2006).

1.5 Later modelling: anthropogenic perturbations of the carbon cycle

Various attempts have been made to quantify the lifetime of the anthropogenic CO_2 perturbation. However, the timescale over which the silicate weathering feedback operates has only been quantified once, using a box model, (Sundquist, 1991). The model had a one-box atmosphere, coupled to a mixed layer ocean underlain by an 11 box deep ocean; each deep ocean box was coupled to a sediment box. Carbon cycle chemistry was performed using interactive variables for atmospheric CO_2, ocean DIC and alkalinity, and sedimentary $CaCO_3$, and the inclusion of analogues of Equations (4), (5) and (6). Expressed as an e-folding timescale, the silicate weathering timescale was calculated to be in the range 3-4x10^5 years. Other future projections of the lifetime of anthropogenic CO_2 have assumed values of 200kyr (Archer et al., 1997) and 400kyr (Archer, 2005).

Taking the parameterisations of weathering temperature dependence from GEOCARB, modified by a plant productivity from COPSE, and applying them to a box model compartmentalised into atmosphere, vegetation, soil and multi-box ocean and sediments (Lenton and Britton, 2006), the silicate weathering timescale was determined to be of the order of a million years. The silicate weathering process has yet to have its timescale quantified using a spatially explicit model.

Recent work using spatially resolved Earth System Models (ESMs) (Montenegro et al., 2007; Ridgwell and Hargreaves, 2007) has incorporated millennial timescale processes into modelling of the anthropocene carbon excursion. Detailed, spatially explicit models of the carbonate sediments in the ocean are included, but terrestrial weathering processes are still only dealt with (in the most basic way) as a global average prescribed flux. As models were "only" integrated over timescales in the 10^4-10^5 year range, silicate weathering is ignored altogether; the weathering flux is from carbonates, and used to quantify the effect of terrestrial neutralisation.

An example future projection using one of these models (GENIE-1, the ESM used for the work in this thesis, see §1.6 below) has 4000GtC of emissions sequestered as follows (Ridgwell and Hargreaves, 2007): 66% are absorbed by the ocean on a timescale of hundreds of years; the dissolution of sea-floor sediments sequesters another 12% on a timescale of ~1.7kyr; carbonate weathering on land consumes a further 14% on a timescale of ~8.3kyr. 8% is left to be removed through silicate weathering. It is worth noting that the proportions of carbon removed from the atmosphere by each of the processes outlined above are different for different sized fossil fuel burns (emissions). For example, with a smaller burn, the proportion of carbon removed by the faster acting process of ocean invasion is greater, due to the fixed ocean reservoir of alkalinity being relatively larger in comparison to the burn size.

Through the ongoing realisation of Moore's Law (Moore, 1965), computer power has now increased to the extent to allow fully realised ESMs with 3D oceans and 2D atmospheres to be integrated over hundreds of thousands of years in a reasonable time (days to weeks), even on desktop-level PCs. This allows the modelling of weathering as a spatially resolved process over timescales relevant to it having a macroscopic effect on the Earth System. Building on the earlier box modelling work (§1.4; this section), and using the parameterisations constrained by field data (including the effect of lithology; §1.2, §1.3), a new weathering model was developed for this thesis. This weathering model is incorporated into the GENIE-1 Earth System Model.

1.6 The GENIE model and GENIE-1

GENIE (www.genie.ac.uk) - Grid ENabled Integrated Earth system model - is a modularised framework for Earth System Modelling. The constituent components of the Earth System (oceans, atmosphere, land, ocean

biogeochemistry, ocean sediments etc) are encapsulated in separate modules, which can be "plugged and played" together; the idea being that for different uses, different modules can be used, and models of differing levels of complexity can be created.

GENIE belongs to the class of models known as EMICs (Earth system Models of Intermediate Complexity). In contrast to General Circulation Models (GCMs) that use underlying low-level physics equations, EMICs are often highly parameterised. Processes that take place over small spatial and temporal scales are aggregated into high level parameterisations in order to minimise computational cost. This has the advantage of allowing more processes to be modelled, and also longer integrations and larger ensembles. However, the increase in parameterisation has the cost of an increase in the uncertainty of model results. In order to address this issue, during the course of it's development, the GENIE model has been tuned using a number of different techniques: an ensemble Kalman filter (Hargreaves et al., 2004); kriging, response surface models and non-dominated sorting genetic algorithms (Price et al., 2006, 2007); "pre-calibration" by emulation and plausibility checking (Holden et al., 2009; Edwards et al., 2010); and using iterative Importance Sampling (Annan and Hargreaves, 2010).

GENIE-1 refers to the first instance of the model created, with a low degree of complexity, and a fast run time. Its basis is a 3D frictional-geostrophic ocean and an energy moisture balance atmosphere (see below). A thousand years of simulation are capable of being run in one hour on a "normal" desktop PC. For this thesis a version of GENIE-1, genie_eb_go_gs_ac_bg_sg_rg(_el), is used. This includes an EMBM (Energy Moisture Balance Model) 2D atmosphere (Weaver et al., 2001) (eb), an 8-layer version of the Goldstein frictional-geostrophic ocean (Edwards and Marsh (2005); and references therein) (go) and sea-ice (gs); AtChem, an atmospheric chemistry module to pass gas fluxes (ac); BioGeM (BioGeochemical Model), the ocean biogeochemistry module (Ridgwell et al., 2007) (bg); SedGeM (Sedimentary-Geochemical Model), the ocean sediments model (Ridgwell and Hargreaves, 2007) (sg); and RokGeM (Rock-Geochemical Model) - the model described here (rg). ENTS, a land surface and vegetation scheme (Williamson et al., 2006) (el) is also used for some (unsuccessful) experiments. A schematic of the model is shown in Figure 3.

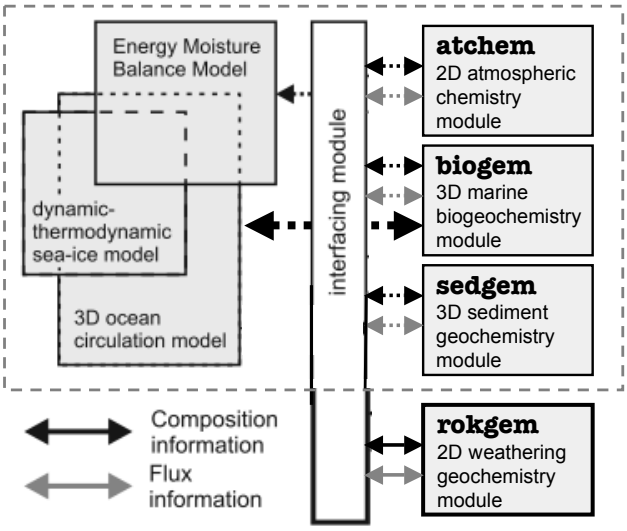

Figure 3: Schematic of the relationship between the different model components comprising the GENIE-1 model. Outlined in bold is the weathering module RoKGeM described in this thesis, while the ocean-atmosphere-sediment carbon cycle + climate model (Ridgwell and Hargreaves (2007)) is delineated by a dashed box. Figure adapted from Ridgwell and Hargreaves (2007)

The "Grid ENabled" part of the acronym GENIE refers to design aspects allowing for the execution of many simultaneous instances of the model across computer clusters, and for the collation, storage, accessing and sharing of results, amongst a geographically spread out community of researchers. Over the course of GENIE's history, a number of bespoke portals, middlewares, and stand alone applications/scripts have been developed to enable more efficient use of the modelling framework. Unfortunately, common standards for usage have not been adopted across the entire GENIE community, leading to many different individual efforts at modelling portals, including much work done on this front for this thesis (see §2.3).

1.7 Thesis outline

For this thesis a new weathering module, called 'RokGeM' (Rock Geochemistry Module) was developed for incorporation into Earth System Models (specifically GENIE; §1.6). Chapter 2 contains descriptions of model development, configuration and running; including the design and implementation of simulations of the long-term future climate and carbon cycle following perturbations in atmospheric CO_2. Chapter 3 contains a description of the RokGeM model: calcium-carbonate and calcium-silicate weathering are modelled using dependencies on temperature, runoff and plant productivity; fluxes are calculated as global averages, or spatially based on lithological data. A sensitivity test was conducted over all relevant variables, including climate sensitivity. In Chapter 4, results are examined in depth for an ensemble covering the switching on/off of carbonate and silicate weathering feedbacks, and two emissions scenarios (1000 and 5000GtC pulses); a timescale analysis of key depletion curves (those of excess global atmospheric pCO_2, surface warming and surface ocean acidification), involving the fitting of exponentials, was performed; all ensemble members analysed; and a commentary on

the most realistic parameter set given. Finally, in Chapter 5, key results are summarised; problems with the methodology, related to the coarse-resolution nature of the model, and the lack of modelled processes, are then examined; an outline of potential future work is given; and conclusions drawn.

The Appendices detail model output and the code used to produce it. Appendix A contains full time-series results: time points for model output (years) are listed in §A.1; graphs of global values of key variables (atmospheric pCO_2, surface warming, ocean acidification, ocean sediment $CaCO_3$, and weathering alkalinity and DIC fluxes) shown in §A.2; tabulated results for societally relevant perturbations (those of atmospheric pCO_2, global warming and ocean acidification) shown in §A.3; graphs showing percentages remaining of said perturbations in §A.4; and graphs showing *e*-folding timescales for the same in §A.5. Appendix B contains information about the scripts used to generate model ensembles, run the model and visualise the output. The "Read Me" file for the scripts is in §B.1; a list of parameters for the main processing script is in §B.2. Appendix C is in digital form; digital media accompanies this thesis containing full model and script code, and results in spreadsheet, graph, 2D array (geographical) and animation form (full details of the contents are given in §C).

2 Model and experimental set-up

Here the computer model set-up is presented, incorporating it's development (§2.1), configuration (§2.2) and running (§2.3). Issues involved in the design and execution of long-term future carbon-cycle perturbation experiments are also discussed, including model-spin-up (§2.4), comparison of key model dependencies with real-world data (§2.5), and emissions scenarios (§2.6). Finally, visualisation of the results of said experiments is briefly discussed (§2.7).

2.1 Model development

The GENIE Earth system Model of Intermediate Complexity (see §1.6) is used as a basis for the modelling done for this thesis. The bulk of GENIE, containing the science modules, is written in Fortran (either FORTRAN 77 or Fortran 90), using code from prior stand-alone models. For this reason, and to aid compatibility, RokGeM was written in Fortran 90. A template was created by copying and renaming the files and directories from AtChem (the directory `genie-atchem` in the root `genie` directory). Thus in `genie-rokgem`, there is a directory `src/fortran` containing files for parameter definitions (`rokgem_lib.f90`), subroutines for handling input and output of data (`rokgem_data.f90`), and subroutines for model calculations (`rokgem_box.f90`); and files for initialisation (`initialise_rokgem.f90`), time-stepping (`rokgem.f90`) and shutdown (`end_rokgem.f90`) of the model. A directory `data/input` contains input files for the model: geographical information used for river routing of weathering fluxes (see §3.6); lists of constants and arrays of lithological data for the 2D weathering schemes (§3.7); and arrays of data used for calibrating model input parameters to data (§2.5.4).

Following software development best practice, the versioning system Subversion was used. Versioning systems allow changes to files to be tracked, and earlier versions to be reverted to at any time, as well as the branching and merging of files, and directory structures. They are indispensable for large software projects, including the development of models containing large code bases, such as GENIE. The Subversion repository for the GENIE project is held on a secure server at the University of Bristol (https://svn.ggy.bris.ac.uk/websvn/listing.php?repname=genie). The main "trunk" of the code base was "branched" (creating `greg-s_branch`) for the purposes of developing RokGeM; the embryonic version of the model held on my local machine was copied across to this branch. Regular commits of the code were performed over the course of development to provide both a record, and a means for reversion to earlier versions of code. After significant developments, the development branch was merged back into the trunk, allowing other GENIE users and developers to use the RokGeM model. Also, the trunk was merged back into the development branch at regular intervals in order to avoid incompatibilities causing conflict. In this respect, the suite of tests developed for GENIE were also run before each committal of code to the repository, to minimise the risk of bugs finding their way into the model. The model runs presented in this thesis are run using the versions of GENIE contained in `greg-s_branch` Revs 5439 - 6324. There is minimal change to model output across this span of versions. A tagged release `tags/Greg_Colbourn_PhD_thesis` is provided in the svn repository for posterity.

2.2 Model configuration

The model was configured using the config files genie_eb_go_gs_ac_bg_sg_rg and worbe2_fullCC_(0-3) and the process described in §2.3 below (and Appendix B.1). This configuration, based on the original GENIE-1 (§1.6), has 36x36 land grid cells and 8 depth levels in the ocean. Climate-CO_2 feedback was switched on, and "tracers" (variables) relevant to the carbon cycle activated and initialised with pre-industrial values. Default physics and biogeochemistry parameters are as in Table 2 (Cao et al., 2009).

A key input to the weathering model is runoff (see §3.3, §3.4 & §3.7) Moisture is transported into continental interiors by the EMBM atmosphere by a combination of diffusion and advection according to prescribed NCEP wind fields. With the values of moisture diffusion and advection given, diffusion is dominant, leading to overly uniform precipitation and hence runoff (see §2.5.2).

Following Ridgwell et al. (2007) there is no seasonality in the model. Climate sensitivity (at equilibrium for a doubling of atmospheric pCO_2) in terms of radiative forcing was adjusted from a default of $4 Wm^{-2}$ to the IPCC's estimate of $3.7 Wm^{-2}$ (§2.3.1 of Solomon et al. (2007)).

2.3 Running the model

The long timescales of the model runs (of the order 10kyr-1Myr) presented here made setting off runs and collating results non-trivial. Bash scripts were employed to break runs into manageable pieces, which were

Table 2: Default physics and biogeochemistry parameters for GENIE-1 as used in this thesis (Cao et al., 2009)

Parameter	Description	Value	Units
	Ocean Physics[a]		
W	Wind-scale	1.93	-
κ_h	Isopycnal diffusion	4489	$m^2\ s^{-1}$
κ_v	Diapycnal diffusion	0.27	$cm^2\ s^{-1}$
λ	1/friction	2.94	days
	Atmospheric Physics[a]		
k_T	Temperature diffusion amplitude	$4.76x10^6$	$m^2\ s^{-1}$
l_d	Temperature diffusion width	1.08	Radians
s_d	Temperature diffusion slope	0.06	-
κ_q	Moisture diffusion	$1.10x10^6$	$m^2\ s^{-1}$
β_T	Temperature advection coefficient	0.11	-
β_q	Moisture advection coefficient	0.23	-
F_a	Fresh water flux factor	0.23	Sv
	Sea-ice Physics[a]		
κ_{hi}	Sea-ice diffusion	6200	$m^2 s^{-1}$
	Ocean biogeochemistry[b]		
$u_0^{PO_4}$	Maximum PO4 uptake rate	1.96	μmol $kg^{-1}yr^{-1}$
K^{PO4}	PO_4 half-saturation concentration	0.22	μmol kg^{-1}
r^{POC}	Partitioning of POC export into fraction #2	0.065	-
l^{POC}	e-folding depth of POC fraction #1	550	m
l_2^{POC}	e-folding depth of POC fraction #2	∞	m
$r_0^{CaCO_3:POC}$	CaCO3:POC export "rain ratio" scalar	0.044	-
η	Calcification rate power	0.81	-
r^{CaCO_3}	Partitioning of CaCO3 export into fraction #2	0.4325	-
l^{CaCO_3}	e-folding depth of CaCO3 fraction #1	1083	m
$l_2^{CaCO_3}$	e-folding depth of CaCO3 fraction #2	∞	m

[a] Edwards and Marsh (2005); Hargreaves et al. (2004)
[b] Ridgwell and Hargreaves (2007); Ridgwell et al. (2007)

submitted as jobs lasting ~5 hours each on the ESCluster supercomputer at UEA. Results were collated by amending saving routines in the original Fortran code of the relevant GENIE modules (BioGeM, SedGeM, RokGeM and ENTS) so that time-series output was appended to previously existing output files for runs restarted as a result of being divided up. In order to further automate running the model, scripts were also used to automatically spin-up the model and set experiments going. A final level of automation was to generate ensembles and groups of ensembles using scripts written in Mathematica.

Scripts are contained in the directory `genie/genie-tools/runscripts`. Typing "`/bin/bashqsub_genie_myr_multipart.sh $1 $2 $3 $4 $5 1 $7 0 $9`" where

- `$1` = MODELID: the config name, e.g `genie_eb_go_gs_ac_bg_sg_rg_el`
- `$2` = BASELINE: the baseline config name - e.g. `worbe2_fullCC`
- `$3` = RUNID: the run ID, e.g. `worbe2_preindustrial_1`
- `$4` = NPARTS: the number of parts to the experiment
- `$5` = K: the experiment part counter
- `$6` = NEWPART: is it the start of a new part? 0=no; 1=yes
- `$7` = MAXYEARS: the individual job length in model years
- `$8` = J: the start year, usually `0`, unless restarting a run.
- `$9` = MINJOBTIME: minimum number of seconds allowed between resubmits before job is killed

at the command line prompt leads to the following: `qsub_genie_myr_multipart.sh` is used to submit `genie_myr_multipart.sh` to the job queue on the computer cluster. `genie_myr_multipart.sh` selects the appropriate parameters by loading them in from files `genie/genie-main/configs/$1`, `genie/genie-configpatches/$2_0` and `genie/genie-configpatches/$2_$5`; `$2_0` contains parameters common to all parts of the experiment. The script `genie/genie-main/configs/$2_$5.sh` is also run, which automates tasks that need doing when progressing from one part of an experiment to the next; it is in this script that the length of the experiment part in years is set with RUNLENGTH. `genie_myr_multipart.sh` then calls `rungenie.sh`, which sets time-stepping and restart locations and launches the job with `genie-main/old_genie_example.job`. After the job has completed (following `$7` years of model time), `genie_myr_multipart.sh` updates the run year and/or part of experiment (and whether it is a new part or not) appropriately and resubmits itself to the job queue.

It terminates when when all parts are finished, or if the time between job submissions is less than the crash tolerance (`$9`). See Appendix B.1.2 for full details of this process.

To automatically generate ensembles, `.csv` file(s) (in `genie_configpatches`) are used. Examples are given in `genie/genie-tools/genie_rootdirstuff/genie_configpatches`. Commas designate values of parameters to loop over in the ensemble (there should be no other commas); `&`s parameters to group together for the purposes of the ensemble; `!`s at the start of lines designate parameters not to be looped over and `%`s at the start of lines give names for output. Settings for the ensemble can be edited in the file `multi_ensemble_params.nb` (a facsimile of which is in Appendix B.2; an explanation of the settings is provided in the file). Executing the contents of `multi_ensemble_params.nb` and then §"**Set-Up For Run:**" in `multi_ensemble_rgexpt.nb` generates the files necessary for the ensemble. A file `qsub_rungenie_expt_XXXXXXXXXX` (where the `X`s represent a date string, e.g. 201102150930 for 9.30 a.m. on the 15th of February 2011) is created in the folder `genie_run log/expts`. This file contains lines of the form "`/bin/bash qsub_genie_myr_multipart.sh $1 $2 $3 $4 $5 1 $7 0 $9`", as above; Executing it sets the ensemble(s) going.

Once runs are finished, or on their way, executing "**Collate Results:**" in `multi_ensemble_rgexpt.nb` collates time-series output. Results are saved in folders in the `results` folder corresponding to ensemble member names, experiment parts and date produced. Options in `multi_ensemble_params.nb` allow different combinations of runs to be collated, spreadsheets to be produced, graphs to be plotted and saved, timescale analysis to be performed (specific to atmospheric CO_2 perturbation experiments), tables to be created and exported along with graphs to LaTeX form, and animated gifs of various forms to be produced from netcdf output; all with a single execution of "**Collate Results:**". See Appendix B.1.5 for full details of ensemble management using Mathematica.

2.4 Spin-up

The model was spun-up using a two stage process (the technical aspects of which are detailed in genie-howto.pdf §5.1). Firstly the sediments were closed (any carbonate hitting the ocean floor was immediately remineralised). For the global average weathering case, terrestrial weathering flux was divided evenly between carbonate and silicate weathering, and set equal to a first approximation of the burial flux of carbonate material in the sediments ($F_{CaSiO_3,0} = F_{CaCO_3,0} = 5$Tmol/yr). For the spatially explicit case, weathering fluxes were left to freely equilibrate with the ocean-atmosphere-sediment system. Silicate weathering was balanced by setting outgassing equal to it ($F_{outgas} = F_{CaSiO_3,0}$; Equation 12). The ocean, atmosphere and biogeochemistry were left to equilibrate under the condition of fixing atmospheric pCO_2 at a pre-industrial level (278ppm). After 25kyr (ample time for equilibrium to be achieved), the sediments were opened and left for 100kyr to equilibrate with the rest of the system. For this second part to the spin-up, in the global average weathering case, terrestrial weathering flux was set to equal the burial flux of carbonate as diagnosed in the first stage of the spin-up. The system is very nearly, but not quite at equilibrium after this, as shown in Figure 4, which shows wt% $CaCO_3$ progressing toward equilibria over the course of 100kyr second-stage spin-ups. The maximum change in wt.% $CaCO_3$ for any run was less than 0.25% in the last 10kyr (after ~75kyr, it is less than 1%, so future second-part spin-ups will be kept to this length). Under control conditions (no emissions), the model remained in a stable pre-industrial state after turning off the restorative forcing used in the spin-up.

Where set, the weathering feedbacks had very little effect on the outcome of the spin-up, on account of baseline parameters being set to their global averages (as diagnosed in the first part) in the second part.

It was thought that a short cut might be introduced in running experiments by way of having a pre-prepared baseline spin-up available for use with different ensembles. However, it was found that, despite model instances being similar in terms of state after the spin-up for most ensembles (the large range in Fig. 4 is mostly down to one particular ensemble), differing settings for parameters between spin-ups and experimental runs makes for unstable experimental runs, which do not tend toward equilibrium. Even different runs in the same ensemble have slightly different outcomes when being run from a single spin-up rather than separate spin-ups (a test showed a difference of 0.07% after 100kyr when looking at atmospheric pCO_2).

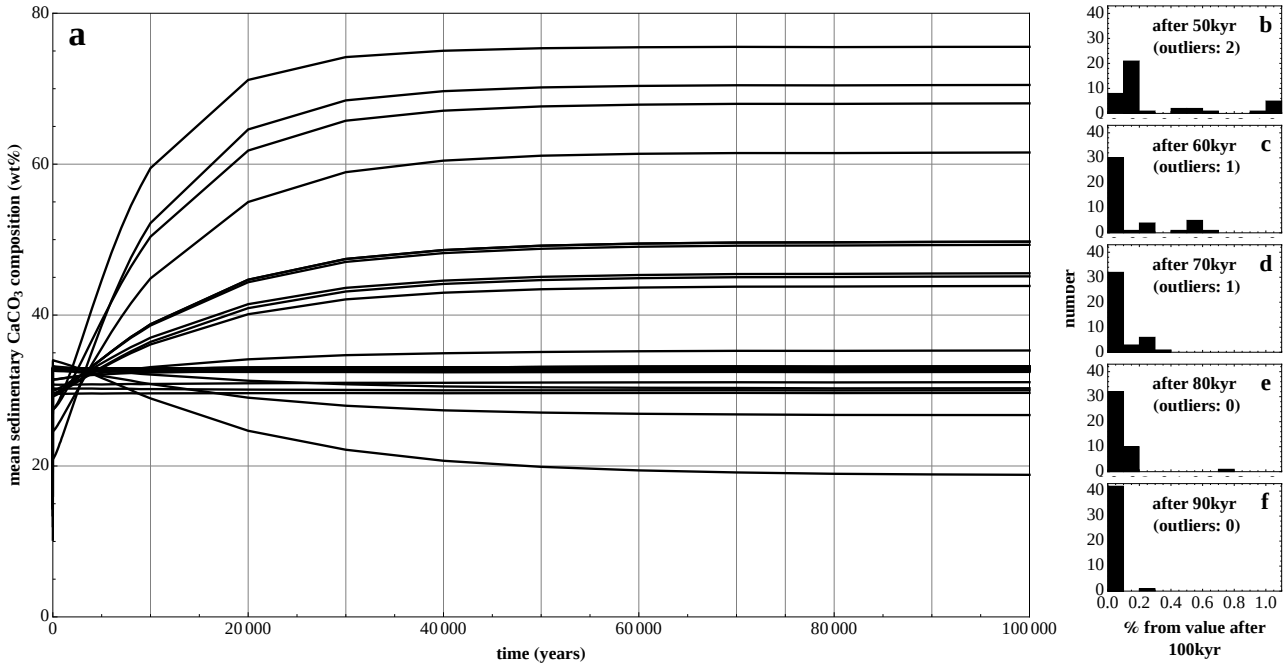

Figure 4: Sedimentary carbonates moving toward equilibrium in model spin-ups. All ensemble runs are shown, covering the full range of parameters explored in this thesis. Note that most of the spread (<30 & >35 wt% $CaCO_3$) is from ensemble members with spatially explicit weathering and greatly differing lithologies (see section §3.8); the observed real-world value is 34.8 wt% (Ridgwell, 2007). After ~50kyr, sedimentary $CaCO_3$ by wt% has levelled off for most runs (a). Some are slower than others to reach equilibrium. The vast majority of runs have $CaCO_3$ wt%s less than 1% different to their final values at 100kyr after 50kyr (b; there are 2 outliers not shown). After 80kyr, all runs runs are less than 1% from their 100kyr values (d). By 90kyr, all but one run has a wt % of sedimentary $CaCO_3$ less than 0.1% away from its value at 100kyr. At this stage, sedimentary $CaCO_3$ is settled at equilibrium, only fluctuating a few parts per ten-thousand over decamillenia.

2.5 Comparison of key dependencies with data

In order for the model to be reasonably in line with reality, one would hope that, after spin-up, the input variables - land temperature (T), runoff (R) and productivity (P) - would have a representation in the model that is in agreement with data. However, due to the coarse nature and intermediate complexity of GENIE, there are large systematic errors.

2.5.1 Land Temperature

Figure 5(b) shows a systematic bias in the model, towards a homogenising of land temperatures. Tropical and Southern Hemisphere areas are consistently too cold, whereas high latitude areas in the Northern Hemisphere are consistently too hot. Overall, this gives a very large rms error, comparable to the mid-low latitude range (the ranges from 45°N-0° and 45°S-0° are 11.4°C and 5.7°C respectively). When temperatures from the ENTS land surface model are looked at (Fig. 5(c)), one can see that there is much less latitudinal homogenisation in temperatures - indeed temperatures are now overly latitudinally stratified. However, using the ENTS land surface model can result in very different temperatures being generated by the EMBM. In the EMBM, moisture is not retained on the land surface; any excess of precipitation minus evaporation (p - E) is run off into the ocean instantaneously. Conversely, the ENTS module designates a bucket of water for each grid cell, which fills and empties according by accumulation of p - E.

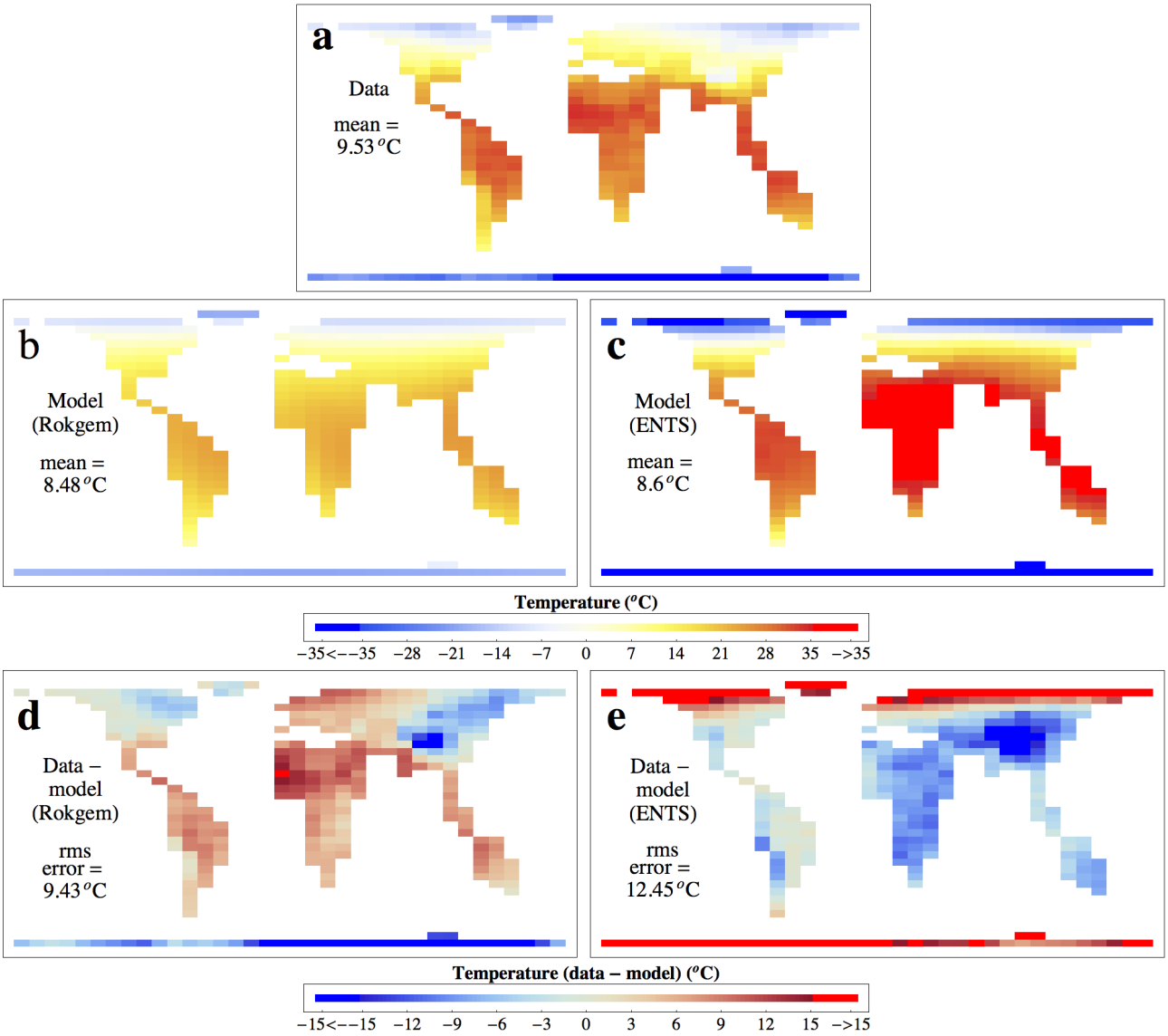

Figure 5: Comparison of modelled annual mean land temperature with data. The model is a pre-industrial spin-up of GENIE, with the output taken from the RokGeM model on the left, and the ENTS model on the right. (The model results are from two different configurations of the model, one with ENTS included, one without; this is because the RokGeM temperature output for the model including ENTS was very different - mean of 4°C. The data is an annual average of the CRU Global 1961-1990 Mean Monthly Surface Temperature Climatology (New et al., 1999)

2.5.2 Runoff

Figure 6 shows that runoff is very poorly represented in GENIE. Without the ENTS land model, precipitation is used as a proxy for runoff. Here (Figure 6(b)), there is at least a comparable amount of average runoff (compare with Fig. 6(a)), even though the distribution is far from realistic. In general tropical and forested areas are under-represented in the model; Fig. 6(i) shows the difference between data and model.

With the land vegetation model ENTS, the default scheme for runoff is overflow of the buckets which hold water on land. On account of the buckets rarely overflowing, there is no runoff over most of the land surface. Buckets capacity is nearly always greater than water content. Water will accumulate up until a point (lower than capacity), but then no further on account of evaporation increasing to match precipitation. As shown in Fig. 6(c) there is only runoff in high latitude regions. The presence of Orography allows lapse rate to influence temperature; higher altitudes have a cooler climate, which leads to more condensation and hence more precipitation and runoff. Switching orography on in the model produces runoff in high altitude areas such as the Himalayas, but there is still no runoff over the vast majority of the land surface (Fig. 6(d)). Fig. 6(j,k) show the difference between data and model for these two cases with and without orography. The way weathering is parameterised, if there is no runoff in a grid cell, there is no weathering flux, so this situation is inadequate for the purpose of the weathering model.

Using precipitation as a proxy no longer works with ENTS; as shown in Fig. 6(e), there is more than five times more precipitation than the required amount of runoff. Switching orography on again produces more land water, leading to an even greater excess of runoff Fig. 6(f). Fig. 6(l,m) show the difference between data and model for these two cases.

Efforts were made to improve the runoff distribution in the model. Changing the constants that affect bucket capacity in the model also affects photosynthesis and albedo. The soil water response of photosynthesis in ENTS is linear function with a range of 0 to 1 for moisture contents ranging from $\frac{1}{2}$ to $\frac{3}{4}$ of bucket capacity. Decreasing bucket capacity to allow more runoff leads to an increase in photosynthesis. Soil albedo, and hence overall land albedo, is also dependent on the parameters used to determine bucket capacity, and can either increase or decrease depending on which of the 3 parameters used to determine bucket capacity are altered. The unintended changes in photosynthesis and albedo serve to destabilise the model, hence adjusting bucket capacity was an unsuccessful approach. Ignoring bucket capacity altogether, and making runoff effectively precipitation minus evaporation, leads to negligible amounts of runoff as nearly all excess land water is evaporated.

In another approach, the "leaky bucket" runoff scheme used in the MOSES land surface model (Meissner et al., 2003) was transcribed into GENIE. Here

$$R = K_s \left(\frac{M}{M_s} \right)^{2b+3} \tag{9}$$

where R is runoff, K_s saturated hydraulic conductivity, M soil moisture, M_s saturated soil moisture and b the Clapp-Hornberger exponent, which is dependent on soil type. There are three types of soil ordered by grain size, each with a correspondingly steeper exponent: coarse (b=4.50), medium (6.63), and fine (11.2). The medium grain soil leaky-bucket scheme gives a non-negligible distribution of runoff (still much less than data over most of the land surface; Figure 6(g,h,n,o)), but the climate is greatly affected (cooled). The fine grain soil scheme gives less runoff (not shown), and the coarse grain scheme crashes the model by way of cooling the land surface to excess and inducing a snowball-Earth state.

An exponential decay formulation of runoff was also tried. An assumed soil moisture time of 1-2 months (Pidwirny, 2006) leads to reasonable amounts of runoff (~150 mm/yr), but takes too much moisture from the land surface, again leading to the model crashing through an induced snowball-Earth state.

Having a separate offline (non-climate-affecting) water cycle for the purposes of calculating runoff for use in RokGeM is a possibility, but such an unphysical representation might as well be supplanted by direct calibration of runoff fields to data, as described below in §2.5.4.

Overall, the instance of the model with the lowest data-model rms error is the first, without the ENTS land model, and with precipitation used as a proxy for runoff. Even so, this rms error is still significantly larger than the data mean (352 vs. 242 mm/yr).

It's also interesting to compare the average runoff from the data (242 mm/yr) with the figures used to calibrate the GKWM and GEM-CO2 models, which use 418 mm/yr (Gibbs et al., 1999) and 374 mm/yr (Amiotte-Suchet et al., 2003). This is quite a large discrepancy.

Although all attempts at modelling an accurate distribution of runoff have substantially failed, the initial model instance - that without the ENTS land surface scheme, and using precipitation as a proxy for runoff - is used

for the purposes of the experiments performed for this thesis. This is on account of it being the least inaccurate when compared with real-world data.

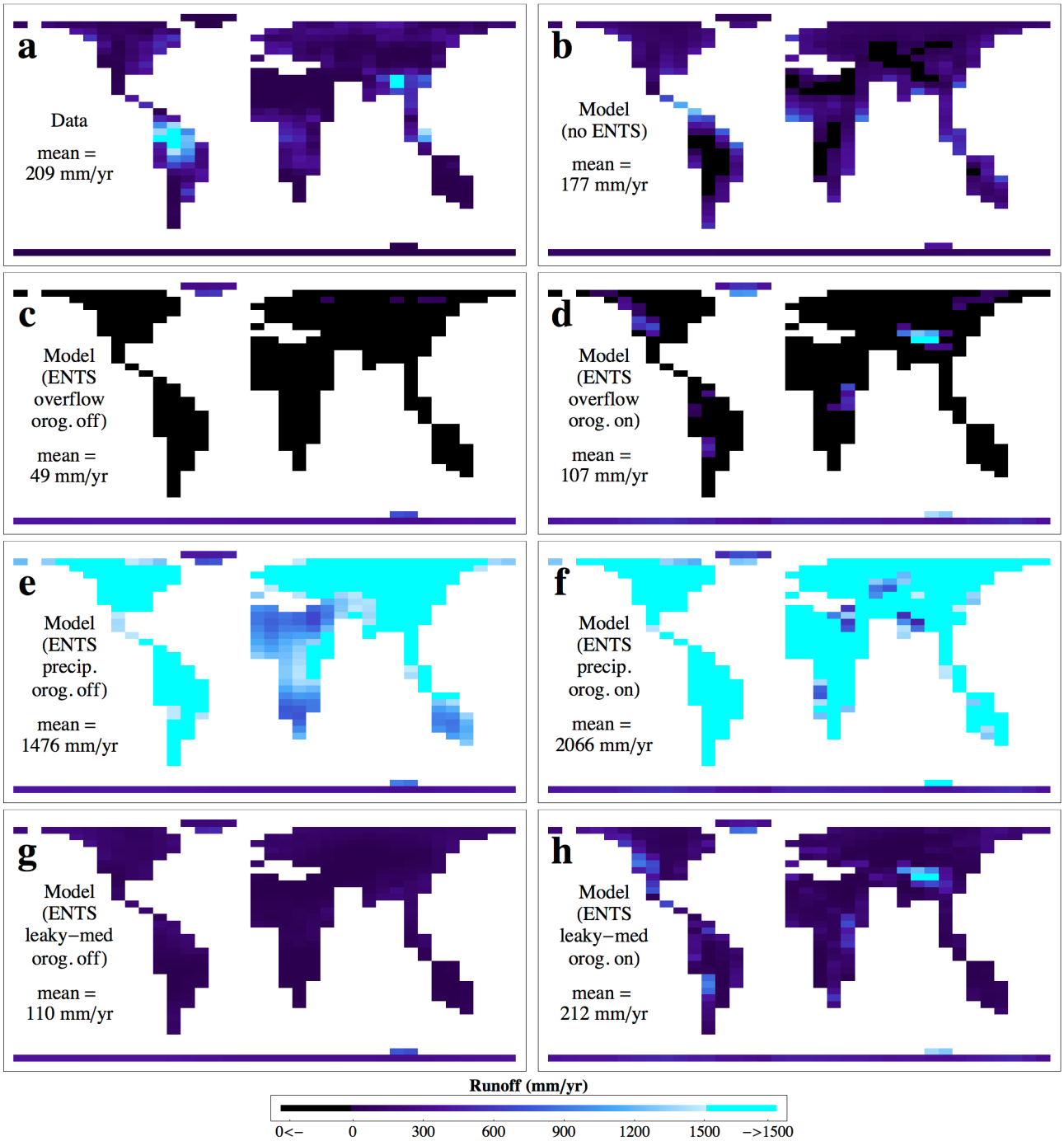

Figure 6: Comparison of modelled runoff (b-h) with data (a). The model is a pre-industrial spin-up of GENIE, with different runoff schemes (described in text), and orography off (c, e, g) or on (d, f, h) . The data is a compilation of observations and simulations (in order to fill a global grid) from the World Meteorological Organization Global Runoff Data Centre (Fekete et al., 2002). The difference between data and the various instances of the model are shown in panels i-o on the next page (i-o correspond to b-h).

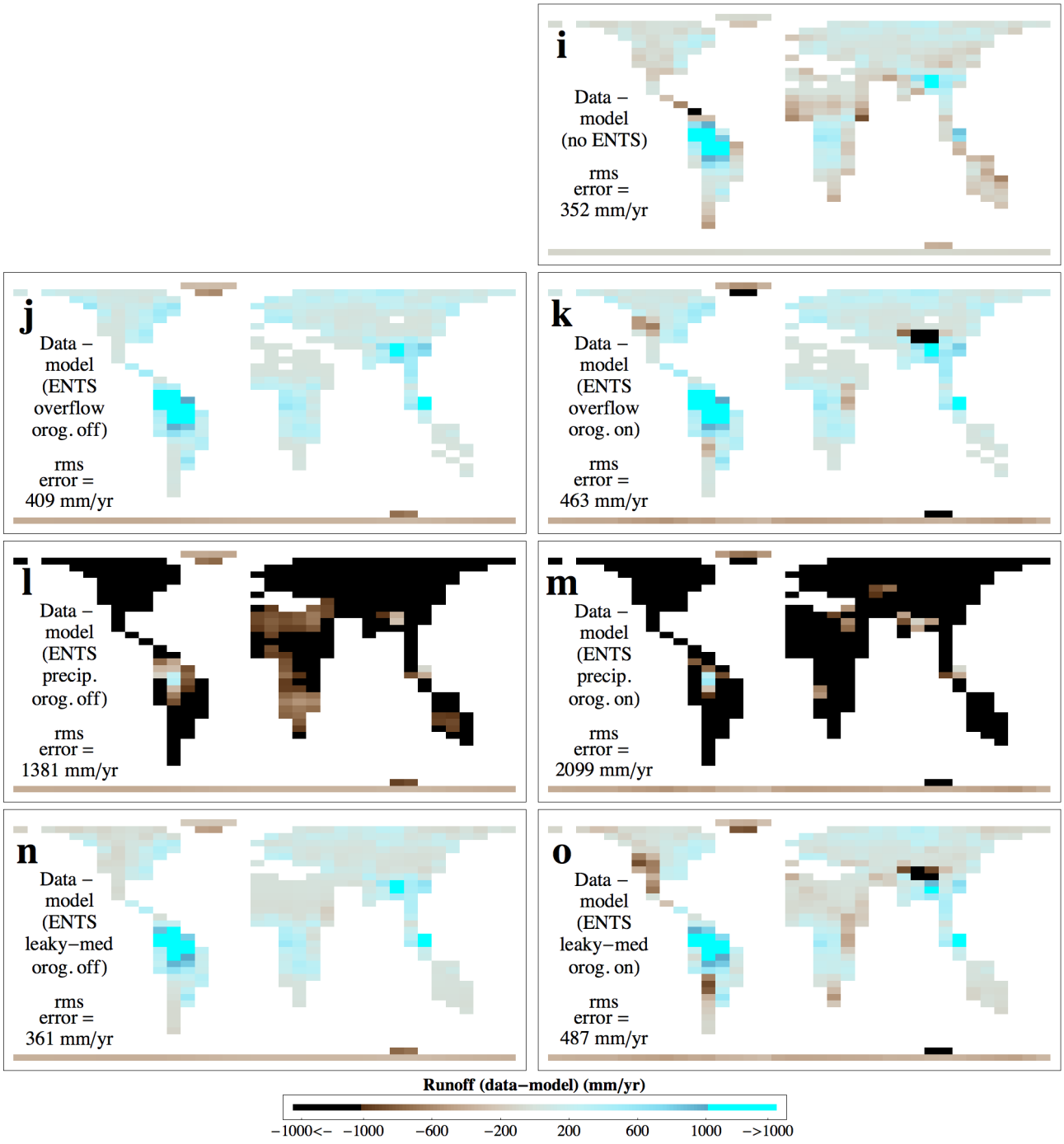
i
Data –
model
(no ENTS)
rms
error =
352 mm/yr
j
Data –
model
(ENTS
overflow
orog. off)
rms
error =
409 mm/yr
k
Data –
model
(ENTS
overflow
orog. on)
rms
error =
463 mm/yr
l
Data –
model
(ENTS
precip.
orog. off)
rms
error =
1381 mm/yr
m
Data –
model
(ENTS
precip.
orog. on)
rms
error =
2099 mm/yr
n
Data –
model
(ENTS
leaky–med
orog. off)
rms
error =
361 mm/yr
o
Data –
model
(ENTS
leaky–med
orog. on)
rms
error =
487 mm/yr
Runoff (data–model) (mm/yr)
−1000<−
−1000
−600
−200
200
600
1000
−>1000

2.5.3 Productivity

Figure 7 shows that the modelled Net Primary Productivity (NPP; the net amount of chemical energy produced by the biosphere) on land is much higher than the data. There is also productivity in regions that should be deserts, such as the Sahara, and most of Australia.

2.5.4 Calibration to data

Because GENIE's coarse resolution does not allow for accurate representation of temperature, runoff and productivity - the input variables for the RokGeM weathering module - options are included to calibrate the fields containing these variables to data. This can be done both by way of normalising fields to global average values from data, thus retaining spatial patterns produced by the model, or by scaling fields directly to data, allowing the pattern from real-world data to be reproduced. These calibrations are done during initialisation of the model, thus allowing for the variables to retain a degree of freedom to vary with climate.

The spin-up procedure of negating feedbacks by setting baseline parameter values (for temperature (T_0), runoff (R_0) and productivity (P_0)) equal to global average values nullifies the effect of calibration to global average data - i.e. with such calibration set, the T, R and P fields are altered in the output, but their changes have no effect on weathering fluxes as T_0, R_0 and P_0 are altered a corresponding amount during spin-up)

Another approach, of scaling one model variable to another (such as runoff to temperature), as described in (Huntingford and Cox, 2000), was discarded on account of there being no adequate variable to anchor patterns to (the temperature distribution also shows large systematic errors, as described above).

This calibration approach (multiplying values by x) is mathematically sound for the weathering parameterisations involving ratios, as

$$\frac{xR}{xR_0} = \frac{R}{R_0} \tag{10}$$

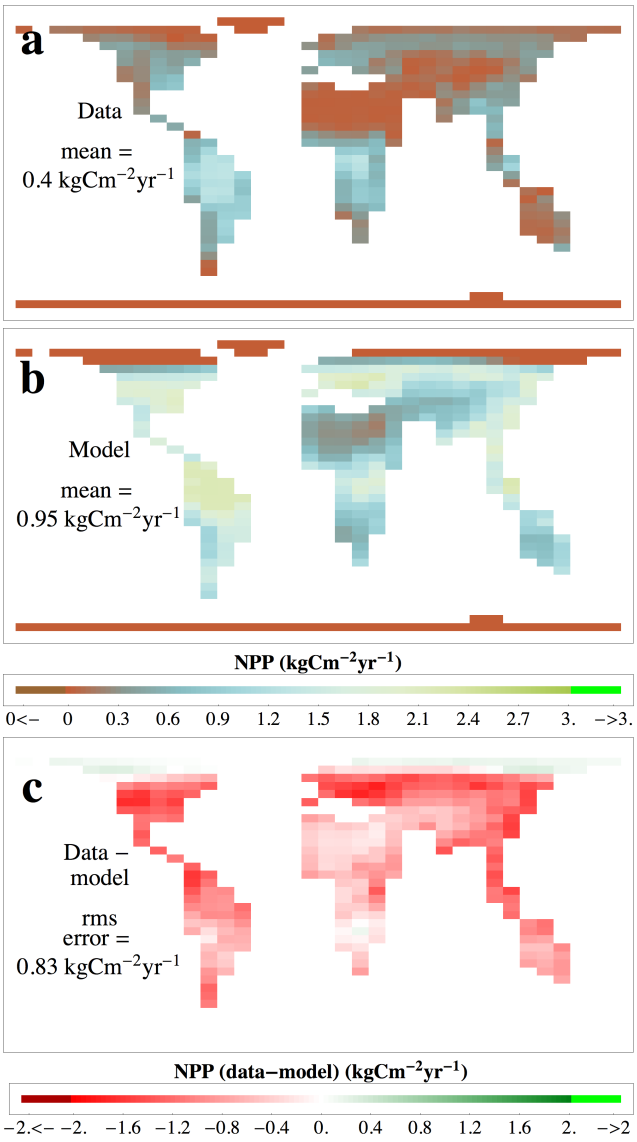

Figure 7: Comparison of modelled productivity with data. The model is a pre-industrial spin-up of genie_eb_go_gs_ac_bg_sg_rg_el. The data is from Socioeconomic Data and Applications Center (SEDAC), http://sedac.ciesin.columbia.edu/es/hanpp.html [accessed 29/09/2009] (Imhoff et al., 2004).

(the same holds for P), but there is a problem with the temperature equation, which uses a difference, as

$$xT - xT_0 = x(T - T_0) \neq T - T_0 \tag{11}$$

However, the difference in average temperature between data and model is only a small fraction of the absolute values involved (a couple of degrees Kelvin out of ~300), so the effect of this mismatch is minimal. Were other weathering functions to be used in the future, this may not always be the case.

Previous work with ENTS demonstrates that even though absolute values are not comparable to data, precipitation *anomalies* under transient climate change simulations are more comparable to NCEP data (see Fig. 7 of (Lenton et al., 2006)). This suggests that precipitation anomalies could be applied to runoff fields as a means to get a more accurate representation of weathering flux variations. However, with the ENTS model, runoff fields are very unreliable and patchy, meaning that this approach cannot be implemented as there is little to work with when doing the scaling. Efforts to improve the runoff fields in GENIE are described in §2.5.2.

2.6 Emission Scenarios

The Emissions scenarios referred to in this thesis are summarised in Table 3 below:

Table 3: Emissions scenarios

GtC released	Scenario
1000	"Producer limited"
1000	Pulse emission in year 1990
5000	Pulse emission in year 1990

The 1000GtC scenario was included in recognition of the fact that most future emissions scenarios (including the IPCC SRES business as usual ones) fail to take into account economic factors that limit the total possible recoverable reserves of fossil fuels. The total economically recoverable supply of fossil fuels is estimated to be 480GtC (Rutledge, 2010); adding this to historical emissions of 357GtC (Boden et al., 2008) yields 837GtC. Factoring in land use change emissions of 137GtC (Enting et al., 1994) historical, and an unknown future amount, it is likely that the upper limit (barring successful mitigation efforts) of total anthropogenic emissions is around the 1000GtC mark. It just so happens that it is likely that this figure of 1000GtC, or a trillion tonnes of carbon, is the upper limit of emissions for global warming to remain within the limit (adopted by numerous institutions, such as the EU (European, 2007)) of 2°C over pre-industrial levels (Allen et al., 2009; Meinshausen et al., 2009).

In realistic scenarios, carbon is input to the atmosphere over the course of a few hundred years; this timescale is a tiny fraction of the simulated time of the model runs presented here (a million years), making it of little importance for results pertaining to the far future. Therefore, as a simplification, and to aid comparison with other models, instantaneous pulse emissions are used in this study. A comparison of pulse emissions with drawn out emissions is shown in Figure 8. There is a trade-off with using pulse emissions however: when analysing results it it useful to look at the fraction of excess pCO_2 remaining in the atmosphere at certain years; these are under-estimated if the peak value is an unrealistic spike. For this reason, and to aid realism, the drawn-out 1000GtC "producer limited" scenario will be used (amongst others) in future work. Nevertheless, the round-number 1000GtC pulse scenario is in the long-term likely very similar with the more reality-based ~1000GtC scenario, hence it is best looked at as a simple long-term carbon perturbation experiment with a justifiable basis in reality. Many more emissions scenarios were going to be included, covering a full range from 500 to 10000GtC, but due to computational constraints, and the fact that there are many variables to test the model over, only the two pulse emissions (of 1000 and 5000GtC) were chosen.

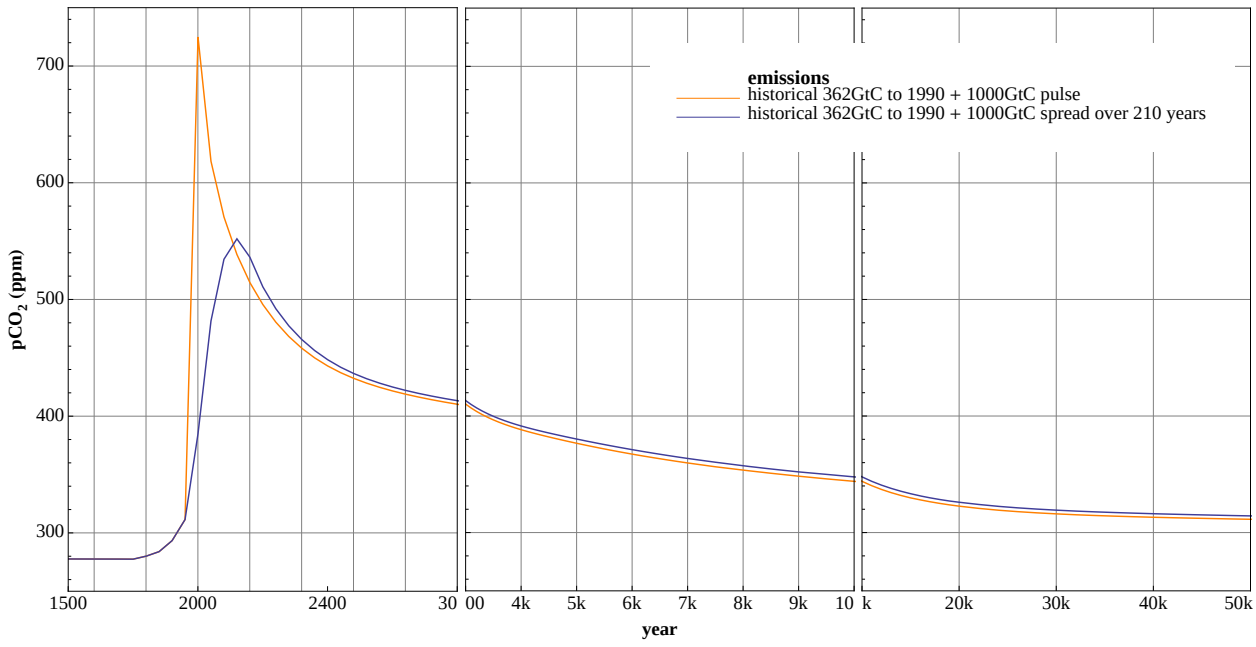

Figure 8: Comparison of a pulse of emissions and a drawn out period (hundreds of years) of emissions. After the initial spike in emissions, the tail of the emissions curves are the same.

2.7 Visualising results

With the production of vast amounts of data from model runs numbering over a hundred, displaying results in a systematic, coherent and concise manner, is a challenge. In the following chapter (§3), an overview of results is shown in the form of a plot of pCO_2 for each section describing a model variable. In depth results are only looked at for a small subset of model runs with interesting parameter variations. Tables of key numbers from graphs are also produced, but most are relegated to Appendix A.

The nature of the experiment, involving a restoration of the Earth System to a preindustrial climate state from pulses of carbon emissions, calls for pertinent data such as percentages of excess CO_2 as well as absolute values of CO_2 at specific times, to be tabulated. Also tabulated are the inverse forms - years where specific target values and fractions remaining are reached. These data are also tabulated for surface global warming, and surface ocean acidification, parameters of wide societal (as well as ecological) significance. A full set of results are in Appendix A.

On a spatial level, gigabytes of NetCDF data-sets were produced as part of the model output. These were converted into time-varying video visualisations including latitudinal trend-lines and comparison amongst ensemble members. A complete set of these animations is included on digital media. For the electronic version of this thesis, links to selected animations are provided at the relevant places.

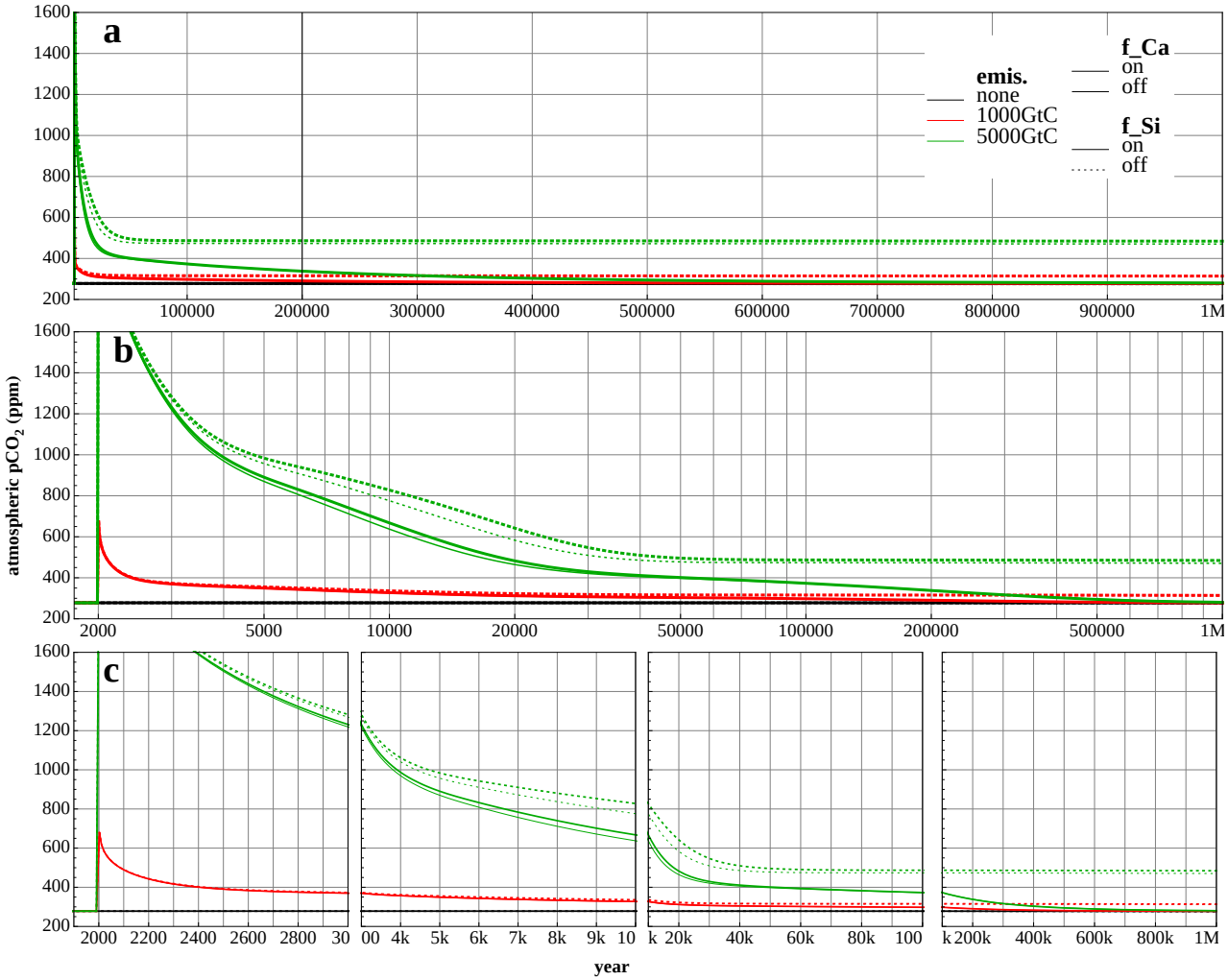

Figure 9: Time-series visualisation using an example result of atmospheric pCO_2 (dependent variable) over 1Myr for two different emissions pulses: linear (a, b, c) and logarithmic (d, e, f) scales for dependent variable with a linear timescale (a, d), a logarithmic timescale (b, e), and multiple linear timescales (c, f); multiple linear scales for both the dependent variable and time (g); separate plots for each emissions scenario (h) [continues on next two pages].

2.7.1 Time-series

The nature of the experiments conducted for this thesis lead to results that are non-linear over time. Carbon cycle perturbations from large emissions pulses are non-linear because there are processes involved that act at different rates. Ocean invasion and mixing are relatively quick (10^0-10^3 year timescales), whereas ocean sediment dissolution and terrestrial weathering are relatively slow (10^3-10^5 year timescales). In order to present line graphs that show in detail the action that is happening, a number of different approaches were tried. These are presented in Figure 9. Plots with a linear timescale (Fig. 9(a)) are dominated by the "long tail" (Archer et al., 2009) of the perturbation. Using multiple timescales in a broken-up plot (Fig. 9(c)) is a good way to visualise processes happening on different timescales, without resorting to a logarithmic timescale (Fig. 9(b)), which is less intuitive to grasp (in everyday thought we are accustomed to thinking of time in a linear way). For the dependent variable, a logarithmic scale (Fig. 9(d, e, f)), or even multiple linear scales (Fig. 9(g)), can also be used to show more detail. Alternately, separate plots can be shown for each emissions scenario (Fig. 9(h)), allowing detail to be seen for the much smaller 1000GtC scenario.

It was decided on balance that using a different linear scales for each emissions scenario for the dependent variable and multiple linear scales for the time axes (Fig. 9(h)) allowed plots to provide the most information in an intuitive manner, whilst retaining a somewhat uncluttered look. All further time-series results are presented in this manner.

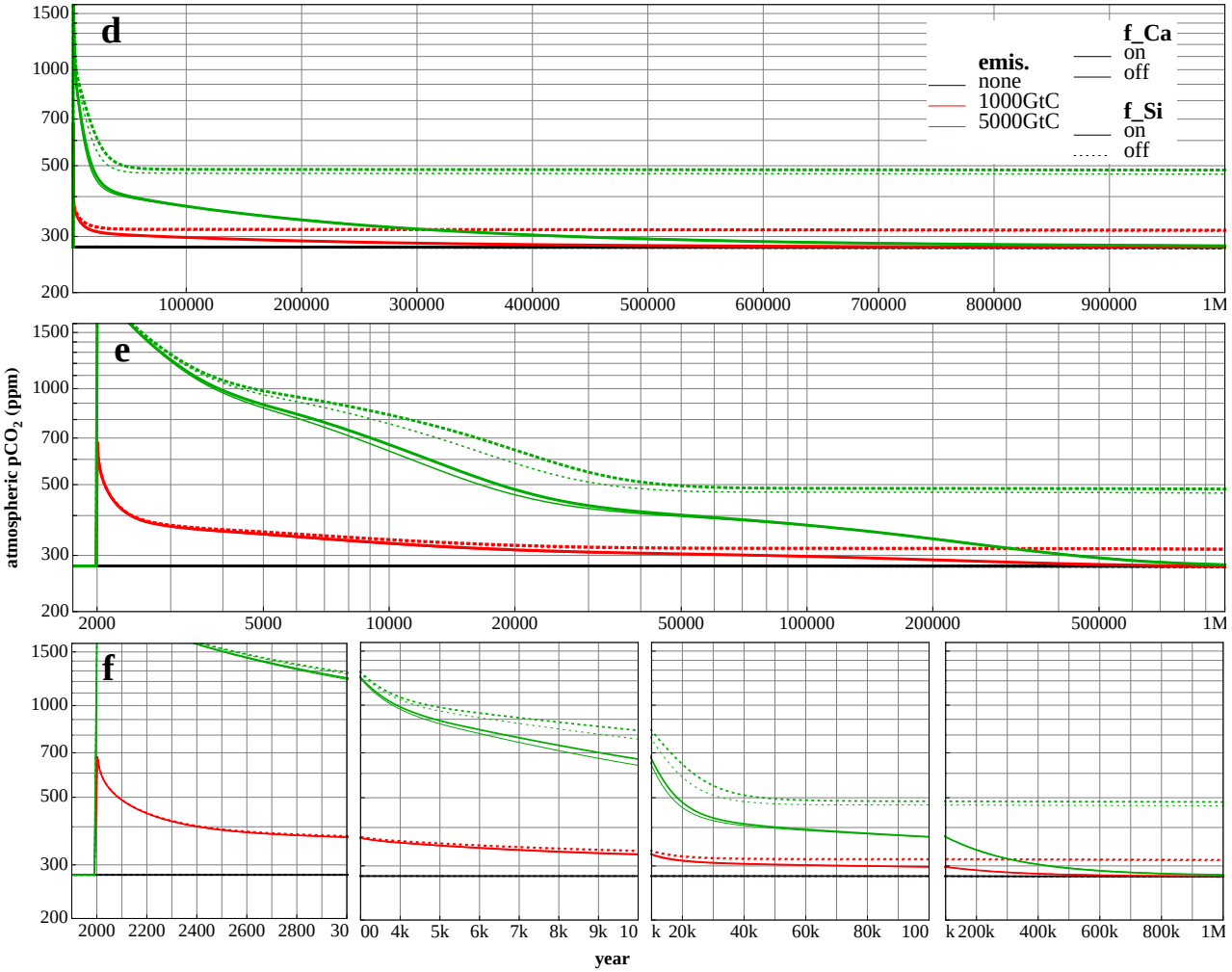

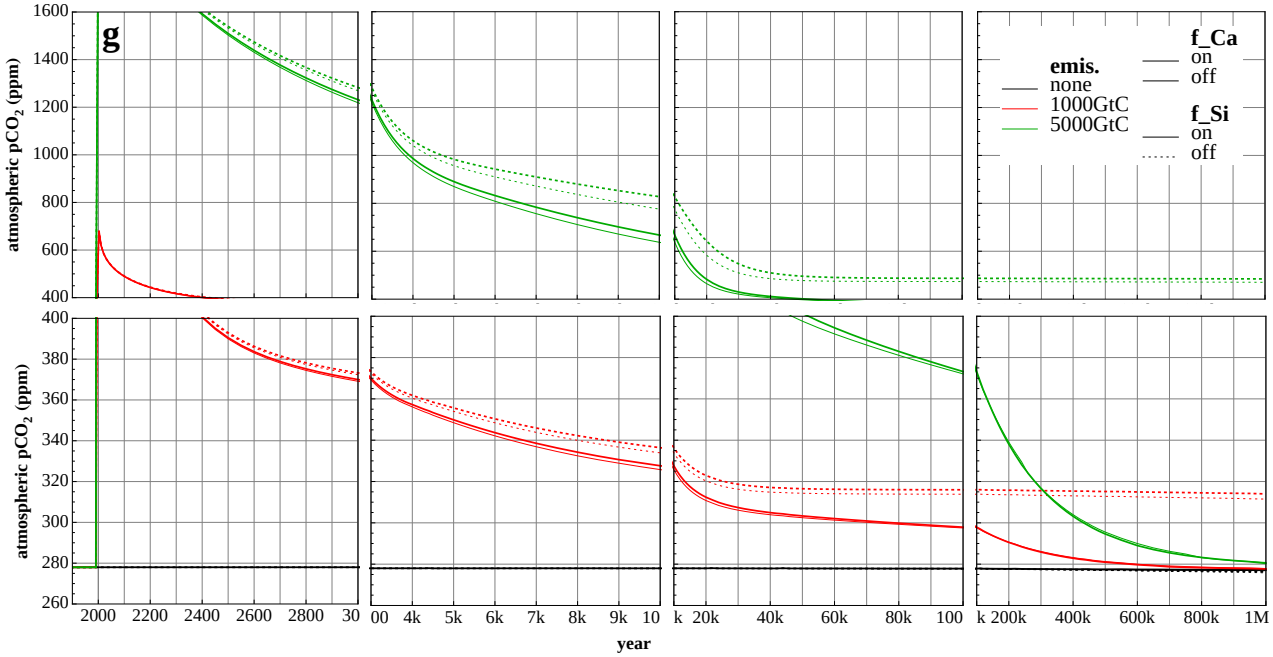
g
atmospheric pCO2 (ppm)
emis.
none
1000GtC
5000GtC
f_Ca
on
off
f_Si
on
off
year

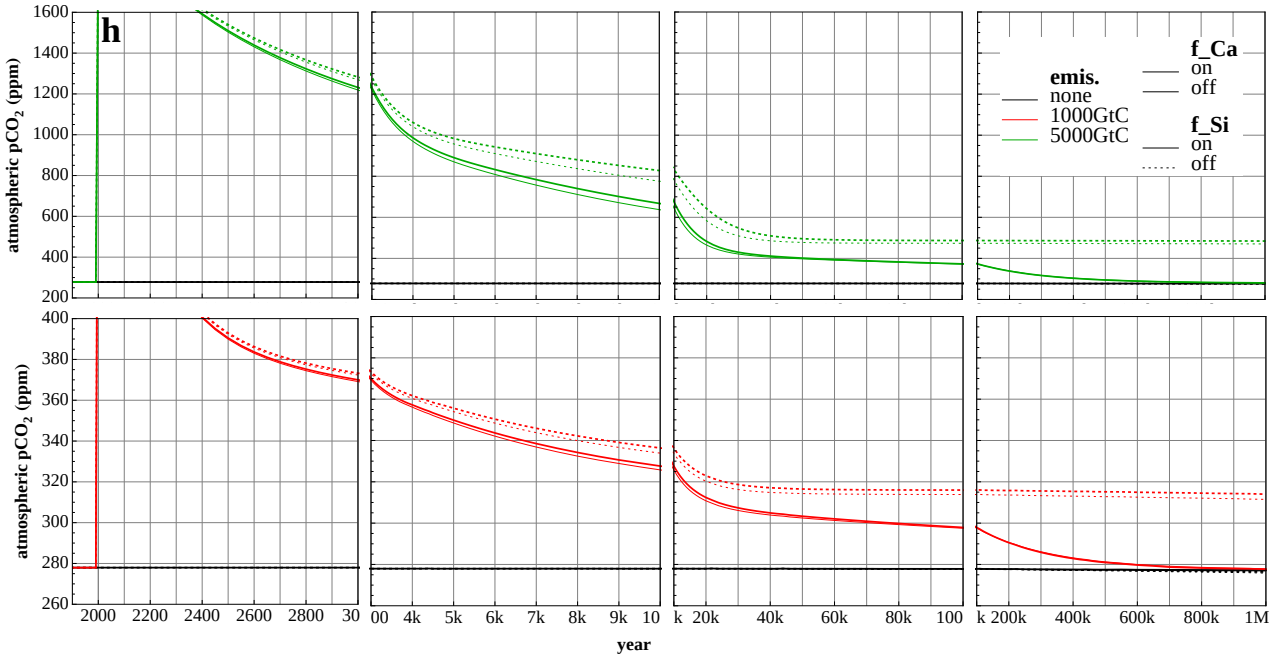
h
atmospheric pCO2 (ppm)
emis.
none
1000GtC
5000GtC
f_Ca
on
off
f_Si
on
off
year

3 Weathering model (RokGeM) description

RokGeM (Rock-Geochemical Model) is a carbon-, calcium- and alkalinity-cycling weathering module with climate feedbacks; it is rooted in the framework of GENIE (Grid ENabled Earth system model) and it's biogeochemistry modules (AtChem, BioGeM and SedGeM; see §1.6). This chapter describes the model's dependencies, processes and sensitivities. Fluxes of calcium ions from carbonate and silicate weathering (§3.1) are either prescribed as global averages (0D) divided evenly over the land surface, or explicitly calculated based on lithological data and runoff (2D) (§3.7, §3.8); they are modulated by feedbacks with temperature (§3.2), runoff (§3.3, §3.4) and productivity (§3.5), and routed to the coastal ocean (§3.6). The effect of changing climate sensitivity is looked at in §3.9.

3.1 Carbonate and Silicate weathering

In the initial zero-dimensional (0D) instance of the model (Globavg), global average fluxes of calcium ions (Ca^{2+}) from calcium-carbonate (F_{CaCO_3}) and calcium-silicate (F_{CaSiO_3}) weathering are prescribed. These are modulated by a simple temperature (T), runoff (R) and productivity (P) feedbacks (see sections §3.2-3.5 below) that can be switched on and off. The fluxes are then used to calculate fluxes of DIC (F_{DIC}) and Alkalinity (F_{Alk}):

$$F_{DIC} = F_{CaCO_3} + F_{outgas} \tag{12}$$

$$F_{Alk} = 2F_{CaCO_3} + 2F_{CaSiO_3} \tag{13}$$

Note that there is only one mole of DIC for each mole of Ca^{2+}; this is a short-circuiting of the atmosphere based on the assumption that the atmosphere and surface ocean are well mixed on the timescales considered here. Instead of removing one mole of CO_2 from the atmosphere - and by implication the ocean - and adding two moles of bicarbonate to the ocean (as in equation 5), nothing is taken from the atmosphere and one mole of bicarbonate is added to the ocean. The same short-circuiting leaves no net DIC flux for silicate weathering (the DIC terms cancel in equation 6). F_{outgas} is a prescribed input of carbon from volcanic outgassing used to counter the prescribed silicate weathering flux (which removes carbon into the geologic reservoir) so as to keep the system in long-term equilibrium.

As shown in Figure 10, short-circuiting the atmosphere has little effect on long-term global atmospheric pCO_2 levels. Even on shortest timescales, there is minimal difference between the runs with short-circuiting on, and those with it off (see Appendix A.2 Fig. 44 (a)). However, it is interesting to note that there is a significant difference in alkalinity flux to the ocean (~10%) between the two (Fig. 44 (e)), which leads to a significant difference in sediment preservation (Fig. 44 (d)).

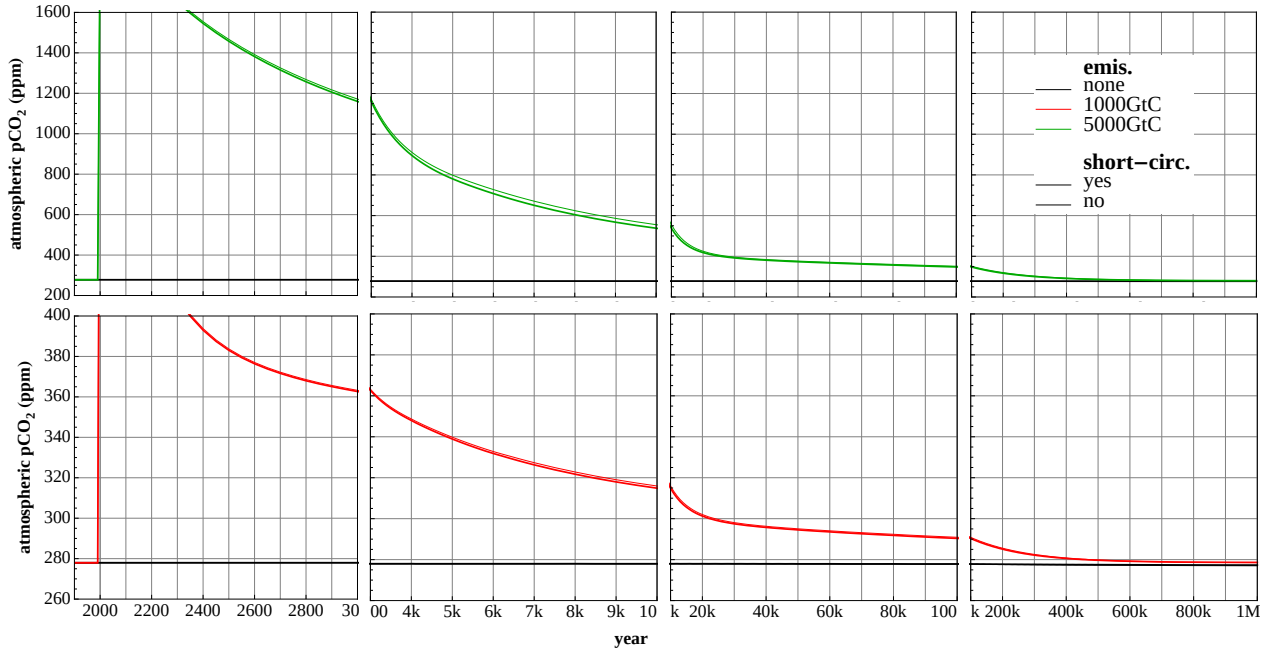

Figure 10: Evolution of atmospheric CO_2 over 1Myr for 1000GtC (red) and 5000GtC (green) emissions pulses, vs. a control run with no emissions (black), with short-circuiting of the atmosphere on/off.

3.2 Temperature dependence of weathering

Temperature affects weathering through controlling the rate of the chemical reactions involved. Following Berner's geologic carbon cycle models (such as BLAG (Berner et al., 1983) and GEOCARB (Berner, 1994)), the dependence of carbonate weathering on temperature is given by:

$$F_{CaCO_3} = F_{CaCO_3,0}\,(1 + k_{Ca}\,(T - T_0)) \tag{14}$$

where T is temperature; 0 stands for the initial value, and the constant $k_{Ca} = 0.049$. This equation is derived by correlating concentrations of bicarbonate in groundwater with the temperature of the groundwater (Harmon et al., 1975). Laboratory studies of the temperature dependence of the dissolution of Ca and Mg silicates form the basis of the silicate weathering-temperature feedback used (Brady, 1991):

$$F_{CaSiO_3} = F_{CaSiO_3,0} e^{-\frac{E_a}{R}\left(\frac{1}{T}-\frac{1}{T_0}\right)} \tag{15}$$

which is an Arrhenius rate law equation; R is the molar gas constant (not to be confused with runoff as it is in all other uses apart from this section) and E_a the activation energy for dissolution. Assuming that $T \approx T_0$, this equation simplifies to:

$$F_{CaSiO_3} = F_{CaSiO_3,0} e^{k_T (T - T_0)} \tag{16}$$

where

$$k_T = \frac{1000 E_a}{R T_0^2} \tag{17}$$

for E_a given in kJ/mol and T_0 in °K. The error induced by this simplification (which lessens the computational resources used by the model - the factor k_T can be calculated at initialisation), is less than 10% for -26°K < (T - T_0) < 31°K (see Fig. 11). A best guess of $E_a = 63$ kJ/mol (Brady, 1991) is used, along with $T_0 = 288$K (global average pre-industrial temperature), to give $k_T = 0.09$ for the model runs presented in this thesis. Another estimate, based on least squares fitting of field based weathering data to multiple controlling variables (temperature, runoff and erosion), is $E_a = 74 \pm 29$ kJ/mol (West et al., 2005). The error gives this estimate of E_a a large range, spanning more than a factor of two, giving very different weathering flux estimates when the exponential function is taken into account, as shown in Figure 11.

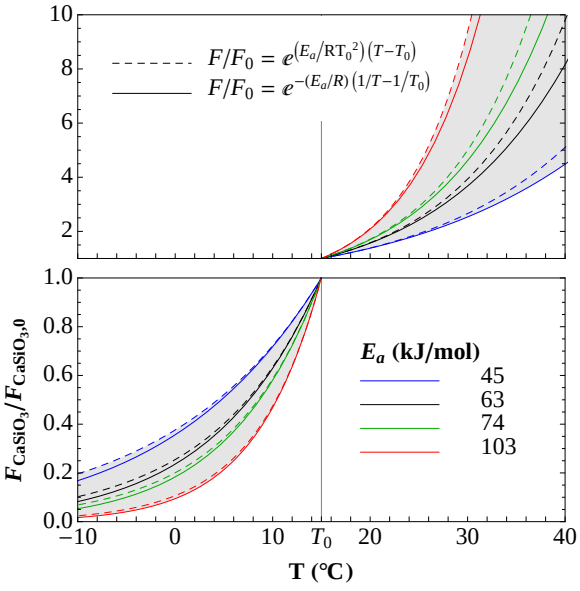

Figure 11: Effects on silicate weathering-temperature feedback of changing activation energy (E_a, different colours), and simplifying Equation 15 (solid lines) to Equation 16 (dashed lines). Values for E_a are taken from (West et al., 2005) (74±29 kJ/mol) and (Brady, 1991) (63 kJ/mol). Note that lower activation energies give bigger fluxes for $T < T_0$ (bottom panel, different y-axis scale).

The effect of the temperature feedback is shown in Figure 12. The silicate weathering-temperature feedback (T_Si) has a greater effect on the draw-down of atmospheric pCO_2 than the carbonate weathering-temperature feedback (T_Ca). The removal of CO_2 from the atmosphere by way of carbonate weathering is completed after c.50kyr; this is when the carbonate ocean sediments are restored, and the burial rate of carbon matches the riverine input of carbon to the ocean from the weathering of carbonate rocks. The case with T_Ca switched on leads to a very slight reduction in the equilibrium pCO_2 (312ppm vs. 314ppm) when compared to the case with no feedback. Silicate weathering continues to reduce atmospheric pCO_2 until it balances volcanic outgassing, at which point pCO_2 levels are returned to approximately pre-industrial levels. This can take up to and over 1Myr depending on the size of the emissions 'slug'; pCO_2 is back to 278ppm 850kyr after a 1000GtC slug, but after 1Myr is only at 289ppm for 5000GtC.

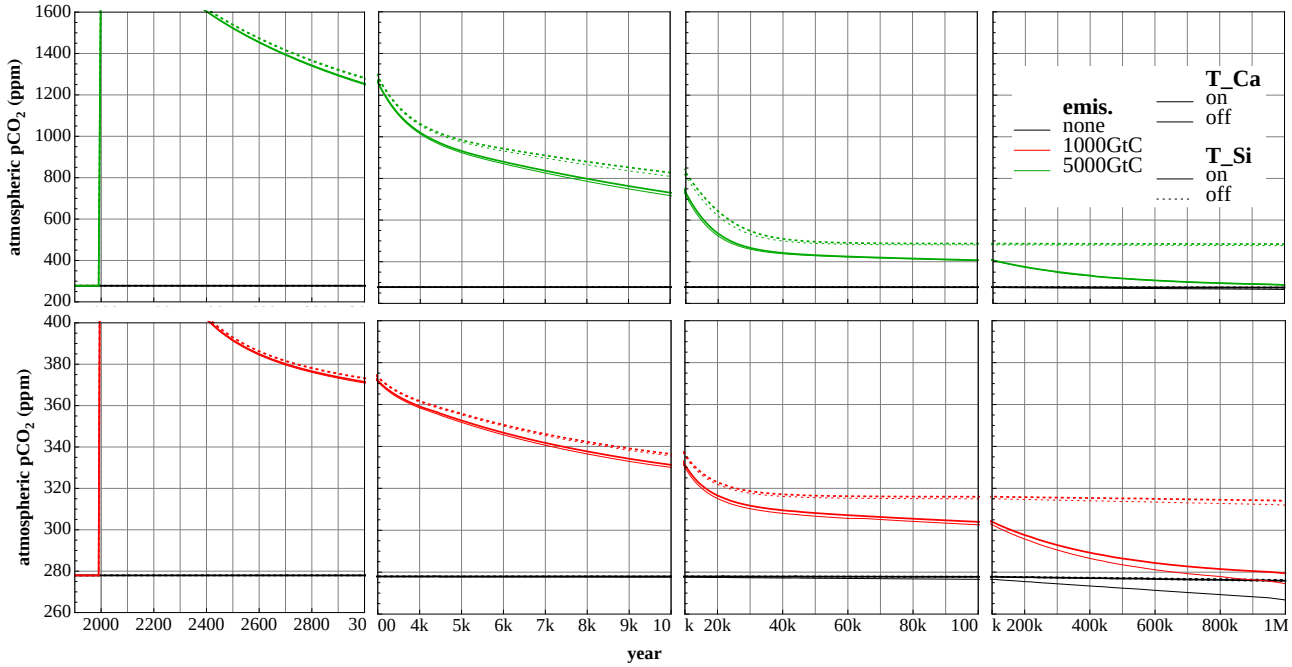

Figure 12: Evolution of atmospheric CO_2 over 1Myr for 1000GtC (red) and 5000GtC (green) emissions pulses, vs. a control run with no emissions (black), with carbonate and silicate weathering-temperature feedbacks (T_Ca and T_Si respectively) on/off.

With both weathering-temperature feedbacks switched on, a sensitivity test was conducted over the range of different estimates for activation energy (E_a). As shown in Figure 13, there is a significant difference between the ensemble members in atmospheric pCO2 drawdown by year 100k; a range of 50ppm for the 5000GtC scenario, compared with 87ppm as the difference between the runs with and without weathering-temperature feedbacks (Fig. 12).

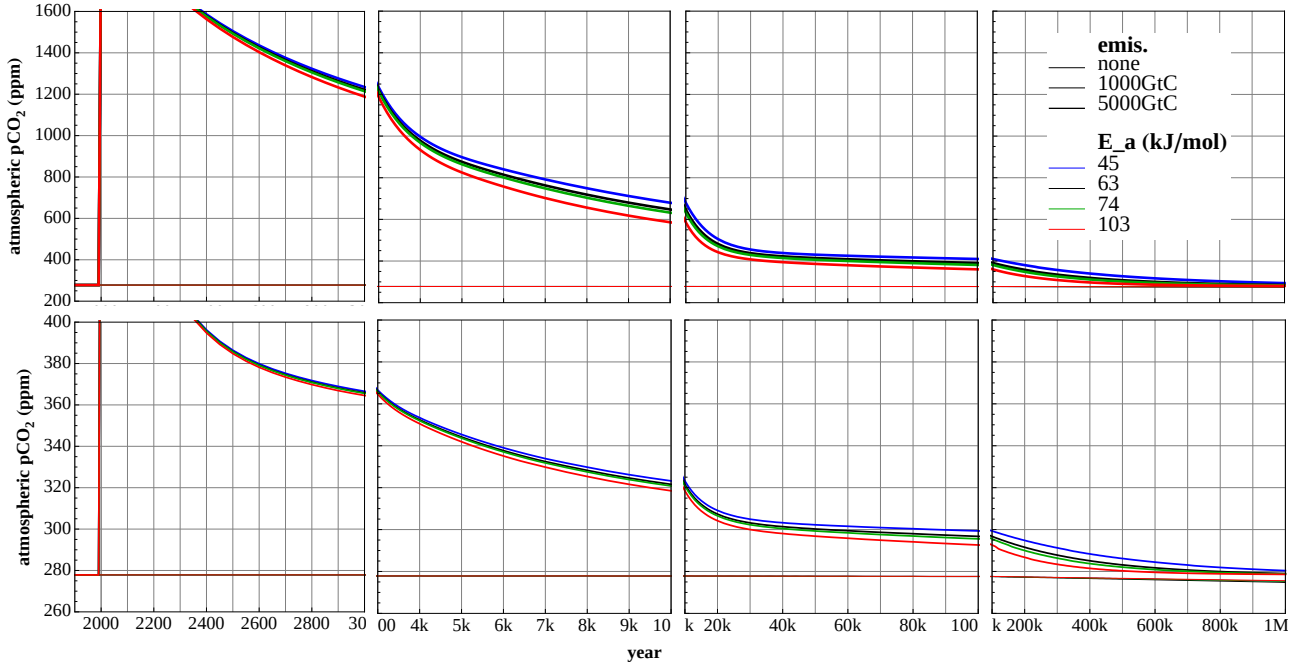

Figure 13: Evolution of atmospheric CO_2 over 1Myr for 1000GtC (red) and 5000GtC (green) emissions pulses, vs. a control run with no emissions (black), with different values of silicate weathering activation energy (E_a)

3.3 Runoff dependence of weathering (0D scheme)

Weathering is dependent on the residence time of water in contact with rocks. Static water in contact with rocks becomes saturated with weathered material; further weathering occurs when water is removed and replenished. Runoff can be used as a proxy for this water cycling that is key to rock weathering. Runoff dependence is factored in following Berner (1994):

$$F_{CaCO_3} = F_{CaCO_3,0} \frac{R}{R_0} \tag{18}$$

$$F_{CaSiO_3} = F_{CaSiO_3,0} \left(\frac{R}{R_0} \right)^{\beta} \tag{19}$$

where R is runoff. The difference between the formulations for carbonate and silicate weathering stems from the assumption that carbonates saturate ground water in contact with them, so that concentrations of weathered bicarbonate are not assumed to be dependent upon runoff (Berner et al., 1983), whereas concentrations of bicarbonate from the weathering of silicate rocks are assumed to be diluted by runoff; β is taken to be 0.65 (Berner, 1994) as a default for the model runs presented in this thesis. More recent work gives $\beta = 0.80 \pm 0.32$ (West et al., 2005). The effect of changing β is modest. As illustrated in Figure 14, there is an ~85% difference in feedback strength between the end members at 25°C below the baseline temperature (T_0), and only a ~35% difference at 25°C above T_0.

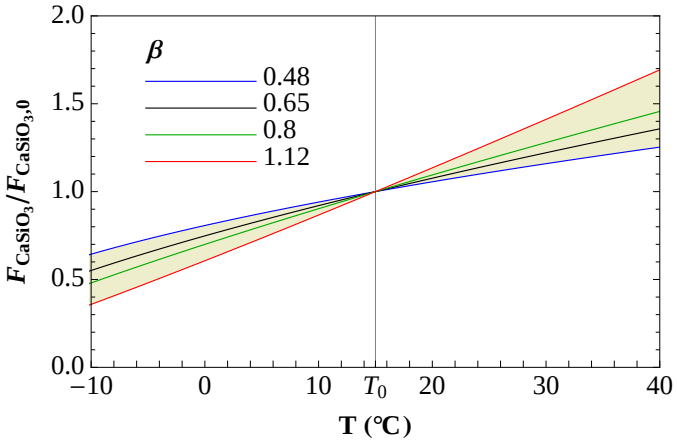

Figure 14: Effect of changing saturation exponent (β) on silicate weathering-runoff feedback. Values for β are taken from the literature (0.65 from Berner (1994); $\beta = 0.80 \pm 0.32$ from West et al. (2005)). Note that lower values of β give bigger fluxes for $T < T_0$.

Runoff is taken explicitly from the coupled EMBM, or alternatively is parameterised as a function of temperature following the approach of Berner:

$$\frac{R}{R_0} = Max\{0, 1 + k_{run} (T - T_0)\} \tag{20}$$

The Max{0,...} is included as only positive values are physical. k_{run} is a constant determined from computer models or observations (see below §3.4). Figure 15 shows a plot of Equations (18) and (19) with the substitution of 20. Even for extreme values of k_{run}, the feedbacks are much less sensitive than the silicate weathering-temperature feedback is to E_a (Fig. 11).

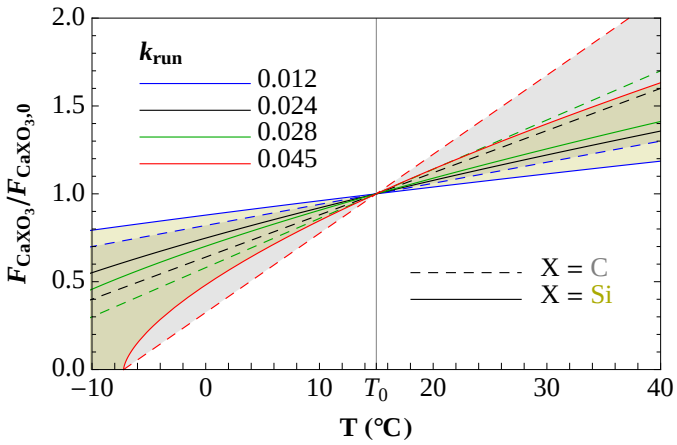

Figure 15: Effects of changing runoff-temperature correlation constant (k_{run}, different colours) on carbonate (solid lines, green shading) and silicate (dashed lines, yellow shading) weathering-runoff feedbacks. Values for k_{run} are taken from model output (0.024 - GENIE; 0.045 - NCAR CCM-3 (Berner and Kothavala, 2001)) and observational data (Fekete et al., 2002; New et al., 1999)(monthly time-series: 0.012 - global average; 0.028 - spatial on GENIE grid); see §3.4 for details and caveats. Note that lower values of k_{run} give bigger fluxes for $T < T_0$.

The effect of the runoff feedback is shown in Figure 16. Only when the emissions pulse is large (5000GtC) is there a significant effect. Even so, the effect is much smaller than that due to temperature feedbacks, the range in pCO_2 between the strongest runoff feedbacks and no feedback being 32ppm 100kyr after a 5000GtC emission, compared with 81ppm for temperature feedbacks. After 1Myr, the model runs with strongest runoff-weathering feedback are only back to 291 and 345ppm respectively for 1000 and 5000GtC emissions.

The effect of whether runoff-dependence is explicit (Eq.s (18) and (19)) or implicit ((18), (19) and (20)) is relatively large. When both carbonate and silicate weathering-runoff feedbacks are switched on, there is a 44ppm difference between the two in atmospheric pCO_2 1Myr after 5000GtC of emissions. This is largely down to differences in k_{run}; $k_{run} \approx 0.02$ for GENIE output, whereas $k_{run} = 0.045$ was used for the implicit calculations, following Berner and Kothavala (2001).

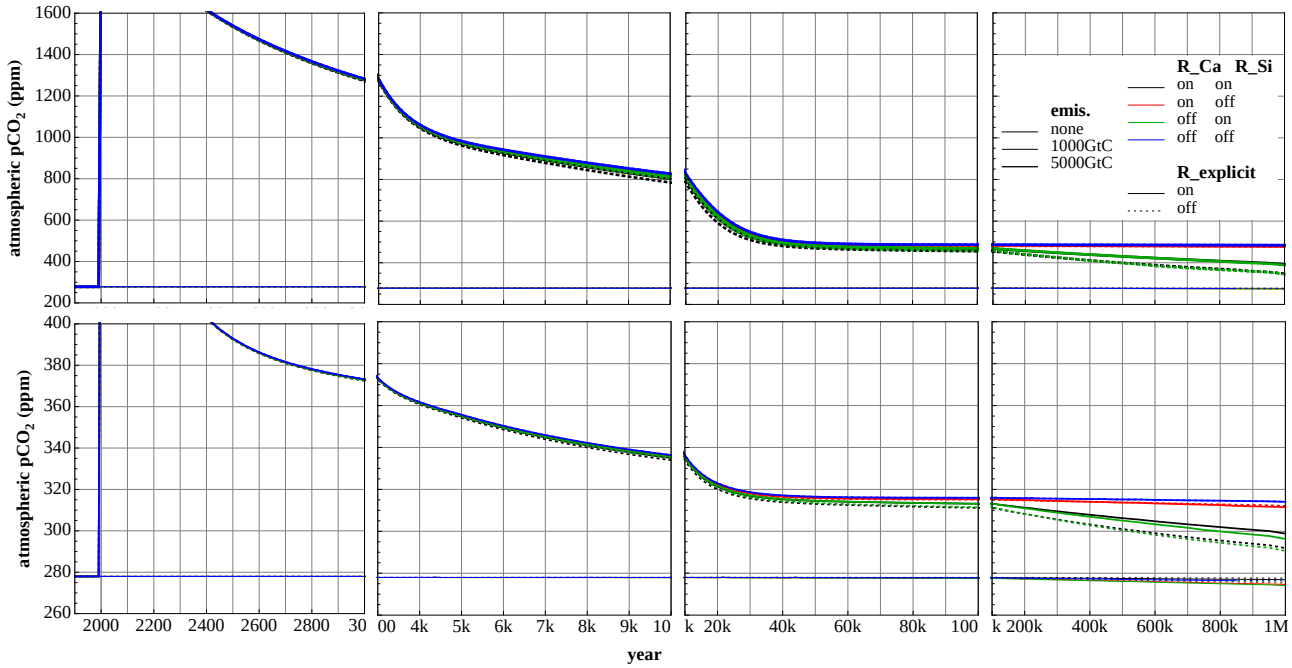

Figure 16: Evolution of atmospheric CO_2 over 1Myr for 1000GtC (bottom) and 5000GtC (top) emissions pulses, vs. a control run with no emissions (thin lines at bottom of plots), with carbonate and silicate weathering-runoff feedbacks (R_Ca and R_Si respectively) on/off and explicit/implicit (R_ex).

Ensembles with both runoff-weathering feedbacks (R_Ca and R_Si) on, covering the published ranges for the constants β and k_{run} are shown in Figures 17 and 18. Like with the overall effect of having the runoff feedbacks switched on or not, ranges in atmospheric pCO_2 values between end members are modest after 100kyr even in the 5000GtC scenario. The difference between β=0.48 and β=1.12 is 16ppm; the difference between k_{run}=0.012 and k_{run}=0.045 is 13ppm. Due to the slow nature of the runoff-silicate weathering feedback, equilibrium is still far enough away for these ranges to be increasing through to year 500k, where they become 43ppm and 69ppm respectively.

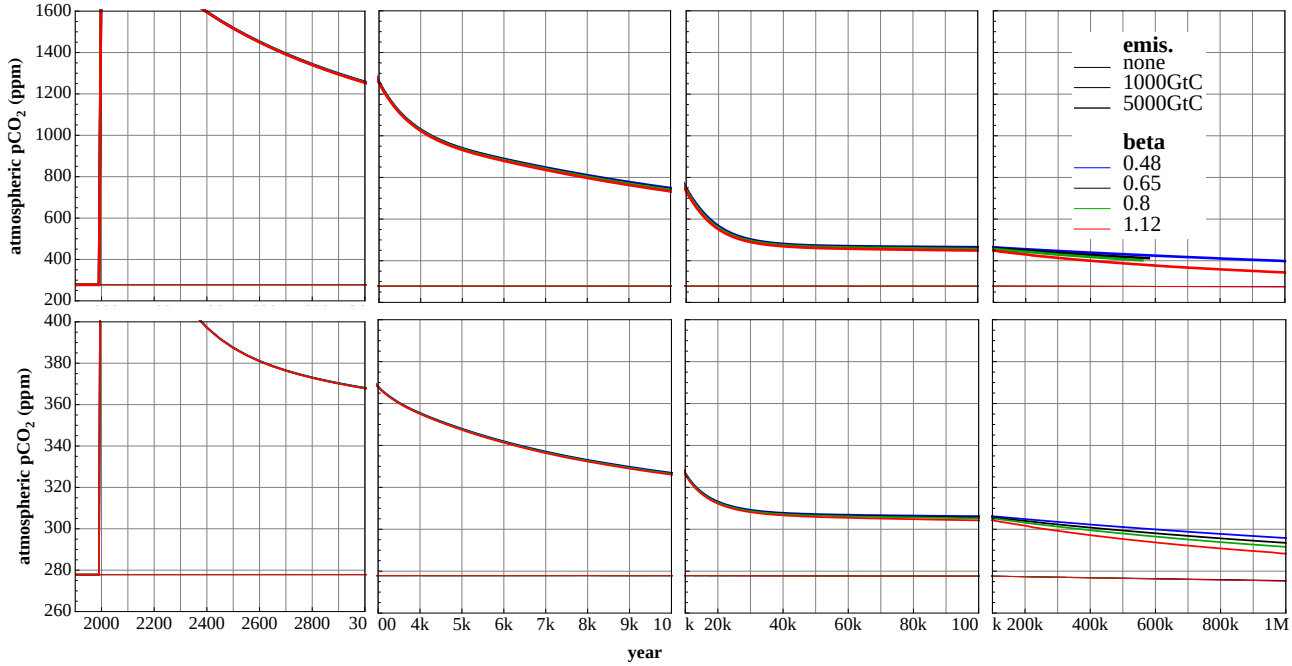

Figure 17: Evolution of atmospheric CO_2 over 1Myr for 1000GtC (bottom) and 5000GtC (top) emissions pulses, vs. a control run with no emissions (thin lines at bottom of plots), with different values of runoff fractional power dependence.

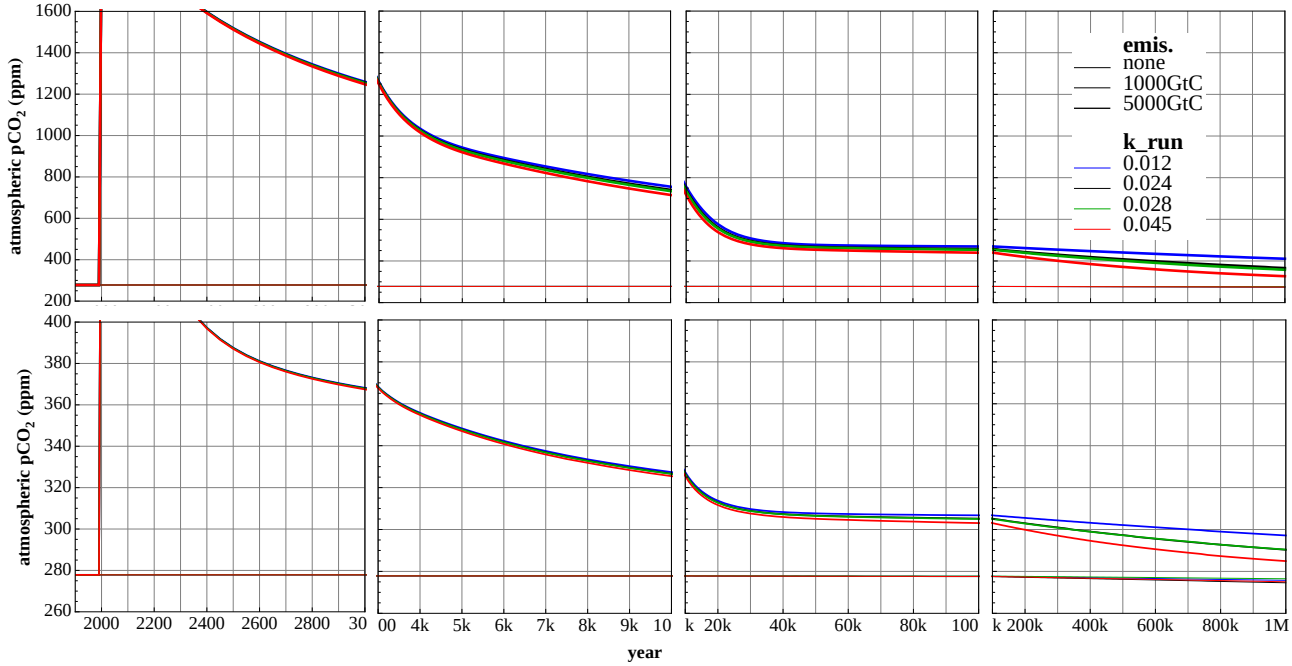

Figure 18: Evolution of atmospheric CO_2 over 1Myr for 1000GtC (bottom) and 5000GtC (top) emissions pulses, vs. a control run with no emissions (thin lines at bottom of plots), with different values of runoff-temperature correlation constant.

3.4 Does runoff depend on temperature?

In GCM modelling, there is a good linear fit between global averages of temperature and runoff. The value of the constant k_{run} in Equation (20) is taken to be 0.045 (Berner and Kothavala, 2001). Note that in the case of the GENIE model used here, $k_{run} = 0.024$, as shown in Fig 19(a). This is close to the value used in GEOCARB III for warmer geological periods (Berner and Kothavala, 2001). R_0 and T_0 are the values of runoff and temperature for the model run to equilibrium with pre-industrial levels of CO_2. The strong correlation between runoff and temperature in GENIE may well be a consequence of the simple 2D energy-moisture balance atmosphere. This strong correlation seems only to apply for global averages; when looking at individual grid cells, the correlation is very low, with R^2 coefficients of only 0.06-0.08 (Figs. 19(b) and 19(c).

When looking at real-world data values, the correlation between T and R is very weak, as shown in Fig. 20. Trend lines follow Equation 20 with k_{run} ranging from 0.012 to 0.050, but with R^2 coefficients of only up to 0.15, as opposed to 0.998 for the global average model results (Fig. 19(a)) . When using data at higher spatial and temporal resolution (monthly instead of annual; data gridded on model grid instead of global averages), it might be expected that the correlation would be better, but this is not the case. Using a time-series instead of a climatology only slightly improves things (Fig. 20: (a) vs. (d), and (g) vs. (f)).

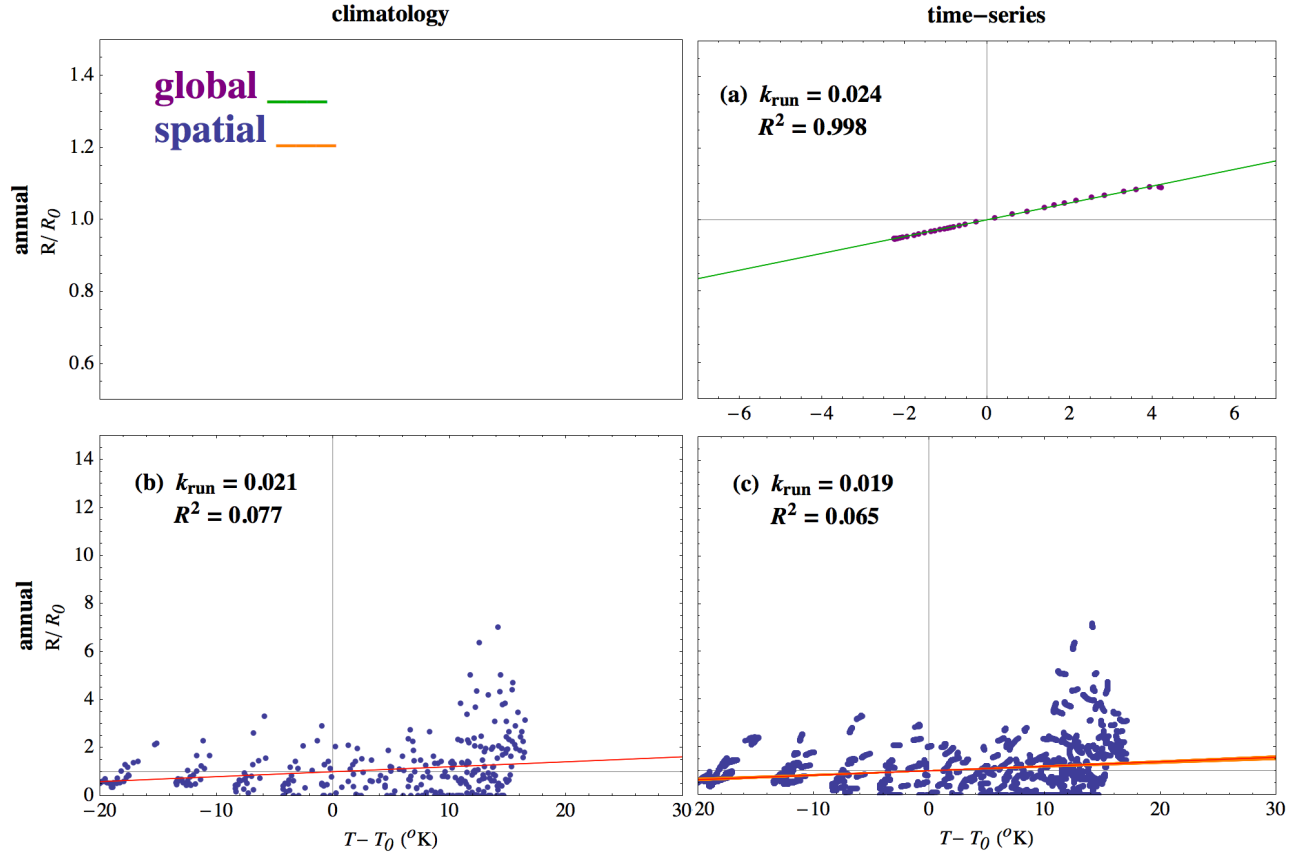

Figure 19: Runoff (R/R_0; relative scale) vs. temperature (T-T_0; °K) in model output from GENIE. Annual climatologies for spatial output (b) and time-series for global averages (a) and spatial output (c). No monthly data is shown as the version of the model used does not have a seasonal cycle. "Climatology" (b), refers to an instance of the model at a stable pre-industrial state; "time-series" is a selection of 40 individual snap-shots (years 1000, 1991, 2200, 2300, 2500, 2750, 3000, 3500, 4002, 5000, 6002, 7000, 8002, 10002, 12002, 15000, 20002, 25000, 30002, 40002, 50002, 60002, 75000, 100002, 125000, 150002, 200002, 250005, 300002, 400002, 500002, 600002, 700002, 800002, 900002, 1000000) of a transient model run with a 5000GtC pulse of emissions at year 2000 (no output was used for the 200 years following this due it being erratic on account of the large emissions pulse). Plots are labelled with fitted line gradients (k_{run}; lines shown in green for global data and red (overall) and orange (individual years in (c)) for spatial data) and coefficients of correlation (R^2). k_{run} ranges from 0.016 to 0.021 for individual years in (c); Corresponding R^2s range from 0.046 to 0.078. R_0 and T_0 are means (averaged over time or space appropriately for each plot).

Berner's original formulation linking runoff and temperature is perhaps valid over the geological timescales it was originally applied to, however, averaging over monthly and yearly timescales, it appears not to hold (despite it being originally based on early GCM modelling (Berner et al., 1983)). This is due to the rapid response and

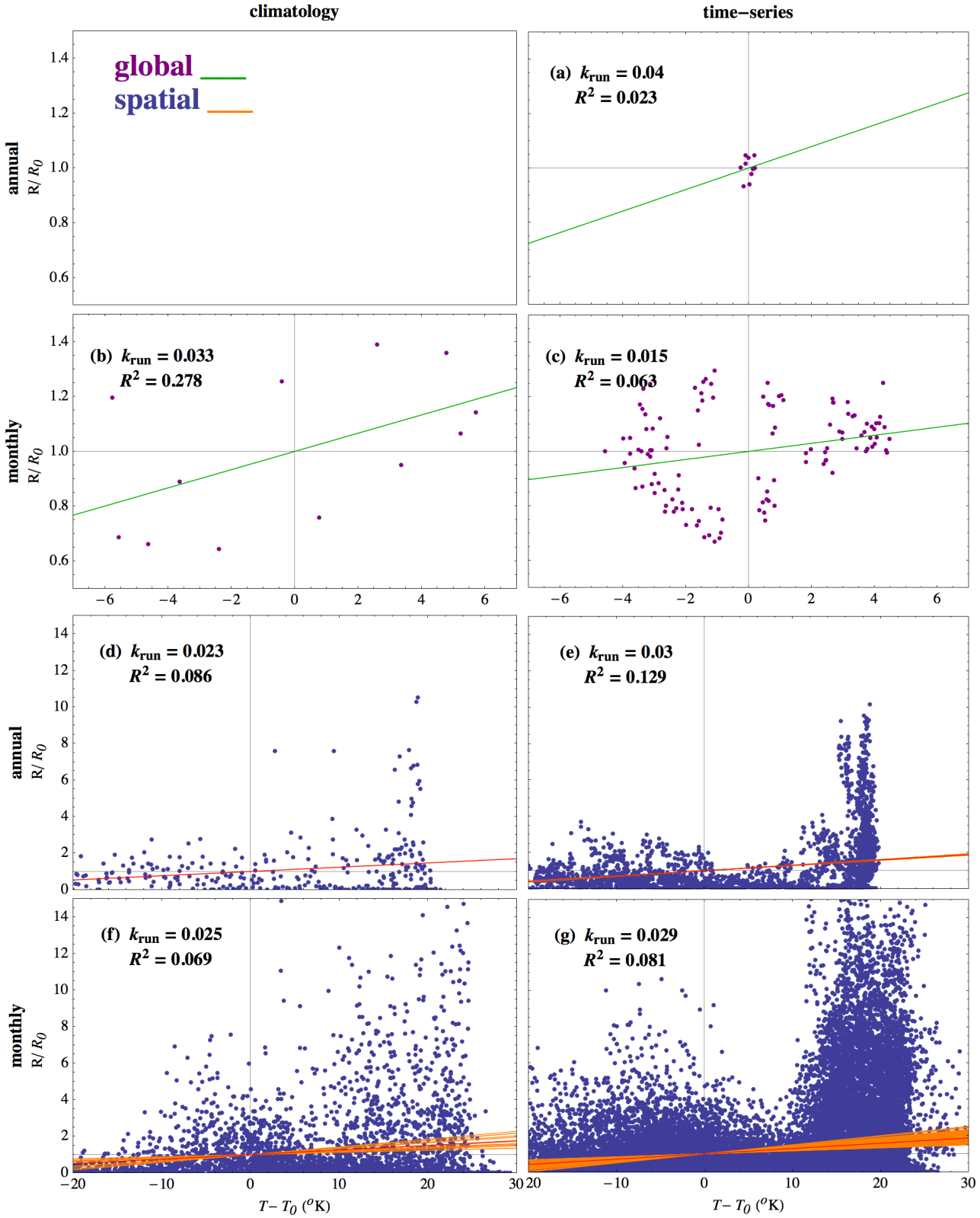

Figure 20: Runoff (R/R_0; relative scale) vs. temperature (T-T_0; °K) in real-world data. Annual (a, d, e) and monthly (b, c, f, g), climatologies (b, d, f) and time-series (a, c, e, g), are shown for global averages (a, b, c) and spatial data placed on the 36x36 GENIE grid (d, e, f, g). The temperature climatology is an average from 1961-1990 (New et al., 1999). The run-off climatology covers different periods for different areas, varying with observer station-specific period of observation; the majority of observations are between 1961 and 1990 however (Fekete et al., 2000). Time-series are from 1986-1995 inclusive. (New et al., 1999; Fekete et al., 2000; Fekete et al., 2002). Plots are labelled with fitted line gradients (k_{run}; lines shown in green for global data and red (overall) and orange (individual months/years in (e, f, g)) for spatial data) and coefficients of correlation (R^2). k_{run} ranges from 0.028 to 0.031 for individual years in (e); 0.012 to 0.042 for individual months in (f); and 0.016 to 0.050 for individual months in (g). Corresponding R^2s range from 0.12 to 0.14 for (e); 0.02 to 0.15 for (f); and 0.04 to 0.15 for (g). R_0 and T_0 are means (averaged over time or space appropriately for each plot).

variable nature of the hydrological cycle in comparison to it's climatic mean, which is affected by temperature (Solomon et al., 2007). Using time-steps of the order of a day (as in GENIE) it can be assumed less likely to hold, as an extrapolation from the fact that there is even less of a correlation for monthly data than there is for annual time-series data (see Fig. 20: (f) vs. (d) and (g) vs. (e)). Ideally, it would be useful to look at time-series at daily resolution, i.e. similar to the model time-step; however, these are not available for global gridded runoff (Global Runoff Data Center, 2010, personal communication).

When looking at at a spatially explicit correlation between T and R, there is largely no significant correlation at all in real world data. This is shown in Fig 21. R^2s of above 0.5 only occur in a few scattered places, notably Western Europe, the Middle East, South and East Asia, middle South America.

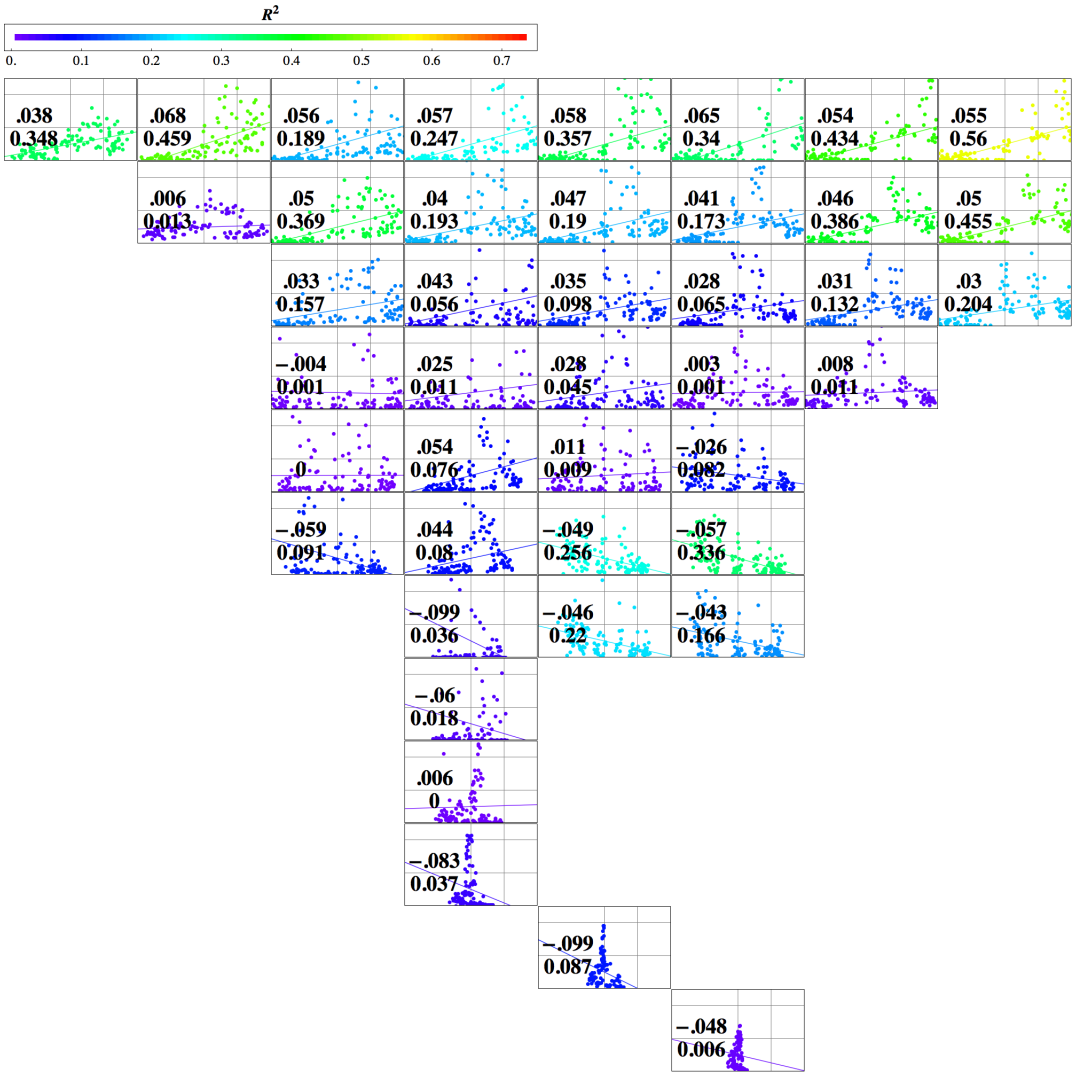

(a) North America

Figure 21: Runoff (y-axes show relative scale of R/R_0; gridlines are 2 and 4) vs. Temperature (x-axes show T-T_0 in °K; gridlines are 0 and 10) for spatial monthly average data, shown on 36x36 GENIE grid (continents in 6 separate sub-figures (a)-(f)), for individual months from 1986 to 1995 inclusive (Fekete et al., 2000) (Fekete et al., 2002). The fitted lines have gradients given by the first number shown on each plot, with a R^2 correlation given by the second number. For each cell, R_0 and T_0 are taken as mean values.

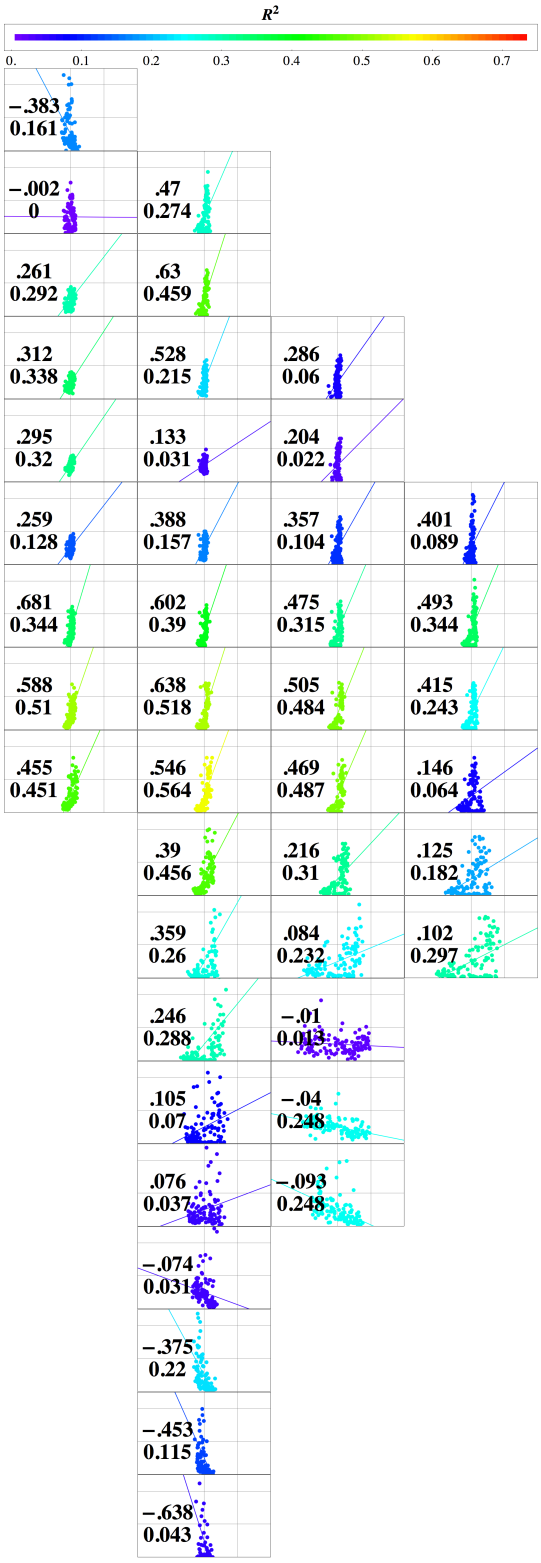

(b) South America

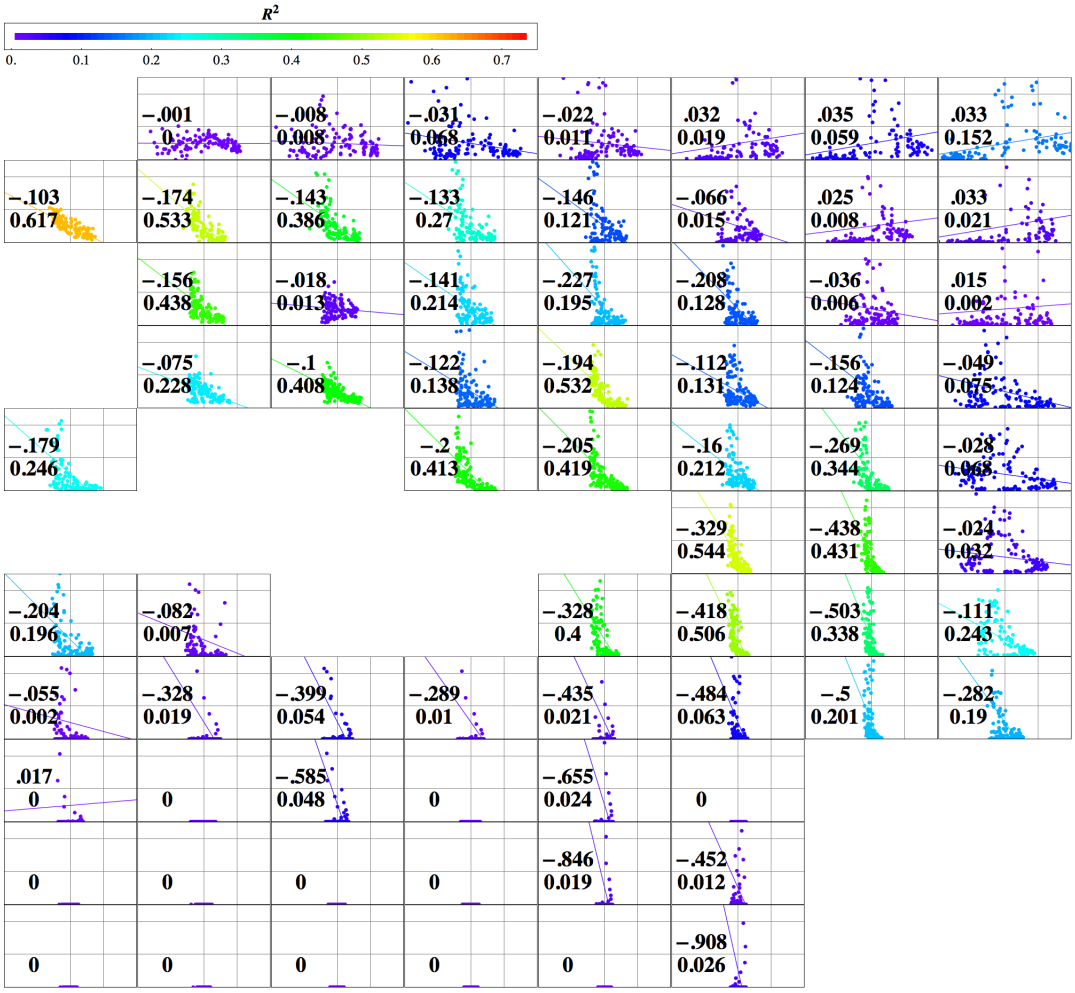

(c) Europe and North Africa

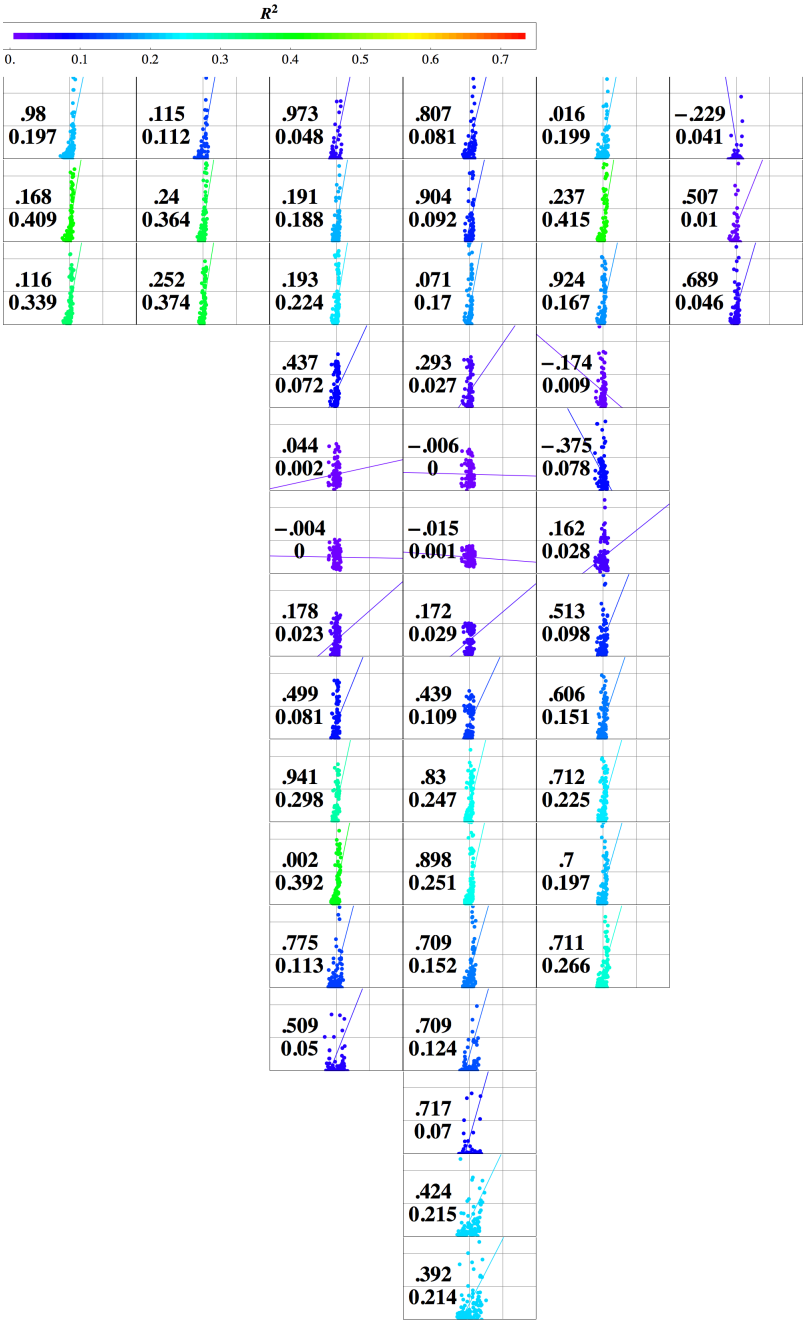

(d) Sub-Saharan Africa

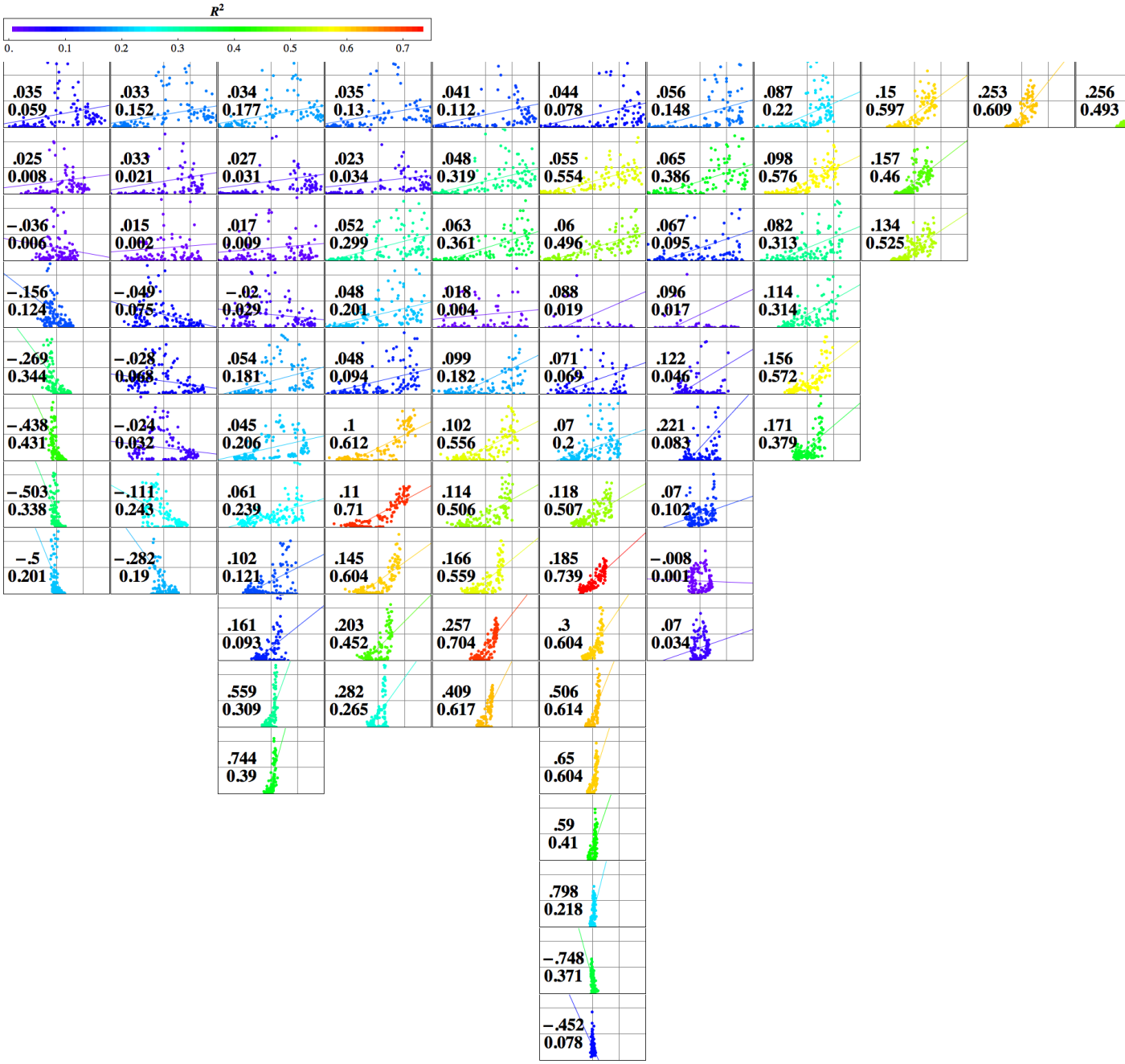
R^2
0. 0.1 0.2 0.3 0.4 0.5 0.6 0.7
.035 0.059
.033 0.152
.034 0.177
.035 0.13
.041 0.112
.044 0.078
.056 0.148
.087 0.22
.15 0.597
.253 0.609
.256 0.493
.025 0.008
.033 0.021
.027 0.031
.023 0.034
.048 0.319
.055 0.554
.065 0.386
.098 0.576
.157 0.46
−.036 0.006
.015 0.002
.017 0.009
.052 0.299
.063 0.361
.06 0.496
.067 0.095
.082 0.313
.134 0.525
−.156 0.124
−.049 0.075
−.02 0.029
.048 0.201
.018 0.004
.088 0.019
.096 0.017
.114 0.314
−.269 0.344
−.028 0.068
.054 0.181
.048 0.094
.099 0.182
.071 0.069
.122 0.046
.156 0.572
−.438 0.431
−.024 0.032
.045 0.206
.1 0.612
.102 0.556
.07 0.2
.221 0.083
.171 0.379
−.503 0.338
−.111 0.243
.061 0.239
.11 0.71
.114 0.506
.118 0.507
.07 0.102
−.5 0.201
−.282 0.19
.102 0.121
.145 0.604
.166 0.559
.185 0.739
−.008 0.001
.161 0.093
.203 0.452
.257 0.704
.3 0.604
.07 0.034
.559 0.309
.282 0.265
.409 0.617
.506 0.614
.744 0.39
.65 0.604
.59 0.41
.798 0.218
−.748 0.371
−.452 0.078

(e) Asia

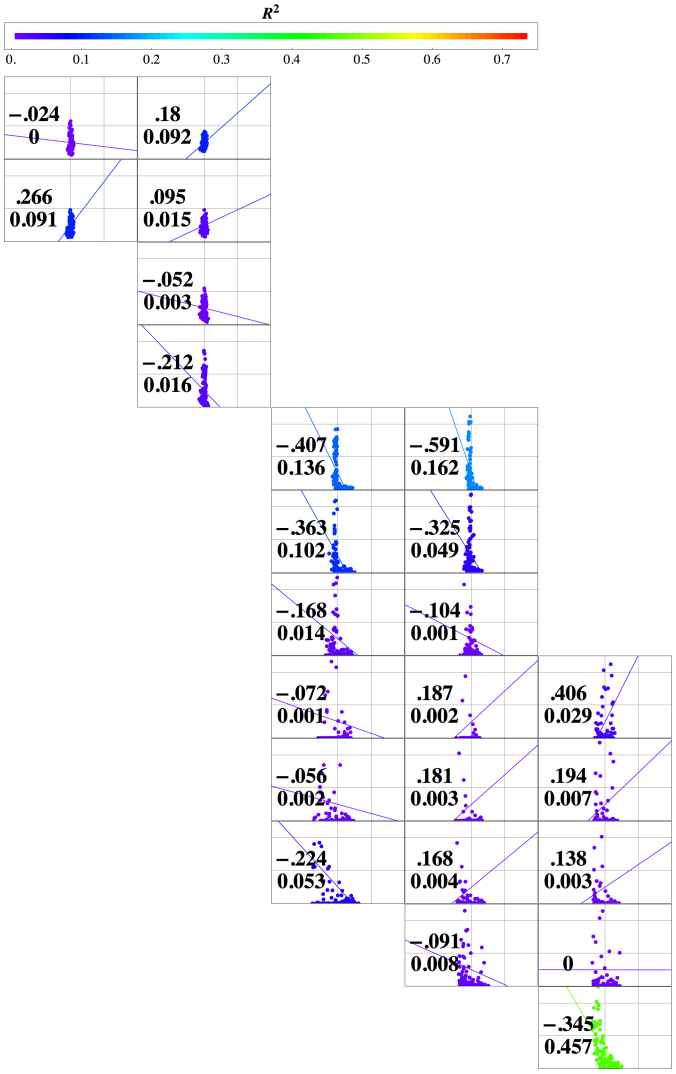

(f) Australasia

Initially, one might think this lack of correlation between T and R would not be too great a problem for the model, as runoff could just be made explicit by using equations 18 and 19. However, reproducing realistic runoff is a challenge for models of as coarse and intermediate complexity a resolution as GENIE, as illustrated in §2.5.2.

Attempts were made to fit non-linear functions (polynomial, exponential, sinusoidal; not shown) to the data, but none of these yielded an R^2 of greater than 0.5. This is expected, given the wide scatter (as shown in Fig. 20). It is interesting to note that there appears to be a secondary peak in runoff at lower temperatures. This is likely down to increased runoff on hardened frozen ground.

Another idea is to parameterise R as a function of precipitation, p, but there is very little correlation here either. See Fig 22. The R^2 is 0.05 for the fitted line.

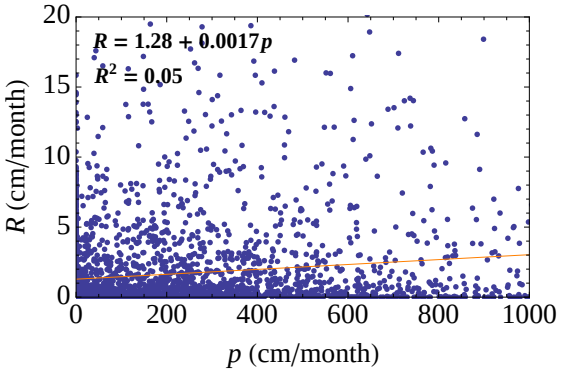

Figure 22: Runoff (R) vs. precipitation (p), for spatial monthly average real-world data on GENIE 36x36 grid. The equation of the fitted line (orange) and it's R^2 correlation are shown on the plot.

So, to answer the question posed: does runoff depend on temperature? Only very loosely and inconsistently. This poses a major problem for the accuracy of the results given by the weathering model when also considering the additional fact that explicit modelling of runoff is difficult (§2.5.2).

3.5 Productivity dependence of weathering

Following Lenton and Britton (2006), weathering fluxes are given an optional (arbitrary) linear dependence on land plant/biosphere productivity (P):

$$(F_{CaCO_3}, F_{CaSiO_3}) = (F_{CaCO_3,0}, F_{CaSiO_3,0})\frac{P}{P_0} \tag{21}$$

Productivity can be measured as either Net or Gross Primary Productivity (NPP or GPP), taken explicitly from a coupled land vegetation scheme such as ENTS. Alternatively, productivity can be parameterised as a function of pCO_2 following the approach of Berner (Berner, 1991):

$$\frac{P}{P_0} = \left(2\frac{C}{C_0}/\left(1+\frac{C}{C_0}\right)\right)^{0.4} \tag{22}$$

where C is atmospheric pCO_2. This is an expression of the fertilisation effect of CO_2 on land plants.

The effect of the productivity feedback is shown in Figure 23. As with the runoff feedback, there is a significant effect only when the emissions pulse is large (5000GtC). Again, the effect is significantly smaller than that due to temperature feedbacks, the range in pCO_2 between the strongest productivity feedback and no feedback being 47ppm 100kyr after a 5000GtC emission, compared with 81ppm for temperature feedbacks.

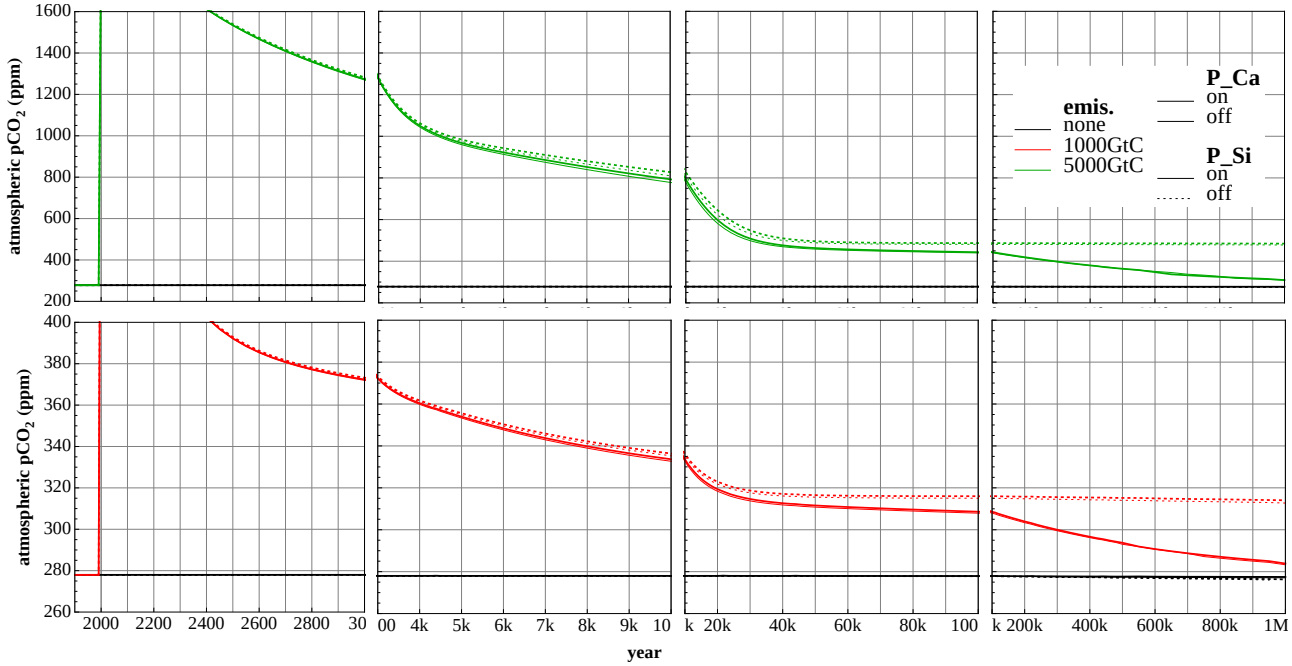

Figure 23: Evolution of atmospheric CO_2 over 1Myr for 1000GtC (red) and 5000GtC (green) emissions pulses, vs. a control run with no emissions (black), with carbonate and silicate weathering-productivity feedbacks (P_Ca and P_Si respectively) on/off [currently no explicit/implicit (P_explicit) - waiting for ENTS results].

3.6 River routing

Weathering fluxes are routed to the coastal ocean using Simulated Topological Network (STN) data (Vörösmarty et al., 2000a,b) and/or simple continental "roof" routing based on average altitude for each land grid cell. There are three routing schemes available.

The first is simple roof routing (using the average altitude of each land grid cell). Here, land grid cells are marked with numbers corresponding to the four cardinal directions (N, S, E, W), and a path is followed from each land cell to a coastal ocean cell.

The second uses the detailed STN routing data, which is similarly marked, but with the addition of the intercardinal directions (NE, NW, SW, SE). Roof data is used for runoff that ends in grid cells that are designated as land on the GENIE grid; this is about half, as due to the low resolution of the GENIE grid - 36x36 cells for the whole globe - coastal land cells can typically cover areas that are half ocean in the much higher resolution grid of the STN data - 0.5°x0.5°. The higher resolution of the STN data, means that for each GENIE land grid cell, water is routed to a number of different coastal ocean cells. A table containing a line for each GENIE land cell was produced; each line lists destination cells and the corresponding fraction of the starting land cell's water that goes to each of them. This table is read in by the RokGeM model, and used to route weathering fluxes from land to ocean.

The third routing scheme only uses the STN data, ignoring runoff that ends inside GENIE land grid cells.

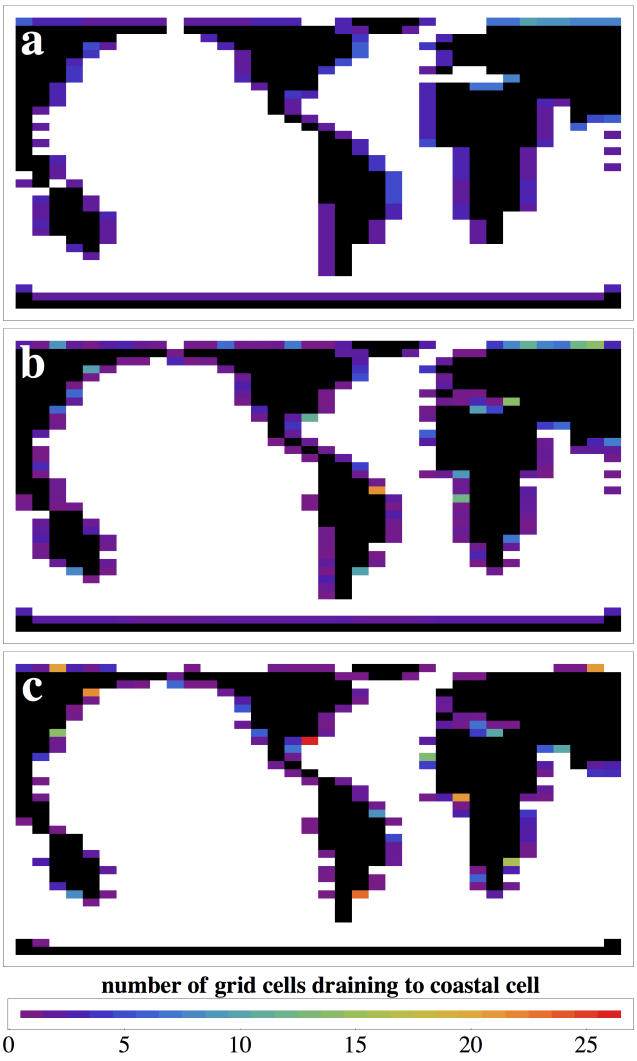

Figure 24: River drainage to the coastal ocean. Using 3 different schemes: a. 'roof' routing only (scheme 1); b. detailed topographical routing and roof routing (scheme 2); c. detailed topographical routing only (scheme 3). See text for explanation.

For both schemes 2 and 3, coastal ocean runoff flux is scaled relative to the total land area, so that runoff flux is conserved. For scheme 2 this factors in endorheic runoff (flux that drains to inland seas and doesn't make it to the global ocean; mainly in central Asia, Africa and Australia - some 18% of the land surface is covered by endorheic basins (Vörösmarty et al., 2000a,b)); for scheme 3 the scaling takes account of both endorheic runoff and the flux ending up in coastal land cells that is dealt with using the roof routing in scheme 2.

Figure 24 shows the distribution of coastal ocean flux for each of the 3 routing schemes assuming constant runoff across the land surface. Scheme 3 - being solely based on the STN data - shows the most realistic distribution. One can clearly see the mouths of some of the world's major rivers, including the Mississippi, the Congo, and the Nile. The Amazon is less pronounced in Scheme 3, although is prominent in Scheme 2.

When comparing the different schemes (Figure 25) one notices little difference to results using schemes 1 and 2, but some difference using scheme 3. This can partly be attributed to the fact that Antarctica isn't included in the STN runoff routing data, whereas it is in the simple roof routing. At first sight it would seem sensible not to include Antarctica as there is no significant river drainage contributing to fluxes of weathered minerals reaching the ocean. However, there is still weathering happening on Antarctica, albeit it bacteria-mediated and sub-glacial (Sharp et al., 1999). This only applies to the simple global average weathering rather than the explicit 2D schemes (see below) as there is no weathering contribution from ice covered areas in the latter.

Something inexplicable seems to go wrong with routing scheme 3; a bug yet to be understood. For this reason, scheme 2 is used as a default.

For the 2D weathering schemes, land lithological data (Amiotte-Suchet et al., 2003; Gibbs et al., 1999) from a 1° resolution map was placed onto the lower resolution GENIE grid, this meant that some land ended up in

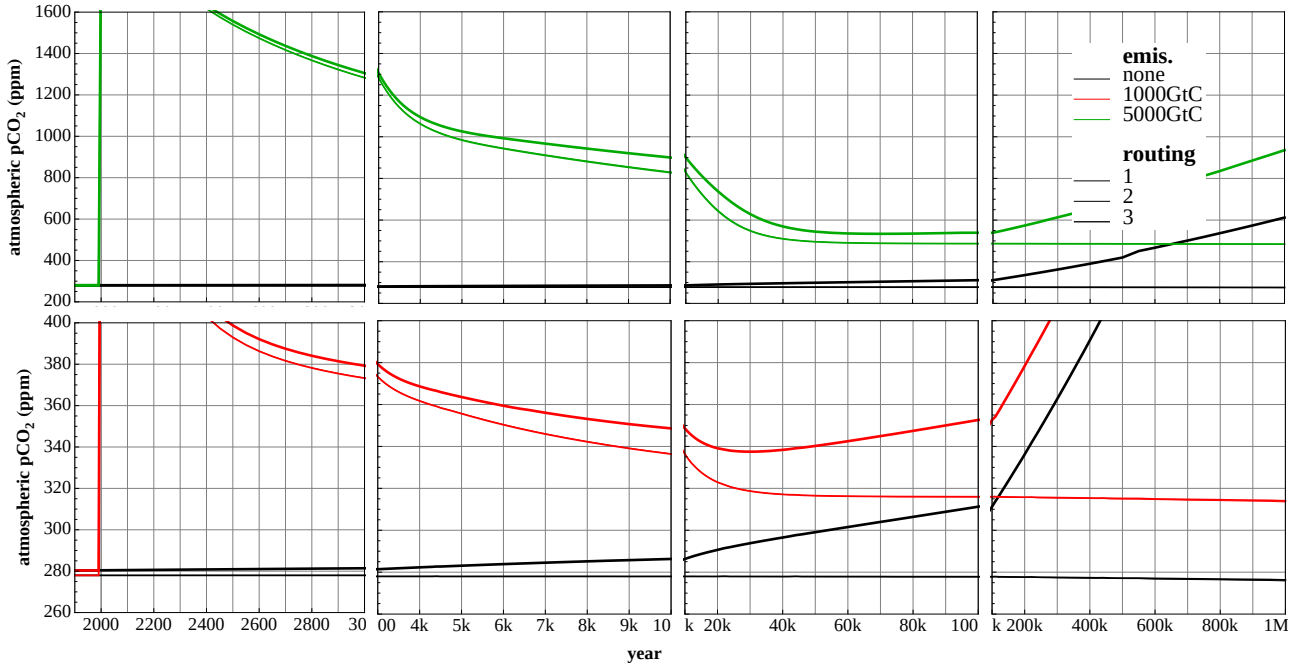

Figure 25: Evolution of atmospheric CO_2 over 1Myr for 1000GtC (red) and 5000GtC (green) emissions pulses, vs. a control run with no emissions (black), for different river routing schemes; schemes 1 and 2 (roof and STN/roof - see text for details) overlap in the thinner line, scheme 3 (STN only) is the thicker line.

the GENIE ocean. This was ignored (resultant weathering fluxes were "truncated" to the GENIE land grid) on account of it not being possible to get accurate values of T, R and P (which weathering fluxes depend on) in the ocean grid cells of the model.

It should be noted that the timescales over which the global ocean mixes are relatively short when compared to those over which the weathering-climate feedbacks operate. This negates the need for high fidelity in the river routing of weathered mineral fluxes.

3.7 Runoff dependence of weathering (2D schemes)

3.7.1 The Global Erosion Model for CO_2 fluxes (GEM-CO2)

The Global Erosion Model for CO_2 fluxes (GEM-CO2) (Amiotte Suchet and Probst, 1995) is based on an empirical linear relationship between the flux of atmospheric/soil CO2 from chemical weathering, and run-off. Subsequent work by the same team (Amiotte-Suchet et al., 2003) dividing the land-surface of the Earth into six different rock types, each with a different rate of weathering, is used as a basis for constructing a spatially explicit model. The types of rock, with their rates of weathering are shown in Table 4. The fractions of each rock type given to weather as either carbonate or silicate rocks is shown, following Gibbs et al. (1999); note that shale and sands and sandstones contain significant amounts of carbonate rock. The global lithological map was placed onto the GENIE-1 grid of 36x36 equal area longitude-sine(latitude) cells. Each grid cell was assigned a value for each rock type (and also water and ice) corresponding to the amount of that rock type present in it. The values for all rock types, water and ice were normalised to sum to 1 for each grid cell. Figure 27 shows the re-gridding.

3.7.2 The Gibbs and Kump Weathering Model (GKWM)

The Gibbs and Kump Weathering Model (GKWM) (Bluth and Kump, 1994; Gibbs and Kump, 1994; Gibbs et al., 1999) is similar to GEM-CO2, but with the run-off dependence modulated by a lithology-dependent fractional power β as well as a linear coefficient k (Equation 23). There are also only five rock types; for the purposes of using the same lithological data (Amiotte-Suchet et al., 2003), the granite class is counted as the sum of the shield and acid-volcanic classes from GEM-CO2. Gibbs and Kump also produced a global lithological dataset, which can be used in lieu of the GEM-CO2 dataset in RokGeM (see Figure 27 (b, l-t)).

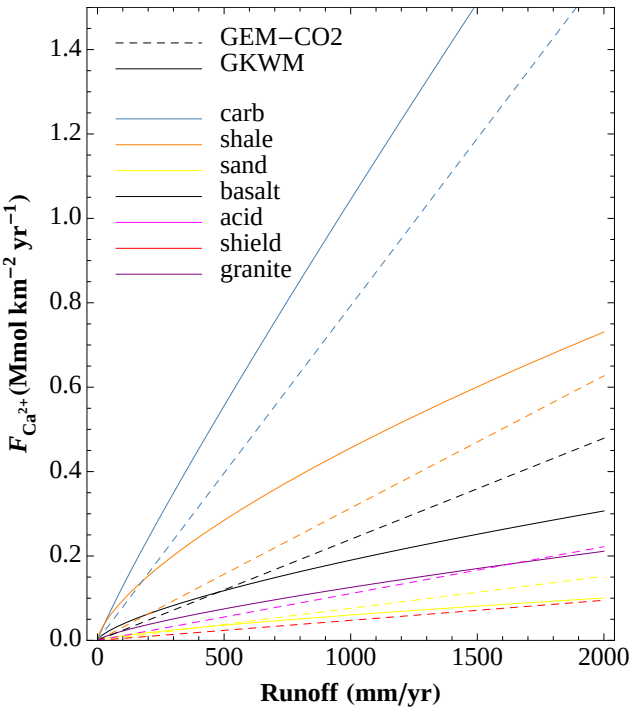

Figure 26: Runoff dependence of weathering for different rock types, in GEM-CO2 (dashed lines) and GKWM (solid lines) (Eq. 23).

3.7.3 Visualising the functions

The run-off dependencies of weathering flux are described by Equation 23 and Table 4 for each of the 2D schemes, where $F_{Ca^{2+}}$ is the weathered flux of Ca^{2+} (Mmol/km^2/yr), R is runoff (mm/yr), and k and β are dimensionless constants; they are plotted in Figure 26. Note that the factor of $\frac{1}{2}$ comes from the fact that in the original papers the weathering flux is described as bicarbonate, whereas for the purposes of this study it is measured as Ca^{2+}. The functions (with the Globavg scheme for comparison) are illustrated along with the temperature feedback of Equations 14 and 16 in Figure 28. Despite their differing formulations, both of the 2D weathering schemes produce similar results.

$$F_{Ca^{2+}} = \tfrac{1}{2} k R^{\beta} \tag{23}$$

Lithology		frac. Ca	frac. Si	GEM-CO2		GKWM	
				$k/10^{-3}$	β	$k/10^{-3}$	β
Carbonate		0.93	0.07	1.586	1	3.890	0.91
Shale		0.39	0.61	0.627	1	8.318	0.68
Sands and Sandstones		0.48	0.52	0.152	1	0.724	0.74
Basalt		0	1	0.479	1	3.236	0.69
Granite	Shield	0	1	0.095	1	1.413	0.75
	Acid Volcanic	0	1	0.222	1		

Table 4: Constants for 2D weathering functions following the formula in Equation 23 with F in units of Mol and R in units of m/yr. Note: Shield and Acid lithologies are combined into Granite in GKWM.

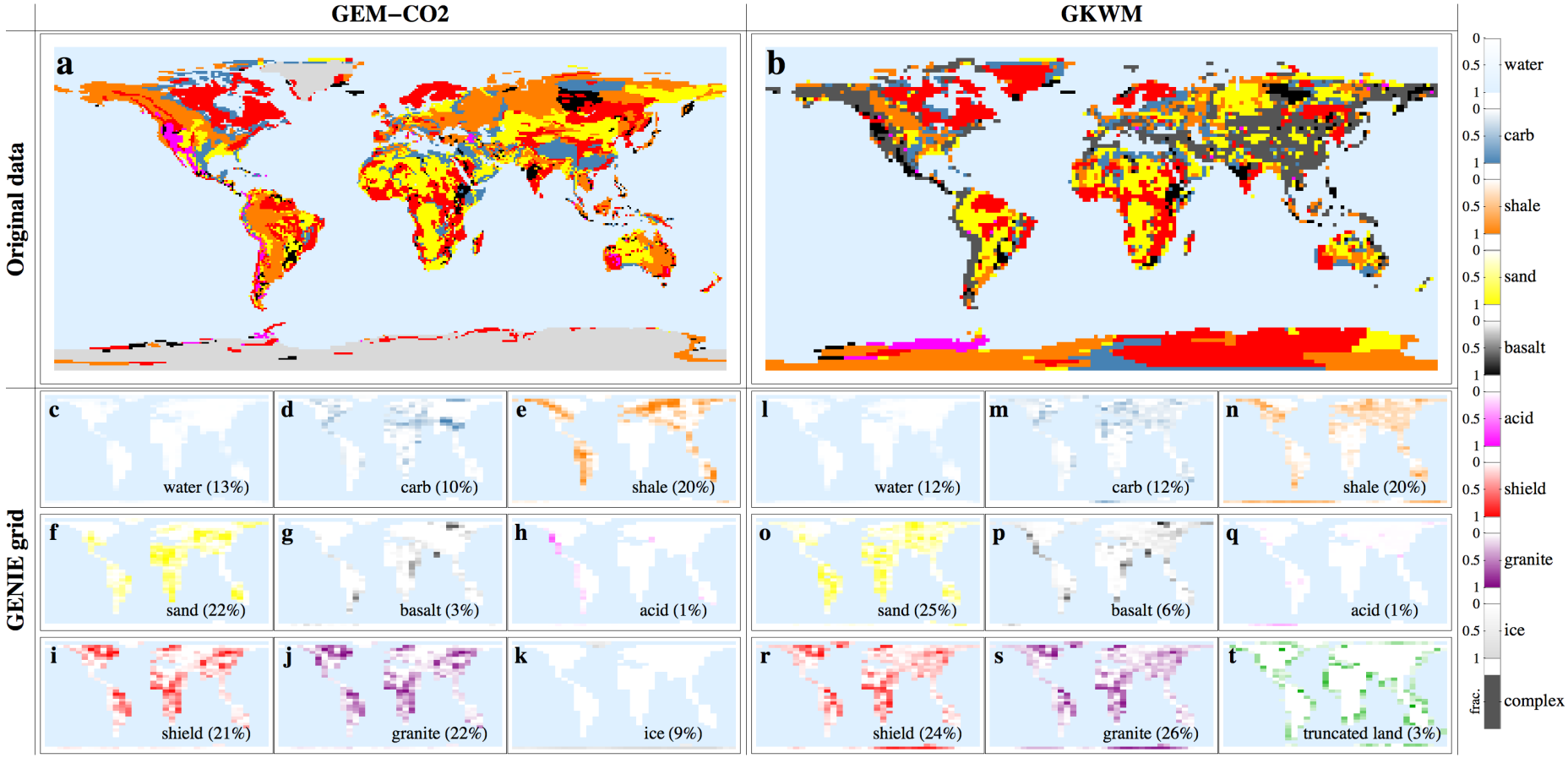

Figure 27: Distribution of lithologies from GEM-CO2 (Amiotte-Suchet et al., 2003) (a, c-k) and GKWM (Gibbs and Kump, 1994) (b, l-t); original source data is shown in the large panels (a, b; GEM-CO2 at 1° resolution and GKWM at 2° resolution); data interpolated onto the GENIE grid (36x36 equal area longitude-sine(latitude) cells) is shown in the smaller panels (c-t). Rock types are colour coded as in (Amiotte-Suchet et al., 2003). For the GENIE grid, each rock type fills a certain fraction of each cell; increasing fractions from 0 to 1 are shown by fading in colour from white (0) to full colour (1). For GKWM, a significant fraction of the land surface is designated "complex"; this signifies none of the main rock types being dominant; for the purposes of the weathering model here described, the complex class was divided into the others in the following fractions: carb=0.172, shale=0.330 sand=0.158, basalt=0.079, acid=0.017, shield=0.243, granite=0.260 (Cirbus Sloan et al., 1997). granite = acid + shield; granite is used in lieu of acid and shield for GKWM; it is not used in GEM-CO2. Note that due to imperfect grid-matching between the data sources and the model, some water appears on the GENIE land grid (c, l; this land does not contribute to weathering flux). Likewise does land appear in the GENIE ocean grid (t, similar for GEM-CO2 but 5%); this land is truncated and not used. After truncating data to the GENIE grid, values are calibrated by scaling to the total number of GENIE land cells.

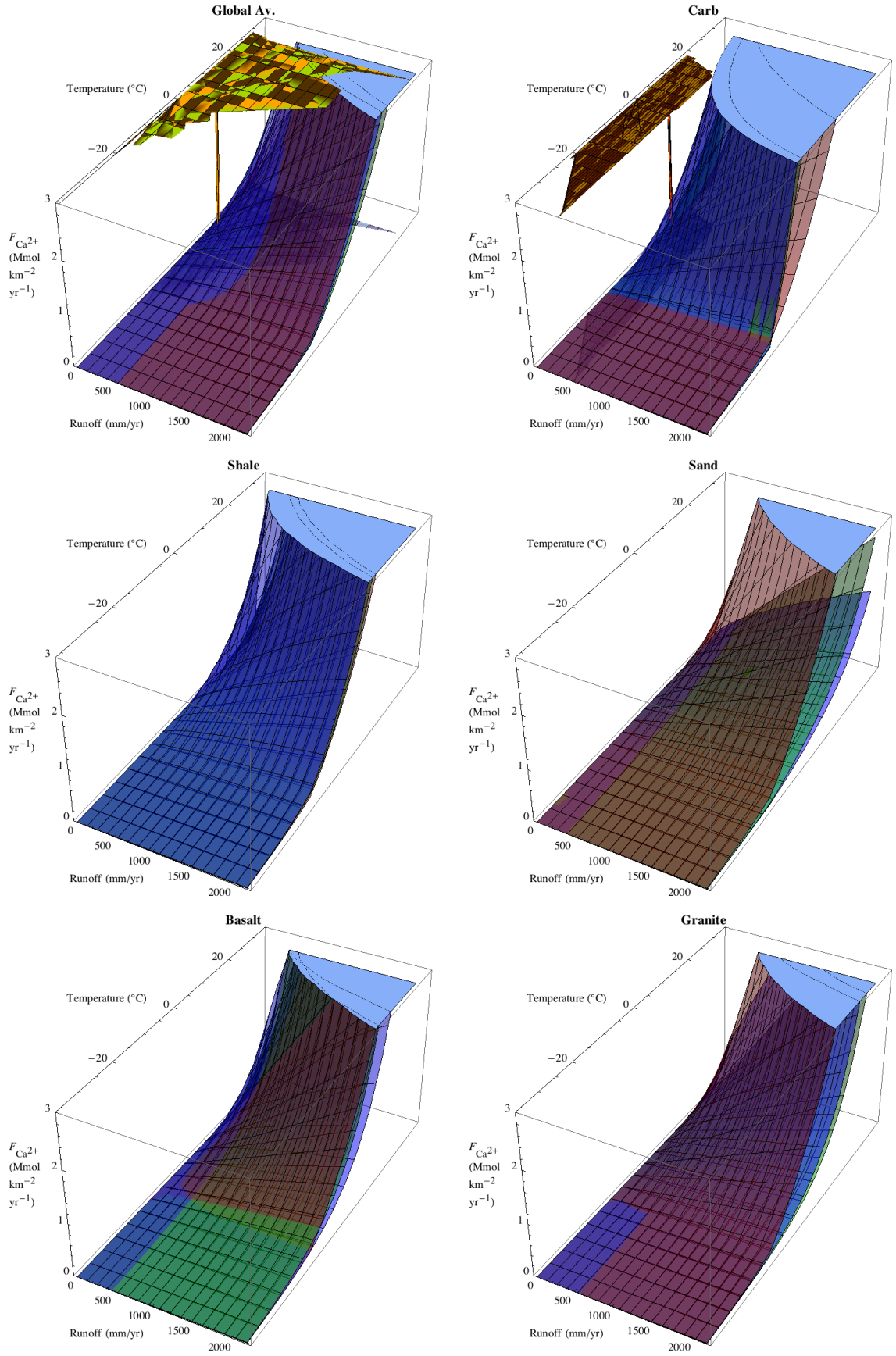

Figure 28: Weathering flux (Ca^{2+}) vs. temperature and run-off for different rock types and weathering schemes (Blue -GKWM, Green - GEM-CO2, Red - Globavg). "Global Av." means the weighted global average lithology, corresponding to 12.1% carbonate, 23.0% shale, 23.8% sandstone, 4.6% basalt, 24.9% shield, 2.0% acid volcanic and 9.7% ice cover. Overlayed on the Global Av. and Carb plots are temperature and runoff observational data (yellow; New et al. (1999); Fekete et al. (2002)) and model output (orange) from GENIE at a steady pre-industrial state after a spin-up (§2.4); global average values are shown as the vertical lines (note that the mottled textures are a plotting artefact).

Figure 29 shows the distribution of terrestrial weathering flux over the land and the ocean. Areas of highest flux are the Eastern side of the Americas in the tropical regions; West, East and South-East Africa; and South, East, and South-East Asia. Of the small differences that appear between the two different schemes (of order 10%), the greatest are in the same regions of high flux.

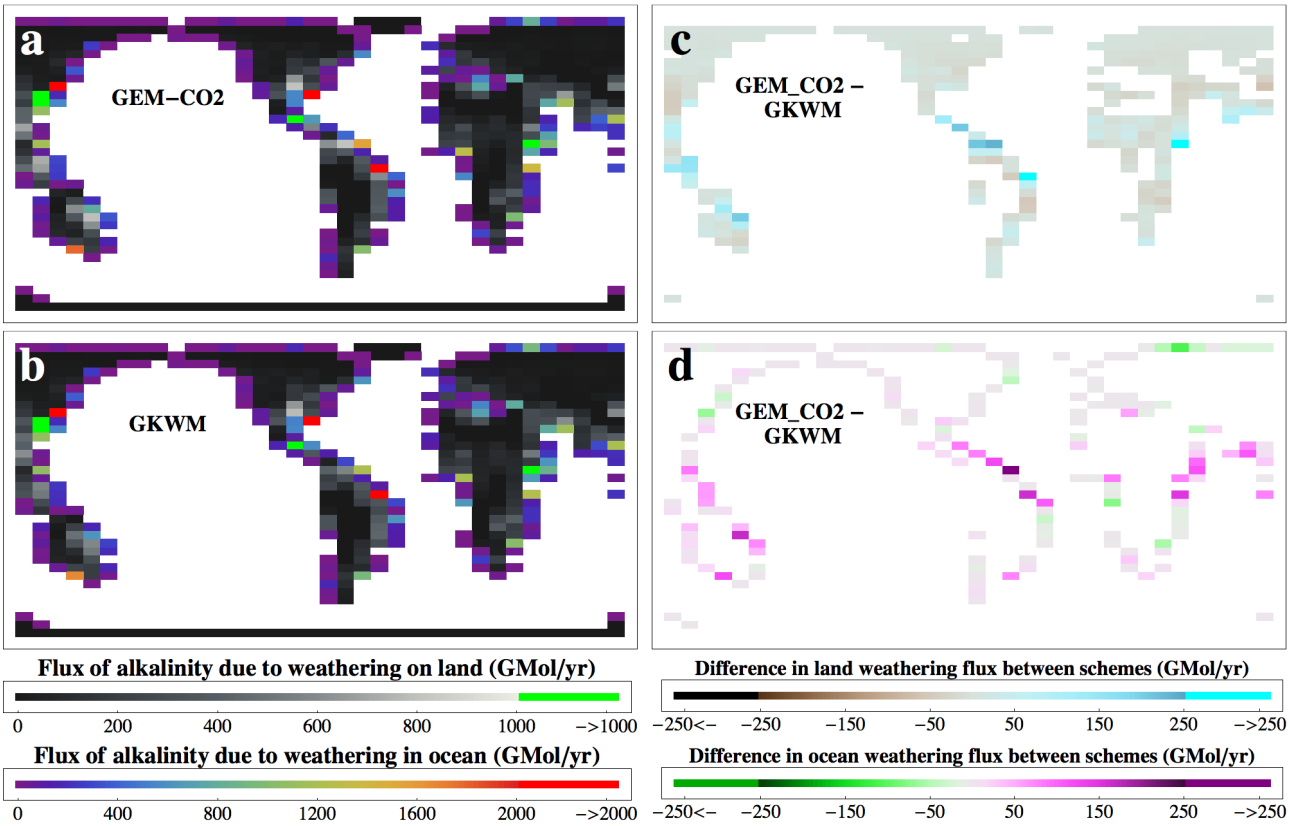

Figure 29: Distribution of weathering flux on land (grey-scale), and once routed to the coast, in the ocean (colour-scale) for a post-spin-up pre-industrial climate, for each of the 2D weathering schemes, GEM-CO2 (a) and GKWM (b). The GEM-CO2 lithological dataset is used. There is a small difference between the schemes, as shown in c (land weathering rate) and d (coastal input rate).

3.7.4 Sensitivity tests of 0D and 2D schemes

Comparing the spatially-explicit (2D) weathering schemes GKWM and GEM-CO2 with Globavg (0D) for the different weathering feedbacks, there is a noticeable difference when f_Si is switched on (Figure 30). Both of the 2D weathering schemes show similar results; 100kyr after a 5000GtC emissions pulse there is a 4ppm difference in atmospheric pCO_2 between the two, whereas there is a 20ppm difference between their mean and 0D Globavg (see Table 27). The 2D weathering schemes respond much faster than the 0D scheme largely on account of post-spin-up steady-state pre-industrial weathering fluxes being much greater for the 2D models (17.5 and 19.8 Tmol DIC $yr^{-}1$ for GKWM and GEM-CO2 respectively) than for the 0D model (11.7 Tmol DIC $yr^{-}1$; in this instance the 0D model starts with prescribed carbonate and silicate weathering fluxes that match the average of the 2D models, but when matched to sediment dissolution rates during spin-up (§2.4), these fluxes diminish to this lower value).

The largest difference between the 0D and 2D schemes in the 5000GtC emissions scenario occurs at year 5800 and is 113ppm. The difference is largest around this period because for the 0D scheme, the $CaCO_3$ sediments almost completely dissolve, whereas for the 2D schemes, due to a higher pre-industrial starting point, sediment dissolution does not become saturated (see Figure 52(d)). For the 1000GtC scenario, where the sediments do not come near to complete dissolution for either the 0D or 2D schemes, there is no pronounced peak in discrepancy between the two.

Runs not including f_Si show a smaller difference (Figure 31). Although the f_Ca-only runs show that f_Ca continues to act for the GKWM throughout the simulation, whereas the Globavg run levels off after ~50kyr.

With 2D weathering, the ocean carbonate system reaches different equilibria at spin-up to those of the 0D weathering model. Surface ocean pH varies by up to 0.018 units between the 0D and 2D schemes (Globavg = 8.149; GKWM = 8.163; GEM-CO2 = 8.167).

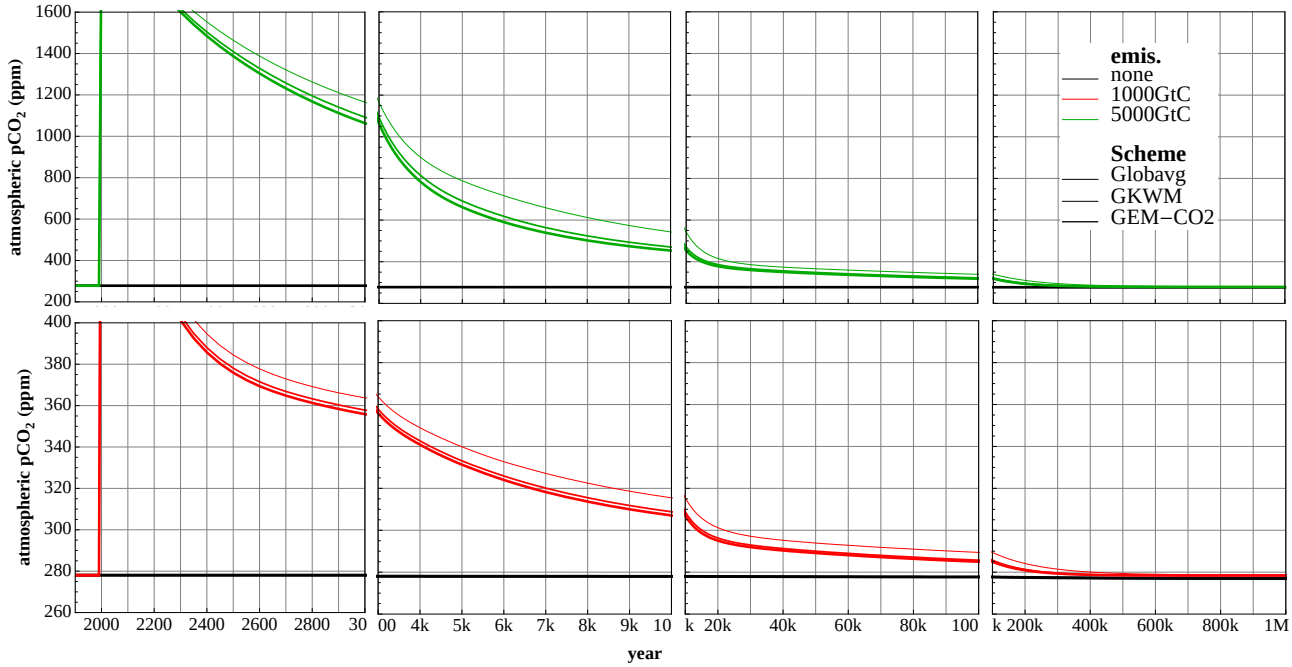

Figure 30: Evolution of atmospheric CO_2 over 1Myr for 1000GtC (red) and 5000GtC (green) emissions pulses, vs. a control run with no emissions (black), for different weathering schemes.

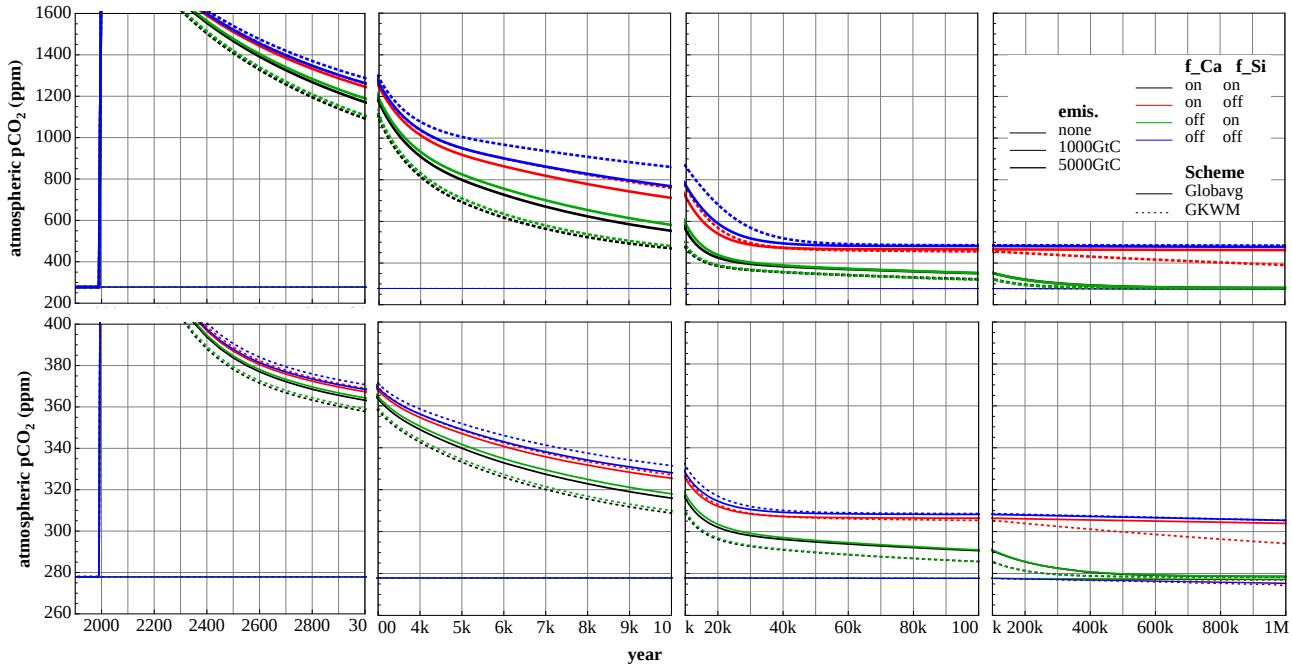

Figure 31: The effect of carbonate and silicate weathering feedbacks (f_Ca and f_Si respectively) on atmospheric CO_2 concentrations over 1Myr for a 5000GtC (red) emissions pulse for the 0D Globavg (thin lines) and 2D GKWM (thick lines) weathering schemes. A control run with no emissions is shown in black. Note the logarithmic time axis.

The distribution of ocean carbonate sediments is very different when the 2D weathering schemes are used, as shown in Figure 32. In general, more of the ocean floor is covered with $CaCO_3$ sediments, at a higher wt%; this is because the weathering flux of alkalinity into the ocean is greater for the 2D cases. At equilibrium, the global average is 13% higher than Globavg for GKWM, and 17% higher for GEM-CO2. For the 5000GtC emissions scenario, for the 0D Globavg case there is a near total dissolution of the sediments (Fig. 32(b) top geographic panels), this is in agreement with previous work using a box model (Archer, 2005); for the 2D cases on the other hand, a significant fraction (7.0 and 4.5 wt% for GKWM and GEM-CO2 respectively) of $CaCO_3$ sediment remains after dissolution ceases (Fig. 32(b) middle and bottom geographic panels).

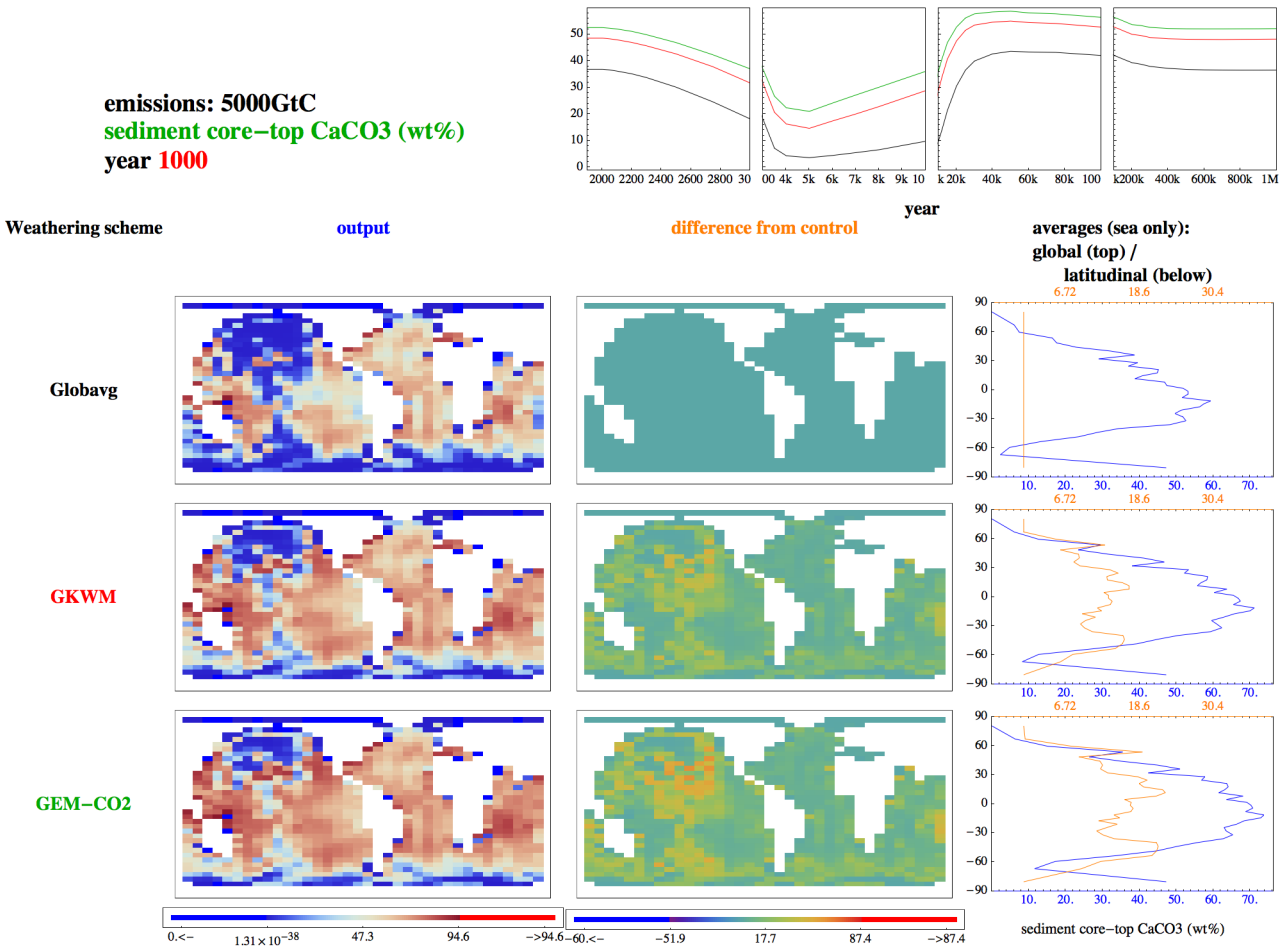

(a) year 1000: after spin-up, there is a noticeable difference between the sediments for runs with the 2D weathering schemes (GKWM and GEM_CO2) and 0D Globavg.

Figure 32: Spatial distribution of sedimentary $CaCO_3$ at selected years (left panels) for 0D (Globavg) and 2D (GKWM and GEM-CO2) weathering schemes, for a 5000GtC emission slug with both f_Ca and f_Si on; their differences from a control run with no emissions (middle panels); and their latitudinal averages (blue lines on right panels, differences from control shown in orange). Global average values are shown as a time-series at the top, with the lines colour coded to the text of the emissions (left), and a vertical line showing the year of the spatial plots. This figure is constructed from frames of an animation generated by the data-processing scripts described in Appendix B (the animation is in the accompanying digital media); it continues on the next page.

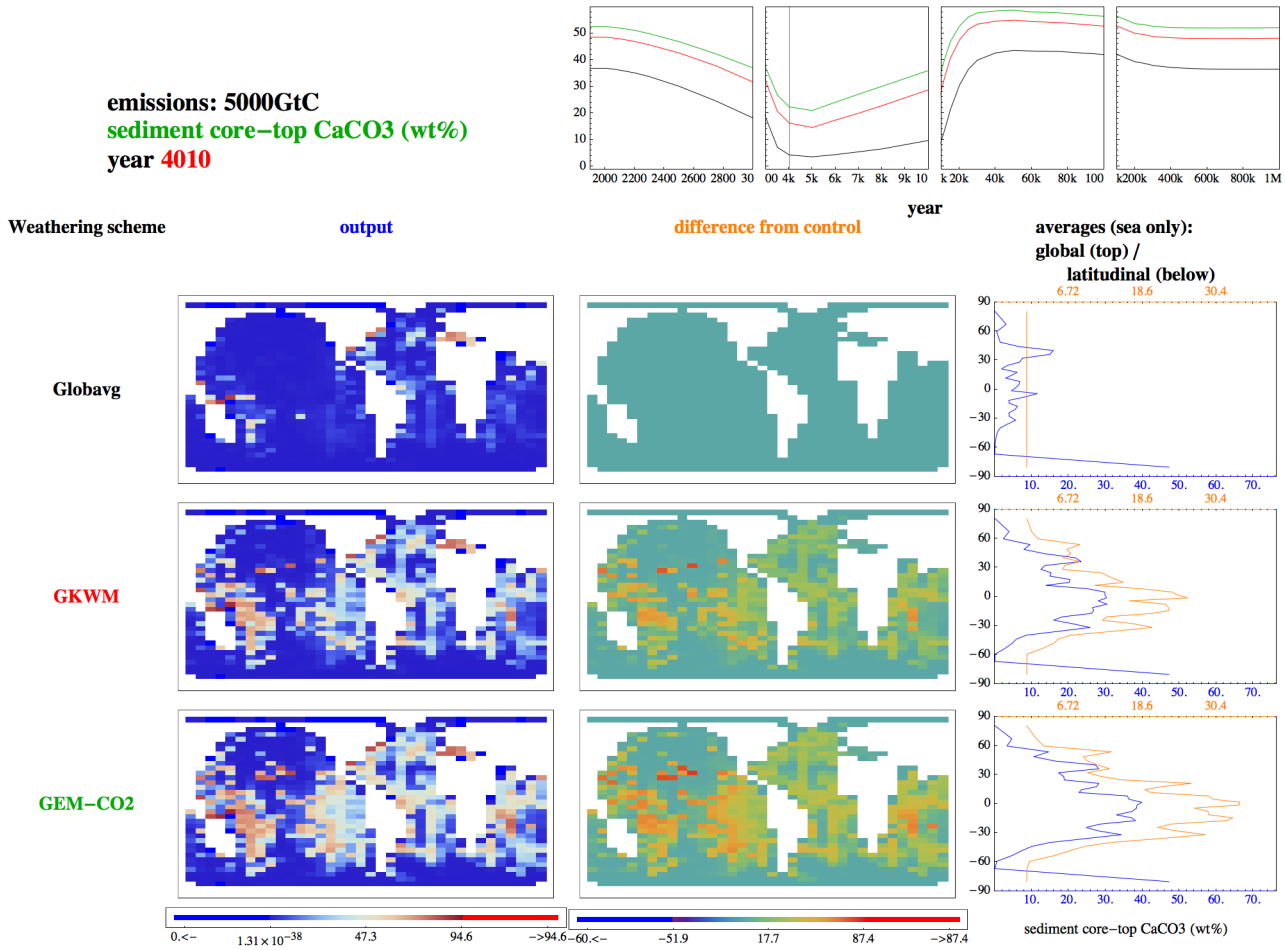

(b) year 4010: sedimentary core-top $CaCO_3$ reaches a minimum. For 0D Globavg there is near total dissolution, whereas for the 2D schemes there is a small persistent distribution of sediment. The minimum at year 4400 (not shown) sees Globavg with 3.4 wt% $CaCO_3$, GKWM with 14.1% and GEM-CO2 with 20.2%. Note that the year (and those in subsequent outputs) is not a round thousand on account of runs being divided up, and output being spurious for the first couple of model years at restarts.

3.8 Lithology dependence of weathering

As a test of sensitivity of the spatially explicit weathering in the model, different lithologies were tried using the GEM-CO2 weathering scheme. Data compiled by the teams behind GKWM (Gibbs et al., 1999) and GEM-CO2 (Amiotte-Suchet et al., 2003) were compared, along with their averages (where each grid cell contained an amount of each rock type equal to it's global average) and monolithic scenarios where the entire land surface was set to a single rock type.

Results are shown in Figure 33; for the individual lithologies, colours follow those in Fig. 27. There is little difference between the datasets of GKWM (the default; light green) and GEM-CO2 (grey line overlapping light green line). There is also little difference between the GKWM lithology and it's average (light green line vs. dark green line). However, there is a significant difference between GEM-CO2 and it's average (grey line vs. brown line).

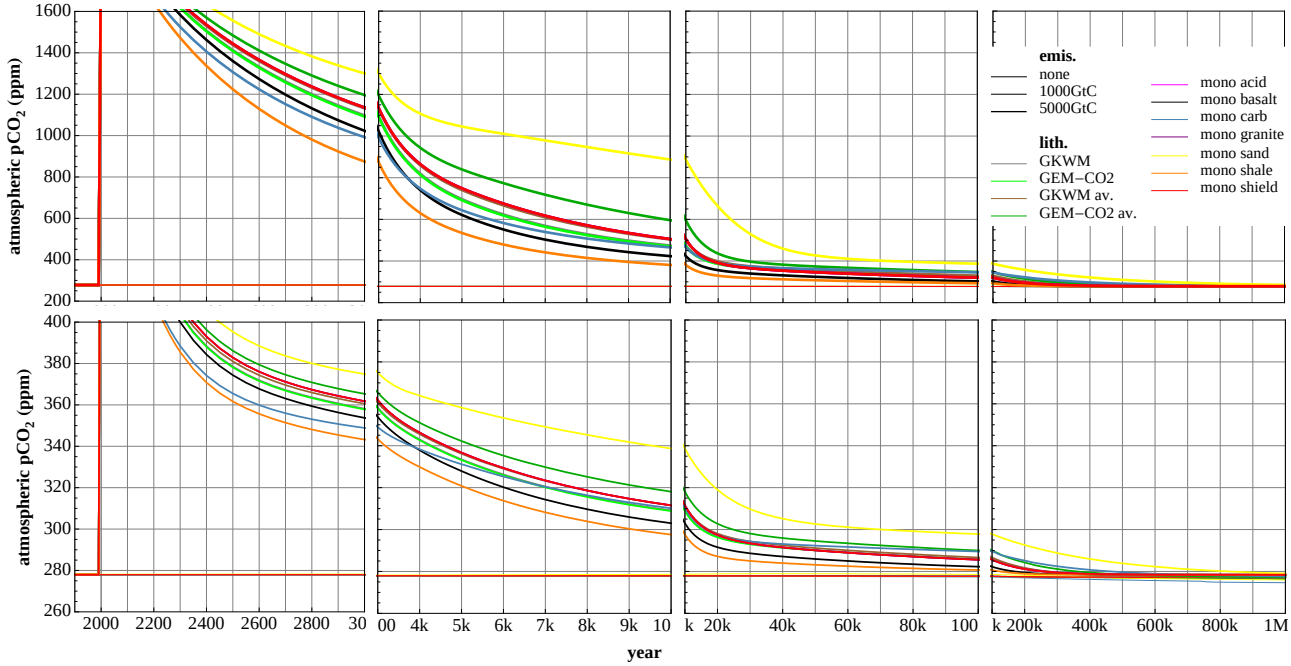

Figure 33: Evolution of atmospheric CO_2 over 1Myr for 1000GtC (medium lines) and 5000GtC (thick lines) emissions pulses, vs. a control run with no emissions (thin lines), for different lithologies using the GEM-CO2 weathering scheme.

There are very large differences between the monolithic end members; shale having the greatest effect, and sandstone the least on global weathering fluxes and hence drawdown of atmospheric pCO_2. The monolithic lithologies closest to reproducing the results of the full model are acid volcanic rock and granite, which closely follow the GKWM and GEM-CO2 full lithologies (the magenta and purple lines of the acid and granite members are in fact hidden underneath the green and grey lines of the GKWM and GEM-CO2 members). In the GEM-CO2 scheme used, granite is not a distinct lithology, and so it is made up of half acid volcanic rock, and half shield rock. The red line shows that a monolithic shield rock world weathers slower, so the granite world must be dominated by it's acid volcanic rock component. The carbonate only world (mono carbonate) weathers quickly to begin with, but then slows after the "terrestrial neutralisation" carbonate weathering-feedback phase. The full model (GKWM or GEM-CO2 lithologies; green and grey lines) overtakes the carbonate world (blue line) after year 14k, when the silicate weathering phase is dominant. This is on account of the carbonate end member containing only a small fraction (7%) of silicate rock.

3.9 Climate sensitivity dependence of weathering

By spinning the model-up in a multi-stage process, parameters affecting radiative forcing in the EMBM were adjusted so as to alter the climate sensitivity (°K of global warming for a doubling of atmospheric pCO_2) by specific amounts. As well as the default climate sensitivity of 2.64°K, climate sensitivities of 1.5, 3, 4.5, 6 and 10°K - covering the full range estimates as reported by the IPCC (Solomon et al., 2007) - were tested. The run with 10°K climate sensitivity was unstable and crashed (not shown). This high a climate sensitivity is ruled out by paleo-data reconstructions (Schneider von Deimling et al., 2006).

Results are shown in Fig. 34. For the 5000GtC emissions scenario, the variation between the middle climate sensitivities of 2.64 to 6°K is relatively small at 36ppm pCO_2 after 100kyr; the difference between 2.64 and 1.5 is equal to this again.

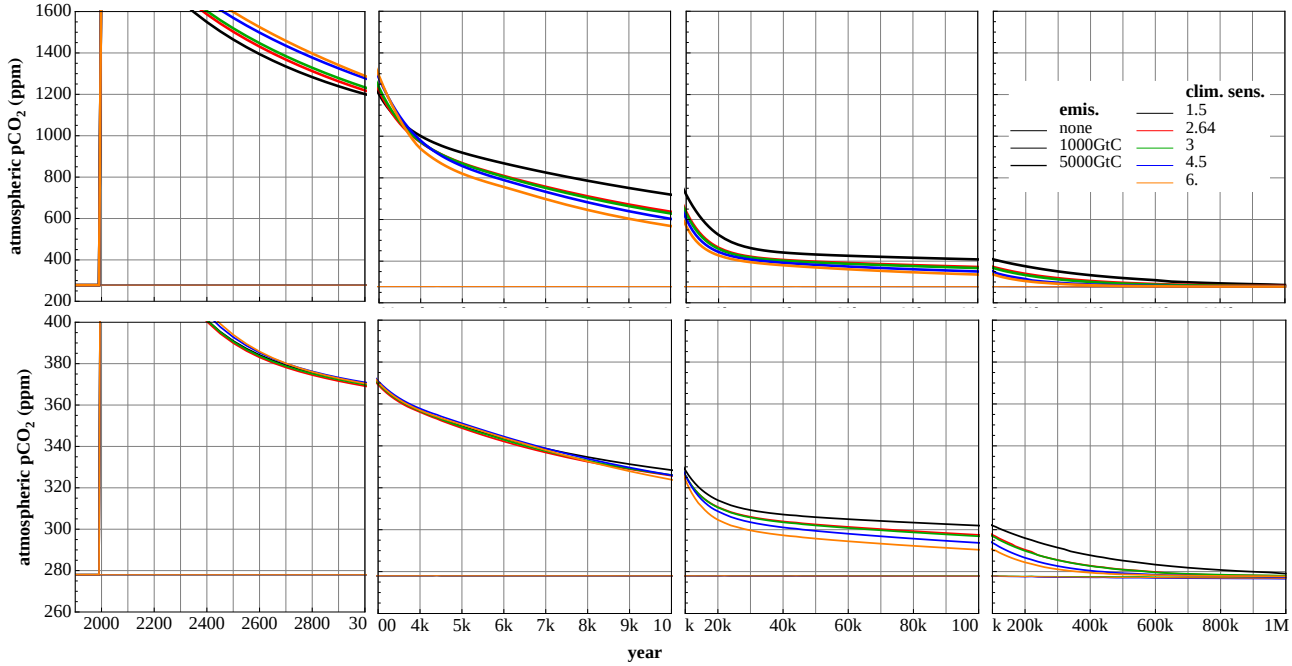

Figure 34: Evolution of atmospheric CO_2 over 1Myr for 1000GtC (red) and 5000GtC (green) emissions pulses, vs. a control run with no emissions (black), for different climate sensitivities.

It is interesting that climate sensitivity exerts less control on the millennial-scale carbon cycle than lithology (see above, §3.8). For the 5000GtC scenario, the range of atmospheric pCO_2 values at year 3000 for the lithology ensemble is 426ppm, whereas it is only 88ppm for the climate sensitivity ensemble. At year 10k it is 506 vs. 151ppm. However, the gap has almost completely closed at year 200k, with a range of 75ppm between the extremes of lithology (shield-shale), and 72ppm between the extremes of climate sensitivity (6-1.5°K). The long endurance of a high range in the climate sensitivity ensemble is largely on account of the lower climate sensitivities having a longer relaxation time than the higher ones. The lowest climate sensitivity (1.5°K) is still 7ppm above preindustrial pCO_2 at year 1M, in contrast to the highest (6°K), which reaches the pre-industrial level of 278ppm by year 850k (300ppm is reached by years 700k and 240k respectively for lowest and highest).

These figures are borne out by timescale analysis performed through fitting exponential curves to the atmospheric pCO_2 model output (see §4.2 and Table 31 in Appendix A). Looking at the 5000GtC scenario, the medium-term timescales associated with deep ocean mixing are lower for lower sensitivities (560±6yr for 1.5°K) and higher for higher sensitivities (860±30yr for 6°K). For higher climate sensitivities, the ocean takes longer to absorb the initial excess CO_2 on account of increases in fresh water flux from melting ice causing a decrease in ocean overturning (particularly in the Atlantic, where overturning shuts down for 2kyr). It is worth noting however, that the percentages of the pCO_2 perturbation sequestered over these medium-term timescales is higher for the higher climate sensitivities (55.0±0.6% for 6°K vs. 47.4±0.1% for 1.5°K).

The situation is reversed when it comes to the long-term timescales associated with carbonate and (especially) silicate weathering. Here, lower climate sensitivities give longer timescales; 9.06±0.09kyr (1.5°K), vs. 6.4±0.4kyr (6°K) for carbonate weathering, and 370±20kyr vs. 120±20kyr for silicate weathering. Higher climate sensitivities amplify perturbations in temperature, runoff and pCO_2, all of which in turn amplify the weathering feedbacks. These results are corroborated for the 1000GtC scenario, which has better fits, and more timescales identified. There is a slight confounding of this result though, in that there are timescales of 3.3-6.9kyr picked out (which are assumed to be associated with dissolution of the ocean sediments, and follow the same pattern as ocean mixing, with longer timescales for higher sensitivities), followed by longer timescales of 9.2-30kyr, which also follow the pattern of increasing with increasing climate sensitivity. This suggests that perhaps some of the third (i=3) timescales for the 5000GtC are from sediment dissolution, and some from carbonate weathering, and in fact the carbonate weathering timescales follow the opposite trend to the silicate ones, i.e. they increase with increasing climate sensitivity.

3.10 Summary of RokGeM model description

RokGeM calculates weathering fluxes of alkalinity and Dissolved Inorganic Carbon (DIC) dependent on, and in feedback with, inputs of land temperature (T), runoff (R) and productivity (P). Carbonate and silicate weathering fluxes of calcium ions (F_{CaCO3} and F_{CaSiO3} respectively) take the form:

$$F_{CaCO_3} = F_{CaCO_3,0}\left(1 + k_{Ca}\left(T - T_0\right)\right)\frac{R}{R_0}\frac{P}{P_0} \tag{24}$$

$$F_{CaSiO_3} = F_{CaSiO_3,0}e^{\frac{1000E_a}{RT_0^2}(T-T_0)}\left(\frac{R}{R_0}\right)^{\beta}\frac{P}{P_0} \tag{25}$$

where 0 denotes an initial value in the feedback ($\{T, R, P\} = \{T_0, R_0, P_0\}$ for switched off feedbacks), k_{Ca} is a constant, E_a the activation energy of the silicate weathering reaction, and β ($0 < \beta < 1$) is a fractional power dependent on lithology. For this thesis the model was run without being coupled to the ENTS land surface scheme. Thus productivity was parameterised as

$$\frac{P}{P_0} = \left(2\frac{C}{C_0}/\left(1 + \frac{C}{C_0}\right)\right)^{0.4} \tag{26}$$

where C is atmospheric pCO_2.

Fluxes are worked out as a global average for the basic 0D implementation of the model, and individually for each grid cell, for the spatially explicit 2D version of the model. In the latter 2D case, each grid cell is apportioned between 5 or 6 distinct lithology classes. Fluxes are routed to the coastal ocean, where they interact with ocean, atmosphere and sediment biogeochemical cycles.

4 Results

An in-depth look at some key results - looking at the operation of the carbonate and silicate weathering feedbacks - are now presented (§4.1), along with timescale analysis for depletion curves of key variables (excess global atmospheric pCO_2, surface warming and surface ocean acidification) (§4.2). Finally, the total ensemble of model runs performed is looked at (§4.3) and a most realistic parameter set chosen and examined (§4.4).

4.1 Carbonate and Silicate weathering feedbacks

Combining temperature, runoff and productivity feedbacks yields the following results. Here we take a more in-depth look at some 1Myr model runs, covering the presence or absence of the carbonate and silicate weathering feedbacks.

For each emissions pulse, it was found that pCO_2 declined relatively rapidly (over the course of a thousand years) initially (Figure 35(a)). This can be attributed to 'ocean invasion' of CO_2 and dissolution of sea-bed carbonate ($CaCO_3$) sediments. pCO_2 then declines more slowly due to the action of first carbonate, and then silicate, weathering feedbacks, referred to as f_Ca and f_Si respectively; these feedbacks include the temperature, runoff and productivity feedbacks described above in §3.2, §3.3 and §3.5.

Compared with a constant weathering flux, the carbonate weathering feedback has only a minimal effect in the long term when switched on; 50kyr after a 5000GtC release, there is only a 22ppm difference in CO_2 concentrations in the atmosphere. Sequestration effectively stops at this point for both constant weathering (carbonate and silicate weathering feedbacks off) and carbonate weathering feedback. The silicate weathering feedback has a more pronounced effect - a 95ppm difference over the same 50kyr time period. Eventually, with the action of the silicate weathering feedback, atmospheric pCO_2 is returned to pre-industrial levels, reaching 300ppm after 440kyr for the 5000GtC scenario (80kyr for 1000GtC). Interestingly, after 50kyr, when the carbonate weathering feedback has run its course, having the carbonate weathering feedback on slightly hinders the silicate weathering feedback; in the case of both carbonate and silicate weathering feedbacks being active, it takes 460kyr - 20kyr longer - to reach 300ppm pCO_2 in the 5000GtC scenario. The cause of this is likely the fact that the carbonate weathering feedback removes CO_2 from the atmosphere, thus leaving less for the stronger silicate weathering feedback to operate on: the silicate weathering feedback is weakened in the presence of the carbonate weathering feedback.

After 1Myr, pCO_2 is 278 and 281ppm respectively for 1000 and 5000GtC emission slugs (pre-industrial pCO_2 was taken to be 278ppm). Even on the millennial timescale, the weathering feedbacks are significant. For the 5000GtC scenario there is a 64ppm difference at year 3000 between having no feedbacks and having both carbonate and silicate weathering feedbacks (this represents 7% of the CO_2 in excess of the pre-industrial). All these figures, and more, are shown in the tables below.

The tables show, for the variables atmospheric CO_2 (Tables 5-8), global surface warming (Tables 9-12), and global surface ocean acidification (Tables 13-16), values (Tables 5, 9 and 13) and percentages remaining (Tables 6, 10 and 14) that are reached at specific years, and years that specific values (Tables 7, 11 and 15) and fractions (Tables 8, 12 and 16) are reached. Negative powers of e are included in the latter tables to allow the gauging of e-folding times (note that $e^{-1}\approx37\%$; $e^{-2}\approx14\%$; $e^{-3}\approx5\%$, $e^{-4}\approx2\%$; and $e^{-5}\approx0.7\%$). The three variables are chosen as they are most defining of the problem of anthropogenic interference in the global carbon cycle. International policy is focused on reductions in atmospheric pCO_2, and their effects on limiting global warming, and ocean acidification.

The airborne fraction of excess pCO_2 (remaining) reaches 50% by the mid 23rd century in the 1000GtC emissions case; this milestone is not reached for a further 650 (carbonate and silicate weathering feedbacks on) to 850 (carbonate and silicate weathering feedbacks off) years for the 5000GtC scenario. Percentages of atmospheric pCO_2, global surface warming, and ocean acidification in excess of pre-industrial levels are plotted up to year 1M in Figure 36. It should be noted that due to the pulse form of emissions here, initial spikes in the values of the variables in question lead to an underestimation of fractions remaining when compared with more realistic scenarios, where emissions are drawn out over decades to centuries. Even so, the difference in shape between the emissions scenarios is substantial, with the larger 5000GtC emissions leading to a steeper initial decline in fractions of excess CO_2, warming and acidification that remain. It should also be noted that discussing temperatures and pHs in terms of fractions (or percentages), is not strictly-speaking meaningful, on account of both being measured on logarithmic scales. These variables are included in the tables below (9–16) and Figure 36 for the sake of allowing rough comparisons with similar figures for pCO_2, and to observe similarities and differences in the shapes and features of the curves.

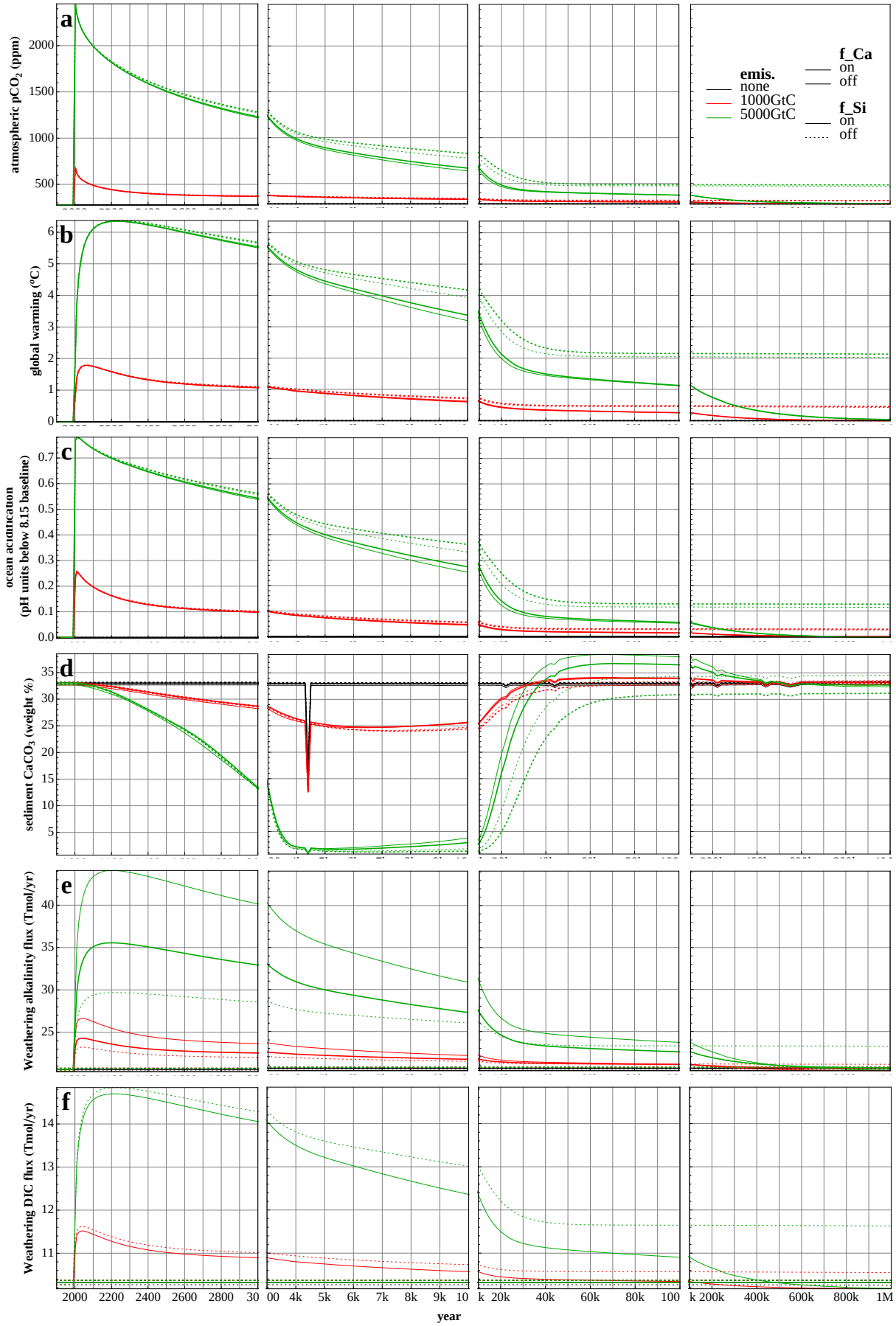

Figure 35: Evolution of (a) atmospheric pCO_2, (b) global surface warming, (c) surface ocean acidification, (d) sea-floor sedimentary carbonates, and weathering ALK (e) and DIC (f) fluxes over 1Myr for 1000GtC (red) and 5000GtC (green) emissions pulses, vs. a control run with no emissions (black), with carbonate and silicate weathering feedbacks (f_Ca and f_Si respectively) on/off. Note that the blips in sediment $CaCO_3$ are an artefact of the model restart process (model runs were restarted every 4.4kyr) caused by the sediments taking a few years to "warm up" and output being taken during this time.

Table 5: **Atmospheric pCO_2** (ppm) reached at specific calendar years

variables			**year**								
emis.	f_Ca	f_Si	3000	5000	10000	20000	50000	100k	200k	500k	1000k
1000GtC	on	on	369	348	326	311	302	298	291	281	278
1000GtC	on	off	372	354	334	320	314	314	314	313	311
1000GtC	off	on	370	350	328	312	303	298	291	281	278
1000GtC	off	off	373	356	336	323	317	316	316	315	314
5000GtC	on	on	1219	870	637	465	398	372	339	296	281
5000GtC	on	off	1269	957	776	583	478	474	473	472	470
5000GtC	off	on	1231	890	668	483	401	373	338	295	280
5000GtC	off	off	1283	984	828	642	496	487	487	486	484

Table 6: **Percentages** of remaining excess **Atmospheric pCO_2** reached at specific calendar years

variables			**year**								
emis.	f_Ca	f_Si	3000	5000	10000	20000	50000	100k	200k	500k	1000k
1000GtC	on	on	22.6	17.5	11.9	8.2	6.1	4.9	3.1	0.8	-0.0
1000GtC	on	off	23.4	18.9	13.9	10.5	9.0	8.9	8.8	8.7	8.3
1000GtC	off	on	22.9	17.9	12.3	8.6	6.3	5.0	3.1	0.7	-0.1
1000GtC	off	off	23.7	19.3	14.5	11.2	9.6	9.4	9.4	9.2	9.0
5000GtC	on	on	43.3	27.2	16.5	8.6	5.5	4.3	2.8	0.8	0.1
5000GtC	on	off	45.6	31.2	22.9	14.0	9.2	9.0	9.0	8.9	8.8
5000GtC	off	on	43.8	28.2	17.9	9.4	5.7	4.4	2.8	0.8	0.1
5000GtC	off	off	46.2	32.5	25.3	16.7	10.0	9.6	9.6	9.6	9.5

Table 7: **Years** that specific values of **Atmospheric pCO_2** are reached

variables			**Atmospheric pCO_2 (ppm)**									
emis.	f_Ca	f_Si	peak	at year	1500	1000	750	500	400	350	300	278
1000GtC	on	on	681	2000	-	-	-	2090	2450	4800	75000	1000000
1000GtC	on	off	681	2000	-	-	-	2090	2450	5800	-	-
1000GtC	off	on	681	2000	-	-	-	2090	2450	5000	80000	950000
1000GtC	off	off	681	2000	-	-	-	2090	2450	6200	-	-
5000GtC	on	on	2453	2000	2550	3900	7500	17000	48000	170000	460000	-
5000GtC	on	off	2453	2000	2550	4400	11000	34000	-	-	-	-
5000GtC	off	on	2453	2000	2550	4000	8000	19000	55000	170000	440000	-
5000GtC	off	off	2453	2000	2600	4800	14000	46000	-	-	-	-

Table 8: **Years** that specific fractions of remaining excess **Atmospheric pCO_2** are reached

variables			**fraction**									
emis.	f_Ca	f_Si	90%	75%	50%	25%	10%	e^{-1}	e^{-2}	e^{-3}	e^{-4}	e^{-5}
1000GtC	on	on	2010	2030	2120	2700	14000	2260	8000	95000	340000	550000
1000GtC	on	off	2010	2030	2120	2800	24000	2280	11000	-	-	-
1000GtC	off	on	2010	2030	2120	2750	15000	2260	8500	100000	320000	550000
1000GtC	off	off	2010	2030	2120	2800	34000	2280	12000	-	-	-
5000GtC	on	on	2030	2160	2750	5800	17000	3500	13000	70000	300000	550000
5000GtC	on	off	2030	2160	2800	8500	36000	3800	22000	-	-	-
5000GtC	off	on	2030	2160	2750	6400	19000	3500	14000	75000	300000	550000
5000GtC	off	off	2030	2160	2850	11000	55000	3900	28000	-	-	-

Table 9: **Surface warming** (°C) reached at specific calendar years

variables			**year**								
emis.	f_Ca	f_Si	3000	5000	10000	20000	50000	100k	200k	500k	1000k
1000GtC	on	on	1.070	0.861	0.596	0.415	0.313	0.251	0.165	0.043	0.000
1000GtC	on	off	1.100	0.918	0.696	0.527	0.455	0.450	0.446	0.437	0.422
1000GtC	off	on	1.080	0.876	0.617	0.434	0.323	0.256	0.163	0.039	0.000
1000GtC	off	off	1.110	0.935	0.724	0.557	0.481	0.475	0.472	0.465	0.451
5000GtC	on	on	5.510	4.370	3.190	1.980	1.370	1.120	0.749	0.227	0.038
5000GtC	on	off	5.650	4.720	3.930	2.840	2.070	2.040	2.040	2.030	2.020
5000GtC	off	on	5.540	4.460	3.370	2.130	1.400	1.130	0.738	0.215	0.032
5000GtC	off	off	5.680	4.820	4.170	3.200	2.210	2.150	2.140	2.140	2.130

Table 10: **Percentages** of remaining excess **Surface warming** reached at specific calendar years

variables			**year**								
emis.	f_Ca	f_Si	3000	5000	10000	20000	50000	100k	200k	500k	1000k
1000GtC	on	on	60.0	48.2	33.4	23.2	17.5	14.1	9.2	2.4	0.0
1000GtC	on	off	61.6	51.3	38.9	29.5	25.4	25.2	24.9	24.4	23.6
1000GtC	off	on	60.4	49.0	34.5	24.3	18.1	14.3	9.1	2.2	0.0
1000GtC	off	off	62.0	52.3	40.5	31.2	26.9	26.6	26.4	26.0	25.2
5000GtC	on	on	86.8	68.9	50.3	31.2	21.5	17.6	11.8	3.6	0.6
5000GtC	on	off	88.7	74.2	61.8	44.6	32.6	32.1	32.0	31.9	31.7
5000GtC	off	on	87.3	70.2	53.0	33.5	22.1	17.8	11.6	3.4	0.5
5000GtC	off	off	89.2	75.6	65.5	50.2	34.7	33.7	33.6	33.5	33.3

Table 11: **Years** that specific values of **Surface warming** are reached

variables			**Surface warming (°C)**									
emis.	f_Ca	f_Si	peak	at year	5	4	3	2	1.5	1	0.5	0
1000GtC	on	on	1.79	2060	-	-	-	-	2260	3500	14000	1000000
1000GtC	on	off	1.79	2060	-	-	-	-	2260	4000	26000	-
1000GtC	off	on	1.79	2060	-	-	-	-	2260	3600	15000	900000
1000GtC	off	off	1.79	2060	-	-	-	-	2260	4200	34000	-
5000GtC	on	on	6.35	2220	3600	6600	12000	20000	36000	130000	300000	-
5000GtC	on	off	6.37	2240	4100	10000	19000	-	-	-	-	-
5000GtC	off	on	6.35	2240	3700	7000	13000	22000	40000	130000	300000	-
5000GtC	off	off	6.37	2240	4300	12000	24000	-	-	-	-	-

Table 12: **Years** that specific fractions of remaining excess **Surface warming** are reached

variables			**fraction**									
emis.	f_Ca	f_Si	90%	75%	50%	25%	10%	e^{-1}	e^{-2}	e^{-3}	e^{-4}	e^{-5}
1000GtC	on	on	2200	2400	4600	18000	190000	9000	110000	360000	600000	750000
1000GtC	on	off	2200	2400	5400	170000	-	12000	-	-	-	-
1000GtC	off	on	2200	2400	4800	19000	190000	9500	120000	340000	550000	700000
1000GtC	off	off	2200	2450	5800	-	-	13000	-	-	-	-
5000GtC	on	on	2850	4000	11000	30000	260000	16000	170000	420000	700000	1000000
5000GtC	on	off	2950	4800	17000	-	-	30000	-	-	-	-
5000GtC	off	on	2850	4200	12000	34000	240000	18000	170000	420000	700000	1000000
5000GtC	off	off	2950	5400	22000	-	-	40000	-	-	-	-

Table 13: **Surface ocean acidification** (pH units below 8.15 baseline) reached at specific calendar years

variables			year								
emis.	f_Ca	f_Si	3000	5000	10000	20000	50000	100k	200k	500k	1000k
1000GtC	on	on	0.098	0.072	0.044	0.025	0.016	0.013	0.008	0.002	0.000
1000GtC	on	off	0.101	0.078	0.053	0.035	0.027	0.027	0.026	0.026	0.025
1000GtC	off	on	0.099	0.074	0.047	0.028	0.018	0.014	0.009	0.002	0.000
1000GtC	off	off	0.102	0.080	0.056	0.039	0.030	0.030	0.029	0.029	0.028
5000GtC	on	on	0.538	0.389	0.253	0.122	0.066	0.052	0.033	0.006	0.000
5000GtC	on	off	0.556	0.430	0.332	0.205	0.119	0.116	0.115	0.115	0.114
5000GtC	off	on	0.543	0.400	0.274	0.139	0.072	0.055	0.035	0.006	0.000
5000GtC	off	off	0.562	0.443	0.362	0.248	0.135	0.128	0.128	0.127	0.127

Table 14: **Percentages** of remaining excess **Surface ocean acidification** reached at specific calendar years

variables			year								
emis.	f_Ca	f_Si	3000	5000	10000	20000	50000	100k	200k	500k	1000k
1000GtC	on	on	37.8	27.9	17.1	9.8	6.4	5.0	3.3	0.8	-0.1
1000GtC	on	off	39.1	30.2	20.5	13.6	10.5	10.3	10.3	10.1	9.7
1000GtC	off	on	38.3	28.6	18.0	10.7	7.0	5.4	3.4	0.8	-0.1
1000GtC	off	off	39.6	31.0	21.7	15.0	11.7	11.5	11.4	11.2	11.0
5000GtC	on	on	68.8	49.8	32.3	15.6	8.4	6.6	4.3	0.8	-0.5
5000GtC	on	off	71.2	55.0	42.5	26.3	15.3	14.8	14.8	14.7	14.6
5000GtC	off	on	69.5	51.3	35.1	17.8	9.2	7.1	4.4	0.8	-0.5
5000GtC	off	off	71.9	56.7	46.3	31.7	17.3	16.4	16.3	16.3	16.2

Table 15: **Years** that specific values of **Surface ocean acidification** are reached

variables			Surface ocean acidification (pH units below 8.15 baseline)									
emis.	f_Ca	f_Si	peak	at year	0.7	0.6	0.5	0.4	0.3	0.2	0.1	0.
1000GtC	on	on	0.26	2010	-	-	-	-	-	2100	2950	950000
1000GtC	on	off	0.26	2010	-	-	-	-	-	2100	3100	-
1000GtC	off	on	0.26	2010	-	-	-	-	-	2100	2950	850000
1000GtC	off	off	0.26	2010	-	-	-	-	-	2100	3100	-
5000GtC	on	on	0.78	2010	2200	2650	3300	4800	8000	13000	26000	750000
5000GtC	on	off	0.78	2010	2220	2700	3600	6400	13000	22000	-	-
5000GtC	off	on	0.78	2010	2200	2650	3400	5200	9000	15000	28000	700000
5000GtC	off	off	0.78	2010	2220	2750	3700	7500	16000	28000	-	-

Table 16: **Years** that specific fractions of remaining excess **Surface ocean acidification** are reached

variables			fraction									
emis.	f_Ca	f_Si	90%	75%	50%	25%	10%	e^{-1}	e^{-2}	e^{-3}	e^{-4}	e^{-5}
1000GtC	on	on	2050	2120	2400	6000	20000	3200	14000	110000	340000	550000
1000GtC	on	off	2050	2120	2450	7500	650000	3400	22000	-	-	-
1000GtC	off	on	2050	2120	2400	6400	24000	3200	15000	120000	340000	550000
1000GtC	off	off	2050	2120	2450	8000	-	3400	26000	-	-	-
5000GtC	on	on	2200	2700	5000	14000	34000	8500	24000	170000	380000	550000
5000GtC	on	off	2200	2800	6800	22000	-	13000	-	-	-	-
5000GtC	off	on	2200	2750	5400	15000	42000	9500	28000	180000	380000	550000
5000GtC	off	off	2200	2850	8000	28000	-	17000	-	-	-	-

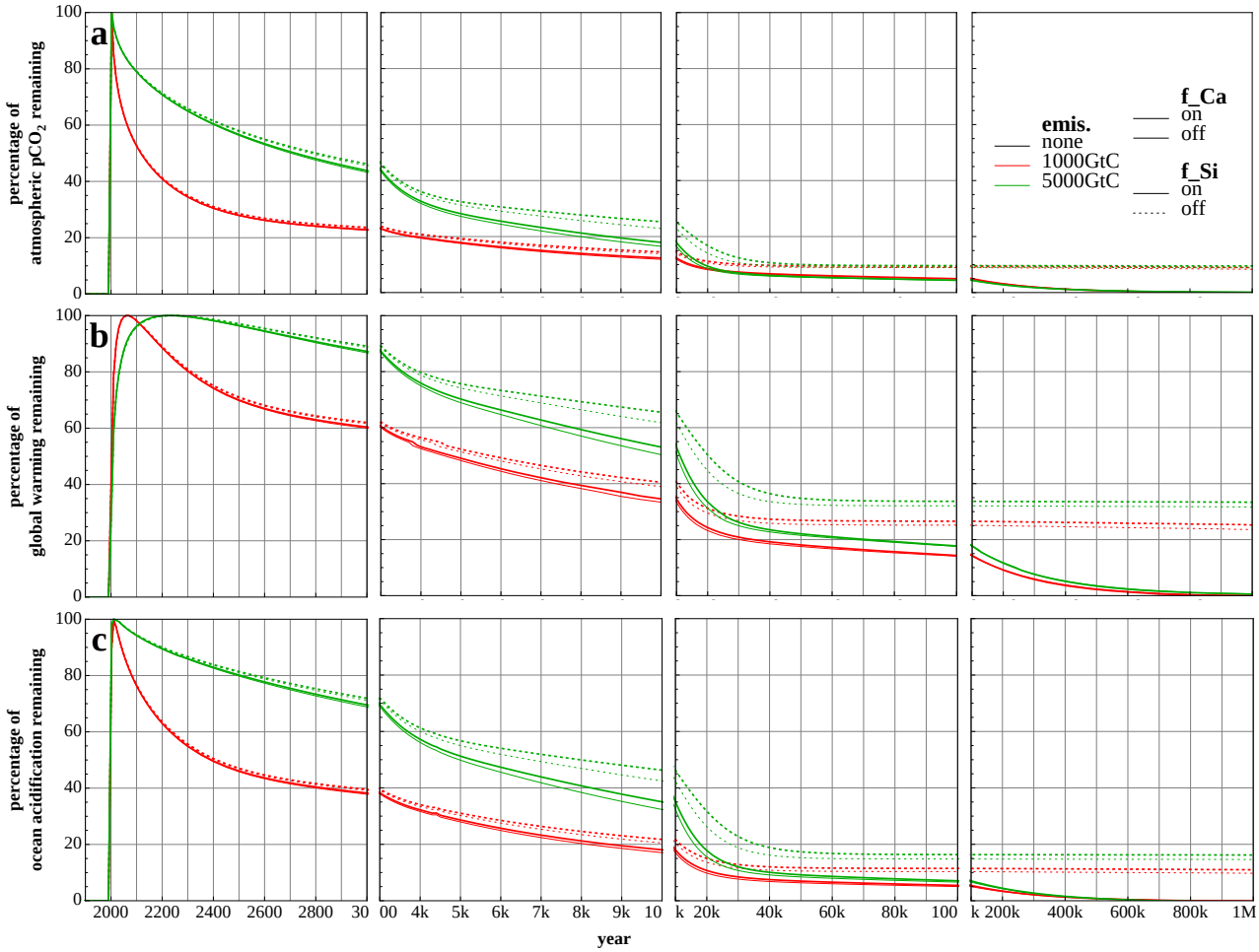

Figure 36: Fractions of initial excess atmospheric pCO_2, global warming and ocean acidification remaining over 1Myr with carbonate and silicate weathering feedbacks on/off.

A rudimentary timescale analysis was carried out as illustrated in Figure 38 (see §4.2). There is a marked distinction in the graph lines between the ensemble members with fixed weathering and the carbonate weathering feedback (f_Ca), and those with the silicate weathering feedback (f_Si). Looking at the case of atmospheric CO_2 sequestration (Fig. 38(a)), for the fixed and f_Ca members there is a clear 10^4 year *e*-folding timescale between the years ~5000 and ~50,000; this is the period of "terrestrial $CaCO_3$ neutralisation" through carbonate weathering (Ridgwell and Edwards, 2007). The exact onset and duration of this timescale is modulated by the strength of the forcing (amount of emissions); the lower forcing scenario has an earlier onset and demise of this timescale and vice-versa for the higher forcing scenario. For the f_Si runs, a ~200kyr *e*-folding timescale emerges from year ~50,000 onwards; this is the period where silicate weathering becomes dominant. Interestingly, after 500kyr, the *e*-folding timescale decreases, indicating an increase in the sequestration due to f_Si, although this may well be an artefact of having few data points here (1 every 50kyr), as looking at Figure 35(a), it looks as though sequestration slows at this point, as preindustrial carbon levels are approached. The peak in sequestration timescale coincides with the completion of the recovery (to preindustrial levels) of carbonate sediments in the ocean (see Fig. 35(d)). For the f_Ca runs, after ~50kyr sequestration of carbon effectively ceases, as seen in Figure 35(a), giving an erratic e-folding timescale. Periods between the plateaus, and at the start of the simulation, are where no single sequestration process dominates.

Figure 35(b) shows the increase in atmospheric temperatures. On a millennial timescale (left panel) there is a clear lag in the system between the lowering of CO_2 levels and the lowering of temperature, illustrated by the more convex shape to the curves. However, the influence of the feedbacks f_Ca and f_Si follow a similar pattern. *e*-folding timescales are similar to those for CO_2 (Figure 38(b)), apart from being slightly higher up until the year ~20000. For the lowest emissions series of 1000GtC, temperatures remain below the 'safe limit' of 2 °C adopted by the European Union (European, 2007) and many other nations (it is part of the non-legally binding Copenhagen Accord (World-Leaders, 2009) drawn up by the USA, China, India, South Africa and Brazil). The highest emissions series of 5000GtC, equivalent to burning all the estimated fossil fuel reserves (including exotic sources such as tar sands) available, results in significantly warmer temperatures that persist for many thousands, even tens of thousands of years; even when the silicate weathering feedback is factored in - temperatures dip back below 2°C above pre-industrial levels only after 20kyr with f_Si on; without f_Si, a third

of warming (>2°C) remains indefinitely.

There is a strong possibility (based on observations of the current and paleo state of the Earth System) that complex feedback mechanisms which aren't included in the model (such as methane release from permafrost melt (Christensen et al., 2004) and from sea-floor hydrates (Archer et al., 2008)) will come into play with these prolonged warming spells. Slow variations in orbital forcing are also omitted from the model. For these reasons, it is difficult to extrapolate these model results into useful predictions for the state of the Earth System in the far future. Models, including versions of GENIE (Lenton et al., 2009), have articulated the possibility of multiple stable states in the Earth System with the possibility of jumps between them (bifurcations), given sufficient perturbations. Here, all emissions scenarios eventually return to the initial pre-industrial state. It is a possibility that were the feedback with land productivity included (see above), the model would end up reaching a different stable state for the larger emissions scenario.

The acidification of the oceans is illustrated in Figure 35(c). Even for the 1000GtC scenario, the decrease in average sea surface pH is around 0.2 - the guardrail proposed by the German Advisory Council on Global Change (WGBU; Schubert et al. (2006)). Like the temperature change, the recovery of sea surface pH lags behind the reduction in atmospheric CO_2 levels (see also Figure 38(c)).

Figures 35(d) and 37 illustrate the dissolution of the ocean carbonate sediments (see individual captions for commentary). The sediments are almost completely dissolved for the 5000GtC emissions scenario, and remain so for ~10kyr. For the case of near complete dissolution, a noticeable slow-down in the sequestration of carbon from the atmosphere is apparent when looking at Figure 36(a). The sediments start to recover after year 10k, allowing the fraction of excess atmospheric pCO_2 remaining in the 5000GtC scenario to converge with the 1000GtC scenario values. Sediments recover after ~50kyr, going on to overshoot their initial pre-industrial level (Fig. 37(d)). Note that the mediterranean maintains it's $CaCO_3$ throughout the perturbation. This is because in the model, ocean circulation is such that the mediterranean basin is warm throughout the water column ($CaCO_3$ solubility is inversely proportional to temperature).

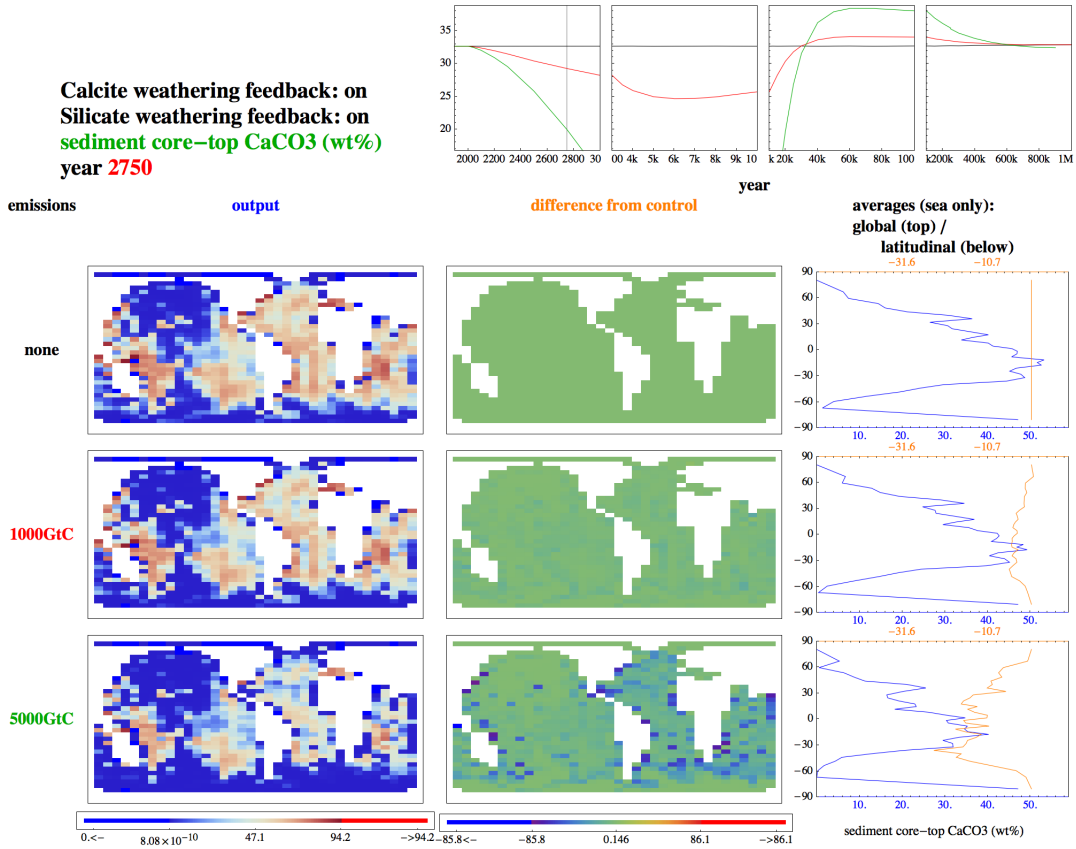

(a) year 2750: sediments are well into their dissolution 760 after emissions pulses, after ocean mixing has taken place.

Figure 37: As Figure 32, but for different emissions scenarios (1000 and 5000GtC), with the 0D Globavg weathering scheme. [Continues on next two pages; animation on accompanying digital media]

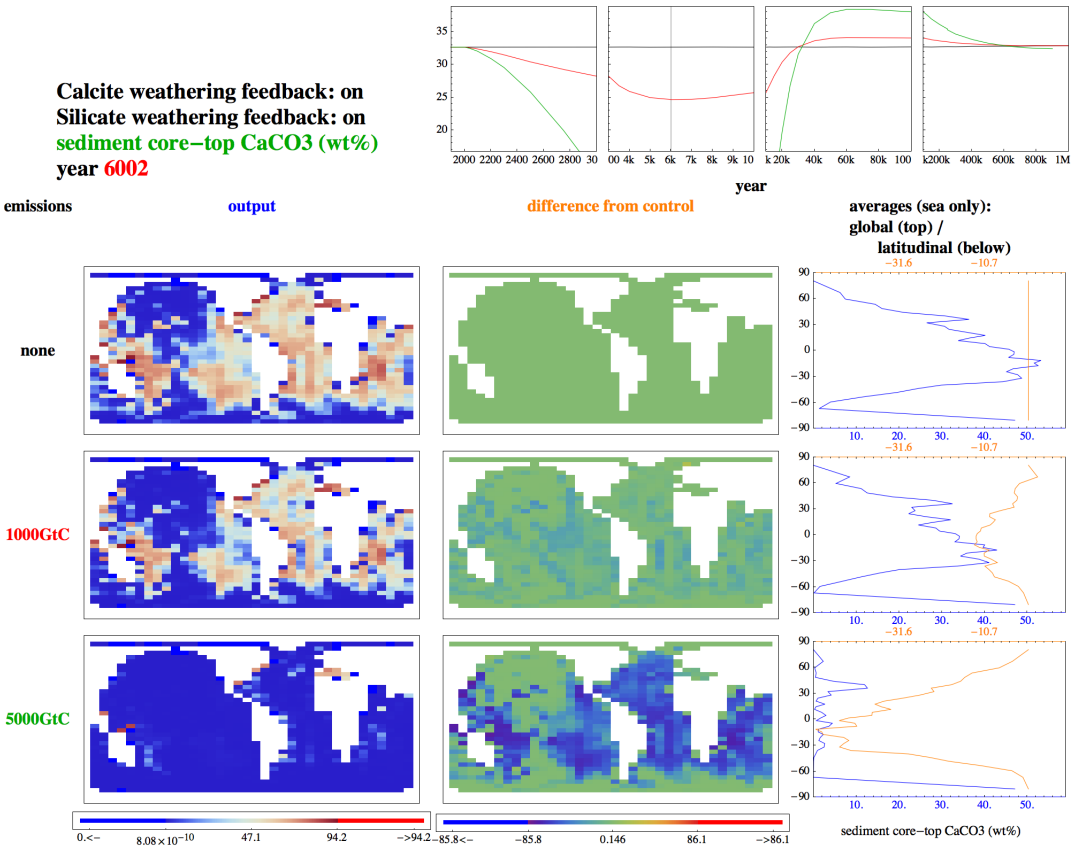

(b) year 6002: sedimentary core-top $CaCO_3$ reaches a minimum (actual minimum is at year ~6200 for 1000GtC emissions, and year ~5200 for 5000GtC).

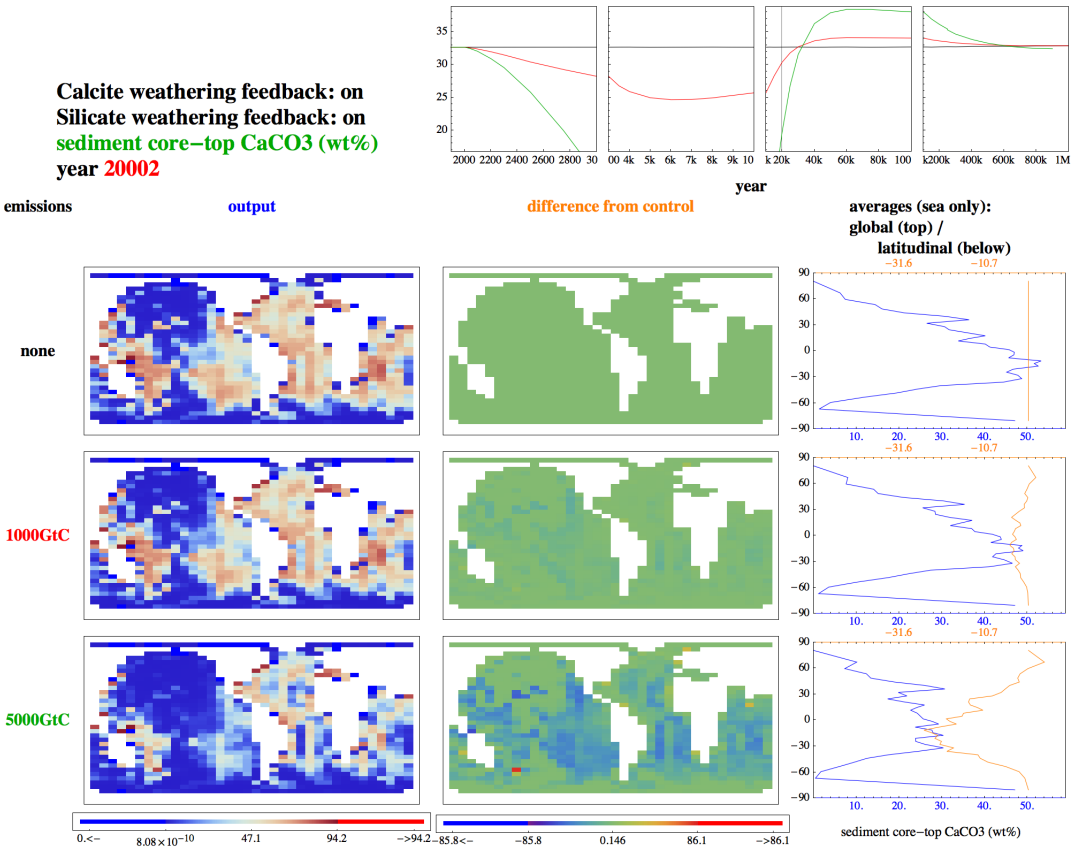

(c) year 20002: sedimentary core-top $CaCO_3$ is recovering as a result of alkalinity and DIC being added to the ocean through terrestrial weathering.

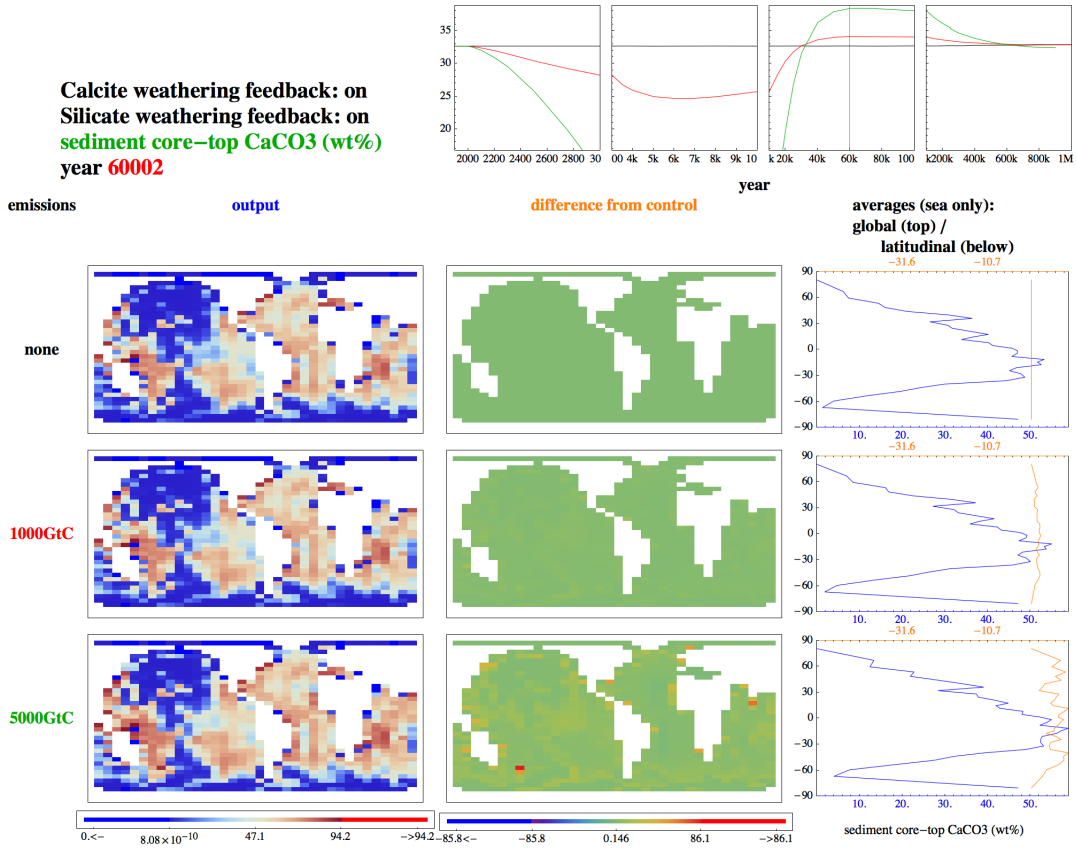

(d) year 60002: sedimentary core-top $CaCO_3$ overshoots pre-industrial equilibrium.

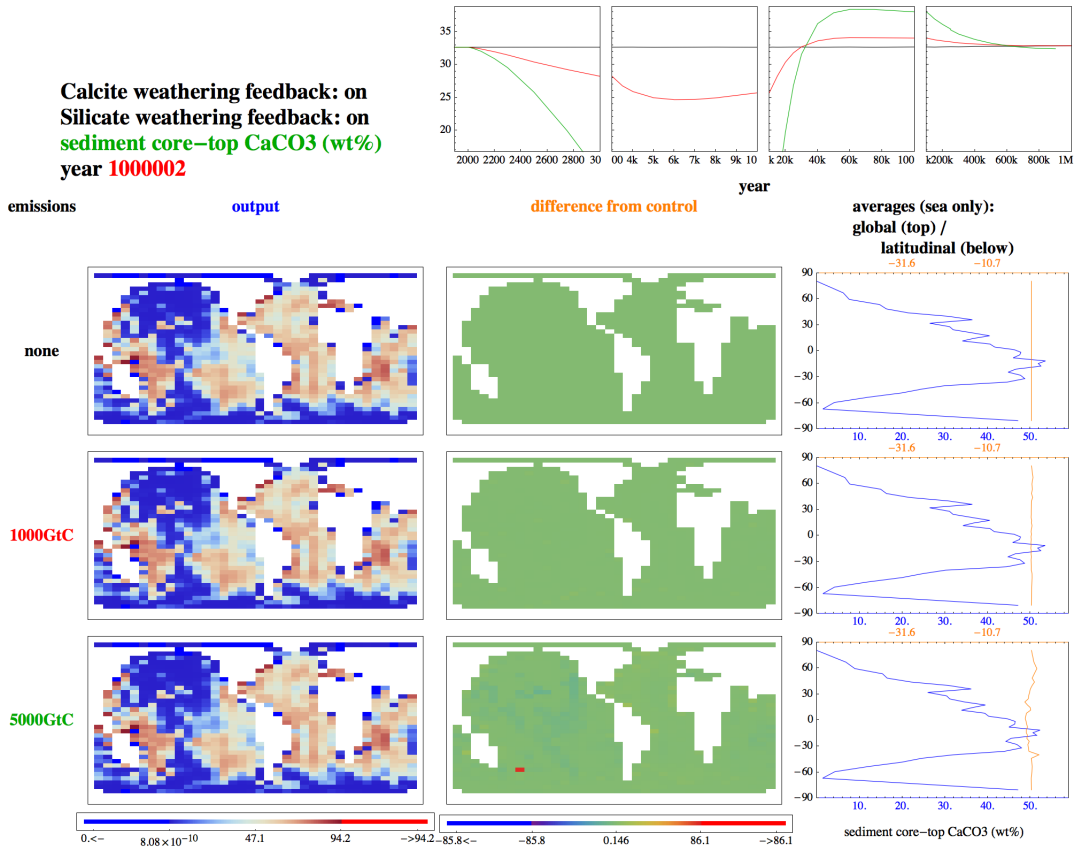

(e) year 1,000,002: sedimentary core-top $CaCO_3$ at equilibrium, at a state only slightly changed from its initial pre-industrial distribution.

4.2 Timescale analysis

All the variables of interest (excess global atmospheric pCO_2, surface warming and ocean acidification) decay in an exponential manner after an initial peak when the (Earth) system is subject to a perturbation in the form of a pulse of carbon emissions. The decay constants, or e-folding timescales, were quantified as follows.

First, the e-folding timescale for each ensemble member was plotted as a function of time. A curve was plotted of the variation with time of the difference between the reduction of each variable from its peak value, and the final reduction of each variable, taken to be at the time when the curves rate of depletion was less than 1 part in 10^6 between successive time outputs (see Appendix X for list of years for time-series model output). The natural logarithm of this curve was taken, and the slope of the resulting curve was taken to be the e-folding timescale (i.e. for pCO_2, the time, at the given year, which it would take for the pCO_2 level to be reduced by a factor of e) Example of these plots are shown in Figure 38; the full set is in Appendix A.

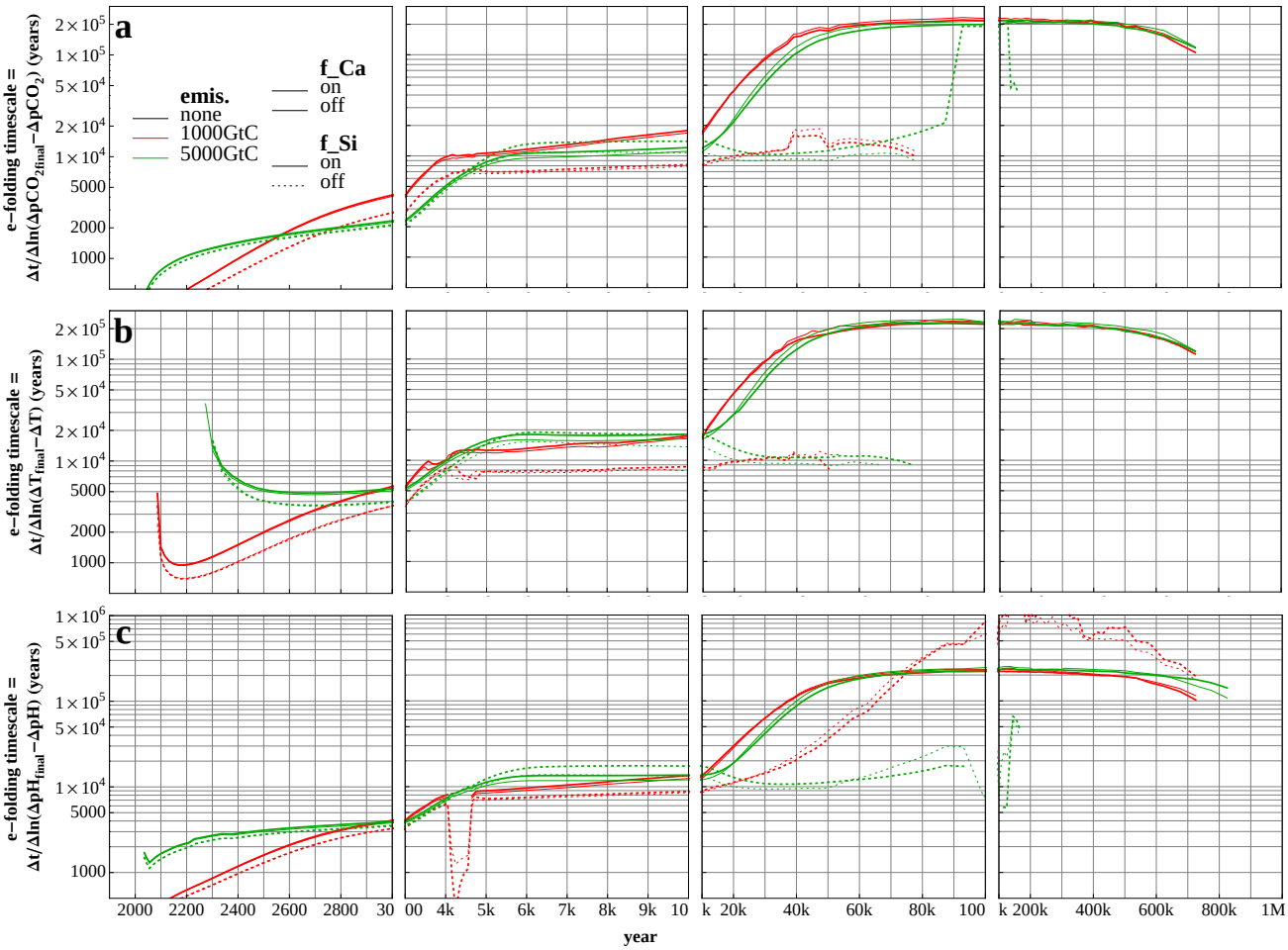

Figure 38: e-folding timescales for (a) the sequestration of CO_2 from the atmosphere, (b) global surface warming and (c) global surface ocean acidification; for 1000GtC (red) and 5000GtC (green) emissions pulses, vs. a control run with no emissions (black), with carbonate and silicate weathering feedbacks (f_Ca and f_Si respectively) on/off. Curves smoothed by taking a 5-point moving average. Note the logarithmic scale on the y-axis.

Second, a series of exponential curves with negative gradients were fitted to model output. The general form of the fit is given by the equation

$$V(t) = b + h\sum_{i=1}^{n} w_i e^{-(t-t_0)/\tau_i} \tag{27}$$

where V is the variable of interest, evaluated at time (year) t. b is the "baseline" of the function, or the value of the variable at the end of the decay where stabilisation occurs. For ensemble members with silicate weathering feedbacks included, this is the pre-industrial level; for runs without silicate weathering, it is slightly above pre-industrial. h is the "height" of the peak above the baseline level; i.e. the peak minus the pre-industrial level (this is equal to the peak for surface warming and ocean acidification as the pre-industrial level for these

is zero by definition). Each curve i is weighted by a normalised weighting w_i. In the initial fitting, which was performed using the function `NonlinearModelFit` in Mathematica, all parameters were unconstrained, which led to the total height of the fitted curve being a product of the total of the weightings w_i and h; for the purposes of presenting the output, the w_i were normalised and h multiplied by the total of the unnormalised w_i. τ_i are e-folding timescales for each curve; the time taken (t - t_0) for the curve to reach e^{-1} of its peak value, where t_0 is the time (year) of the peak.

The number of curves fitted (n), was looped over, up to a maximum of n=10 (no fits had n>7), in order to determine the best fitting curve. The Bayesian Information Criterion (BIC) (Schwarz, 1978) was used to rank curves in order of best fit, as it penalises over-fitting by giving a higher score (lower scores are best) to equal fits with more parameters. In general, fits with the lowest BIC also have the highest R^2, but this is not universally the case. Of the best fit curves, those with parameters with relative confidence intervals (taken at the 95% level) greater than two, or very large (>10^7) or negative (except b which is sometimes slightly negative for a legitimate fit) values, were discarded in favour of the next best fit.

Nearly all time-series decay curves were able to be fitted to equation 27 with a very high level of accuracy (R^2>0.99999; note that BIC is a relative term so cannot be used to give an absolute measure of the degree of fit). The exceptions were the surface warming decay curves, which were not particularly amenable to the fitting process (fewer timescales were picked out; n≤4); perhaps they are better approximated by a different function class than exponential. The surface ocean acidification decay curves were not quite as well fitted as the atmospheric pCO_2 curves (n≤6 vs. n≤7); and the 5000GtC scenario had less impressive fits than the 1000GtC scenario. An example of a good fit (to pCO_2 model output) is shown in Figure 39(a); note that the fit is so close, that the model output, the fit, and the lines showing the 95% confidence interval of the fit all overlap. An example of a bad fit (to surface warming model output) is shown in Fig. 39(b) Note that even for the fits which look bad, R^2 values appear high (>0.9); this is on account of R^2 being a measure of linear correlation, and the well-fitted values at the peak end of the time-series biasing the result. For the tabulated fits (a complete set for all ensemble members is given in Appendix A, Tables 31, 36 and 41), those with an R^2<0.999 should not be given much weight.

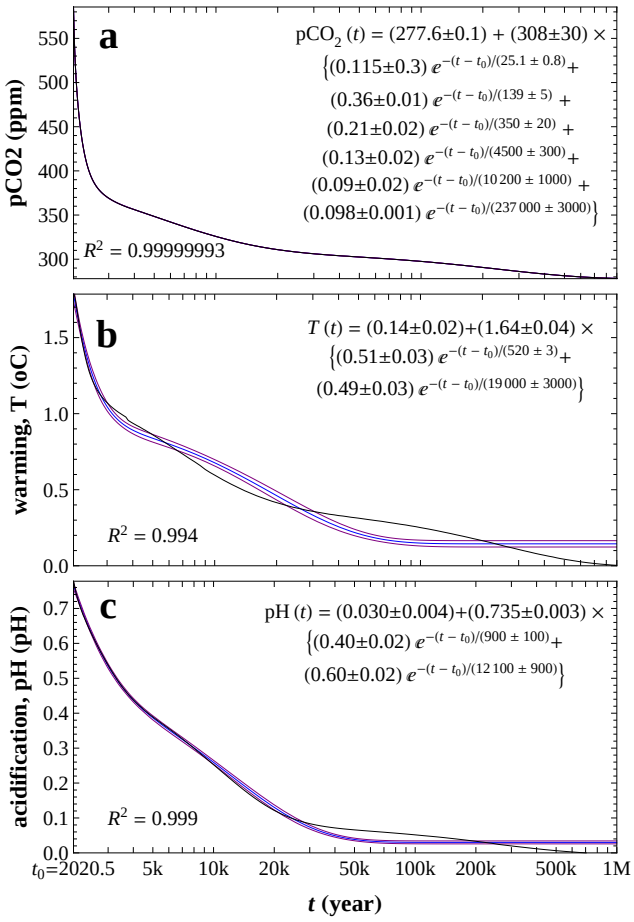

Figure 39: Fits (blue lines; purple lines show 95% confidence intervals; equations on plots) to model output (black lines) of atmospheric pCO_2 (a), surface global warming (b), and surface ocean acidification (c), for global average weathering with carbonate and silicate weathering feedbacks on for 1000GtC (a, b) and 5000GtC (c) emissions. Model runs are chosen to show (a) a good fit (fit with confidence interval coincides with model output); (b) a fit that has an R^2 that appears high (0.994) but a fit is clearly less than optimal when visualised; and (c) a fit that is initially good, but fits the long tail of the output poorly, yet still has a high R^2. Note logarithmic scale on time axis.

The fits produced for the carbonate and silicate weathering feedback ensemble, are shown in Tables 17-19 (entries are left blank for output where the fitting process was unsuccessful; all numbers are given an appropriate number of significant figures dependent on their uncertainty, which is determined from the fitting). A number of distinct timescales are picked out, with some ensemble members having more than others. For the carbonate weathering feedback off, silicate weathering feedback on, 1000GtC scenario, there are 7 timescales. Each is likely representative of a different process in the model. The first corresponds to "ocean invasion" of CO_2, and has a short timescale of only 6 years; the second is perhaps carbonate chemistry reactions in seawater (29yr); the third mixing of the upper layers of the ocean (148yr); the fourth, mixing of the ocean down to depth (370yr); the fifth, dissolution of the ocean-floor carbonate sediments (4.5kyr); the sixth carbonate weathering (10.3kyr), and the seventh and final, silicate weathering (237kyr).

The first 3-4 timescales (up to the century level) compare approximately to earlier work of exponential fit-

ting using the "Bern" climate model (Joos et al., 1996). The latter timescale of 10.2-11.6kyr for carbonate weathering, compares favourably to the figures given by (Sundquist, 1991) of 6.3-14kyr ("carbonate-ion compensation"). However, the (fourth or fifth) timescale of 4.5-4.7kyr for sediment dissolution is significantly larger than Sundquist's 1.5-2.7kyr timescale for "calcite dissolution kinetics". The timescale for silicate weathering is significantly lower than previous estimates at ~225-237kyr vs. 325-400kyr (Sundquist, 1991; Archer, 2005). Note that the lower end of the range (225kyr) is for silicate weathering feedback on, carbonate weathering feedback off; as mentioned in section §4.1, the carbonate weathering feedback appears to slightly hinder the silicate weathering feedback. For the version of the model with spatially resolved weathering, the silicate weathering timescale is much lower still, at ~100kyr (see §4.4 below).

The 5000GtC scenario gives fits with a lower number of terms n. This is perhaps due to processes being "blended" together; their distinct timescales blurred. It could be an artefact of the low resolution of the model output time-series; only 143 quasi-logarithmically distributed outputs were taken over the 1Myr runs (see Appendix A.1). There is the possibility that with more points included, the fits would come out differently. There is also a possibility that the arrangement (spacing) of points along the time axis has an effect.

A scatter plot of all successful fits is shown in Figure 40. There is a clear clustering of points, indicating robust timescales of ~30-100yr, ~150-200yr, ~400-800yr, ~4-7kyr, ~10-20kyr and ~100-200kyr. Also, ΔpH timescales appear to shadow ΔpCO_2 timescales at slightly higher (longer) values. There is also a considerable spread in weightings (fractions sequestered) for the ~5kyr (sediment dissolution) and ~12kyr timescales (carbonate weathering), but less so for the others.

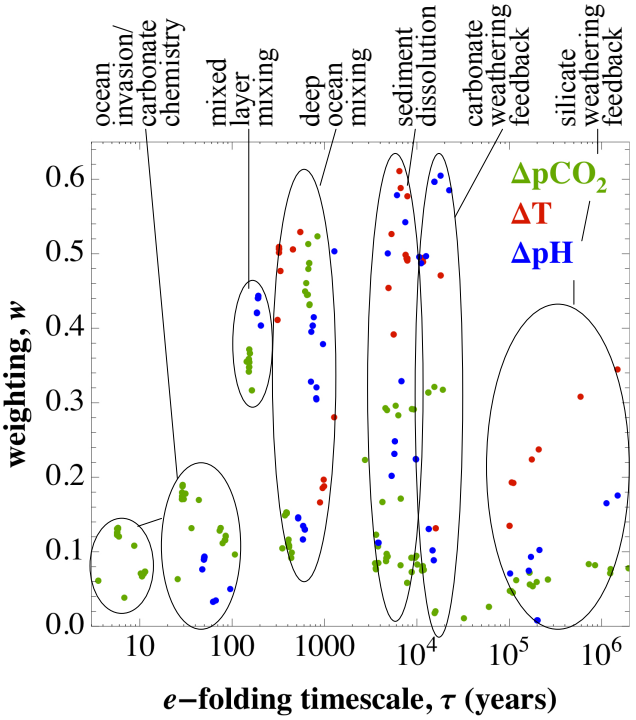

Figure 40: Scatter plot of e-folding timescales and their weightings for the depletion of excess atmospheric pCO_2 (ΔpCO_2), surface global warming (ΔT) and surface ocean acidification (ΔpH) for all fitted ensemble members. Lack of points for ΔT indicates poor curve-fitting. Annotation highlights processes corresponding to distinct timescales; ocean invasion and carbonate chemistry are grouped together on account of very few model runs having 7 distinct timescales, and many having 6.

Table 17: **Timescale fitting** for excess **Surface warming** decay

variables			fit to $T(t) = b + h\sum_i w_i e^{-(t-t_0)/\tau_i}$					
emis.	f_Ca	f_Si		warming (°C)	i	1	2	R^2
1000GtC	on	on	b	0.14±0.02	w_i (%)	51±3	49±3	0.994
			h	1.64±0.04	τ_i (yr)	520±90	19000±3000	
1000GtC	on	off	b	0.458±0.004	w_i (%)	50.2±0.6	49.8±0.5	0.99994
			h	1.371±0.005	τ_i (yr)	320±10	7500±200	
1000GtC	off	on	b	0.23±0.04	w_i (%)	100.00±0.06		0.97
			h	1.25±0.07	τ_i (yr)	4900±800		
1000GtC	off	off	b	0.484±0.005	w_i (%)	50.9±0.6	49.1±0.5	0.99994
			h	1.346±0.006	τ_i (yr)	320±10	7900±200	
5000GtC	on	on	b	0.1±0.1	w_i (%)	71±1	29±2	0.998
			h	6.01±0.1	τ_i (yr)	6100±400	190000±40000	
5000GtC	on	off	-	-	-	-	-	-
5000GtC	off	on	b	0.8±0.1	w_i (%)	100.0±0.4		0.99
			h	5.0±0.1	τ_i (yr)	12000±1000		
5000GtC	off	off	-	-	-	-	-	-

Table 18: **Timescale fitting** for excess **Atmospheric pCO_2** decay

variables			fit to $pCO_2(t) = b + h\sum_i w_i e^{-(t-t_0)/\tau_i}$									
emis.	f_Ca	f_Si		pCO_2 (ppm)	i	1	2	3	4	5	6	7	R^2
1000GtC	on	on	b	277.56±0.09	w_i (%)	11.8±0.4	17.0±0.2	32.0±0.8	15±2	11±1	6±1	7.5±0.1	0.99999996
			h	403±40	τ_i (yr)	5.8±0.2	29±1	148±5	370±20	4500±300	10300±800	237000±2000	
1000GtC	on	off	b	313.89±0.07	w_i (%)	13.1±0.5	18.8±0.3	35.7±0.9	15±2	10±1	7±1		0.99999994
			h	367±36	τ_i (yr)	5.8±0.2	29±1	151±6	390±20	4700±300	11400±800		
1000GtC	off	on	b	277.42±0.09	w_i (%)	11.9±0.4	17.0±0.3	32.1±0.9	15±2	10.0±1	7±1	7.9±0.1	0.99999995
			h	403±40	τ_i (yr)	5.8±0.2	29±1	149±5	370±20	4600±300	10700±800	225000±2000	
1000GtC	off	off	b	316.02±0.07	w_i (%)	13.2±0.5	19.0±0.3	35.9±0.9	15±2	8.7±0.9	8±1		0.99999995
			h	364±36	τ_i (yr)	5.8±0.2	29±1	151±6	390±20	4600±300	11600±700		
5000GtC	on	on	b	2172±2172	w_i (%)	6.1±0.6	11.4±0.4	45.2±0.1	30.7±0.2	6.63±0.08			0.999997
			h	2172±217	τ_i (yr)	11±1	74±5	653±7	7180±70	223000±9000			
5000GtC	on	off	b	1980±1980	w_i (%)	7±1	12.9±0.9	48.4±0.2	32.0±0.3				0.999992
			h	1980±198	τ_i (yr)	11±3	75±10	670±10	10800±200				
5000GtC	off	on	b	2172±2172	w_i (%)	6.2±0.6	11.5±0.4	45.0±0.1	30.5±0.1	6.81±0.09			0.999997
			h	2172±217	τ_i (yr)	11±1	76±6	663±7	8020±80	215000±9000			
5000GtC	off	off	b	1970±1970	w_i (%)	7±2	13±1	48.7±0.3	31.4±0.3				0.99999
			h	1970±197	τ_i (yr)	11±3	80±10	680±10	13300±200				

Table 19: **Timescale fitting** for excess **Surface ocean acidification** decay

variables			fit to $pH(t) = b + h\sum_i w_i e^{-(t-t_0)/\tau_i}$								
emis.	f_Ca	f_Si		acidification (pH)	i	1	2	3	4	5	6	R^2
1000GtC	on	on	b	-0.0005±0.0002	w_i (%)	8±2	38±4	13±5	17±6	16±7	7.8±0.1	0.999995
			h	0.2594±0.0003	τ_i (yr)	50±9	190±20	500±100	4400±900	10000±2000	240000±10000	
1000GtC	on	off	b	0.02621±0.0001	w_i (%)	9±3	44±3	13±4	25±3	9±4		0.999990
			h	0.2328±0.0003	τ_i (yr)	50±10	190±20	600±200	5800±700	15000±3000		
1000GtC	off	on	b	-0.0006±0.0002	w_i (%)	8±2	38±4	13±5	16±5	16±6	8.6±0.1	0.999995
			h	0.2594±0.0004	τ_i (yr)	50±9	190±20	500±100	4300±900	10000±1000	228000±9000	
1000GtC	off	off	b	0.02921±0.00009	w_i (%)	9±3	44±3	13±5	20±4	13±4		0.999992
			h	0.2298±0.0002	τ_i (yr)	50±10	190±20	600±100	5300±800	13000±2000		
5000GtC	on	on	b	0.05±0.01	w_i (%)	100.0±0.8						0.99
			h	0.65±0.01	τ_i (yr)	5200±400						
5000GtC	on	off	b	0.113±0.002	w_i (%)	39.0±0.8	61.0±0.6					0.99990
			h	0.661±0.001	τ_i (yr)	730±30	12400±300					
5000GtC	off	on	b	-0.007±0.003	w_i (%)	33.1±0.6	55.6±0.5	11.3±0.4				0.99994
			h	0.780±0.001	τ_i (yr)	720±20	9700±200	260000±30000				
5000GtC	off	off	b	0.123±0.002	w_i (%)	40.3±0.8	59.7±0.6					0.9999
			h	0.650±0.003	τ_i (yr)	750±40	15500±500					

4.3 Analysis of all model ensemble members

All ensembles are shown together in Figure 41. The full set of all ensemble runs (63 for each emissions scenario) are plotted together with their mean and standard deviations in Figure 42 (the crashed run from the river routing ensemble has been omitted). Most of the runs are unrepresentative of the real world; they have parameter settings that are designed to test the limits of the RokGeM model. Examples of such settings include the switching off of carbonate and silicate weathering feedbacks, having a uniform global average weathering flux across the whole land surface, or covering the whole land surface with a monolithic rock distribution.

Of the runs including the silicate weathering feedback, most return to their preindustrial equilibrium (or very close too it), by year 1M. Exceptions are runs only including the weathering-runoff feedback (and not the weathering-temperature or weathering-productivity feedbacks), and those with extremes of lithology or climate sensitivity. The outliers in the global warming perturbation plots (which greatly affect the standard deviation, see Fig. 42(b, e)) are the runs with extreme values of climate sensitivity.

In order to quantify the effect of changing different parameters in the model, various metrics were applied to the results of the different ensembles of model runs. First, the ranges of atmospheric pCO_2 at selected times after the pulse of emissions (years 3000, 10000, and 100k) in the 1000GtC scenario were collated. As shown in Table 20, these ranges are largest for the "lithologies" ensemble (different distribution of rock types over the land surface, including monolithological end members; §3.8), and the combined ensemble with different schemes (0D and 2D) and the silicate and carbonate weathering feedback switches (§3.7.4). The latter is at an unfair advantage in terms of influence in that it involves a combined effect of changing two different features of the model. It's notable that the weathering-temperature feedbacks ensemble (§3.2) has a disproportionately greater effect at year 100k when compared with years 10000 and 3000. The calcite and silicate weathering feedback ensemble (§4.1) echoes this result, through it's inclusion of the weathering-temperature feedback (it also includes the weathering-runoff and weathering-productivity feedback, which do not exhibit this effect). All but two ensembles show an stabilisation or increase in atmospheric pCO_2 range from year 3000, through year 10000 to year 100k. The notable exception is the lithologies ensemble, which has a greater range at year 10000 than year 100k. This is because many of the runs in this ensemble have a strong weathering and are already starting to approach equilibrium by year 100k.

Other quantifications of ensemble (or parameter) strength are ranges of calcite and silicate weathering e-fold response times. There is some difficulty in accurately compiling such figures (Table 20) as produced by the timescale analysis procedure outlined above (§4.2). This is on account of some analyses not producing reliable timescales for all sequestration processes (including weathering), and also the blurring of boundaries between different processes. It was arbitrarily decided that timescales over 40kyr were associated with silicate weathering, and those between 6.5kyr and 40kyr, when accompanied by a greater timescale, carbonate weathering. These ranges show a different pattern to looking at the individual time-slices. Dominant ensembles are the ones involving runoff parameters. This is on account of these ensembles having very long equilibrium times. Whilst the absolute ranges are large for these ensembles, the relative ranges are less so (see pale green and orange in Figure 43). When looking at these relative ranges, the lithologies and weathering schemes and feedback switches ensembles are also prominent once again, in addition to the runoff related ensembles. Worthy of special mention is the climate sensitivities ensemble, which has by far the greatest relative and absolute range for the carbonate weathering timescale. This may well be an artefact of incorrect attribution of timescales to the carbonate weathering process.

Table 20: Quantitative comparison of ensembles (1000GtC scenario): ranges of **Atmospheric pCO_2**

Ensemble	at year			Weathering timescale		Integral
	3000	10000	100k	Calcite	Silicate	over 1Myr
short-circuit test	0	1	1	225	9900	2670
weathering-temperature feedbacks	2	6	13	2290	20400	5220
weathering activation energy	2	5	6	969	233000	30500
weathering-runoff feedbacks	1	2	5	1010	1090000	2200
frac. power of explicit weathering-runoff dependence	0	1	2	286	1130000	6290
runoff-temperature correlation constant	1	2	4	537	2050000	29000
weathering-productivity feedbacks	1	3	8	648	50500	3540
calcite and silicate weathering feedbacks	4	10	18	1270	11800	7260
weathering schemes	8	8	4	615	44500	9750
weathering schemes with f_Ca and f_Si on/off	13	22	23	3400	1850000	5530
river routing schemes	0	1	0	271	0	52
lithologies	32	41	17	6080	278000	25100
climate sensitivity	2	4	12	5330	200000	82700

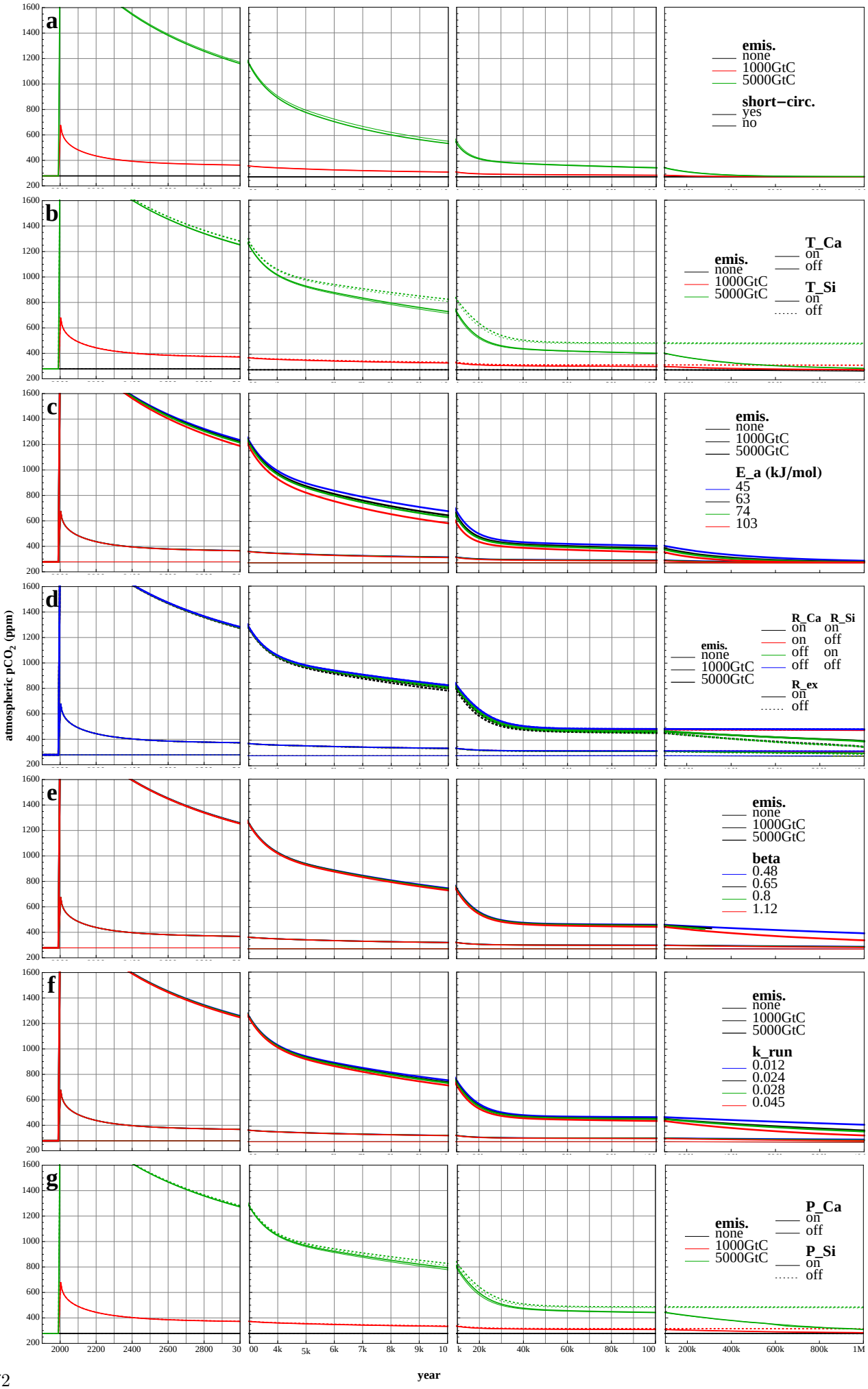

Figure 41: Atmospheric pCO_2 over 1Myr for all model ensembles.

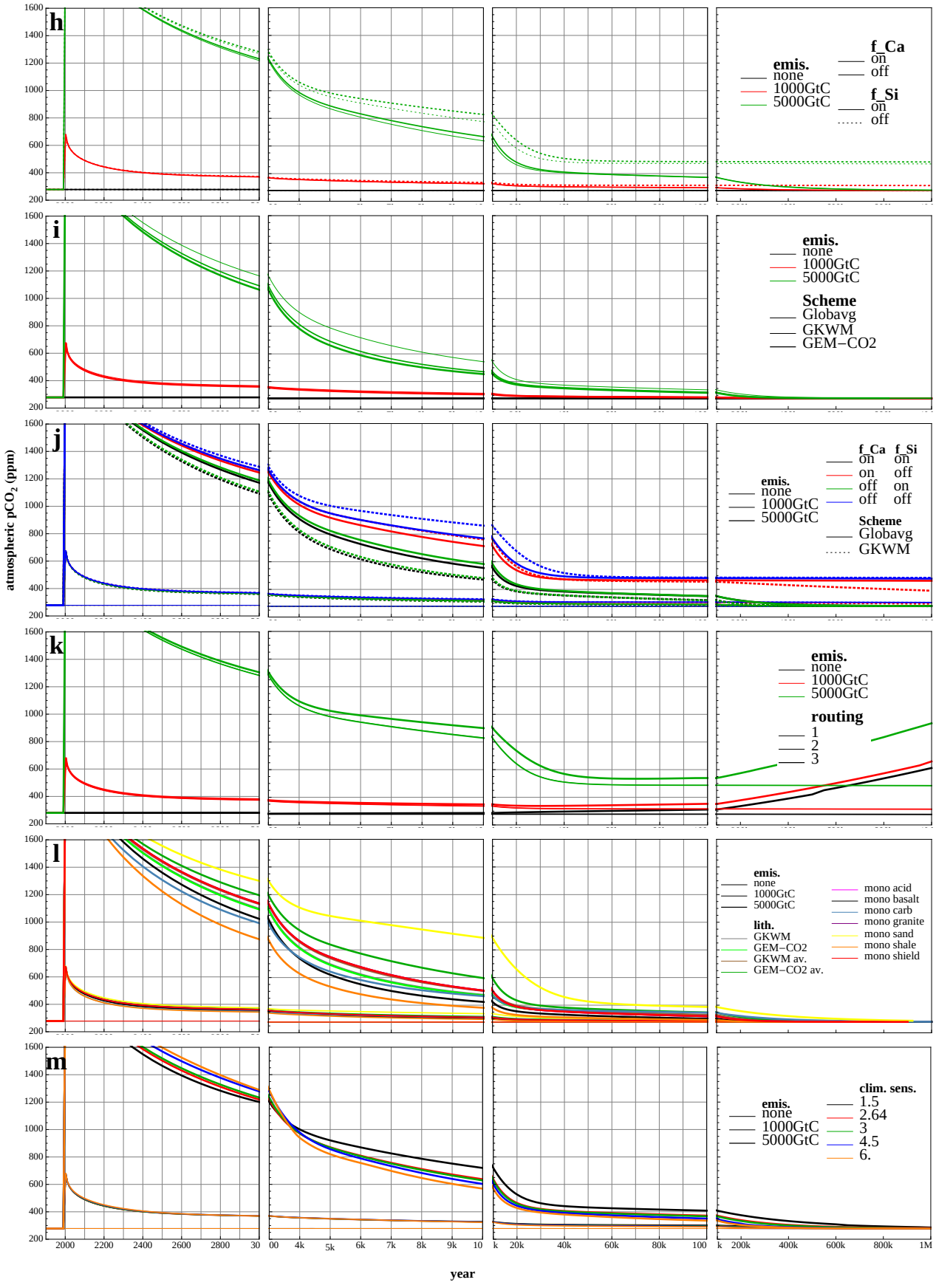

Figure 41: continued

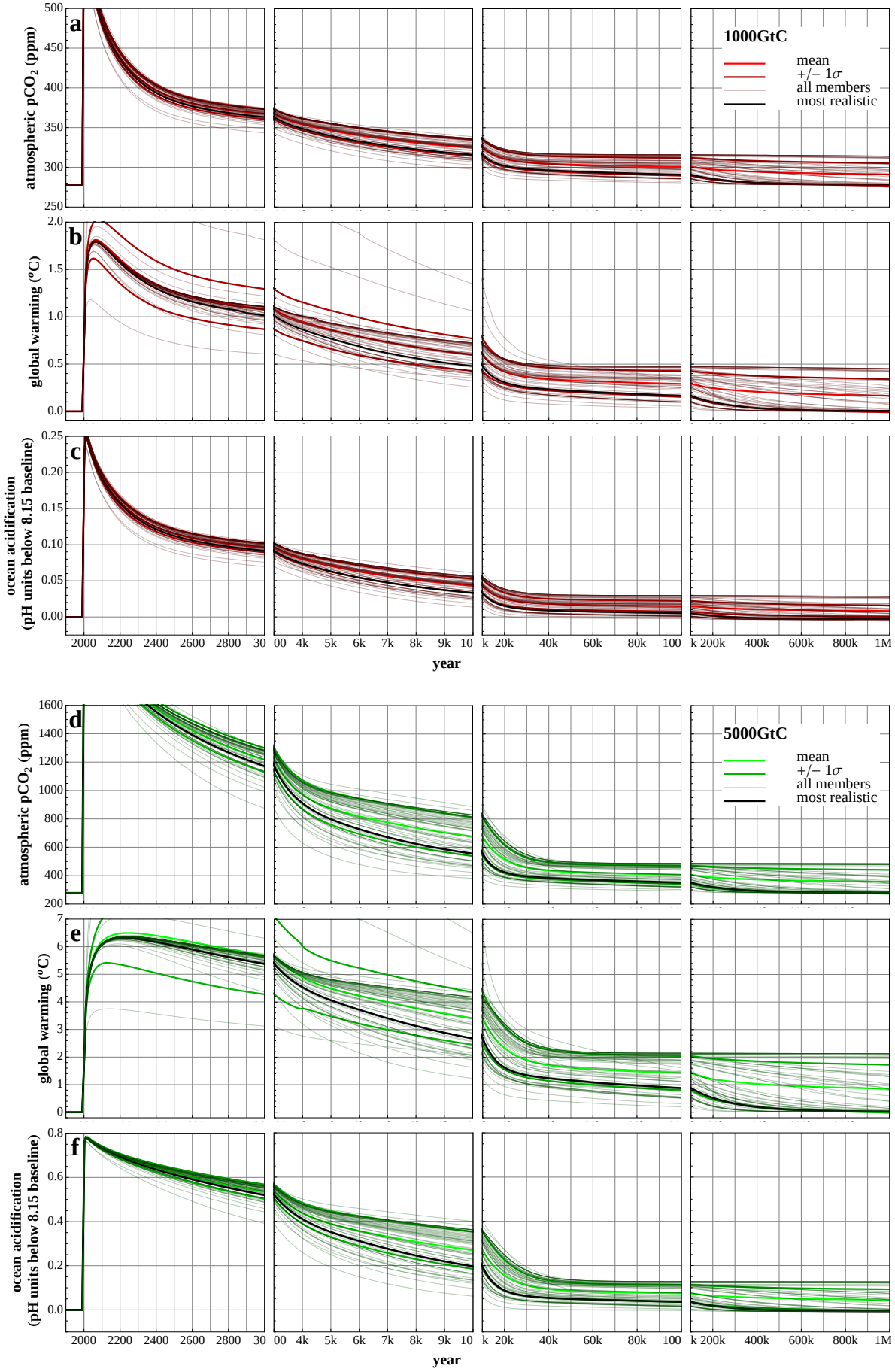

Figure 42: Atmospheric pCO_2 (a,d), global warming (b, e) and ocean acidification (e,f) for 1000GtC (a, b, c) and 5000GtC (d, e, f) emissions pulses. All model runs, shown with their mean and standard deviation range. The most realistic run is shown in black.

A final quantification, that is perhaps the most objective of all measures is taking the range of the areas under the atmospheric pCO_2 curves for each ensemble (last column of Table 20). Here, climate sensitivity has by far the greatest effect (>80,000ppm yr), lithologies, weathering activation energy and runoff-temperature correlation constant all have a significant effect (~25,000ppm yr), and river routing and whether or not to "short-circuit" the atmosphere as regards to weathering in the carbon cycle (§3.1) have a small effect. However, there is a caveat in that many runs have not yet reached equilibrium by the end of the integration after 1Myr (notably the fractional power of explicit weathering-runoff feedback and runoff-temperature correlation constant ensembles (§3.3)). For full accuracy, all model runs would have to be integrated over complete runs to equilibrium. This was not done due to time and computational constraints.

Taking the ranges of Table 20, dividing them by their respective arithmetic means to obtain relative ranges, and then normalising their cumulative totals, a visualisation of parameter sensitivity of the RokGeM model is shown in Figure 43. Different patterns across the set of ensembles, as discussed in above in relation to the numbers in Table 20, are seen for each metric. Clearly dominant however, is the multiple ensemble across weathering scheme dimensionality (0D and 2D) and feedbacks, and the ensembles over different 2D lithologies, and different climate sensitivities. The first of these shows a greater effect than it's two component ensembles (immediately to the left of it), combined. This illustrates the complexity of the interlocking feedbacks in the model, whereby effects of combining features are not linear or indeed orthogonal.

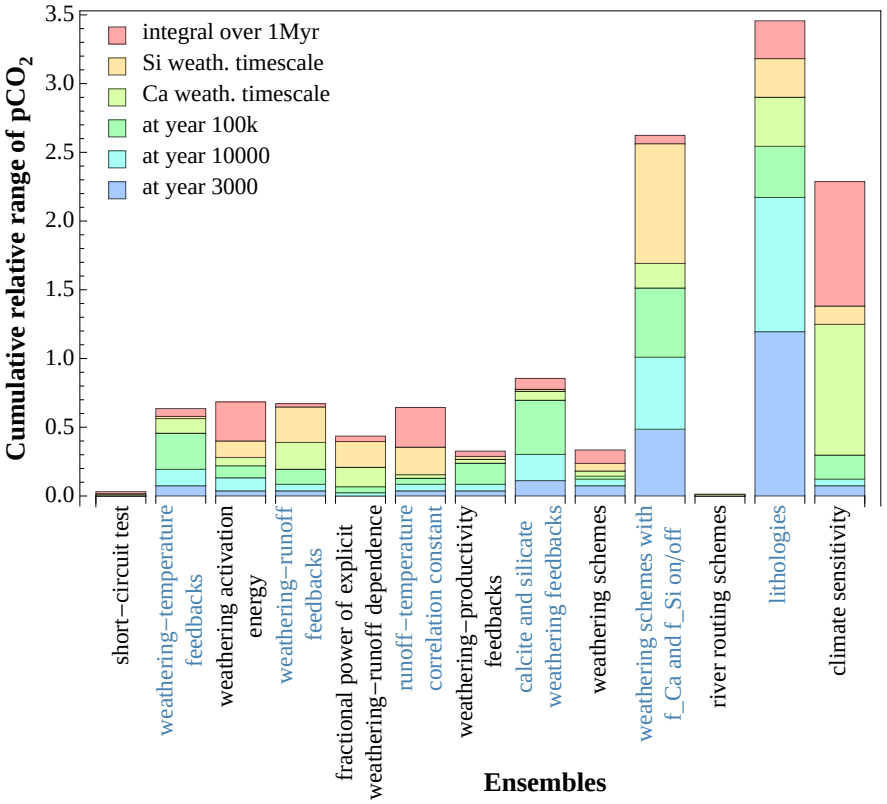

Figure 43: Parameter sensitivity in RokGeM: quantitative comparison of ensembles. Metrics are colour coded, and stacked. Ranges are normalised by taking means over all ensembles and then dividing by the number of metrics, so that a score of 1 on the y-axis represents the ensemble parameter(s) being of average significance when compared to the set of sensitivity ensembles explored.

4.4 Model run with the most realistic parameter set

The most realistic ensemble member was also picked out and put on the plots in Figure 42. This run includes all carbonate and silicate weathering feedbacks, spatially explicit weathering (GKWM scheme), the default data-based lithology distribution, default best estimate climate sensitivity, and the 1000GtC emissions scenario. From hence forth, this model run will be referred to as model run alpha. It appears (in black) low down near the (mean - 1σ) lines on account of it including silicate weathering feedbacks, when a sizeable fraction of the total ensemble (23 out of 63) do not.

Tables 21-25 show key values of the chosen key variables for model run alpha. Peak global warming is restricted to 1.77°C, which is about at the "safe" limit (1.7°C above the pre-industrial level) given by James Hansen and others (Hansen et al., 2008). Translated into a sustained pCO_2 level, the limit is 350ppm which has been much popularised by advocacy groups attempting to mitigate climate change. This pCO_2 limit is based on studies of paleo-climate, which point toward the long-term equilibrium climate sensitivity being ~6°C for a doubling of pCO_2. For model run alpha, pCO_2 remains above 350ppm until the year 3500. The discrepancy with the temperature, when compared to Hansen's result, is down to a prescribed climate sensitivity of ~3°C in GENIE, and a lack of land-surface feedbacks, such as permafrost melt, in the model (model runs presented here are done so without the ENTS land scheme - see §1.6 - which nevertheless does not include permafrost). Other feedbacks that have triggered flips in climate in the geological past include the release of methane from clathrates on the sea bed, these are also not included in GENIE.

From the curve fitting performed (see above), it was determined that atmospheric pCO_2 (in ppm) at year t following an instantaneous release of 1000GtC of CO_2 emissions into the atmosphere, is given by

$$pCO_2(t) = 278.37 + 399 f(t) \tag{28}$$

where

$$\begin{aligned} f(t) \quad = \quad & 0.131e^{-\Delta t/5.7} + 0.18e^{-\Delta t/28.7} + 0.372e^{-\Delta t/153} + 0.092e^{-\Delta t/440} + \\ & 0.121e^{-\Delta t/3600} + 0.06e^{-\Delta t/7800} + 0.0451e^{-\Delta t/109000} \end{aligned} \tag{29}$$

is the fraction of excess pCO_2 remaining after time Δt ($=t$-t_0 from Eq. 27; the time after the peak). The numbers above are shown complete with errors at the 95% confidence level from the fitting in Table 25 below. Or, to put it in more common language, translating the e-folding timescales of Equation 29 into half lives: 13.1% of excess pCO_2 is removed (or "decays") with a half-life of 4.0 years; 18% has a half-life of 19.9 years; 37.2% has a half-life of 106 years; 9.2% has a half-life of 300 years; 12.1% has a half-life of 2,500 years; 6% has a half-life of 5,400 years; and 4.51% has a half-life of 76,000 years. It should be noted that the fractions of the perturbation attributed to the longer timescales are underestimates on account of the emissions scenario being a pulse, rather than being drawn out over a decades to centuries as with our current real-world perturbation. The first three (sub-millennial) timescales are best quantified using models more complex than GENIE (GCMs); the latter three (supra-millennial) timescales are now able to be quantified using EMICs such as GENIE, as demonstrated. It would be interesting to test the quantification on output from other EMICs, such as the UVic model (Weaver et al., 2001).

The new result is the quantification of the silicate weathering timescale, which has only before been determined using box models (such as Sundquist (1991)), or estimated using geological evidence and reasoning (Berner and Caldeira, 1997).

Table 21: **Atmospheric pCO_2**, **Surface warming** and **Surface ocean acidification** reached at specific calendar years for model run with the most realistic parameter set

year	3000	5000	10000	20000	50000	100k	200k	500k	1000k
Atmospheric pCO_2 (ppm)	358	333	309	296	290	286	281	279	278
Surface warming (^{o}C)	0.959	0.697	0.394	0.235	0.155	0.100	0.042	0.006	0.003
Surface ocean acidification (pH units below 8.15 baseline)	0.085	0.055	0.025	0.009	0.004	0.001	-0.002	-0.003	-0.004

Table 22: **Percentages** of remaining excess **Atmospheric pCO_2**, **Surface warming** and **Surface ocean acidification** reached at specific calendar years for model run with the most realistic parameter set

year	3000	5000	10000	20000	50000	100k	200k	500k	1000k
Atmospheric pCO_2 (%)	20.0	13.8	7.7	4.6	3.0	1.9	0.8	0.1	0.1
Surface warming (%)	54.2	39.4	22.3	13.3	8.8	5.6	2.4	0.3	0.2
Surface ocean acidification (%)	34.1	22.1	10.0	3.7	1.4	0.4	-0.7	-1.4	-1.5

Table 23: **Years** that specific values of **Atmospheric pCO_2**, **Surface warming** and **Surface ocean acidification** are reached for model run with the most realistic parameter set

Atmospheric pCO_2 (ppm)	peak	677	value	500	400	350	300	278
	at year	2000	at year	2080	2350	3500	16010	-
Surface warming (^{o}C)	peak	1.77	value	2	1.5	1	0.5	0
	at year	2060	at year	-	2220	2850	8010	-
Surface ocean acidification	peak	0.25	value	0.2	0.15	0.1	0.05	0
(pH units below 8.15 baseline)	at year	2010	at year	2080	2220	2600	5600	130010

Table 24: **Years** that specific fractions of remaining excess **Atmospheric pCO_2**, **Surface warming** and **Surface ocean acidification** are reached for model run with the most realistic parameter set

fraction	90%	75%	50%	25%	10%	e^{-1}	e^{-2}	e^{-3}	e^{-4}	e^{-5}
Atmospheric pCO_2	2010	2020	2100	2550	7500	2220	5200	18010	110010	230010
Surface warming	2180	2350	3400	9000	38010	5600	20010	120010	240010	370010
Surface ocean acidification	2040	2100	2350	4400	10010	2800	8010	17000	40010	85000

Table 25: **Timescale fitting** for excess **Atmospheric pCO_2**, **Surface warming** and **Surface ocean acidification** decay for model run with the most realistic parameter set

Variable (V)	fit to $V(t) = b + h\sum_i w_i e^{-(t-t_0)/\tau_i}$										
			i	1	2	3	4	5	6	7	R^2
Atmospheric pCO_2 (ppm)	b	278.37±0.04	w_i (%)	13.1±0.3	18.0±0.2	37.2±0.2	9.2±0.7	12±1	6±1	4.51±0.06	0.99999998
	h	399±39	τ_i (yr)	5.7±0.1	28.7±0.6	153±2	440±20	3600±200	7800±700	109000±1000	
Surface warming (°C)	b	0.007±0.005	w_i (%)	41.1±0.4	45.4±0.4	13.5±0.4					0.99994
	h	1.802±0.007	τ_i (yr)	310±8	4900±100	101000±9000					
Surface ocean acidification (pH units below 8.15 baseline)	b	0.004±0.003	w_i (%)	100±1							0.95
	h	0.180±0.006	τ_i (yr)	1700±200							

5 Discussion & Conclusion

5.1 Key results

Using the RokGeM weathering model as described in this thesis, long-term carbon cycle perturbations (up to 1Myr) in scenarios of 1000 and 5000GtC fossil fuel emissions have been modelled with the GENIE Earth system model. It was discovered that (see Fig. 43):

- Parameters that had a significant effect on timescales for the draw-down of CO2 included:
  - the silicate weathering feedback switch;
  - the distribution of lithologies;
  - climate sensitivity.
- Parameters that had less of an effect were:
  - whether weathering was spatially explicit or not;
  - the formulation of runoff and productivity weathering feedbacks (whether explicit, or implicitly dependent on other variables);
  - weathering activation energy;
  - the fractional power dependence of weathering on runoff;
  - the temperature dependence of runoff.
- Parameters that did not have a significant effect were:
  - the river-routing scheme used;
  - whether or not the atmosphere was "short-circuited" in the carbon cycle.

5.1.1 Timescales for weathering effects on the carbon cycle

Fitting model output of atmospheric pCO_2 (amongst other variables) to a series of decaying exponentials enabled a precise quantification of the *e*-folding timescales for various sequestration processes. The longest timescales to come out of this analysis correspond to those of "terrestrial neutralisation" through the action of carbonate weathering, and removal of carbon to the geologic reservoir through the process of silicate weathering.

Dependent on the settings of various model parameters, carbonate weathering *e*-folding timescales were elucidated to be between 7.9 and 15kyr. It should be stated however that the picture is complicated somewhat by the fact that some fittings contain more timescales than others. This leaves room for confusion of terrestrial neutralisation timescales with those of sediment dissolution (or even these two timescales being combined into one) where there is only one timescale in the region of 10^3-10^4 years. Ambiguous timescales were omitted when looking in the range given above, as were timescales for the 5000GtC runs, which mostly had imperfect fits. Taking the parameter set deemed most realistic, the carbonate weathering timescale for GENIE-RokGeM is 7.8±0.7kyr. This figure is in agreement with previous estimates of 8.2kyr (Archer et al., 1997) and 8.3kyr (Ridgwell and Hargreaves, 2007), although it should be noted that these are results from models with a prescribed carbonate weathering flux.

Silicate weathering *e*-folding timescales were in the range 60-2800kyr (Here, picking the timescale is easier as it is merely the longest one). This very large range comes from extreme end member runs: a monolithological world covered in basalt gives the lower timescale (60±2kyr); a world with a global average silicate weathering flux in sole feedback with runoff (parameterised by temperature with a minimal linear coefficient) gives the upper timescale (2.8±0.2Myr, although note that the graphing method, as opposed to the curve-fitting method (§4.2) gives a timescale of only 800kyr). Again taking the most realistic parameter set, the timescale for silicate weathering for GENIE-RokGeM is 109±1kyr. This figure, which comes from using the spatially explicit (2D) GKWM, is much lower than previous box-modelling estimates of 300-400kyr (Sundquist, 1991). The shorter timescale is the result of a stronger weathering feedback. Silicate weathering is stronger in the spatially explicit model because it is amplified in the warm and wet climates of the low latitudes to a degree that more than compensates for weaker weathering at high latitudes; non-linear feedbacks mean that the overall global average weathering rates are greater in the 2D model than the 0D model.

Using the 0D Globavg version of RokGeM gives a timescale of 148kyr for an otherwise similar parameter set with all silicate weathering feedbacks switched on. This is still significantly shorter than the box-modelling estimates of Sundquist (1991). It should be noted that Sundquist's study is not directly comparable, as the perturbations are formulated as instantaneous changes in weathering rates rather than injections of CO_2 into the atmosphere (another study by Sundquist (1990) has such perturbations, but only over a shorter timescale

of 50kyr that does not include a full silicate weathering response). The silicate weathering feedback equation of Sundquist (1991) is

$$\frac{F_{ws}}{F_{wsi}} = \left(\frac{2R_{CO_2}}{1 + R_{CO_2}} \right)^{0.4} R_{CO_2}^{0.22} \tag{30}$$

where F_{ws} is the rate of silicate weathering; F_{wsi} the initial rate of silicate weathering, and R_{CO_2} the ratio of atmospheric CO_2 to it's initial value. Rearranging, and solving for $F_{ws} = 1.1F_{wsi}$ (a 10% increase in silicate weathering), yields an equivalent increase in atmospheric pCO_2 of 26%, or 153GtC (from the preindustrial level). This is somewhat smaller than the emissions pulses used here (1000GtC for the 109kyr and 148kyr timescales given above); but this merely emphasises the discrepancy between the two sets of results on account of larger perturbations giving longer timescales in general (as borne out by results from both Sundquist (1991) and this study). Taking the reverse approach, and applying Equation 30 to the instantaneous increase in atmospheric pCO_2 following a 1000GtC release, gives an increase in silicate weathering of 45%. This is greater than the GENIE-RokGeM output of a 22% instantaneous increase in silicate weathering (which rises to a peak of 34% after feedback with the maximal global warming that occurs by year 2050). Thus the silicate weathering feedback is stronger in the box model, yet it still has a longer timescale of action.

Other estimates of the silicate weathering timescale in the literature (200-400kyr) are from the work of Archer (Archer et al., 1997; Archer, 2005). These are taken as given (from Sundquist), without calculation or elaboration. Neverthless, Archer has done a good job popularising the notion of the "long tail" of climate change, drawing analogies with nuclear waste (Archer, 2008).

It should be stressed that these RokGeM-derived timescales as presented, are provisional, and subject to revisions due to various limitations of the model (see §5.2 below). Assuming minimal change from removing the short-circuiting of the atmosphere (§3.1), preindustrial weathering fluxes of DIC into the ocean can be exchanged for fluxes of CO_2 from the atmosphere. With this, weathering fluxes from the 2D weathering schemes of RokGeM compare favourably to previous estimates from the literature, although they are slightly lower: 17.5 and 19.8 Tmol CO_2 yr^{-1} vs. 21.5 - 26.8 Tmol CO_2 yr^{-1} (see Table 1; this is to be expected on account of the 2D RokGeM schemes being based on two of the offline models used to create the previous estimates). Were the modelled fluxes scaled to match the literature, even shorter timescales for the operation of the weathering feedbacks can be expected. On the other hand, including seasonality (which was omitted for the model runs here presented) slightly reduces annual average weathering, and would thus presumably slightly lengthen sequestration timescales. This is on account of a low in summer runoff more than compensating for a high in summer temperatures, and summer weathering fluxes being therefore only half of winter ones.

By performing an ensemble of otherwise-identically configured model runs across many different emissions sizes (say 10 in a range from 1000-10000GtC), it may be possible to fit a dependence on perturbation size to the various timescales to come out of the exponential fitting procedure. It would be interesting to marry this to recent work on solving the long-term carbon cycle by analytical means (Goodwin et al., 2008; Goodwin and Ridgwell, 2010).

Finally, a word of caution should be given about the *e*-fold timescale fitting as described. It was performed using a built in function of the technical software package Mathematica ("`NonlinearModelFit`"), which is essentially a black-box on account of it being closed-source code. This is not such a drawback when the arrived at functions can be manually tested to determine goodness-of-fit, however.

5.1.2 The effect of lithology on weathering over geological timescales

The large effect of lithology suggests that over geological timescales, weathering and hence climate can be greatly affected by tectonism leading to different rock-types presenting weatherable surfaces to the atmosphere. Looking at Earth history, tectonism's effect on continental lithology, as well as prominence and position, may well have played a major role in the regulation of atmospheric CO_2. The early Earth had a CO_2 rich atmosphere (Haqq-Misra et al., 2008), and no continental land masses. With the rise of volcanic arcs, the first continents were born, composed mainly of basalt. The results presented here (§3.8) show that a world (albeit with the present continental configuration) covered completely in basalt weathers significantly faster than the world including other types of rock. However, despite the presence of highly-weatherable basalt, CO_2 concentrations in the atmosphere remained high enough - factoring in the Faint Young Sun (Sagan and Mullen, 1972) - to sustain early life and liquid water; this was in part because there was much lower a continental area to weather. With the growth of the continents, more weatherable land surface was created; but, through subductive, metamorphic and then sedimentary recycling processes, other less weatherable rock types than basalt presented themselves as part of these land surfaces. These competing processes of continental growth and changing lithology likely

modulate geological-scale carbon cycling (and hence atmospheric pCO_2) in addition to the fundamental silicate-weathering-carbon-climate feedback. The degree of this modulation is a ripe subject for further study, using such models as GENIE with RokGeM.

5.1.3 Climate implications

The long tail of the climate-carbon cycle perturbation allows for said perturbation to interact with features of the Earth System not commonly associated with the Anthropocene. Although only perhaps 6% of the perturbation will persist over timescales in the 10^4yr range and 5% in the 10^5yr range (§4.4), given a large enough perturbation this gives ample room for effects on glacial-interglacial dynamics through interaction with ice-sheets or seafloor clathrate deposits. This is a target for future modelling with RokGeM and GENIE (see §5.3.2). Will the next ice age be "put on ice" (if you'll excuse the contradictory pun!)?

5.2 Limitations

5.2.1 Additional factors affecting weathering

With weathering, there are many variables to consider, which have a high degree of interdependence. As well as temperature and run-off, there are also the biotic components vegetation and soil to consider. These are to some degree summarised in the basic productivity dependence outlined in §3.5, although there is the risk of double-counting in that the temperature and runoff dependencies arise from field data on an Earth that is clearly biotic, and so presumably already include the effects of biology. It should be re-iterated here that the model runs for this thesis do not include an actively determined productivity as they are performed without the ENTS land surface component of GENIE (difficulties were experienced in obtaining a reasonably calibrated model setup). Assuming the problems with ENTS are overcome, an idea for future model runs would be to parameterise biologically enhanced soil CO_2 levels, which accelerate weathering (Lovelock and Whitfield, 1982).

Further nuances of weathering lead to the consideration that perhaps chemical and physical weathering processes should be separated out. Erosion has been shown to be a major influence on weathering (West et al., 2005); and differing levels of erosion divide weathering into "transport limited" and "kinetically limited" regimes (§1.2), which should also perhaps be separated in any weathering model that strives for realism. Physical weathering is also highly dependent on wind (dust abrasion) and relief, which is in turn a function of altitude. Wind driven dust is also a source of minerals that add to riverine flux usually deigned to be from weathering (Hilley and Porder, 2008). Another factor is ground frost, that leads to cracking and, therefore, mineral release.

A recent study of weathering in Japan (Hartmann et al., 2009) emphasises the role of slope as a factor influencing weathering flux. With the switching-on of orography GENIE-1, it may be possible to parameterise this in a crude way as another input for RokGeM. Hartmann also focuses on the role of dissolved silica (DSi) - a product of silicate weathering - in providing nutrients for ocean-dwelling diatoms, part of the "biological pump" involved in the sequestration of atmospheric pCO_2. High tectonic activity in the Pacific "ring of fire" leads to high levels of weathering, a high DSi flux entering the ocean, and hence significant CO_2 sequestration. The ocean biogeochemistry module of GENIE, BioGeM, includes a silica cycle already, so this should be a relatively straight forward addition to RokGeM.

The natural world is very complicated even when omitting anthropogenic factors; including the effects of the human habitation of Earth in modelling studies is a whole other challenge. It's easy to specify adding a certain amount of the greenhouse gas CO_2 to a well mixed atmosphere (as is done for the perturbation experiments for this thesis), but this is just one component of the multi-faceted interference of the human race in the biogeochemical cycles of Earth. Features of the Anthropocene (Zalasiewicz et al., 2008) particularly pertinent in their effects on carbonate and silicate weathering processes include: large increases in erosion rates due to unsustainable agricultural practices; the production of acid rain; the altering of vegetation types and areal cover; and the addition of mineral fertilisers to soil. These may be specified as boundary conditions, but applying them in a time-dependent manner over model runs spanning decamillennia (10^4) to lakhs (10^5) of years would involve pure speculation, considering global macro-economic effects cannot be predicted even years (cf. the "credit crunch") or centuries (cf. the industrial revolution) in advance.

Unfortunately, many of these factors will likely never be adequately parameterised in models on the scale of today's EMICs. This is on account of their variability over small spatial scales. Even across single kilometer-scale watersheds there can be wildly different weathering regimes; mountainous regions where erosion is dominant, merging into forested regions downstream, where thick soils mediate the weathering reaction.

Progress has been made recently in formulating general weathering rate relationships (Lasaga and Lüttge, 2001; Lüttge, 2006; Hellmann et al., 2010). Through looking at the molecular surface interactions involved, and

using equations analogous to those for crystal growth, general relationships based on Gibbs Free Energy and separate near- and far-from-equilibrium regimes were determined. Attempting to parameterise these for use in an EMIC proves to be problematic, however, on account of variables relating to concentrations in land water of the necessary aqueous carbonate species not being readily modelled.

A mechanistic model of weathering has recently been developed however (Roelandt et al., 2010). The Biosphere-Weathering at the Catchment Scale (B-WITCH) models soil geochemistry and upscales it to a 0.5°x0.5° continental scale. Chemistry is modelled directly through kinetic laws derived from Transition State Theory. Carbon and water inputs are provided through a coupling to a dynamical vegetation model. This mechanistic approach has the advantage over the parametric approach employed in RokGeM (and the other global models it was based on) in that it captures more detail on both temporal and spatial scales. Global parametric weathering models can only capture broad features relating to climate (temperature and runoff). Mechanistic models such as B-WITCH however, are more able to capture the rapid changes of the anthropocene, by modelling smaller scale changes in soil composition and chemistry. However, this comes with a computational overhead, and so far B-WITCH has only been used to model sub-continental scales.

So, as described above, the factors affecting weathering are multiple and interlinked; this poses a challenge for their teasing apart, which would be necessary in an ESM weathering module designed to be truly modular (as RokGeM strives to be). The inputs to the weathering module are dependant on the modules that it is run with, i.e. whether or not vegetation carbon affects weathering is dependant on whether the model includes a vegetation module (such as ENTS). Also, temperature and runoff fields are dependent on the atmospheric module coupled.

Ideally, a number of things would need to be in place within the GENIE model for a weathering module to provide realistic results. Accurate temperature and moisture fields for the continental interiors would be important, as would wind fields and orography for physical weathering. If it is the case that a 3D atmosphere (i.e. the IGCM) is necessary for this, then the feasibility of very long runs (10^5-10^6 years) becomes an issue as the IGCM 3D atmosphere module runs nearly 100 times slower than GENIE-1.

5.2.2 Errors in modelling

As documented in §2.5, a significant source of error in the RokGeM model is the quality of the model fields produced by the wider GENIE model (in particular the EMBM and ENTS) used as inputs. The ideal solution of course would be for these inputs to be better modelled (or simply better tuned) so as to get more accurate (in comparison to real-world data) results. Short of this - which is perhaps an unrealistic expectation given the very coarse resolution of the model as configured - an attempt was made to add an option to calibrate input fields to data (§2.5.4). This "quasi-offline" mode of operation for RokGeM, however, is still yet to be realised in a working example (model runs so far have crashed, presumably due to some as-yet unspotted bug in either the mathematical or computer-code implementation of the calibration).

Another source of error is the runoff-as-a-function-of-temperature parameterisation (§3.4). Using relations from box-modelling (Berner and Kothavala, 2001), the option is available in RokGeM to use temperature as a proxy for runoff. This might be considered a windfall, in light of the fact that runoff fields (§2.5.2) are perhaps even worse (less accurate) than temperature fields (§2.5.1) in GENIE (as configured). However, the correlation between runoff and temperature in real world data seems tenuous enough to stretch the credibility of the parameterisation. It is interesting to note that in the archetype WHAK weathering model (Walker et al., 1981), runoff is given an exponential dependence on temperature. Eyeballing the plots of Figure 20, it seems plausible that such a relation exists in the real world, at least for higher temperatures (>20°C), although attempts to fit such a function still give low correlations (R^2 <0.4) on account of the very wide scatter. An idea for further exploration is the dividing of the temperature scale into different runoff regimes, with different functional dependencies. Perhaps a linear function followed by an exponential give a better fit, although what looks like an increase in runoff at lower temperatures (water running off less-permeable frozen or near-frozen ground more easily) would also need to be factored in.

5.3 Further work

5.3.1 Higher resolutions

The GENIE model is capable of being run at a number of different spatial (and temporal) resolutions and grids. The option to run RokGeM at different resolutions is included by way of a parameter which specifies the directory that contains the lithological data files used. The GKWM and GEM-CO2 lithological data (see §3.7.1 and §3.7.2) were also gridded onto a 72x72 equal-area longitude-sine(latitude) grid (double the default

resolution), but this has not been tested on account of other climate and biogeochemical model configuration that is yet to be done, and the longer run times involved in running the model (it already takes ~5 weeks of CPU time to run 1Myr with the 36x36 version; the 72x72 version would run 8 or even 16 times slower on account of it also including the 16 level ocean.

A version of GENIE using a 16 level, rather than 8 level (GOLDSTEIN) ocean is now being widely used (Ridgwell et al., 2007; Goodwin and Ridgwell, 2010) on account of its higher-resolution ocean better reproducing biogeochemical tracer distributions. This version, which is only twice as slow to run as the version used for all results previously presented, is currently undergoing testing using RokGeM. With the current latest CPUs, it is now likely feasible to run a full carbon-cycle version of GENIE (including RokGeM, which only takes ~3% of the model run time) at 36x36x16 resolution, for 1Myr, inside a month.

Moves are underfoot (Simon Mueller, personal communication) to have spatial grids specified in GENIE as a run-time option. For RokGeM to take full advantage of this, the re-gridding of lithological data would have to be performed as part of the model initialisation; at present it has been done separately for each individual grid using stand-alone code written in Mathematica.

5.3.2 Applying the model to glacial-interglacial cycles

As highlighted above (§5.1.3), there is potential for the anthropogenic perturbation of the carbon cycle to cancel the next ice age, or even flip the Earth System into an ice-free "Hothouse" climate, last seen in the far-distant past, 3Ma in the Pliocence. This poses the unresolved question of just how large the perturbation has to be for this to occur.

Mysak (2008) reviews glacial inceptions. He concludes that due to Milankovitch forcing alone, the next glacial inception is unlikely to be within 50kyr, as long as atmospheric pCO_2 remains above preindustrial levels (>280ppm). Mysak models glacial inceptions using the McGill Paleoclimate Model (MPM), an EMIC that has detailed vegetation and ice-sheet parameterisations that allow a good representation of the important albedo feedbacks affecting the timing of glacial inception, despite it's 2D latitude-depth ocean, and compartmentalised continent grid being of lower resolution than GENIE. Other important feedbacks modelled in the MPM are the orography-temperature feedback, and freshwater fluxes and their affect on polar heat transport via the thermohaline circulation. For the case of atmospheric pCO_2 fixed at 300ppm, it was also found with the MPM that glaciation is avoided for the totality of a 100kyr run. Runs including a large anthropogenic warming perturbation (equivalent to thousands of GtC) show climate has little memory following global warming; i.e the timing of far distant glaciations is unaffected. However, (Archer, 2005) argues, and results presented in this thesis suggest, that this is not necessarily the case with an interactive carbon cycle present. The long tail in the perturbation stretches to possibly subsume future glaciations.

Using the CLIMBER-2 Earth System Model, and including a parameterisation of ice-sheet dynamics and a summer insolation-minimum for glacial inception, it was determined that with 5000GtC of emissions, the next glaciation is postponed indefinitely (Archer and Ganopolski, 2005), as an atmospheric concentration of >400ppm CO_2 persists. For 1000GtC emissions, the next glaciation is postponed from 50kyr to 130kyr hence; this is in agreement with Mysak (2008), as the atmospheric pCO_2 stabilises at a level slightly above 300ppm in this case.

The above results are without the inclusion of weathering, however. With the inclusion of the draw-down of atmospheric pCO_2 through weathering, presumably the delay in the inception of glaciation will be less. In the case of the 5000GtC, the delay will not be permanent. That is, unless the climate reaches a new equilibrium on account of changes in the land carbon inventory. In order to resolve the question satisfactorily with (the fully interactive ESM) GENIE, in addition to the RokGeM weathering model, the key processes of ice-sheet dynamics and methane clathrate release need to be adequately parameterised. There is an option to include the 3D ice sheet model GLIMMER (see Supplementary Information of Lenton et al. (2007)) in GENIE. The land model ENTS needs to be active in GENIE to determine whether there is a shifting in the equilibrium land carbon storage. The silicate weathering feedback timescale of ~110kyr given by GENIE-RokGeM is similar to the glacial-interglacial timescale over the past few cycles, as measured in the polar ice cores (Lüthi et al., 2008). This suggests that it could be sufficient to mitigate against severe anthropogenic disruption of the glacial-interglacial cycle.

5.3.3 Applying the model to Phanerozoic events

The inclusion of RokGeM into GENIE allows for long-term carbon cycle experiments to be performed in a manner general enough (geographic boundary conditions can be readily changed) to be applied to any geological interval or event. Past events in Earth history involving large perturbations in climate and the carbon cycle

include the Devonian rise of plants, basalt outpourings at the End Permian (Siberian traps) and End Cretaceous (Deccan traps), and the release of fossil carbon at the Paleocene-Eocene Thermal Maximum (PETM). These events are all future possibilities for modelling with GENIE-RokGeM.

The PETM is arguably the best analogue of future anthropogenic climate change we have from the geological past (Pagani et al., 2006). Previous work with GENIE (Panchuk et al., 2008) used a sediment data-model comparison, and modelled ocean circulation patterns resultant from relevant paleogeography, to constrain the source and amount of carbon released during the PETM. A pulse of 6800GtC into the atmosphere (and/or ocean) is modelled as the minimum required to match the sedimentary records. The version of GENIE used by Panchuk et al. (2008) has a fixed weathering flux applied uniformly throughout the global ocean. This is similar to the 0D version of RokGeM described herein, but without the coastal placement of weathering flux. Switching to coastal input only minimally slows down oceanic uptake of atmospheric carbon. However, the switching on of active feedbacks, and 2D weathering, has a large impact, even on the 10^2-10^3 year timescale relevant to initial "upward" perturbation of the carbon system following the PETM (see Fig. 31). This suggests a limit somewhat lower than 6800GtC as a lower bound for atmosphere-ocean input of carbon at the PETM.

Preliminary to GENIE-RokGeM PETM experiments, lithological data pertaining to the Eocene (55Ma) has been obtained from Lee Kump (personal communication; maps from (Gibbs et al., 1999) are also available). The dataset was re-gridded from its native 2° resolution onto the 36x36 GENIE grid. It was then shifted geographically to conform to already extant boundary conditions for a 55Ma version of GENIE. This involved a 1-2 grid square shifting of North America, Africa and Asia, and a significant shifting of Australia (6 grid cells South) to join it to Antarctica (this join was done in GENIE in order to simplify the solution to the barotropic streamfunction in the ocean model). Experiments are to be performed in the near future.

5.3.4 The entire Phanerozoic in a single EMIC model run?

Moving into the speculative realm, a perhaps ultimate instance of the EMIC class of models would be a model capable of being integrated over truly geological timescales; multi-millions of years: the inclusion of plate tectonics altering geography and cycling biogeochemical tracers between the mantle and lithospheric crust. This may seem a rather fantastic idea, but it is not wholly within the realms of science fiction. New advances in GPGPU (General Purpose Graphics Processing Unit) computation have enabled legacy code to be run at turbo-charged speeds; speed-ups of up to 100-fold are possible. Re-writing code in a manner that allows for interpretation by a GPU may not be a simple task (although efforts are being made to make the transition easier for the scientific community (Fortran CUDA), but were GENIE ever to have a substantial re-write, it would be a great boost to it's capabilities were it made GPU compliant. Not only could complete Phanerozoic runs be envisaged, but also ensembles for the purposes of tuning far larger than those that have been performed to date (Annan et al., 2005; Holden et al., 2009). From the point of view of a model developer, one major drawback (and bottleneck to progress) in the development of RokGeM has been the speed of iteration from code-writing to testing and back, on account of the long integration times needed for model spin-up. A GPGPU version of GENIE would also significantly speed up this process.

5.4 Conclusion

A new spatially-explicit weathering model, RokGeM, was developed for this thesis, designed as a modular component of a wider Earth System Model (GENIE). Following earlier modelling (GKWM (Bluth and Kump, 1994); GEM-CO2 (Amiotte-Suchet et al., 2003)) it has dependencies on runoff and temperature. It also has an explicit dependency on biological productivity, although this is yet to be thoroughly implemented on account of problems with the configuration of the coupled land surface scheme (ENTS). Other works in progress include the better optimising of input fields (of temperature, runoff and productivity), and the extension of the model into higher-resolution and paleo configurations. Not to mention the many factors complicating the accurate modelling of carbonate and silicate weathering on a global scale. Nevertheless, RokGeM is the first weathering model to be fully dynamically interactive with the carbon and climate cycles.

Following experimentation involving modelling of anthropogenic pulses of CO_2 emissions, new quantifications of the carbonate and (especially) silicate weathering feedback (e-folding) timescales were obtained. The technique used, of auto-fitting a variable number of exponentials to elucidate multiple e-folding timescales, is a useful tool for the accurate quantification of carbon cycle perturbations of any length and size. There is good potential for further work exploring the implications of this technique for quick but accurate analytical calculations of the form given by (Goodwin et al., 2008). The weathering timescale estimates for RokGeM cover a wide range depending on the parameter settings chosen. However, using parameters deemed to be most realistic, e-folding timescales of ~8kyr for carbonate weathering, and ~110kyr for silicate weathering are taken to be the headline

result of this thesis. Although shorter than previous estimates (200-400kyr), the silicate weathering timescale, through its definition by a full Earth System Model for the first time, should ideally be used to focus public attention on the future "long tail" of our in-progress carbon- and climate-cycle perturbation. A large section of the public are against nuclear technology on account of the long lifetimes of its waste. It would perhaps ultimately be good for us all if more people were aware of the vast timescales that the Anthropocene may stretch to.

References

Allen, M. R., D. J. Frame, C. Huntingford, C. D. Jones, J. A. Lowe, M. Meinshausen, and N. Meinshausen (2009, April). Warming caused by cumulative carbon emissions towards the trillionth tonne. *Nature 458*, 1163–1166, doi:10.1038/nature08019 Cited on page 27.

Amiotte-Suchet, Probst, and Ludwig (2003, April). Worldwide distribution of continental rock lithology: Implications for the atmospheric/soil CO_2 uptake by continental weathering and alkalinity river transport to the oceans. *GLOBAL BIOGEOCHEMICAL CYCLES 17*, 1038–1051, doi:10.1029/2002GB001891 Cited on pages 11, 13, 14, 23, 46, 47, 49, 55, and 84.

Amiotte Suchet, P. and J. L. Probst (1995, February). A global model for present-day atmospheric/soil CO_2 consumption by chemical erosion of continental rocks (GEM-CO_2). *Tellus Series B Chemical and Physical Meteorology B 47*, 273–280, doi:10.1034/j.1600-0889.47.issue1.23.x Cited on pages 13, 14, and 47.

Annan, J. D. and J. C. Hargreaves (2010, February). Efficient identification of ocean thermodynamics in a physical/biogeochemical ocean model with an iterative Importance Sampling method. *Ocean Modelling 33*, 205–215. Cited on page 16.

Annan, J. D., J. C. Hargreaves, N. R. Edwards, and R. Marsh (2005, January). Parameter estimation in an intermediate complexity earth system model using an ensemble kalman filter. *Ocean Modelling 8*(1-2), 135–154, doi:DOI: 10.1016/j.ocemod.2003.12.004 Cited on page 84.

Archer, D. (2005, September). Fate of fossil fuel CO_2 in geologic time. *Journal of Geophysical Research (Oceans) 110*(C9), 9–14, doi:10.1029/2004JC002625 Cited on pages 9, 15, 52, 69, 80, and 83.

Archer, D. (2008, October). *The long thaw: how humans are changing the next 100,000 years of Earth's climate*. Princeton. Cited on page 80.

Archer, D., B. Buffett, and V. Brovkin (2008, September). Ocean methane hydrates as a slow tipping point in the global carbon cycle. *PNAS*, 20596–20601, doi:10.1073/pnas.0800885105 Cited on page 64.

Archer, D., M. Eby, V. Brovkin, A. Ridgwell, L. Cao, U. Mikolajewicz, K. Caldeira, K. Matsumoto, G. Munhoven, A. Montenegro, and K. Tokos (2009, May). Atmospheric Lifetime of Fossil Fuel Carbon Dioxide. *Annual Review of Earth and Planetary Sciences 37*, 117–134, doi:10.1146/annurev.earth.031208.100206 Cited on page 29.

Archer, D. and A. Ganopolski (2005, May). A movable trigger: Fossil fuel CO_2 and the onset of the next glaciation. *Geochemistry, Geophysics, Geosystems 6*, 5003–+, doi:10.1029/2004GC000891 Cited on page 83.

Archer, D., H. Kheshgi, and E. Maier-Reimer (1997, February). Multiple timescales for neutralization of fossil fuel CO_2. *Geophysical Research Letters 24*, 405–408, doi:10.1029/97GL00168 Cited on pages 15, 79, and 80.

Bergman, N. M., T. M. Lenton, and W. A. J. (2004, May). Copse: A new model of biogeochemical cycling over phanerozoic time. *American Journal of Science 304*, 397–437. Cited on pages 13 and 15.

Berner (1991, April). A model for atmospheric CO_2 over phanerozoic time. *American Journal of Science 291*, 339–376, doi:10.1126/science.249.4975.1382 Cited on pages 14 and 45.

Berner, Lasanga, and Garrels (1983, September). The carbonate-silicate geochemical cycle and its effect on atmospheric carbon dioxide over the past 100 million years. *American Journal of Science 283*, 641–683. Cited on pages 14, 32, 34, and 37.

Berner, E. K. and R. A. Berner (1987). *Global Water Cycle: Geochemistry and Environment*. Prentice-Hall, Inc., Englewood Cliffs, New Jersey. Cited on page 13.

Berner, R. (1990, September). Atmospheric carbon dioxide levels over Phanerozoic time. *Science 249*, 1382–1386, doi:10.1126/science.249.4975.1382 Cited on page 14.

Berner, R. A. (1992, August). Weathering, plants, and the long-term carbon cycle. *Geochimica et Cosmochimica Acta 56*, 3225–3231, doi:10.1016/0016-7037(92)90300-8 Cited on page 13.

Berner, R. A. (1994, January). GEOCARB II; a revised model of atmospheric CO_2 over Phanerozoic time. *American Journal of Science 294*(1), 56–91. Cited on pages 14, 32, and 34.

Berner, R. A. and K. Caldeira (1997, October). The need for mass balance and feedback in the geochemical carbon cycle. *Geology 25*, 955–956, doi:10.1130/0091-7613(1997)025¡0955:TNFMBA¿2.3.CO;2 Cited on pages 11, 15, and 76.

Berner, R. A. and Z. Kothavala (2001, February). Geocarb III: A Revised Model of Atmospheric CO_2 over Phanerozoic Time. *American Journal of Science 301*(2), 182–204, doi:10.2475/ajs.301.2.182 Cited on pages 14, 34, 35, 37, and 82.

Bluth and Kump (1994, May). Lithologic and climatologic controls of river chemistry. *Geochimica et Cosmochimica Acta 58*, 2341–2359, doi:10.1016/0016-7037(94)90015-9 Cited on pages 11, 13, 47, and 84.

Boden, T., G. Marland, and R. Andres (2008), Global, Regional, and National Fossil-Fuel CO_2 Emissions. Carbon Dioxide Information Analysis Center, Oak Ridge National Laboratory, U.S. Department of Energy, Oak Ridge, Tenn., U.S.A., http://cdiac.ornl.gov/trends/emis/overview Cited on page 27.

Brady, P. V. (1991, October). The effect of silicate weathering on global temperature and atmospheric CO_2. *Journal of Geophysical Research 96*, 18101–18106, doi:10.1029/91JB01898 Cited on page 32.

Caldeira, K. and J. F. Kasting (1992, December). The life span of the biosphere revisited. *Nature 360*, 721–723, doi:10.1038/360721a0 Cited on page 14.

Canadell, J., D. Pataki, R. Gifford, R. Houghton, Y. Luo, M. Raupach, P. Smith, and W. Steffen (2007). *Saturation of the Terrestrial Carbon Sink*, Chapter 6, pp. 59–78. Springer-Verlag, doi:10.1007/978-3-540-32730-1_6 Cited on page 9.

Cao, L., M. Eby, A. Ridgwell, K. Caldeira, D. Archer, A. Ishida, F. Joos, K. Matsumoto, U. Mikolajewicz, A. Mouchet, J. C. Orr, G. Plattner, R. Schlitzer, K. Tokos, I. Totterdell, T. Tschumi, Y. Yamanaka, and A. Yool (2009, March). The role of ocean transport in the uptake of anthropogenic CO_2. *Biogeosciences 6*, 375–390, doi:10.5194/bg-6-375-2009 Cited on pages 7, 18, and 19.

Christensen, T. R., T. Johansson, H. J. Åkerman, M. Mastepanov, N. Malmer, T. Friborg, P. Crill, and B. H. Svensson (2004, February). Thawing sub-arctic permafrost: Effects on vegetation and methane emissions. *Geophysical Research Letters 31*, 4501–4503, doi:10.1029/2003GL018680 Cited on page 64.

Cirbus Sloan, L., G. J. S. Bluth, and G. M. Filippelli (1997, February). A comparison of spatially resolved and global mean reconstructions of continental denudation under ice-free and present conditions. *Paleoceanography 12*, 147–160, doi:10.1029/96PA03070 Cited on page 49.

Cochran, M. F. and R. A. Berner (1996, October). Promotion of chemical weathering by higher plants: field observations on hawaiian basalts. *Chemical Geology 132*(1-4), 71–77, doi:DOI: 10.1016/S0009-2541(96)00042-3 Cited on page 13.

Dessert, C., B. Dupré, J. Gaillardet, L. M. François, and C. J. Allégre (2003, December). Basalt weathering laws and the impact of basalt weathering on the global carbon cycle. *Chemical Geology 202*(3-4), 257–273, doi:DOI: 10.1016/j.chemgeo.2002.10.001 Cited on page 13.

Edwards, N. R., D. Cameron, and J. Rougier (2010, October). Precalibrating an intermediate complexity climate model. *Climate Dynamics*, 250–263, doi:10.1007/s00382-010-0921-0 Cited on page 16.

Edwards, N. R. and R. Marsh (2005, February). Uncertainties due to transport-parameter sensitivity in an efficient 3-D ocean-climate model. *Climate Dynamics 24*, 415–433, doi:10.1007/s00382-004-0508-8 Cited on pages 16 and 19.

Enting, Wigley, and Heimann (1994). Future emissions and concentrations of carbon dioxide: Key ocean-atmosphere-land analyses. Technical report, CSIRO. Cited on page 27.

European, U. (2007), European Commission, http://eur-lex.europa.eu/LexUriServ/LexUriServ.do?uri=CELEX:52007DC0002:EN:NOT Cited on pages 27 and 63.

Fekete, B. M., C. J. Vorosmarty, and W. Grabs (2000, February). Global, composite runoff fields based on observed river discharge and simulated water balances. Technical report, Global Runoff Data Center. Cited on pages 38 and 39.

Fekete, B. M., C. J. Vörösmarty, and W. Grabs (2002, August). High-resolution fields of global runoff combining observed river discharge and simulated water balances. *Global Biogeochemical Cycles 16*(3), 1042–1052, doi:10.1029/1999GB001254 Cited on pages 24, 34, 38, 39, and 50.

Foster, G. L. and D. Vance (2006, December). Negligible glacial-interglacial variation in continental chemical weathering rates. *Nature 444*, 918–921, doi:10.1038/nature05365 Cited on page 15.

Friedlingstein, P., P. Cox, R. Betts, L. Bopp, W. von Bloh, V. Brovkin, P. Cadule, S. Doney, M. Eby, I. Fung, G. Bala, J. John, C. Jones, F. Joos, T. Kato, M. Kawamiya, W. Knorr, K. Lindsay, H. D. Matthews, T. Raddatz, P. Rayner, C. Reick, E. Roeckner, K. Schnitzler, R. Schnur, K. Strassmann, A. J. Weaver, C. Yoshikawa, and N. Zeng (2006, July). Climate Carbon Cycle Feedback Analysis: Results from the C4MIP Model Intercomparison. *Journal of Climate 19*, 3337–3353, doi:10.1175/JCLI3800.1 Cited on page 9.

Gaillardet, J., B. Dupré, P. Louvat, and C. J. Allégre (1999, July). Global silicate weathering and CO_2 consumption rates deduced from the chemistry of large rivers. *Chemical Geology 159*(1-4), 3–30, doi:DOI: 10.1016/S0009-2541(99)00031-5 Cited on pages 13 and 14.

Gibbs, M. T., G. J. S. Bluth, P. J. Fawcett, and L. R. Kump (1999, November). Global chemical erosion over the last 250My; variations due to changes in paleogeography, paleoclimate, and paleogeology. *American Journal of Science 299*(7-9), 611–651, doi:10.2475/ajs.299.7-9.611 Cited on pages 11, 13, 14, 23, 46, 47, 55, and 84.

Gibbs, M. T. and L. R. Kump (1994, August). Global chemical erosion during the last glacial maximum and the present: Sensitivity to changes in lithology and hydrology. *Paleoceanography 9*, 529–544, doi:10.1029/94PA01009 Cited on pages 47 and 49.

Gislason, S. R., E. H. Oelkers, E. S. Eiriksdottir, M. I. Kardjilov, G. Gisladottir, B. Sigfusson, A. Snorrason, S. Elefsen, J. Hardardottir, P. Torssander, and N. Oskarsson (2008, February). The feedback between climate and weathering. *Mineral Mag 72*(1), 317–320, doi:10.1180/minmag.2008.072.1.317 Cited on page 12.

Gislason, S. R., E. H. Oelkers, E. S. Eiriksdottir, M. I. Kardjilov, G. Gisladottir, B. Sigfusson, A. Snorrason, S. Elefsen, J. Hardardottir, P. Torssander, and N. Oskarsson (2009, January). Direct evidence of the feedback between climate and weathering. *Earth and Planetary Science Letters 277*(1-2), 213–222, doi:10.1016/j.epsl.2008.10.018 Cited on page 12.

Gislason, S. R., E. H. Oelkers, and Á. Snorrason (2006, January). Role of river-suspended material in the global carbon cycle. *Geology 34*, 49–52, doi:10.1130/G22045.1 Cited on page 12.

Goodwin, P., M. J. Follows, and R. G. Williams (2008, September). Analytical relationships between atmospheric carbon dioxide, carbon emissions, and ocean processes. *Global Biogeochemical Cycles 22*, B3030+, doi:10.1029/2008GB003184 Cited on pages 80 and 84.

Goodwin, P. and A. Ridgwell (2010, May). Ocean-atmosphere partitioning of anthropogenic carbon dioxide on multimillennial timescales. *Global Biogeochemical Cycles 24*, GB2014–2026, doi:10.1029/2008GB003449 Cited on pages 10, 80, and 83.

Hansen, J., M. Sato, P. Kharecha, D. Beerling, R. Berner, V. Masson-Delmotte, M. Pagani, M. Raymo, D. L. Royer, and J. C. Zachos (2008, April). Target atmospheric CO_2: Where should humanity aim? *ArXiv e-prints*, doi:10.2174/1874282300802010217 Cited on page 76.

Haqq-Misra, J. D., S. D. Domagal-Goldman, P. J. Kasting, and J. F. Kasting (2008, December). A Revised, Hazy Methane Greenhouse for the Archean Earth. *Astrobiology 8*, 1127–1137, doi:10.1089/ast.2007.0197 Cited on page 80.

Hargreaves, J. C., J. D. Annan, N. R. Edwards, and R. Marsh (2004, December). An efficient climate forecasting method using an intermediate complexity Earth System Model and the ensemble Kalman filter. *Climate Dynamics 23*, 745–760, doi:10.1007/s00382-004-0471-4ELECTR: 7 Cited on pages 16 and 19.

Harmon, R. S., W. B. White, J. J. Drake, and J. W. Hess (1975, December). Regional Hydrochemistry of North American Carbonate Terrains. *Water Resources Research 11(6)*, 963–967, doi:10.1029/WR011i006p00963 Cited on page 32.

Hartmann, J., N. Jansen, H. H. Dürr, S. Kempe, and P. Köhler (2009, August). Global CO_2-consumption by chemical weathering: What is the contribution of highly active weathering regions? *Global and Planetary Change 69*(4), 185–194, doi:DOI: 10.1016/j.gloplacha.2009.07.007 Cited on page 81.

Hellmann, R., D. Daval, and D. Tisserand (2010). The dependence of albite feldspar dissolution kinetics on fluid saturation state at acid and basic ph: Progress towards a universal relation. *Comptes Rendus Geoscience 342*(7-8), 676–684, doi:DOI: 10.1016/j.crte.2009.06.004 Cited on page 81.

Hilley, G. E. and S. Porder (2008, November). A framework for predicting global silicate weathering and CO_2 drawdown rates over geologic time-scales. *Proceedings of the National Academy of Science 105*, 16855–16859, doi:10.1073/pnas.0801462105 Cited on pages 12 and 81.

Holden, P. B., N. R. Edwards, K. I. C. Oliver, T. M. Lenton, and R. D. Wilkinson (2009, July). A probabilistic calibration of climate sensitivity and terrestrial carbon change in GENIE-1. *Climate Dynamics*, 785–806, doi:10.1007/s00382-009-0630-8 Cited on pages 16 and 84.

Huntingford, C. and P. M. Cox (2000). An analogue model to derive additional climate change scenarios from existing GCM simulations. *Climate Dynamics 16*, 575–586, doi:10.1007/s003820000067 Cited on page 26.

Imhoff, M. L., L. Bounoua, T. Ricketts, C. Loucks, R. Harriss, and W. T. Lawrence (2004, June). Global patterns in human consumption of net primary production. *Nature 429*, 870–873, doi:10.1038/nature02619 Cited on page 26.

Joos, F., M. Bruno, R. Fink, U. Siegenthaler, T. F. Stocker, C. Le Quéré, and J. L. Sarmiento (1996, July). An efficient and accurate representation of complex oceanic and biospheric models of anthropogenic carbon uptake. *Tellus Series B Chemical and Physical Meteorology B 48*, 397–417, doi:10.1034/j.1600-0889.1996.t01-2-00006.x Cited on page 69.

Kelly, E., O. Chadwick, and T. Hilinski (1998, August). The effect of plants on mineral weathering. *Biogeochemistry 42*, 21–53. Cited on page 13.

Kump, L. R., S. L. Brantley, and M. A. Arthur (2000, May). Chemical Weathering, Atmospheric CO_2, and Climate. *Annual Review of Earth and Planetary Sciences 28*, 611–667, doi:10.1146/annurev.earth.28.1.611 Cited on page 12.

Lasaga, A. C. and A. Lüttge (2001, March). Variation of Crystal Dissolution Rate Based on a Dissolution Stepwave Model. *Science 291*(5512), 2400–2404, doi:10.1126/science.1058173 Cited on page 81.

Le Quere, C., M. R. Raupach, J. G. Canadell, and G. Marland (2009, November). Trends in the sources and sinks of carbon dioxide. *Nature Geoscience 2*(12), 831–836, doi:10.1038/ngeo689 Cited on page 9.

Le Quéré, C., C. Rödenbeck, E. T. Buitenhuis, T. J. Conway, R. Langenfelds, A. Gomez, C. Labuschagne, M. Ramonet, T. Nakazawa, N. Metzl, N. Gillett, and M. Heimann (2007, June). Saturation of the Southern Ocean CO_2 Sink Due to Recent Climate Change. *Science 316*, 1735–1738, doi:10.1126/science.1136188 Cited on page 9.

Lenton, T. M. and C. Britton (2006, August). Enhanced carbonate and silicate weathering accelerates recovery from fossil fuel CO_2 perturbations. *Global Biogeochemical Cycles 20*, B3009–3021, doi:10.1029/2005GB002678 Cited on pages 13, 15, and 45.

Lenton, T. M., R. Marsh, A. R. Price, D. J. Lunt, Y. Aksenov, J. D. Annan, T. Cooper-Chadwick, S. J. Cox, N. R. Edwards, S. Goswami, J. C. Hargreaves, P. P. Harris, Z. Jiao, V. N. Livina, A. J. Payne, I. C. Rutt, J. G. Shepherd, P. J. Valdes, G. Williams, M. S. Williamson, and A. Yool (2007, June). Effects of atmospheric dynamics and ocean resolution on bi-stability of the thermohaline circulation examined using the Grid ENabled Integrated Earth system modelling (GENIE) framework. *Climate Dynamics 29*, 591–613, doi:10.1007/s00382-007-0254-9 Cited on page 83.

Lenton, T. M., R. J. Myerscough, R. Marsh, V. N. Livina, A. R. Price, S. J. Cox, and The Genie Team (2009, March). Using GENIE to study a tipping point in the climate system. *Royal Society of London Philosophical Transactions Series A 367*, 871–884, doi:10.1098/rsta.2008.0171 Cited on page 64.

Lenton, T. M. and W. von Bloh (2001, May). Biotic feedback extends the life span of the biosphere. *Geophysical Research Letters 28*, 1715–1718, doi:10.1029/2000GL012198 Cited on pages 13 and 14.

Lenton, T. M., M. S. Williamson, N. R. Edwards, R. Marsh, A. R. Price, A. J. Ridgwell, J. G. Shepherd, and S. J. Cox (2006, June). Millennial timescale carbon cycle and climate change in an efficient Earth system model. *Climate Dynamics 26*, 687–711, doi:10.1007/s00382-006-0109-9 Cited on page 26.

Lovelock, J. E. and A. J. Watson (1982, August). The regulation of carbon dioxide and climate: Gaia or geochemistry. *Planetary and Space Science 30*(8), 795–802, doi:DOI: 10.1016/0032-0633(82)90112-X Cited on page 14.

Lovelock, J. E. and M. Whitfield (1982, April). Life span of the biosphere. *Nature 296*, 561–563, doi:10.1038/296561a0 Cited on pages 14 and 81.

Lüthi, D., M. Le Floch, B. Bereiter, T. Blunier, J.-M. Barnola, U. Siegenthaler, D. Raynaud, J. Jouzel, H. Fischer, K. Kawamura, and T. F. Stocker (2008, May). High-resolution carbon dioxide concentration record 650,000-800,000 years before present. *Nature 453*, 379–382, doi:10.1038/nature06949 Cited on page 83.

Lüttge, A. (2006). Crystal dissolution kinetics and gibbs free energy. *Journal of Electron Spectroscopy and Related Phenomena 150*(2-3), 248–259, doi:DOI: 10.1016/j.elspec.2005.06.007 Cited on page 81.

Meinshausen, M., N. Meinshausen, W. Hare, S. C. B. Raper, K. Frieler, R. Knutti, D. J. Frame, and M. R. Allen (2009, April). Greenhouse-gas emission targets for limiting global warming to 2^{o}C. *Nature 458*, 1158–1162, doi:10.1038/nature08017 Cited on page 27.

Meissner, K. J., A. J. Weaver, H. D. Matthews, and P. M. Cox (2003, October). The role of land surface dynamics in glacial inception: a study with the UVic Earth System Model. *Climate Dynamics 21*, 515–537, doi:10.1007/s00382-003-0352-2 Cited on page 23.

Meybeck (1987, May). Global chemical weathering of surfical rocks estimated from river disolved loads. *American Journal of Science 287*, 401–428. Cited on pages 13 and 14.

Montenegro, A., V. Brovkin, M. Eby, D. Archer, and A. J. Weaver (2007, October). Long term fate of anthropogenic carbon. *Geophysical Research Letters 34*, 19707–19711, doi:10.1029/2007GL030905 Cited on page 15.

Moore, G. E. (1965, April). Cramming More Components Onto Integrated Circuits. *Electronics 38*(8), 114–117. Cited on page 15.

Munhoven, G. (2002, June). Glacial interglacial changes of continental weathering: estimates of the related CO_2 and HCO_3^- flux variations and their uncertainties. *Global and Planetary Change 33*, 155–176, doi:10.1016/S0921-8181(02)00068-1 Cited on page 15.

Mysak, L. A. (2008, Sep). Glacial inceptions: Past and future. *ATMOSPHERE-OCEAN 49*, 317–341, doi:10.3137/ao.460303 Cited on page 83.

New, M., M. Hulme, and P. Jones (1999, March). Representing Twentieth-Century Space-Time Climate Variability. Part I: Development of a 1961-90 Mean Monthly Terrestrial Climatology. *Journal of Climate 12*, 829–856, doi:10.1175/1520-0442(1999)012¡0829:RTCSTC¿2.0.CO;2 Cited on pages 22, 34, 38, and 50.

Pagani, M., K. Caldeira, D. Archer, and J. C. Zachos (2006, December). An Ancient Carbon Mystery. *Science 314*(5805), 1556–1557, doi:10.1126/science.1136110 Cited on page 84.

Panchuk, K., A. Ridgwell, and L. R. Kump (2008, April). Sedimentary response to Paleocene-Eocene Thermal Maximum carbon release: A model-data comparison. *Geology 36*, 315–318. Cited on page 84.

Pidwirny, M. (2006). *Fundamentals of Physical Geography*, Chapter The Hydrological Cycle, pp. 1. http://www.physicalgeography.net/fundamentals/8b.html. Cited on page 23.

Price, A., I. Voutchkov, G. Pound, N. Edwards, T. Lenton, and S. Cox (2006, December). Multiobjective Tuning of Grid-Enabled Earth System Models Using a Non-dominated Sorting Genetic Algorithm (NSGA-II). *e-Science and Grid Computing, International Conference on 0*, 117, doi:http://doi.ieeecomputersociety.org/10.1109/E-SCIENCE.2006.103 Cited on page 16.

Price, A. R., G. Xue, A. Yool, D. J. Lunt, P. J. Valdes, T. M. Lenton, J. L. Wason, G. E. Pound, and S. J. Cox (2007, February). Optimization of integrated earth system model components using grid-enabled data management and computation: Research articles. *Concurr. Comput. : Pract. Exper. 19*(2), 153–165, doi:http://dx.doi.org/10.1002/cpe.v19:2 Cited on page 16.

Raymo, M. E. and W. F. Ruddiman (1992, September). Tectonic forcing of late Cenozoic climate. *Nature 359*, 117–122, doi:10.1038/359117a0 Cited on page 15.

Raymo, M. E., W. F. Ruddiman, and P. N. Froelich (1988, July). Influence of late Cenozoic mountain building on ocean geochemical cycles. *Geology 16*, 649–653, doi:10.1130/0091-7613(1988)016¡0649:IOLCMB¿2.3.CO;2 Cited on page 13.

Revelle, R. and H. E. Suiss (1957, February). Carbon dioxide exchange between atmosphere and ocean and the question of an increase of atmospheric CO_2 during the past decades. *Telus 9*, 18–27, doi:10.1111/j.2153-3490.1957.tb01849.x Cited on page 9.

Ridgwell, A. (2007, October). Interpreting transient carbonate compensation depth changes by marine sediment core modeling. *Paleoceanography 22*(26), PA4102–4111, doi:10.1029/2006PA001372 Cited on page 21.

Ridgwell, A. and U. Edwards (2007). *Geological Carbon Sinks*, Chapter 6, pp. 74–97. CAB International, doi:10.1079/9781845931896.0074 Cited on pages 10, 11, and 63.

Ridgwell, A. and J. C. Hargreaves (2007, May). Regulation of atmospheric CO_2 by deep-sea sediments in an Earth system model. *Global Biogeochemical Cycles 21*, GB2008–2021, doi:10.1029/2006GB002764 Cited on pages 15, 16, 19, and 79.

Ridgwell, A., J. C. Hargreaves, N. R. Edwards, J. D. Annan, T. M. Lenton, R. Marsh, A. Yool, and A. Watson (2007, January). Marine geochemical data assimilation in an efficient Earth System Model of global biogeochemical cycling. *Biogeosciences 4*, 87–104, doi:10.5194/bg-4-87-2007 Cited on pages 16, 18, 19, and 83.

Riebe, C. S., J. W. Kirchner, and R. C. Finkel (2004, August). Erosional and climatic effects on long-term chemical weathering rates in granitic landscapes spanning diverse climate regimes. *Earth and Planetary Science Letters 224*, 547–562, doi:10.1016/j.epsl.2004.05.019 Cited on page 11.

Roelandt, C., Y. Godderis, M.-P. Bonnet, and F. Sondag (2010, April). Coupled modeling of biospheric and chemical weathering processes at the continental scale. *Global Biogeochem. Cycles 24*(2), GB2004–. Cited on page 82.

Rutledge, D. (2010). Estimating long-term world coal production with logit and probit transforms. *International Journal of Coal Geology In Press, Corrected Proof*, –, doi:DOI: 10.1016/j.coal.2010.10.012 Cited on page 27.

Sagan, C. and G. Mullen (1972, July). Earth and Mars: Evolution of Atmospheres and Surface Temperatures. *Science 177*, 52–56, doi:10.1126/science.177.4043.52 Cited on page 80.

Schneider von Deimling, T., H. Held, A. Ganopolski, and S. Rahmstorf (2006, August). Climate sensitivity estimated from ensemble simulations of glacial climate. *Climate Dynamics 27*, 149–163, doi:10.1007/s00382-006-0126-8 Cited on page 55.

Schubert, R., H.-J. Schellnhuber, N. Buchmann, A. Epiney, R. Griebhammer, M. Kulessa, D. Messner, S. Rahmstorf, and J. Schmid (2006, March). The future oceans - warming up, rising high, turning sour. Technical report, German Advisory Council on Global Change (WBGU). Cited on page 64.

Schwartzman, D. W. and T. Volk (1989, August). Biotic enhancement of weathering and the habitability of Earth. *Nature 340*, 457–460, doi:10.1038/340457a0 Cited on pages 13 and 14.

Schwartzman, D. W. and T. Volk (1991, October). Biotic enhancement of weathering and surface temperatures on earth since the origin of life. *Global and Planetary Change 4*, 357–371, doi:10.1016/0921-8181(91)90002-E Cited on page 14.

Schwarz, G. (1978, March). Estimating the dimension of a model. *The annals of statistics 6*(2), 461–464. Cited on page 68.

Sharp, M., J. Parkes, B. Cragg, I. J. Fairchild, H. Lamb, and M. Tranter (1999, February). Widespread bacterial populations at glacier beds and their relationship to rock weathering and carbon cycling. *Geology 27*, 107–110, doi:10.1130/0091-7613(1999)027¡0107:WBPAGB¿2.3.CO;2 Cited on page 46.

Solomon, S., D. Qin, M. Manning, R. Alley, T. Berntsen, N. Bindoff, Z. Chen, A. Chidthaisong, J. Gregory, G. Hegerl, M. Heimann, B. Hewitson, B. Hoskins, F. Joos, J. Jouzel, V. Kattsov, U. Lohmann, T. Matsuno, M. Molina, N. Nicholls, J. Overpeck, G. Raga, V. Ramaswamy, J. Ren, M. Rusticucci, R. Somerville, T. Stocker, P. Whetton, R. Wood, and D. Wratt (2007). Climate Change 2007: The Physical Science Basis. Contribution of Working Group I to the Fourth Assessment Report of the Intergovernmental Panel on Climate Change. Technical report, Intergovernmental Panel on Climate Change. Cited on pages 18, 39, and 55.

Sundquist, E. (1991, March). Steady- and non-steady-state carbonate-silicate controls on atmospheric CO_2. *Quaternary Science Reviews 10*, 283–296, doi:10.1016/0277-3791(91)90026-Q Cited on pages 15, 69, 76, 79, and 80.

Sundquist, E. T. (1990, June). Influence of Deep-Sea Benthic Processes on Atmospheric CO_2. *Royal Society of London Philosophical Transactions Series A 331*, 155–165. Cited on page 79.

Tans, P. (2010), NOAA/ESRL, `http://www.esrl.noaa.gov/gmd/ccgg/trends` Cited on page 9.

Tipper, E. T., M. J. Bickle, A. Galy, A. J. West, C. Pomiès, and H. J. Chapman (2006, June). The short term climatic sensitivity of carbonate and silicate weathering fluxes: Insight from seasonal variations in river chemistry. *Geochimica et Cosmochimica Acta 70*, 2737–2754, doi:10.1016/j.gca.2006.03.005 Cited on page 11.

Vörösmarty, C. J., B. M. Fekete, M. Meybeck, and R. B. Lammers (2000a, October). Geomorphometric attributes of the global system of rivers at 30-minute spatial resolution. *Journal of Hydrology 237*(1-2), 17–39, doi:10.1016/S0022-1694(00)00282-1 Cited on page 46.

Vörösmarty, C. J., B. M. Fekete, M. Meybeck, and R. B. Lammers (2000b, June). Global system of rivers: Its role in organizing continental land mass and defining land-to-ocean linkages. *Global Biogeochemical Cycles 14*, 599–622, doi:10.1029/1999GB900092 Cited on page 46.

Walker, J. C. G., P. B. Hays, and J. F. Kasting (1981, October). A negative feedback mechanism for the long-term stabilization of the earth's surface temperature. *Journal of Geophysical Research 86*, 9776–9782, doi:10.1029/JC086iC10p09776 Cited on pages 11, 14, and 82.

Weaver et al. (2001, April). The UVic earth system climate model: Model description, climatology, and application to past, present and future climates. *ATMOSPHERE-OCEAN 39*, 1–68. Cited on pages 16 and 76.

West, A. J., A. Galy, and M. Bickle (2005, June). Tectonic and climatic controls on silicate weathering. *Earth and Planetary Science Letters 235*, 211–228, doi:10.1016/j.epsl.2005.03.020 Cited on pages 11, 32, 34, and 81.

Williamson, M., T. Lenton, J. Shepherd, and N. Edwards (2006, October). An efficient numerical terrestrial scheme (ents) for earth system modelling. *Ecological Modelling 198*(3-4), 362–374, doi:10.1016/j.ecolmodel.2006.05.027 Cited on page 16.

World-Leaders (2009), United Nations Framework Convention on Climate Change (UNFCC), http://unfccc.int/resource/docs/2009/cop15/eng/l07.pdf Cited on page 63.

Zalasiewicz, J., M. Williams, A. Smith, T. Barry, A. Coe, P. Bown, P. Brenchley, D. Cantrill, A. Gale, P. Gibbard, F. Gregory, M. Hounslow, A. Kerr, P. Pearson, R. Knox, J. Powell, C. Waters, J. Marshall, M. Oates, P. Rawson, and P. Stone (2008, February). Are we now living in the Anthropocene? *GSA Today*, 4–8, doi:10.1130/GSAT01802A.1 Cited on page 81.

A Full time-series results

A.1 Time-series output years

1,000.5	3,000.5	10,010.5	100,010.5
1,990.5	3,100.5	11,000.5	110,010.5
2,002.5	3,200.5	12,010.5	120,010.5
2,010.5	3,300.5	13,000.5	130,010.5
2,020.5	3,400.5	14,010.5	140,010.5
2,030.5	3,500.5	15,000.5	150,010.5
2,040.5	3,600.5	16,010.5	160,010.5
2,050.5	3,700.5	17,000.5	170,010.5
2,060.5	3,800.5	18,010.5	180,010.5
2,070.5	3,900.5	19,000.5	190,010.5
2,080.5	4,010.5	20,010.5	200,010.5
2,090.5	4,100.5	22,010.5	220,010.5
2,100.5	4,200.5	24,010.5	240,010.5
2,120.5	4,300.5	26,010.5	260,010.5
2,140.5	4,400.5	28,010.5	280,010.5
2,160.5	4,500.5	30,010.5	300,010.5
2,180.5	4,600.5	32,010.5	320,010.5
2,200.5	4,700.5	34,010.5	340,010.5
2,220.5	4,800.5	36,010.5	360,010.5
2,240.5	4,900.5	38,010.5	380,010.5
2,260.5	5,000.5	40,010.5	400,010.5
2,280.5	5,200.5	42,010.5	420,010.5
2,300.5	5,400.5	44,010.5	440,010.5
2,350.5	5,600.5	46,010.5	460,010.5
2,400.5	5,800.5	48,010.5	480,010.5
2,450.5	6,010.5	50,010.5	500,010.5
2,500.5	6,200.5	55,000.5	550,010.5
2,550.5	6,400.5	60,010.5	600,010.5
2,600.5	6,600.5	65,000.5	650,010.5
2,650.5	6,800.5	70,010.5	700,010.5
2,700.5	7,000.5	75,000.5	750,010.5
2,750.5	7,500.5	80,010.5	800,010.5
2,800.5	8,010.5	85,000.5	850,010.5
2,850.5	8,500.5	90,010.5	900,010.5
2,900.5	9,000.5	95,000.5	950,010.5
2,950.5	9,500.5		1,000,010.5

Table 26: Time-series output years for pulse emissions scenarios with pulse at year 1990. Half-years are specified as some output (from BioGeM and SedGeM) is averaged over a year straddling the time-point specified. Each vertical block of numbers corresponds to a panel in the broken linear time-series plots throughout the thesis.

A.2 Time-series of key variables

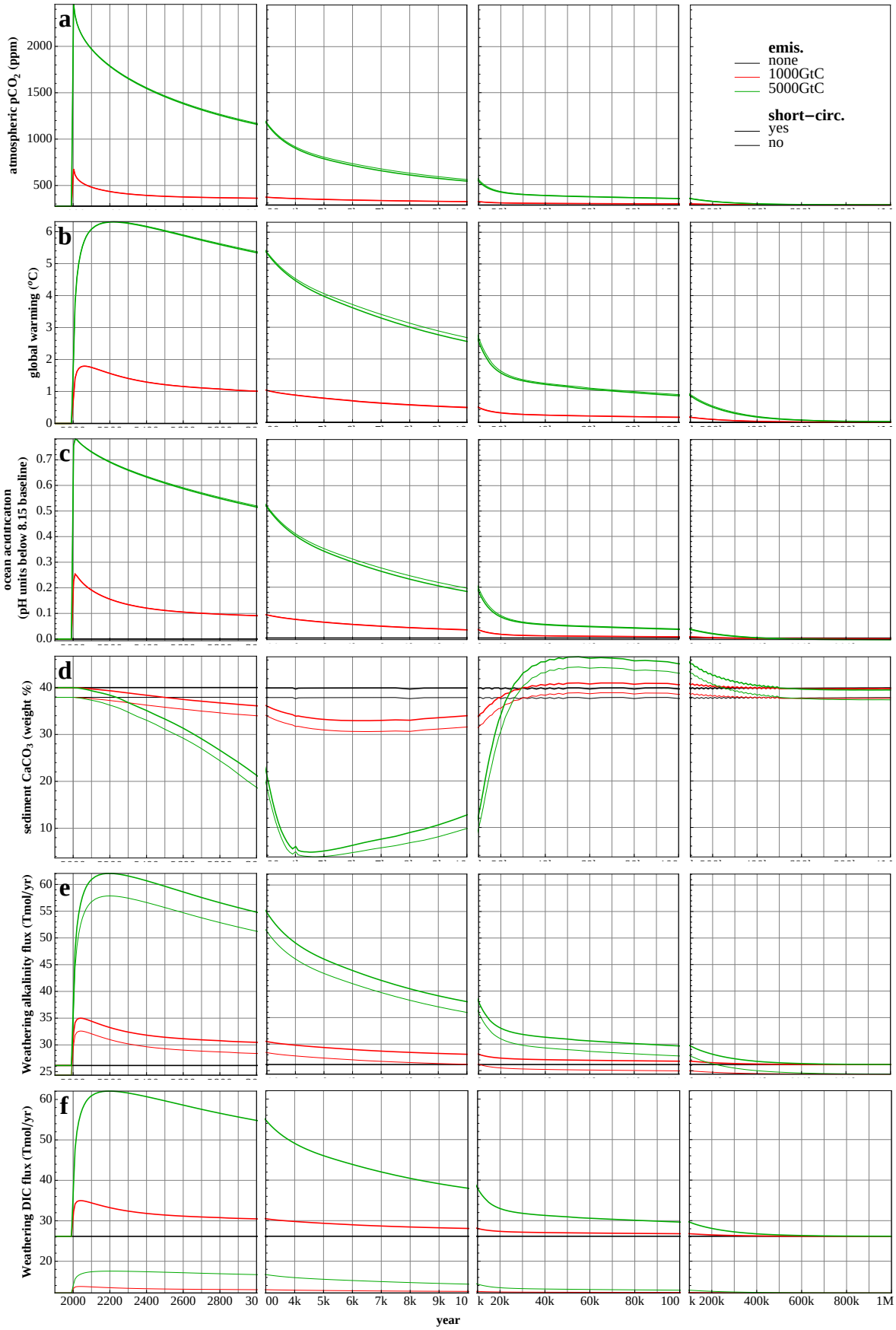

Figure 44: Timeseries of key variables for short-circuit test ensemble

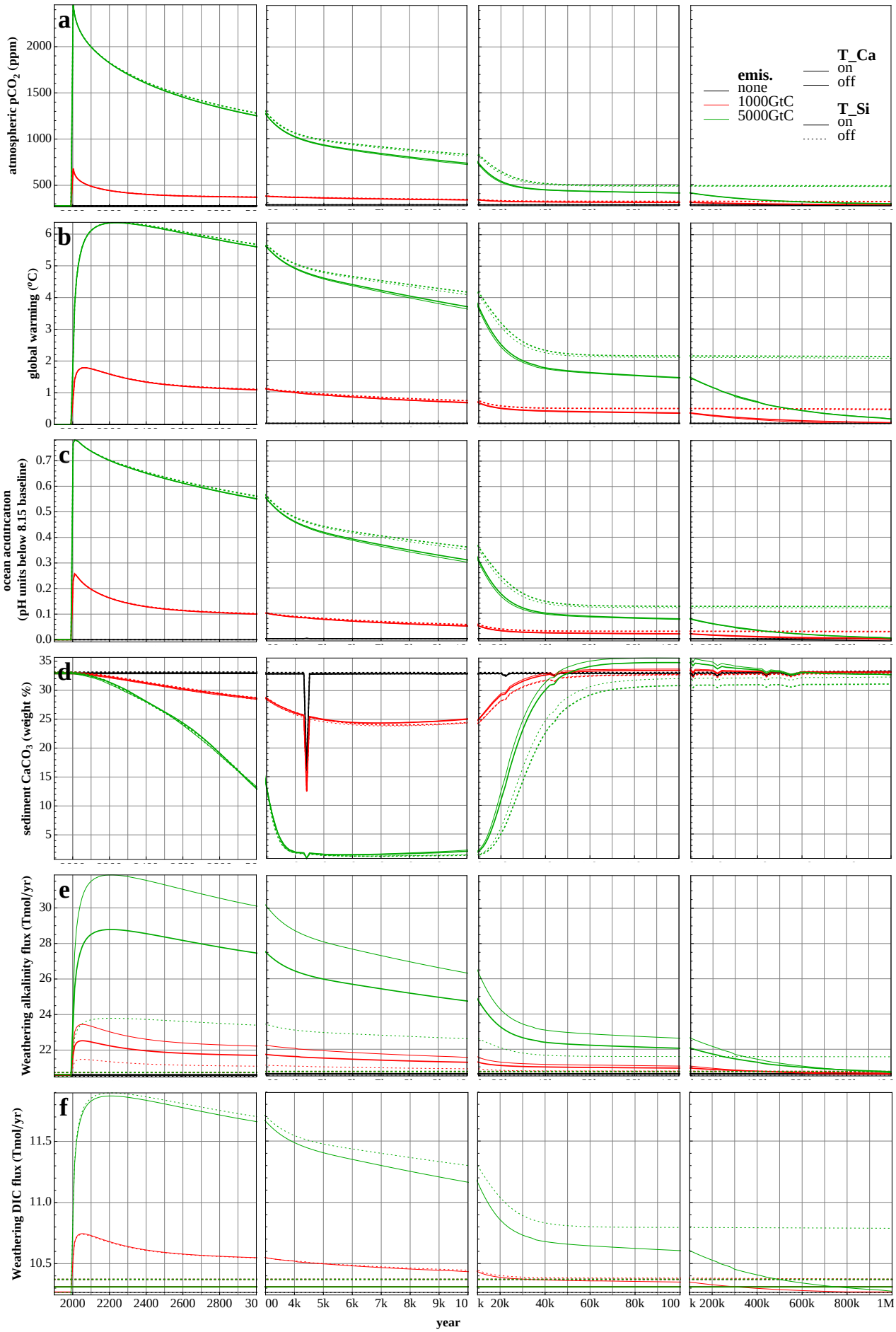

Figure 45: Timeseries of key variables for weathering-temperature feedbacks ensemble

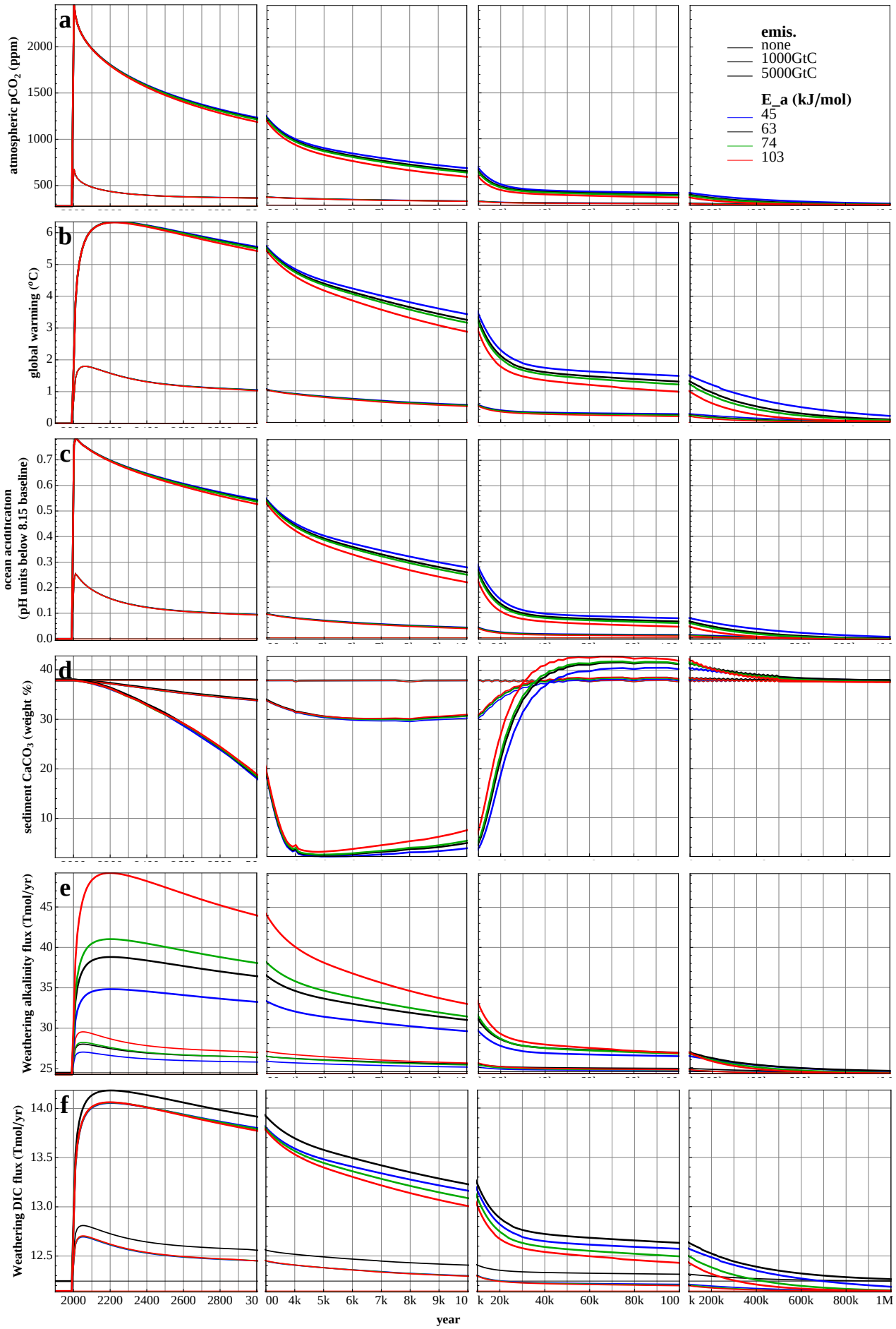

Figure 46: Timeseries of key variables for weathering activation energy ensemble

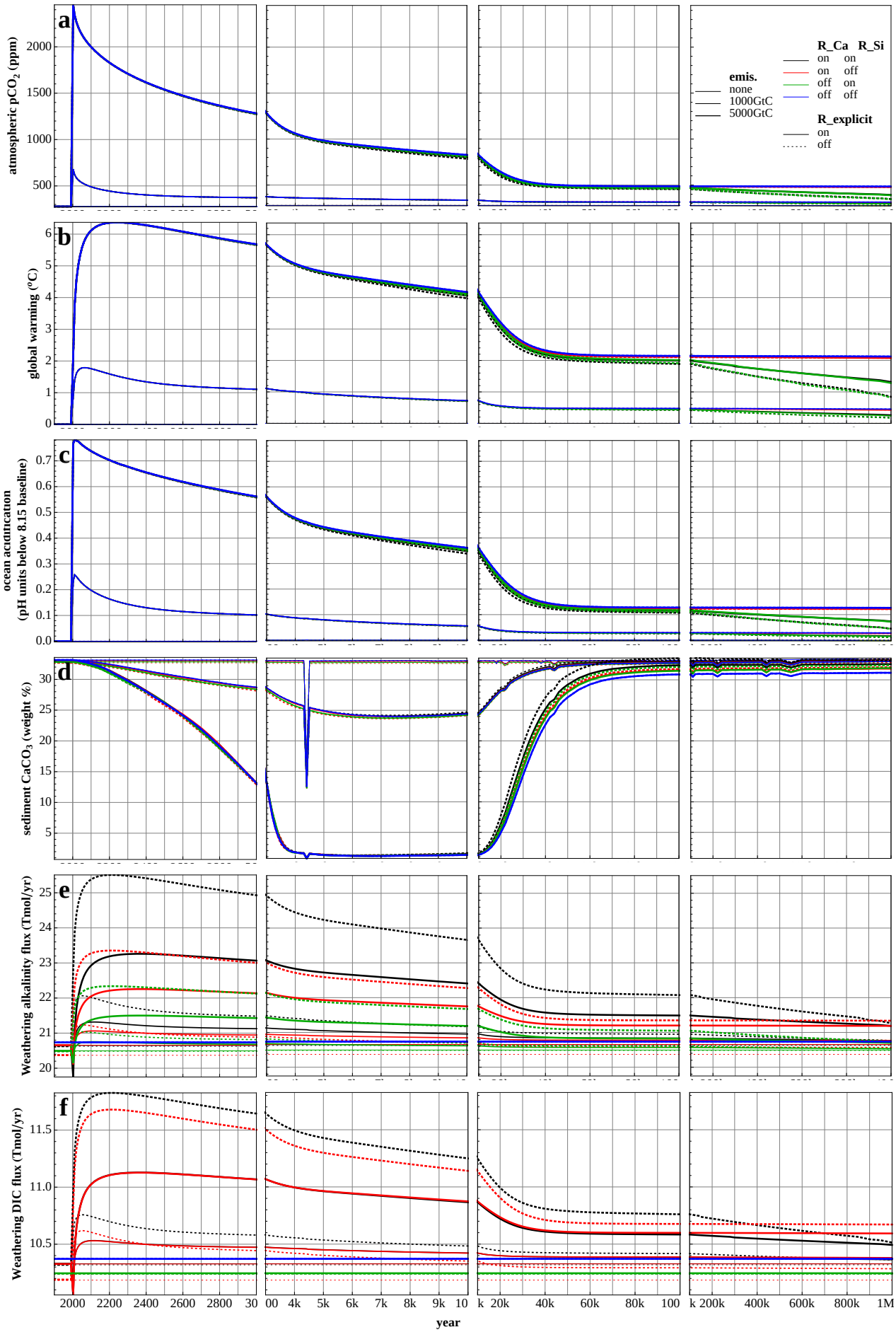

Figure 47: Timeseries of key variables for weathering-runoff feedbacks ensemble

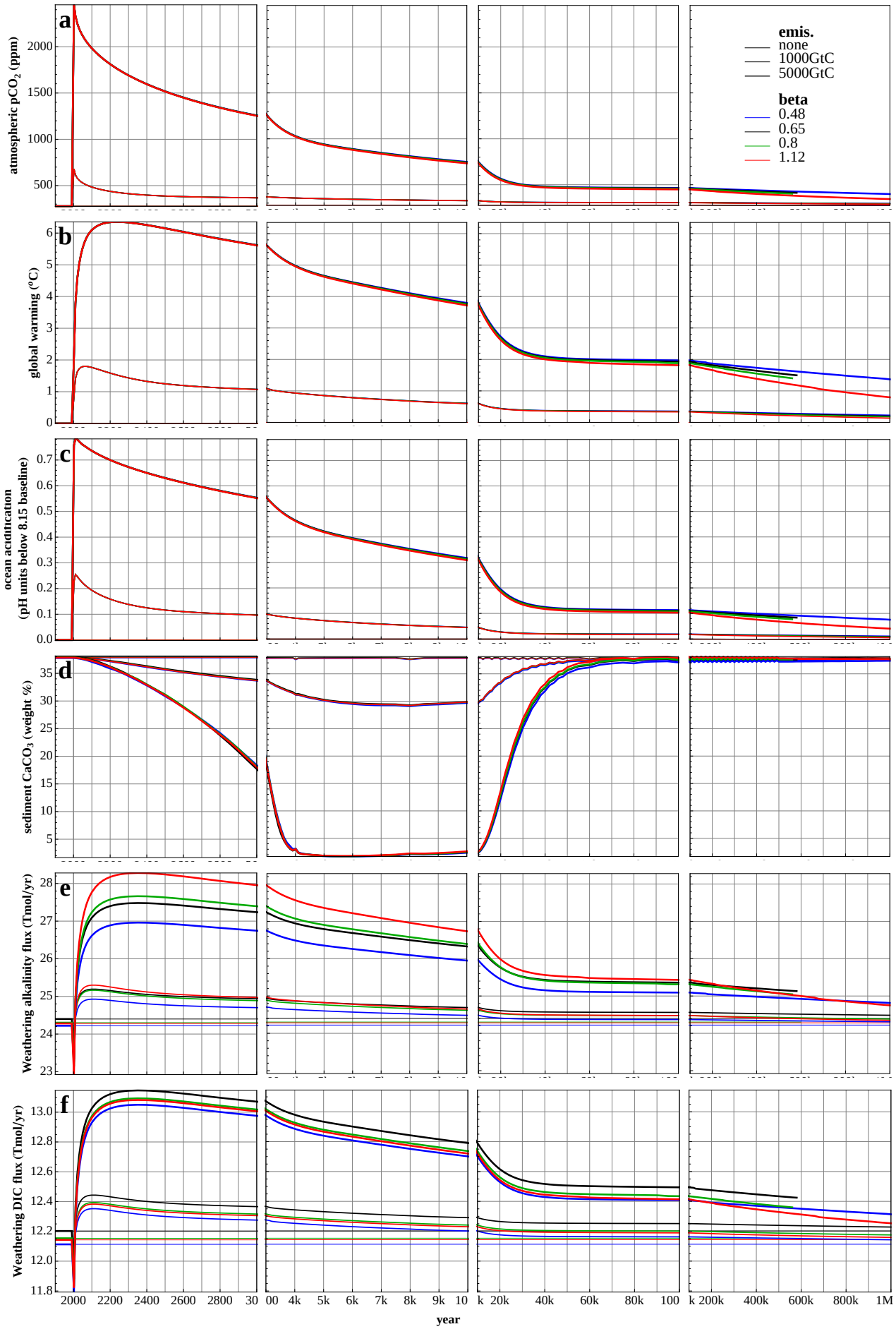

Figure 48: Timeseries of key variables for fractional power of explicit weathering-runoff dependence ensemble

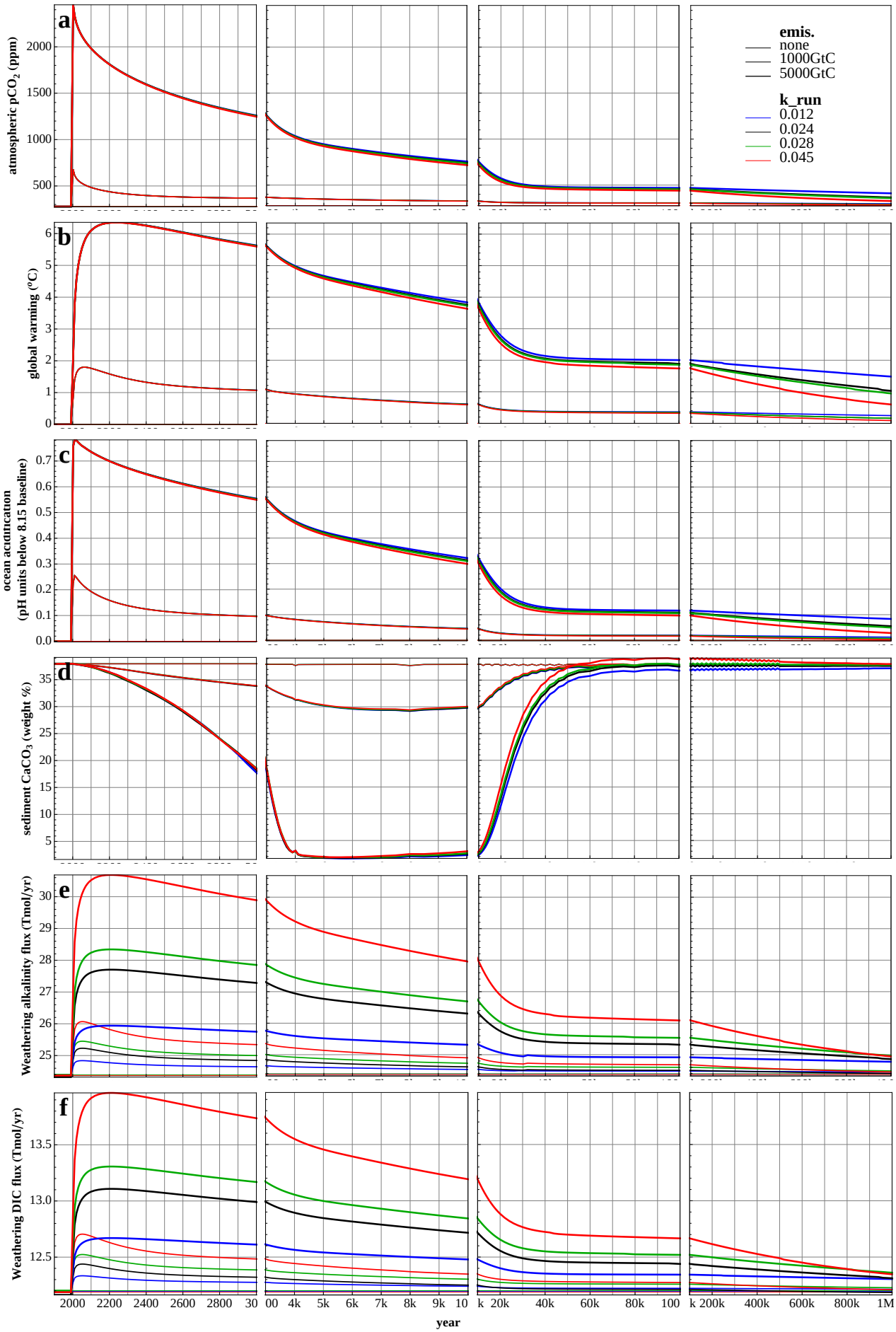

Figure 49: Timeseries of key variables for runoff-temperature correlation constant ensemble

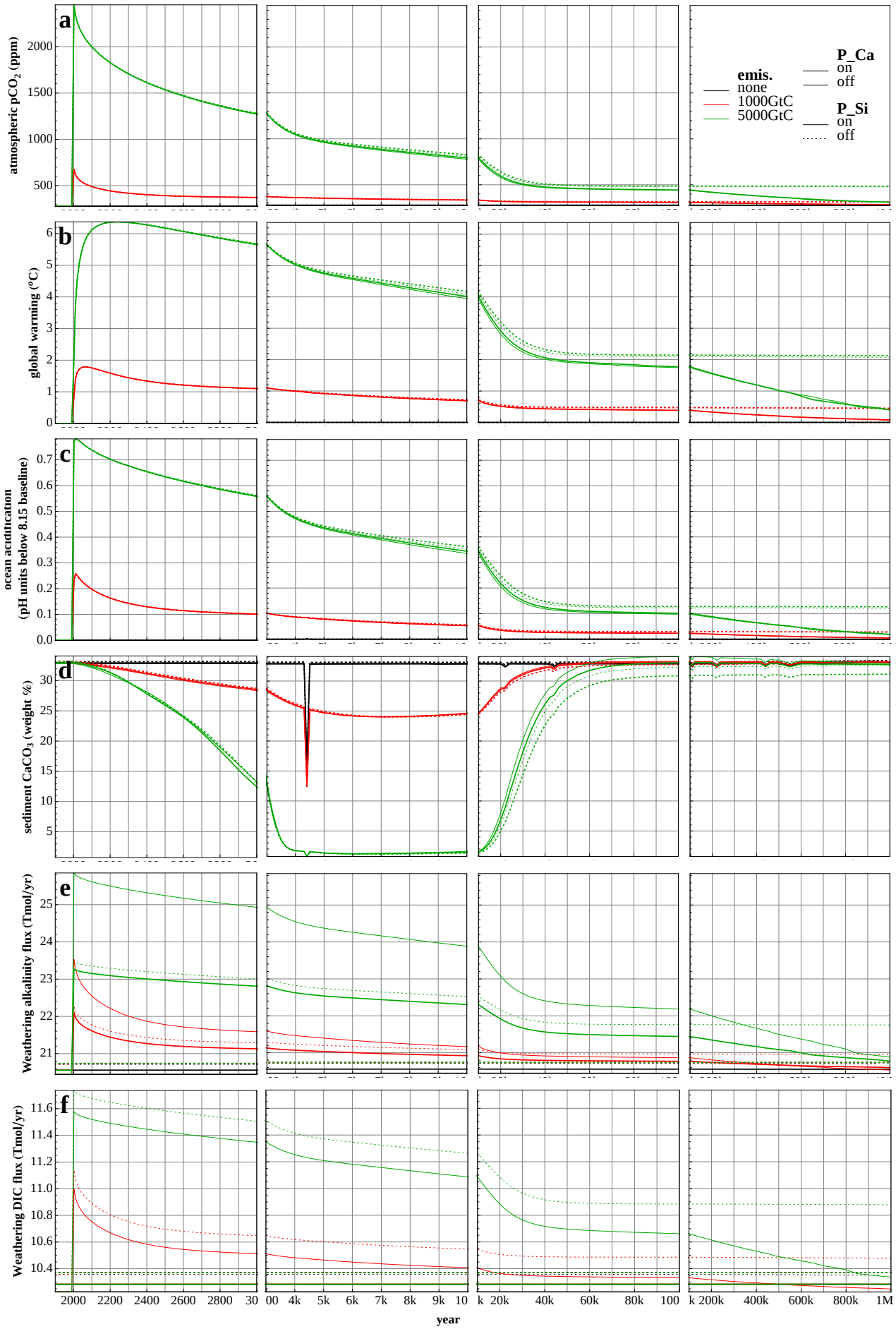

Figure 50: Timeseries of key variables for weathering-productivity feedbacks ensemble

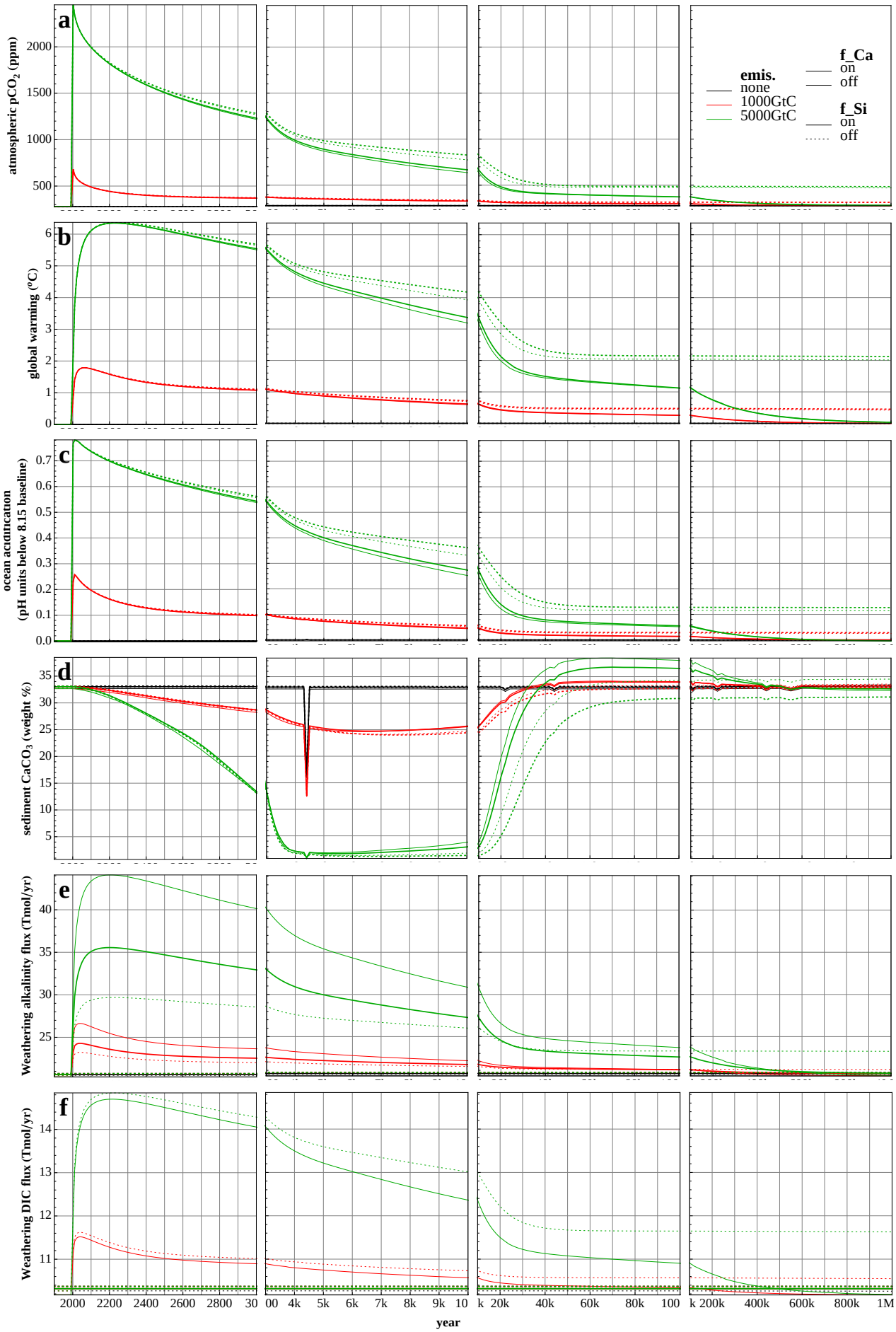

Figure 51: Timeseries of key variables for calcite and silicate weathering feedbacks ensemble

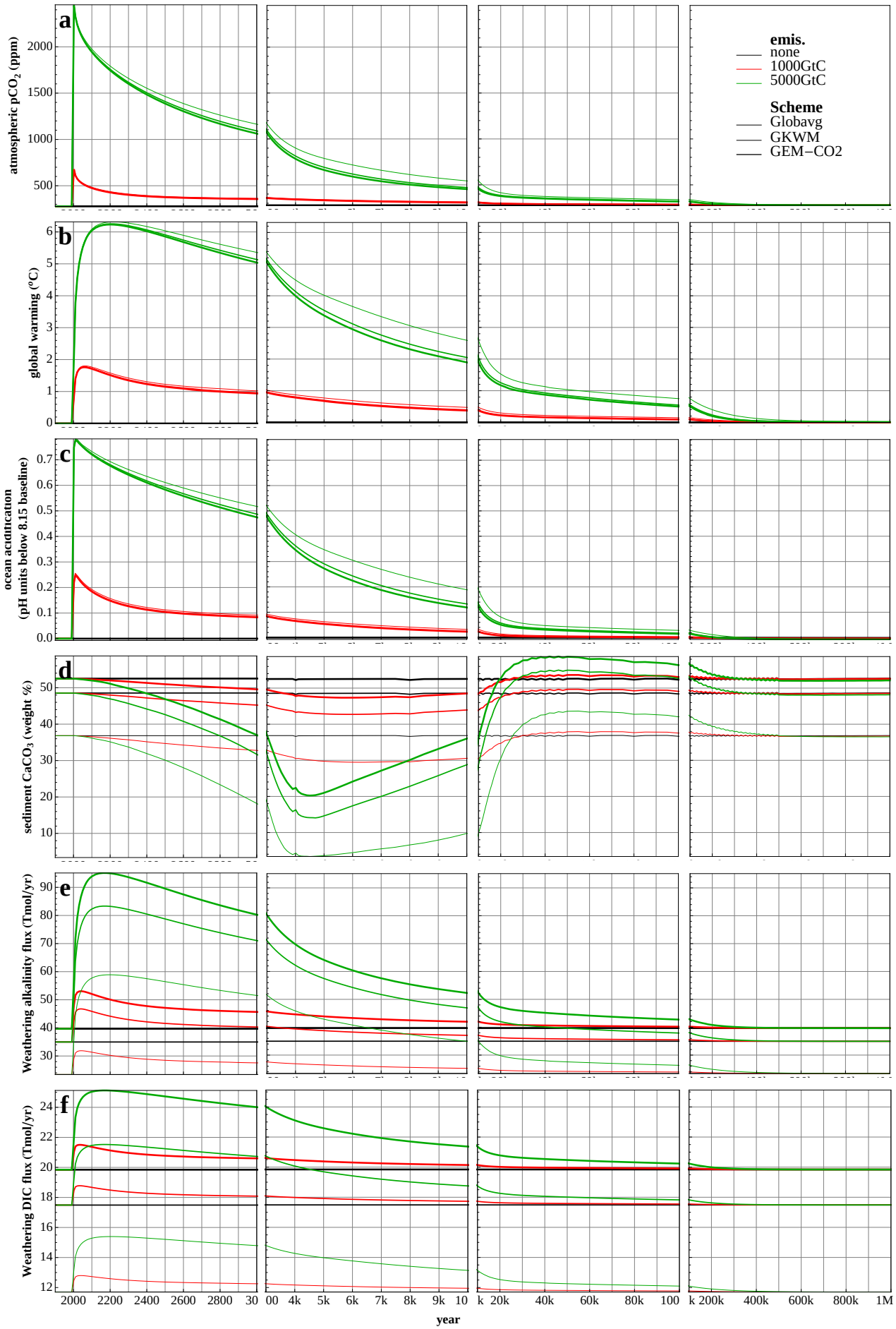

Figure 52: Timeseries of key variables for weathering schemes ensemble

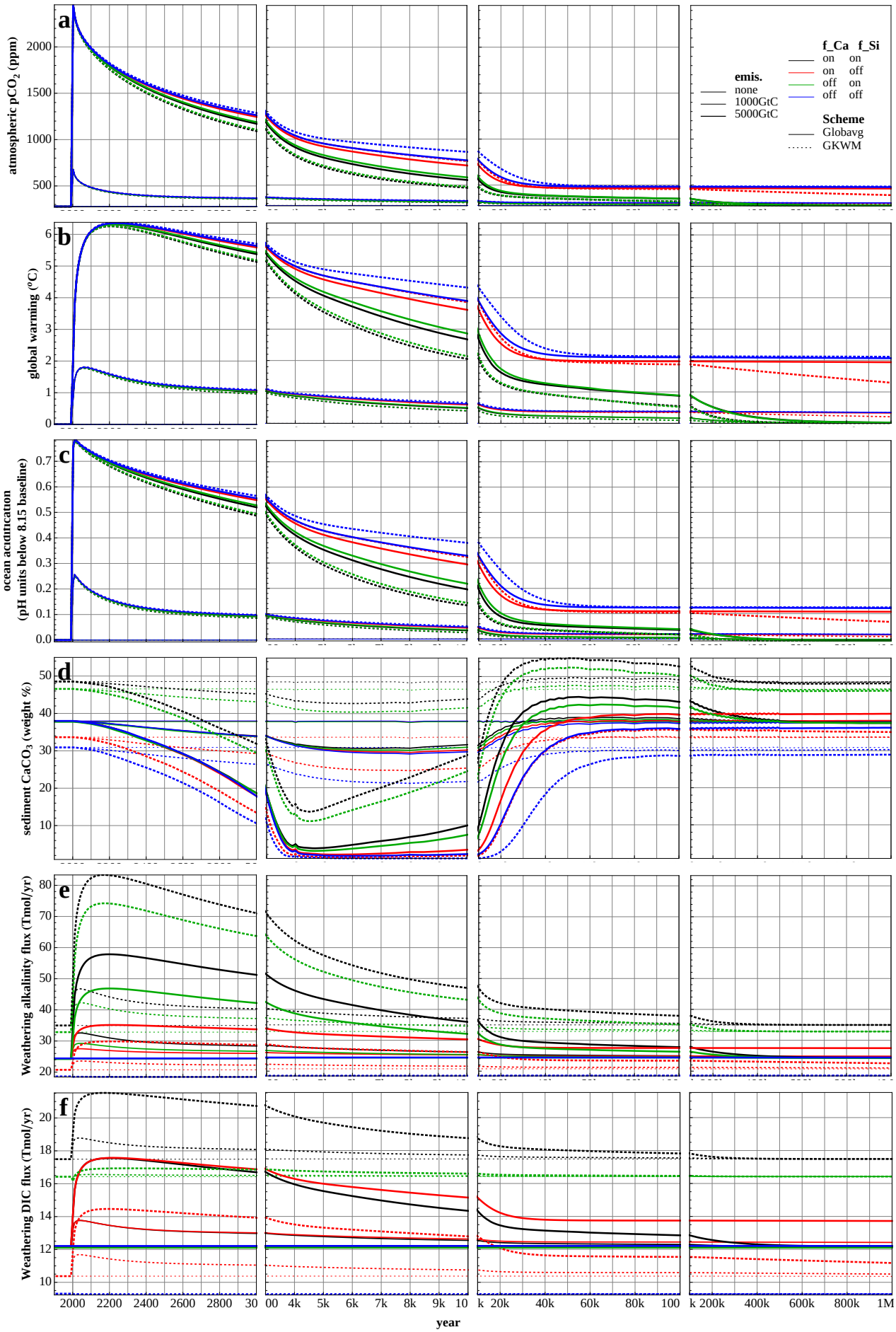

Figure 53: Timeseries of key variables for weathering schemes with f_Ca and f_Si on/off ensemble

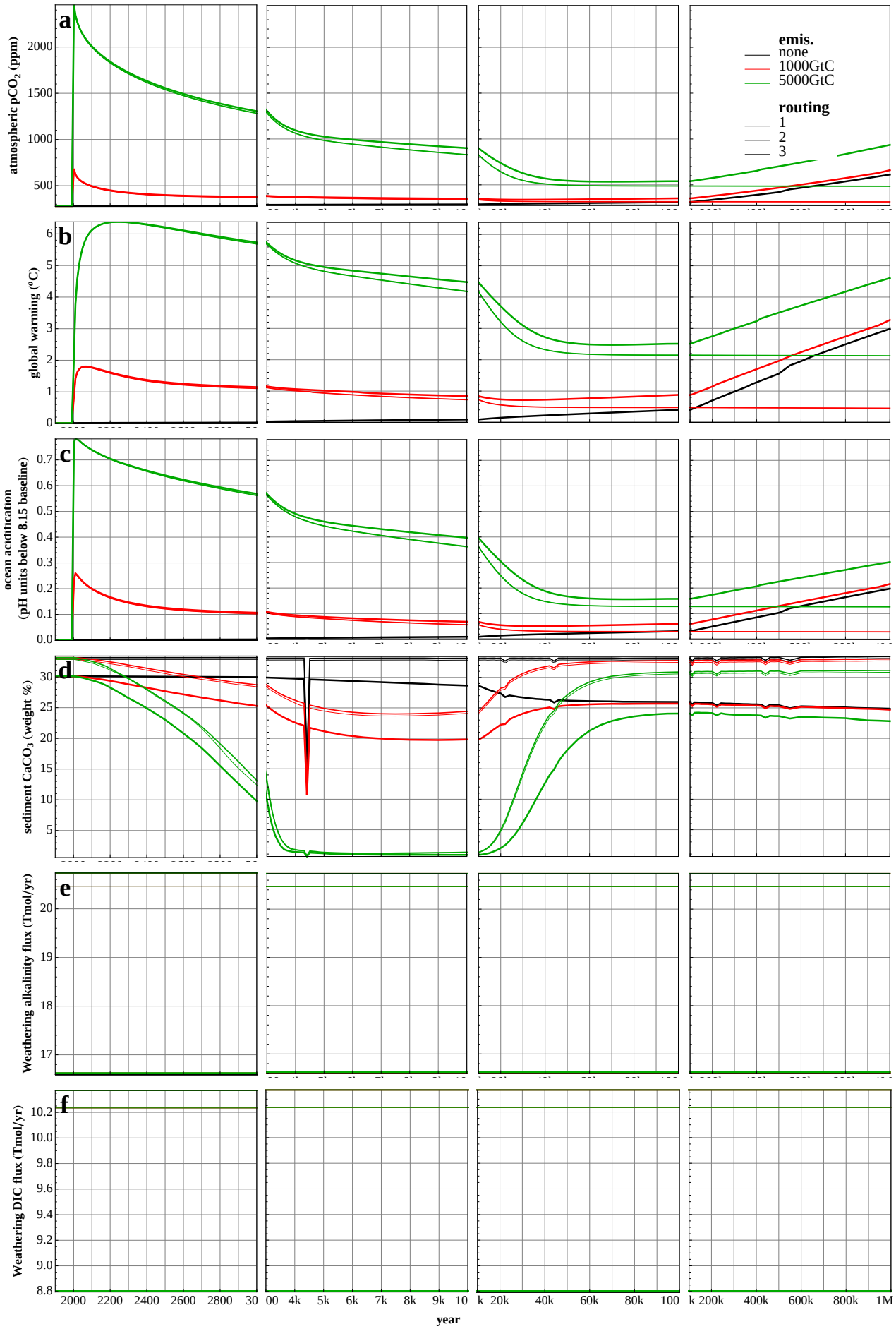

Figure 54: Timeseries of key variables for river routing schemes ensemble

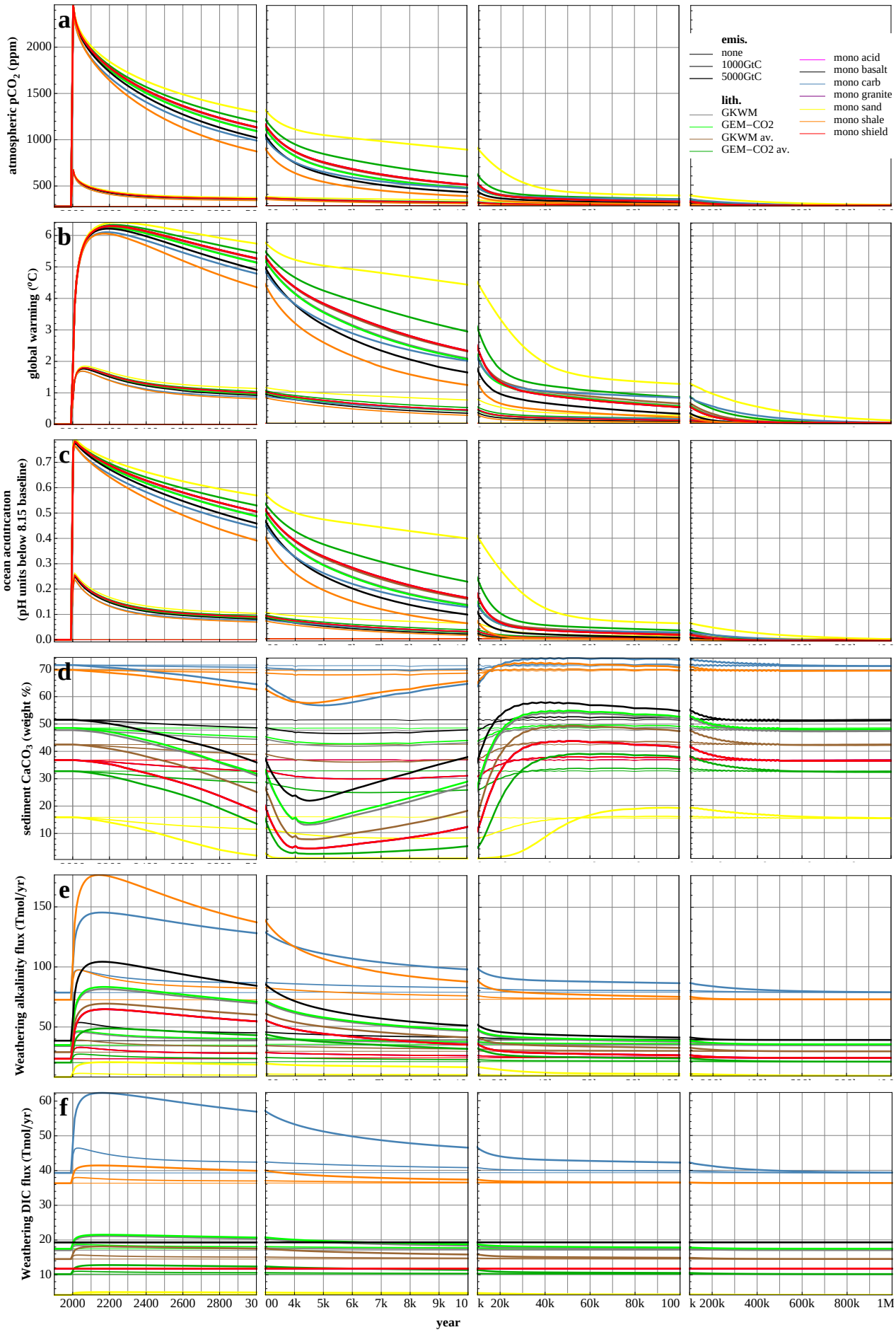

Figure 55: Timeseries of key variables for lithologies ensemble

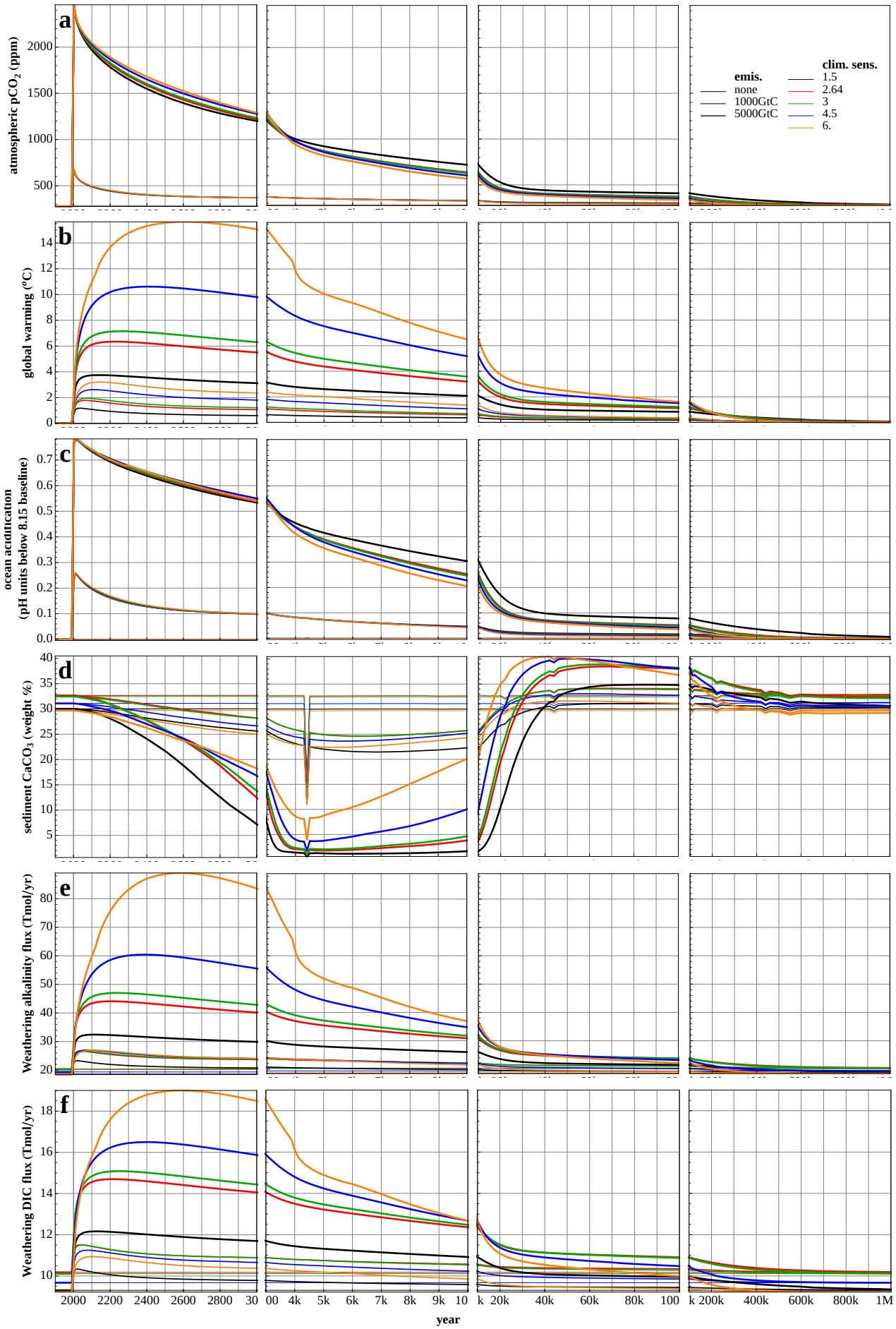

Figure 56: Timeseries of key variables for climate sensitivity ensemble

A.3 Tabulated results for key variables

Table 27: **Atmospheric pCO_2** (ppm) reached at specific calendar years

variables		year								
emis.	short-circ.	3000	5000	10000	20000	50000	100k	200k	500k	1000k
1000GtC	yes	363	340	316	302	295	291	286	280	279
1000GtC	no	363	339	315	301	295	290	285	280	279
5000GtC	yes	1171	798	555	425	377	351	320	287	280
5000GtC	no	1160	780	538	418	373	348	317	286	280

variables			year								
emis.	T_Ca	T_Si	3000	5000	10000	20000	50000	100k	200k	500k	1000k
1000GtC	on	on	371	351	330	315	307	303	296	284	275
1000GtC	on	off	373	355	335	322	316	315	315	314	312
1000GtC	off	on	371	352	331	317	308	304	298	287	279
1000GtC	off	off	373	356	336	323	317	316	316	315	314
5000GtC	on	on	1250	923	717	523	429	406	374	320	289
5000GtC	on	off	1278	975	810	620	488	481	480	479	477
5000GtC	off	on	1254	931	732	535	432	407	374	319	288
5000GtC	off	off	1283	984	828	642	496	487	487	486	485

variables		year								
emis.	E_a (kJ/mol)	3000	5000	10000	20000	50000	100k	200k	500k	1000k
1000GtC	45	367	345	323	309	302	299	295	286	280
1000GtC	63	366	344	322	307	300	297	292	283	279
1000GtC	74	366	344	321	307	299	296	290	282	279
1000GtC	103	365	342	318	304	297	293	287	280	279
5000GtC	45	1235	899	680	505	430	410	380	327	294
5000GtC	63	1221	876	647	482	414	391	358	308	285
5000GtC	74	1214	865	632	471	406	381	348	302	283
5000GtC	103	1188	825	586	442	386	360	327	290	281

variables				year								
emis.	R_Ca	R_Si	R_explicit	3000	5000	10000	20000	50000	100k	200k	500k	1000k
1000GtC	on	on	on	373	355	335	321	314	313	311	306	299
1000GtC	on	on	off	372	354	334	320	313	311	308	301	292
1000GtC	on	off	on	373	355	336	322	316	315	315	314	312
1000GtC	on	off	off	373	355	336	322	316	315	315	314	312
1000GtC	off	on	on	373	355	336	322	315	313	311	305	296
1000GtC	off	on	off	373	355	335	321	314	311	308	300	291
1000GtC	off	off	on	373	356	336	323	317	316	316	315	314
1000GtC	off	off	off	373	356	336	323	317	316	316	315	314
5000GtC	on	on	on	1276	971	803	611	480	468	457	431	392
5000GtC	on	on	off	1272	962	785	590	469	455	439	400	348
5000GtC	on	off	on	1280	978	818	629	491	484	483	481	478
5000GtC	on	off	off	1279	977	814	624	489	482	481	480	479
5000GtC	off	on	on	1280	978	816	625	483	470	459	431	389
5000GtC	off	on	off	1277	973	805	611	474	458	441	398	345
5000GtC	off	off	on	1283	984	828	642	496	487	487	486	484
5000GtC	off	off	off	1283	984	828	642	496	487	487	486	484

variables		year								
emis.	beta	3000	5000	10000	20000	50000	100k	200k	500k	1000k
1000GtC	0.48	368	348	327	313	307	306	305	301	296
1000GtC	0.65	368	348	327	313	307	306	304	299	294
1000GtC	0.8	368	348	326	313	307	305	303	298	292
1000GtC	1.12	368	347	326	312	306	304	302	295	288
5000GtC	0.48	1258	940	749	566	473	465	455	431	398
5000GtC	0.65	1256	938	743	561	470	460	449	419	-
5000GtC	0.8	1256	936	740	558	467	457	443	408	-
5000GtC	1.12	1254	932	733	550	461	449	430	388	344

variables		year								
emis.	k_run	3000	5000	10000	20000	50000	100k	200k	500k	1000k
1000GtC	0.012	368	348	327	314	308	307	306	302	297
1000GtC	0.024	368	348	327	313	307	305	303	297	290
1000GtC	0.028	368	348	326	313	306	305	303	297	290
1000GtC	0.045	367	347	325	312	305	303	300	292	285
5000GtC	0.012	1259	944	756	574	477	470	462	441	411
5000GtC	0.024	1255	936	741	559	467	457	442	408	366
5000GtC	0.028	1254	932	735	554	465	454	439	401	358
5000GtC	0.045	1247	922	717	537	454	440	419	372	327

variables			year								
emis.	P_Ca	P_Si	3000	5000	10000	20000	50000	100k	200k	500k	1000k
1000GtC	on	on	372	353	333	318	311	308	303	293	283
1000GtC	on	off	373	355	335	322	316	315	315	314	313
1000GtC	off	on	372	354	334	319	312	309	304	294	284
1000GtC	off	off	373	356	336	323	317	316	316	315	314
5000GtC	on	on	1270	959	778	579	458	440	416	363	310
5000GtC	on	off	1278	975	810	620	488	481	481	480	478
5000GtC	off	on	1274	967	793	595	463	443	419	364	309
5000GtC	off	off	1283	984	828	642	496	487	487	486	484

variables			year								
emis.	f_Ca	f_Si	3000	5000	10000	20000	50000	100k	200k	500k	1000k
1000GtC	on	on	369	348	326	311	302	298	291	281	278
1000GtC	on	off	372	354	334	320	314	314	314	313	311
1000GtC	off	on	370	350	328	312	303	298	291	281	278
1000GtC	off	off	373	356	336	323	317	316	316	315	314
5000GtC	on	on	1219	870	637	465	398	372	339	296	281
5000GtC	on	off	1269	957	776	583	478	474	473	472	470
5000GtC	off	on	1231	890	668	483	401	373	338	295	280
5000GtC	off	off	1283	984	828	642	496	487	487	486	484

variables		year								
emis.	Scheme	3000	5000	10000	20000	50000	100k	200k	500k	1000k
1000GtC	Globavg	364	340	315	301	294	289	284	279	279
1000GtC	GKWM	358	333	309	296	290	286	281	279	278
1000GtC	GEM-CO2	356	331	307	295	289	285	281	279	278
5000GtC	Globavg	1165	788	543	415	366	340	310	284	280
5000GtC	GKWM	1092	692	471	386	348	322	296	280	279
5000GtC	GEM-CO2	1063	662	454	378	343	318	293	280	279

variables				year								
emis.	f_Ca	f_Si	Scheme	3000	5000	10000	20000	50000	100k	200k	500k	1000k
1000GtC	on	on	Globavg	363	340	316	302	295	291	286	280	279
1000GtC	on	on	GKWM	358	333	309	296	290	286	281	279	278
1000GtC	on	off	Globavg	367	347	325	312	307	306	306	305	304
1000GtC	on	off	GKWM	369	348	327	313	306	305	304	300	294
1000GtC	off	on	Globavg	364	342	318	304	296	291	286	280	279
1000GtC	off	on	GKWM	359	334	310	297	290	286	281	279	278
1000GtC	off	off	Globavg	368	349	328	315	309	308	308	307	305
1000GtC	off	off	GKWM	371	351	331	317	309	309	308	307	305
5000GtC	on	on	Globavg	1171	798	555	425	377	351	320	287	280
5000GtC	on	on	GKWM	1092	692	471	386	348	322	296	280	279
5000GtC	on	off	Globavg	1246	919	713	539	469	466	465	464	462
5000GtC	on	off	GKWM	1262	951	761	567	465	456	447	423	391
5000GtC	off	on	Globavg	1189	825	583	438	380	352	319	287	280
5000GtC	off	on	GKWM	1107	710	482	389	349	320	294	280	279
5000GtC	off	off	Globavg	1263	951	769	588	486	482	481	480	478
5000GtC	off	off	GKWM	1288	1005	861	678	499	486	485	485	484

variables		year								
emis.	routing	3000	5000	10000	20000	50000	100k	200k	500k	1000k
1000GtC	1	373	356	337	323	316	316	316	315	314
1000GtC	2	373	356	336	323	317	316	316	315	314
1000GtC	3	379	364	349	339	340	353	378	469	660
5000GtC	1	1283	986	831	646	496	487	487	486	484
5000GtC	2	1283	984	828	642	496	487	487	486	484
5000GtC	3	1305	1026	901	737	544	539	575	701	936

variables		year								
emis.	lith.	3000	5000	10000	20000	50000	100k	200k	500k	1000k
1000GtC	GKWM	358	333	309	297	290	286	281	279	278
1000GtC	GEM-CO2	358	333	309	296	290	286	281	279	-
1000GtC	GKWM av.	361	336	312	298	291	287	282	278	277
1000GtC	GEM-CO2 av.	365	342	318	303	295	290	284	279	277
1000GtC	mono acid	362	337	311	297	290	286	281	279	278
1000GtC	mono basalt	354	328	303	292	286	282	279	278	278
1000GtC	mono carb	349	331	310	297	292	290	285	280	278
1000GtC	mono granite	362	337	311	297	290	286	281	279	278
1000GtC	mono sand	375	358	339	319	303	298	293	284	279
1000GtC	mono shale	343	321	298	287	283	281	279	278	278
1000GtC	mono shield	362	337	311	297	290	286	281	279	278
5000GtC	GKWM	1097	697	474	387	350	323	297	280	279
5000GtC	GEM-CO2	1092	692	471	386	348	322	295	280	279
5000GtC	GKWM av.	1131	741	503	398	356	330	302	281	279
5000GtC	GEM-CO2 av.	1196	840	596	435	374	347	315	285	279
5000GtC	mono acid	1136	749	505	390	346	320	295	280	279
5000GtC	mono basalt	1023	621	423	356	324	302	285	279	279
5000GtC	mono carb	992	644	465	392	361	345	322	291	280
5000GtC	mono granite	1136	749	505	390	346	320	295	280	279
5000GtC	mono sand	1300	1046	887	661	427	387	357	310	285
5000GtC	mono shale	874	535	381	329	308	293	282	279	279
5000GtC	mono shield	1136	749	505	390	346	320	295	280	279

variables		year								
emis.	clim. sens.	3000	5000	10000	20000	50000	100k	200k	500k	1000k
1000GtC	1.5	370	349	328	314	306	302	296	285	279
1000GtC	2.64	369	348	326	311	302	298	290	281	278
1000GtC	3	370	349	326	311	302	297	290	281	278
1000GtC	4.5	371	351	326	309	299	294	287	279	277
1000GtC	6.	370	350	324	305	296	290	284	279	278
5000GtC	1.5	1201	921	720	526	432	408	375	319	285
5000GtC	2.64	1219	871	637	465	398	372	339	296	281
5000GtC	3	1233	868	629	459	394	367	333	292	279
5000GtC	4.5	1278	857	603	444	382	350	314	283	278
5000GtC	6.	1289	820	569	427	370	336	304	281	278

Table 28: **Percentages** of remaining excess **Atmospheric pCO_2** reached at specific calendar years

variables		year								
emis.	short-circ.	3000	5000	10000	20000	50000	100k	200k	500k	1000k
1000GtC	yes	21.3	15.4	9.5	6.0	4.2	3.2	1.9	0.4	0.1
1000GtC	no	21.1	15.2	9.2	5.8	4.1	3.1	1.8	0.4	0.1
5000GtC	yes	41.1	23.9	12.7	6.7	4.5	3.4	1.9	0.4	0.1
5000GtC	no	40.5	23.1	11.9	6.4	4.4	3.2	1.8	0.4	0.1

variables			year								
emis.	T_Ca	T_Si	3000	5000	10000	20000	50000	100k	200k	500k	1000k
1000GtC	on	on	23.1	18.3	12.9	9.2	7.2	6.1	4.4	1.4	-0.8
1000GtC	on	off	23.6	19.1	14.3	10.9	9.3	9.2	9.1	8.9	8.5
1000GtC	off	on	23.2	18.5	13.2	9.6	7.5	6.5	4.9	2.1	0.4
1000GtC	off	off	23.7	19.3	14.5	11.2	9.6	9.4	9.4	9.2	9.0
5000GtC	on	on	44.7	29.7	20.2	11.3	6.9	5.9	4.4	1.9	0.5
5000GtC	on	off	46.0	32.0	24.5	15.7	9.7	9.3	9.3	9.3	9.2
5000GtC	off	on	44.9	30.0	20.9	11.8	7.1	5.9	4.4	1.9	0.5
5000GtC	off	off	46.2	32.5	25.3	16.7	10.0	9.6	9.6	9.6	9.5

variables		year								
emis.	E_a (kJ/mol)	3000	5000	10000	20000	50000	100k	200k	500k	1000k
1000GtC	45	22.1	16.8	11.3	7.8	6.0	5.3	4.2	2.0	0.6
1000GtC	63	21.9	16.5	10.9	7.3	5.5	4.7	3.4	1.3	0.2
1000GtC	74	21.9	16.4	10.7	7.1	5.3	4.4	3.0	1.0	0.2
1000GtC	103	21.6	16.0	10.1	6.5	4.7	3.6	2.2	0.6	0.1
5000GtC	45	44.0	28.5	18.5	10.4	7.0	6.1	4.7	2.2	0.7
5000GtC	63	43.4	27.5	17.0	9.4	6.3	5.2	3.7	1.4	0.3
5000GtC	74	43.0	27.0	16.3	8.9	5.9	4.7	3.2	1.1	0.2
5000GtC	103	41.9	25.1	14.1	7.5	5.0	3.8	2.3	0.6	0.1

variables				year								
emis.	R_Ca	R_Si	R_explicit	3000	5000	10000	20000	50000	100k	200k	500k	1000k
1000GtC	on	on	on	23.6	19.1	14.2	10.8	9.1	8.7	8.3	7.0	5.2
1000GtC	on	on	off	23.5	18.9	13.9	10.4	8.7	8.2	7.5	5.7	3.5
1000GtC	on	off	on	23.6	19.2	14.4	11.0	9.4	9.3	9.2	8.9	8.3
1000GtC	on	off	off	23.6	19.2	14.3	10.9	9.4	9.2	9.1	8.9	8.5
1000GtC	off	on	on	23.6	19.2	14.3	10.9	9.1	8.7	8.2	6.7	4.6
1000GtC	off	on	off	23.5	19.1	14.1	10.6	8.8	8.3	7.5	5.6	3.2
1000GtC	off	off	on	23.7	19.3	14.5	11.2	9.6	9.4	9.4	9.2	9.0
1000GtC	off	off	off	23.7	19.3	14.5	11.2	9.6	9.4	9.4	9.2	9.0
5000GtC	on	on	on	45.9	31.9	24.1	15.3	9.3	8.7	8.2	7.0	5.3
5000GtC	on	on	off	45.7	31.5	23.3	14.3	8.8	8.1	7.4	5.6	3.2
5000GtC	on	off	on	46.1	32.2	24.8	16.2	9.8	9.5	9.4	9.3	9.2
5000GtC	on	off	off	46.0	32.1	24.7	15.9	9.7	9.4	9.3	9.3	9.2
5000GtC	off	on	on	46.1	32.2	24.7	16.0	9.4	8.8	8.3	7.0	5.1
5000GtC	off	on	off	45.9	32.0	24.2	15.3	9.0	8.3	7.5	5.5	3.1
5000GtC	off	off	on	46.2	32.5	25.3	16.7	10.0	9.6	9.6	9.6	9.5
5000GtC	off	off	off	46.2	32.5	25.3	16.7	10.0	9.6	9.6	9.6	9.5

variables		year								
emis.	beta	3000	5000	10000	20000	50000	100k	200k	500k	1000k
1000GtC	0.48	22.5	17.5	12.2	8.8	7.3	7.0	6.7	5.7	4.4
1000GtC	0.65	22.5	17.4	12.1	8.7	7.2	6.9	6.5	5.3	3.9
1000GtC	0.8	22.5	17.4	12.1	8.7	7.1	6.8	6.3	5.0	3.4
1000GtC	1.12	22.4	17.3	12.0	8.5	7.0	6.5	5.9	4.3	2.6
5000GtC	0.48	45.1	30.4	21.6	13.3	9.0	8.6	8.1	7.1	5.5
5000GtC	0.65	45.0	30.4	21.4	13.0	8.8	8.4	7.9	6.5	-
5000GtC	0.8	44.9	30.2	21.2	12.9	8.7	8.2	7.6	6.0	-
5000GtC	1.12	44.9	30.1	20.9	12.5	8.4	7.8	7.0	5.0	3.0

variables		year								
emis.	k_run	3000	5000	10000	20000	50000	100k	200k	500k	1000k
1000GtC	0.012	22.5	17.5	12.3	8.9	7.4	7.2	6.9	6.0	4.8
1000GtC	0.024	22.5	17.4	12.1	8.7	7.1	6.8	6.2	4.8	3.1
1000GtC	0.028	22.4	17.4	12.1	8.7	7.1	6.7	6.2	4.8	3.1
1000GtC	0.045	22.3	17.2	11.8	8.4	6.8	6.2	5.5	3.6	1.7
5000GtC	0.012	45.1	30.6	22.0	13.6	9.2	8.8	8.4	7.5	6.1
5000GtC	0.024	44.9	30.2	21.3	12.9	8.7	8.2	7.5	6.0	4.0
5000GtC	0.028	44.9	30.1	21.0	12.7	8.6	8.1	7.4	5.7	3.7
5000GtC	0.045	44.6	29.6	20.2	11.9	8.1	7.4	6.5	4.3	2.2

variables			year								
emis.	P_Ca	P_Si	3000	5000	10000	20000	50000	100k	200k	500k	1000k
1000GtC	on	on	23.3	18.7	13.6	10.0	8.2	7.4	6.3	3.8	1.3
1000GtC	on	off	23.6	19.1	14.2	10.9	9.3	9.2	9.1	9.0	8.6
1000GtC	off	on	23.4	18.9	13.8	10.3	8.3	7.6	6.5	3.9	1.5
1000GtC	off	off	23.7	19.3	14.5	11.2	9.6	9.4	9.4	9.2	9.0
5000GtC	on	on	45.6	31.3	23.0	13.8	8.3	7.4	6.4	3.9	1.5
5000GtC	on	off	46.0	32.0	24.5	15.7	9.7	9.3	9.3	9.3	9.2
5000GtC	off	on	45.8	31.7	23.7	14.6	8.5	7.6	6.5	4.0	1.4
5000GtC	off	off	46.2	32.5	25.3	16.7	10.0	9.6	9.6	9.6	9.5

variables			year								
emis.	f_Ca	f_Si	3000	5000	10000	20000	50000	100k	200k	500k	1000k
1000GtC	on	on	22.6	17.5	11.9	8.2	6.1	4.9	3.1	0.8	-0.0
1000GtC	on	off	23.4	18.9	13.9	10.5	9.0	8.9	8.8	8.7	8.3
1000GtC	off	on	22.9	17.9	12.3	8.6	6.3	5.0	3.1	0.7	-0.1
1000GtC	off	off	23.7	19.3	14.5	11.2	9.6	9.4	9.4	9.2	9.0
5000GtC	on	on	43.3	27.2	16.5	8.6	5.5	4.3	2.8	0.8	0.1
5000GtC	on	off	45.6	31.2	22.9	14.0	9.2	9.0	9.0	8.9	8.8
5000GtC	off	on	43.8	28.2	17.9	9.4	5.7	4.4	2.8	0.8	0.1
5000GtC	off	off	46.2	32.5	25.3	16.7	10.0	9.6	9.6	9.6	9.5

variables		year								
emis.	Scheme	3000	5000	10000	20000	50000	100k	200k	500k	1000k
1000GtC	Globavg	21.4	15.4	9.3	5.8	3.9	2.8	1.5	0.3	0.1
1000GtC	GKWM	20.0	13.8	7.7	4.6	3.0	1.9	0.8	0.1	0.1
1000GtC	GEM-CO2	19.5	13.4	7.3	4.3	2.8	1.7	0.7	0.1	0.1
5000GtC	Globavg	40.7	23.5	12.2	6.3	4.0	2.8	1.5	0.3	0.1
5000GtC	GKWM	37.5	19.0	8.9	5.0	3.2	2.0	0.8	0.1	0.0
5000GtC	GEM-CO2	36.2	17.7	8.1	4.6	3.0	1.9	0.7	0.1	0.0

variables				year								
emis.	f_Ca	f_Si	Scheme	3000	5000	10000	20000	50000	100k	200k	500k	1000k
1000GtC	on	on	Globavg	21.3	15.4	9.5	6.0	4.2	3.2	1.9	0.4	0.1
1000GtC	on	on	GKWM	20.0	13.8	7.7	4.6	3.0	1.9	0.8	0.1	0.1
1000GtC	on	off	Globavg	22.3	17.2	11.8	8.5	7.2	7.1	7.0	6.8	6.5
1000GtC	on	off	GKWM	22.7	17.6	12.2	8.7	7.1	6.8	6.4	5.4	4.1
1000GtC	off	on	Globavg	21.6	15.9	10.0	6.4	4.4	3.3	1.9	0.4	0.1
1000GtC	off	on	GKWM	20.3	14.1	8.0	4.7	3.0	1.9	0.8	0.1	0.1
1000GtC	off	off	Globavg	22.6	17.7	12.5	9.1	7.6	7.5	7.5	7.2	6.8
1000GtC	off	off	GKWM	23.1	18.3	13.3	9.7	7.8	7.6	7.5	7.3	6.8
5000GtC	on	on	Globavg	41.1	23.9	12.7	6.7	4.5	3.4	1.9	0.4	0.1
5000GtC	on	on	GKWM	37.5	19.1	8.9	5.0	3.2	2.0	0.8	0.1	0.0
5000GtC	on	off	Globavg	44.5	29.5	20.0	12.0	8.8	8.6	8.6	8.6	8.5
5000GtC	on	off	GKWM	45.2	30.9	22.2	13.3	8.6	8.2	7.8	6.7	5.2
5000GtC	off	on	Globavg	41.9	25.1	14.0	7.3	4.7	3.4	1.9	0.4	0.1
5000GtC	off	on	GKWM	38.2	19.9	9.4	5.1	3.3	2.0	0.7	0.1	0.0
5000GtC	off	off	Globavg	45.3	31.0	22.6	14.2	9.6	9.4	9.3	9.3	9.2
5000GtC	off	off	GKWM	46.4	33.4	26.8	18.4	10.1	9.5	9.5	9.5	9.5

variables		year								
emis.	routing	3000	5000	10000	20000	50000	100k	200k	500k	1000k
1000GtC	1	23.7	19.3	14.5	11.2	9.6	9.4	9.4	9.2	8.8
1000GtC	2	23.7	19.3	14.5	11.2	9.6	9.4	9.4	9.2	9.0
1000GtC	3	24.7	20.8	17.1	14.8	15.1	18.1	24.5	46.8	94.1
5000GtC	1	46.2	32.6	25.5	16.9	10.0	9.6	9.6	9.5	9.5
5000GtC	2	46.2	32.5	25.3	16.7	10.0	9.6	9.6	9.6	9.5
5000GtC	3	47.1	34.3	28.5	21.0	12.2	11.9	13.6	19.4	30.1

variables		year								
emis.	lith.	3000	5000	10000	20000	50000	100k	200k	500k	1000k
1000GtC	GKWM	20.1	13.9	7.8	4.6	3.0	2.0	0.8	0.1	0.1
1000GtC	GEM-CO2	20.0	13.8	7.7	4.6	3.0	1.9	0.8	0.1	-
1000GtC	GKWM av.	20.6	14.5	8.4	5.0	3.3	2.1	0.9	-0.0	-0.2
1000GtC	GEM-CO2 av.	21.8	16.0	10.0	6.2	4.1	3.0	1.5	0.1	-0.2
1000GtC	mono acid	20.9	14.6	8.3	4.8	3.0	1.9	0.8	0.1	0.1
1000GtC	mono basalt	19.0	12.5	6.3	3.4	2.0	1.1	0.4	0.1	0.1
1000GtC	mono carb	17.9	13.4	8.1	4.9	3.6	2.9	1.8	0.4	-0.1
1000GtC	mono granite	20.9	14.6	8.3	4.8	3.0	1.9	0.8	0.1	0.1
1000GtC	mono sand	24.0	19.9	15.0	10.2	6.1	4.9	3.6	1.4	0.2
1000GtC	mono shale	16.5	10.8	4.9	2.3	1.3	0.7	0.2	0.1	0.1
1000GtC	mono shield	20.9	14.6	8.3	4.8	3.0	1.9	0.8	0.1	0.1
5000GtC	GKWM	37.7	19.3	9.0	5.0	3.3	2.1	0.9	0.1	0.0
5000GtC	GEM-CO2	37.5	19.1	8.9	5.0	3.2	2.0	0.8	0.1	0.0
5000GtC	GKWM av.	39.2	21.3	10.3	5.5	3.6	2.4	1.1	0.1	0.0
5000GtC	GEM-CO2 av.	42.2	25.8	14.6	7.2	4.4	3.2	1.7	0.3	0.0
5000GtC	mono acid	39.4	21.7	10.4	5.2	3.1	1.9	0.8	0.1	0.0
5000GtC	mono basalt	34.3	15.8	6.7	3.6	2.1	1.1	0.3	0.1	0.0
5000GtC	mono carb	33.3	17.0	8.7	5.3	3.9	3.1	2.0	0.6	0.1
5000GtC	mono granite	39.4	21.7	10.4	5.2	3.1	1.9	0.8	0.1	0.0
5000GtC	mono sand	46.9	35.2	27.9	17.6	6.8	5.0	3.6	1.4	0.3
5000GtC	mono shale	27.8	11.9	4.8	2.4	1.4	0.7	0.2	0.1	0.1
5000GtC	mono shield	39.4	21.7	10.4	5.2	3.1	1.9	0.8	0.1	0.0

variables		year								
emis.	clim. sens.	3000	5000	10000	20000	50000	100k	200k	500k	1000k
1000GtC	1.5	22.8	17.7	12.5	8.9	6.9	5.9	4.4	1.8	0.2
1000GtC	2.64	22.6	17.5	11.9	8.2	6.1	4.9	3.1	0.8	-0.0
1000GtC	3	22.8	17.6	11.9	8.1	6.0	4.7	3.0	0.7	0.0
1000GtC	4.5	23.0	18.0	11.9	7.6	5.3	3.9	2.1	0.3	-0.2
1000GtC	6.	22.9	17.8	11.3	6.6	4.4	3.1	1.6	0.2	-0.1
5000GtC	1.5	42.4	29.5	20.3	11.4	7.1	6.0	4.5	1.9	0.3
5000GtC	2.64	43.3	27.2	16.5	8.6	5.5	4.3	2.8	0.8	0.1
5000GtC	3	43.9	27.1	16.1	8.3	5.3	4.1	2.5	0.7	0.1
5000GtC	4.5	45.9	26.6	14.9	7.6	4.8	3.3	1.6	0.3	-0.0
5000GtC	6.	46.4	24.9	13.3	6.9	4.2	2.6	1.2	0.1	-0.0

Table 29: **Years** that specific values of **Atmospheric pCO_2** are reached

variables		**Atmospheric pCO_2 (ppm)**									
emis.	short-circ.	peak	at year	1500	1000	750	500	400	350	300	278
1000GtC	yes	678	2000	-	-	-	2080	2400	3900	24010	-
1000GtC	no	678	2000	-	-	-	2080	2350	3900	24010	-
5000GtC	yes	2453	2000	2500	3600	5800	13000	28010	110010	330010	-
5000GtC	no	2453	2000	2450	3500	5400	12010	26010	95000	310010	-

variables			**Atmospheric pCO_2 (ppm)**									
emis.	T_Ca	T_Si	peak	at year	1500	1000	750	500	400	350	300	278
1000GtC	on	on	680	2000	-	-	-	2090	2450	5400	140000	850000
1000GtC	on	off	681	2000	-	-	-	2090	2450	6000	-	-
1000GtC	off	on	681	2000	-	-	-	2090	2450	5400	170000	-
1000GtC	off	off	681	2000	-	-	-	2090	2450	6200	-	-
5000GtC	on	on	2453	2000	2550	4200	9500	24000	120000	300000	800000	-
5000GtC	on	off	2453	2000	2600	4600	13000	40000	-	-	-	-
5000GtC	off	on	2453	2000	2550	4200	9500	24000	120000	320000	750000	-
5000GtC	off	off	2453	2000	2600	4800	14000	46000	-	-	-	-

variables		**Atmospheric pCO_2 (ppm)**									
emis.	E_a (kJ/mol)	peak	at year	1500	1000	750	500	400	350	300	278
1000GtC	45	678	2000	-	-	-	2080	2400	4400	90010	-
1000GtC	63	678	2000	-	-	-	2080	2400	4300	55000	-
1000GtC	74	678	2000	-	-	-	2080	2400	4300	44010	-
1000GtC	103	678	2000	-	-	-	2080	2400	4100	30010	-
5000GtC	45	2453	2000	2550	4010	8010	22010	130010	340010	860010	-
5000GtC	63	2453	2000	2500	3900	7500	18010	80010	230010	620010	-
5000GtC	74	2453	2000	2500	3800	7000	17000	65000	200010	520010	-
5000GtC	103	2453	2000	2500	3700	6200	15000	36010	130010	370010	-

variables				Atmospheric pCO_2 (ppm)									
emis.	R_Ca	R_Si	R_explicit	peak	at year	1500	1000	750	500	400	350	300	278
1000GtC	on	on	on	681	2000	-	-	-	2090	2450	6000	1000000	-
1000GtC	on	on	off	681	2000	-	-	-	2090	2450	5800	600000	-
1000GtC	on	off	on	681	2000	-	-	-	2090	2450	6000	-	-
1000GtC	on	off	off	681	2000	-	-	-	2090	2450	6000	-	-
1000GtC	off	on	on	681	2000	-	-	-	2090	2450	6000	800000	-
1000GtC	off	on	off	681	2000	-	-	-	2090	2450	6000	550000	-
1000GtC	off	off	on	681	2000	-	-	-	2090	2450	6200	-	-
1000GtC	off	off	off	681	2000	-	-	-	2090	2450	6200	-	-
5000GtC	on	on	on	2453	2000	2600	4600	13000	38000	950000	-	-	-
5000GtC	on	on	off	2452	2000	2550	4500	12000	34000	500000	1000000	-	-
5000GtC	on	off	on	2453	2000	2600	4700	13000	44000	-	-	-	-
5000GtC	on	off	off	2453	2000	2600	4700	13000	42000	-	-	-	-
5000GtC	off	on	on	2453	2000	2600	4700	13000	40000	900000	-	-	-
5000GtC	off	on	off	2453	2000	2600	4600	13000	36000	500000	1000000	-	-
5000GtC	off	off	on	2453	2000	2600	4800	14000	46000	-	-	-	-
5000GtC	off	off	off	2453	2000	2600	4800	14000	46000	-	-	-	-

variables		Atmospheric pCO_2 (ppm)									
emis.	beta	peak	at year	1500	1000	750	500	400	350	300	278
1000GtC	0.48	678	2000	-	-	-	2080	2400	4700	600010	-
1000GtC	0.65	678	2000	-	-	-	2080	2400	4700	450010	-
1000GtC	0.8	678	2000	-	-	-	2080	2400	4700	370010	-
1000GtC	1.12	678	2000	-	-	-	2080	2400	4700	270010	-
5000GtC	0.48	2453	2000	2550	4300	10010	32010	980010	-	-	-
5000GtC	0.65	2453	2000	2550	4300	10010	30010	-	-	-	-
5000GtC	0.8	2453	2000	2550	4300	10010	30010	-	-	-	-
5000GtC	1.12	2453	2000	2550	4200	9500	28010	400010	920010	-	-

variables		Atmospheric pCO_2 (ppm)									
emis.	k_run	peak	at year	1500	1000	750	500	400	350	300	278
1000GtC	0.012	678	2000	-	-	-	2080	2400	4800	700010	-
1000GtC	0.024	678	2000	-	-	-	2080	2400	4700	350010	-
1000GtC	0.028	678	2000	-	-	-	2080	2400	4700	340010	-
1000GtC	0.045	678	2000	-	-	-	2080	2400	4600	200010	-
5000GtC	0.012	2453	2000	2550	4300	11000	34010	-	-	-	-
5000GtC	0.024	2453	2000	2550	4300	10010	30010	600010	-	-	-
5000GtC	0.028	2453	2000	2550	4200	10010	28010	520010	-	-	-
5000GtC	0.045	2453	2000	2550	4200	9000	26010	310010	700010	-	-

variables			Atmospheric pCO_2 (ppm)									
emis.	P_Ca	P_Si	peak	at year	1500	1000	750	500	400	350	300	278
1000GtC	on	on	681	2000	-	-	-	2090	2450	5600	300000	-
1000GtC	on	off	681	2000	-	-	-	2090	2450	6000	-	-
1000GtC	off	on	681	2000	-	-	-	2090	2450	5800	320000	-
1000GtC	off	off	681	2000	-	-	-	2090	2450	6200	-	-
5000GtC	on	on	2453	2000	2550	4500	12000	30000	300000	650000	-	-
5000GtC	on	off	2453	2000	2600	4600	13000	40000	-	-	-	-
5000GtC	off	on	2453	2000	2550	4600	12000	32000	300000	600000	-	-
5000GtC	off	off	2453	2000	2600	4800	14000	46000	-	-	-	-

variables			Atmospheric pCO_2 (ppm)									
emis.	f_Ca	f_Si	peak	at year	1500	1000	750	500	400	350	300	278
1000GtC	on	on	681	2000	-	-	-	2090	2450	4800	75000	1000000
1000GtC	on	off	681	2000	-	-	-	2090	2450	5800	-	-
1000GtC	off	on	681	2000	-	-	-	2090	2450	5000	80000	950000
1000GtC	off	off	681	2000	-	-	-	2090	2450	6200	-	-
5000GtC	on	on	2453	2000	2550	3900	7500	17000	48000	170000	460000	-
5000GtC	on	off	2453	2000	2550	4400	11000	34000	-	-	-	-
5000GtC	off	on	2453	2000	2550	4000	8000	19000	55000	170000	440000	-
5000GtC	off	off	2453	2000	2600	4800	14000	46000	-	-	-	-

variables		Atmospheric pCO_2 (ppm)									
emis.	Scheme	peak	at year	1500	1000	750	500	400	350	300	278
1000GtC	Globavg	679	2000	-	-	-	2080	2400	3900	22010	-
1000GtC	GKWM	677	2000	-	-	-	2080	2350	3500	16010	-
1000GtC	GEM-CO2	677	2000	-	-	-	2070	2350	3300	14010	-
5000GtC	Globavg	2454	2000	2500	3500	5600	12010	24010	80010	260010	-
5000GtC	GKWM	2450	2000	2450	3300	4500	9000	17000	48010	180010	-
5000GtC	GEM-CO2	2448	2000	2400	3200	4300	8500	15000	42010	170010	-

variables				Atmospheric pCO_2 (ppm)									
emis.	f_Ca	f_Si	Scheme	peak	at year	1500	1000	750	500	400	350	300	278
1000GtC	on	on	Globavg	678	2000	-	-	-	2080	2400	3900	24010	-
1000GtC	on	on	GKWM	677	2000	-	-	-	2080	2350	3500	16010	-
1000GtC	on	off	Globavg	678	2000	-	-	-	2080	2400	4600	-	-
1000GtC	on	off	GKWM	679	2000	-	-	-	2090	2400	4800	490010	-
1000GtC	off	on	Globavg	678	2000	-	-	-	2080	2400	4100	28010	-
1000GtC	off	on	GKWM	677	2000	-	-	-	2080	2350	3500	16010	-
1000GtC	off	off	Globavg	678	2000	-	-	-	2080	2400	4800	-	-
1000GtC	off	off	GKWM	679	2000	-	-	-	2090	2450	5400	-	-
5000GtC	on	on	Globavg	2453	2000	2500	3600	5800	13000	28010	110010	330010	-
5000GtC	on	on	GKWM	2450	2000	2450	3300	4500	9000	17000	48010	180010	-
5000GtC	on	off	Globavg	2453	2000	2550	4200	9000	28010	-	-	-	-
5000GtC	on	off	GKWM	2454	2000	2550	4400	11000	30010	860010	-	-	-
5000GtC	off	on	Globavg	2453	2000	2500	3700	6200	14010	32010	110010	320010	-
5000GtC	off	on	GKWM	2451	2000	2450	3300	4600	9500	18010	50010	180010	-
5000GtC	off	off	Globavg	2453	2000	2550	4400	11000	38010	-	-	-	-
5000GtC	off	off	GKWM	2454	2000	2600	5200	16010	50010	-	-	-	-

variables		Atmospheric pCO_2 (ppm)									
emis.	routing	peak	at year	1500	1000	750	500	400	350	300	278
1000GtC	1	681	2000	-	-	-	2090	2450	6200	-	-
1000GtC	2	681	2000	-	-	-	2090	2450	6200	-	-
1000GtC	3	684	2000	-	-	-	2100	2500	9000	-	-
5000GtC	1	2453	2000	2600	4800	14000	48000	-	-	-	-
5000GtC	2	2453	2000	2600	4800	14000	46000	-	-	-	-
5000GtC	3	2457	2000	2600	5800	19000	-	-	-	-	-

variables		Atmospheric pCO_2 (ppm)									
emis.	lith.	peak	at year	1500	1000	750	500	400	350	300	278
1000GtC	GKWM	677	2000	-	-	-	2080	2350	3500	16010	-
1000GtC	GEM-CO2	677	2000	-	-	-	2080	2350	3500	16010	-
1000GtC	GKWM av.	678	2000	-	-	-	2080	2350	3700	18010	490010
1000GtC	GEM-CO2 av.	679	2000	-	-	-	2080	2400	4100	26010	620010
1000GtC	mono acid	678	2000	-	-	-	2080	2350	3700	17000	-
1000GtC	mono basalt	677	2000	-	-	-	2070	2300	3200	12010	-
1000GtC	mono carb	673	2000	-	-	-	2060	2260	2950	17000	820010
1000GtC	mono granite	678	2000	-	-	-	2080	2350	3700	17000	-
1000GtC	mono sand	681	2000	-	-	-	2100	2450	6800	70010	-
1000GtC	mono shale	674	2000	-	-	-	2060	2240	2750	9500	-
1000GtC	mono shield	678	2000	-	-	-	2080	2350	3700	17000	-
5000GtC	GKWM	2451	2000	2450	3300	4500	9000	17000	50010	190010	-
5000GtC	GEM-CO2	2450	2000	2450	3300	4500	9000	17000	48010	180010	-
5000GtC	GKWM av.	2452	2000	2450	3400	4900	11000	20010	60010	210010	-
5000GtC	GEM-CO2 av.	2454	2000	2500	3700	6600	15000	30010	95000	290010	-
5000GtC	mono acid	2453	2000	2450	3400	5000	11000	19000	46010	170010	-
5000GtC	mono basalt	2449	2000	2400	3100	4010	7500	12010	24010	110010	-
5000GtC	mono carb	2423	2000	2350	3000	4010	8500	18010	85000	370010	-
5000GtC	mono granite	2453	2000	2450	3400	5000	11000	19000	46010	170010	-
5000GtC	mono sand	2458	2000	2600	6400	16010	34010	75000	230010	640010	-
5000GtC	mono shale	2426	2000	2300	2800	3400	5600	9000	14010	75000	-
5000GtC	mono shield	2453	2000	2450	3400	5000	11000	19000	46010	170010	-

variables		Atmospheric pCO_2 (ppm)									
emis.	clim. sens.	peak	at year	1500	1000	750	500	400	350	300	278
1000GtC	1.5	681	2000	-	-	-	2090	2450	5000	130000	-
1000GtC	2.64	681	2000	-	-	-	2090	2450	4800	75000	1000000
1000GtC	3	681	2000	-	-	-	2090	2450	4900	70000	-
1000GtC	4.5	682	2000	-	-	-	2100	2450	5200	48000	750000
1000GtC	6.	682	2000	-	-	-	2100	2450	5200	30000	750000
5000GtC	1.5	2453	2000	2500	4100	9500	24000	130000	320000	700000	-
5000GtC	2.64	2453	2000	2550	3900	7500	17000	48000	170000	460000	-
5000GtC	3	2454	2000	2550	3900	7500	16000	44000	150000	420000	-
5000GtC	4.5	2457	2000	2600	3900	6800	15000	36000	110000	280000	1000000
5000GtC	6.	2458	2000	2650	3800	6200	13000	28000	75000	240000	800000

Table 30: **Years** that specific fractions of remaining excess **Atmospheric pCO_2** are reached

variables		fraction									
emis.	short-circ.	90%	75%	50%	25%	10%	e^{-1}	e^{-2}	e^{-3}	e^{-4}	e^{-5}
1000GtC	yes	2010	2030	2120	2600	9500	2240	6200	32010	210010	410010
1000GtC	no	2010	2030	2120	2600	9000	2240	6010	30010	200010	390010
5000GtC	yes	2030	2140	2650	4800	13000	3300	9500	38010	210010	410010
5000GtC	no	2030	2140	2650	4600	12010	3300	9000	36010	200010	380010

variables			fraction									
emis.	T_Ca	T_Si	90%	75%	50%	25%	10%	e^{-1}	e^{-2}	e^{-3}	e^{-4}	e^{-5}
1000GtC	on	on	2010	2030	2120	2750	17000	2280	9500	170000	460000	650000
1000GtC	on	off	2010	2030	2120	2800	28000	2280	12000	-	-	-
1000GtC	off	on	2010	2030	2120	2750	19000	2280	10000	200000	600000	900000
1000GtC	off	off	2010	2030	2120	2800	34000	2280	12000	-	-	-
5000GtC	on	on	2030	2160	2750	7500	24000	3700	17000	160000	550000	950000
5000GtC	on	off	2030	2160	2800	10000	44000	3900	26000	-	-	-
5000GtC	off	on	2030	2160	2800	7500	26000	3700	18000	170000	550000	950000
5000GtC	off	off	2030	2160	2850	11000	55000	3900	28000	-	-	-

variables		fraction									
emis.	E_a (kJ/mol)	90%	75%	50%	25%	10%	e^{-1}	e^{-2}	e^{-3}	e^{-4}	e^{-5}
1000GtC	45	2010	2030	2120	2650	13000	2260	7500	130010	560010	960010
1000GtC	63	2010	2030	2120	2650	12010	2240	7500	85000	390010	700010
1000GtC	74	2010	2030	2120	2650	12010	2240	7000	70010	340010	620010
1000GtC	103	2010	2030	2120	2650	11000	2240	6600	42010	240010	460010
5000GtC	45	2030	2140	2750	6400	22010	3600	15000	180010	600010	-
5000GtC	63	2030	2140	2700	6010	19000	3500	14010	120010	410010	740010
5000GtC	74	2030	2140	2700	5800	18010	3500	13000	90010	360010	640010
5000GtC	103	2030	2140	2700	5200	15000	3400	11000	50010	250010	460010

variables				fraction									
emis.	R_Ca	R_Si	R_explicit	90%	75%	50%	25%	10%	e^{-1}	e^{-2}	e^{-3}	e^{-4}	e^{-5}
1000GtC	on	on	on	2010	2030	2120	2800	26000	2280	12000	-	-	-
1000GtC	on	on	off	2010	2030	2120	2800	24000	2280	11000	700000	-	-
1000GtC	on	off	on	2010	2030	2120	2800	30000	2280	12000	-	-	-
1000GtC	on	off	off	2010	2030	2120	2800	30000	2280	12000	-	-	-
1000GtC	off	on	on	2010	2030	2120	2800	28000	2280	12000	950000	-	-
1000GtC	off	on	off	2010	2030	2120	2800	26000	2280	11000	650000	-	-
1000GtC	off	off	on	2010	2030	2120	2800	34000	2280	12000	-	-	-
1000GtC	off	off	off	2010	2030	2120	2800	34000	2280	12000	-	-	-
5000GtC	on	on	on	2030	2160	2800	9500	40000	3900	24000	-	-	-
5000GtC	on	on	off	2030	2160	2800	9000	34000	3800	22000	650000	-	-
5000GtC	on	off	on	2030	2160	2800	10000	46000	3900	26000	-	-	-
5000GtC	on	off	off	2030	2160	2800	10000	44000	3900	26000	-	-	-
5000GtC	off	on	on	2030	2160	2800	10000	42000	3900	26000	-	-	-
5000GtC	off	on	off	2030	2160	2800	9500	38000	3900	24000	600000	-	-
5000GtC	off	off	on	2030	2160	2850	11000	55000	3900	28000	-	-	-
5000GtC	off	off	off	2030	2160	2850	11000	55000	3900	28000	-	-	-

variables		fraction									
emis.	beta	90%	75%	50%	25%	10%	e^{-1}	e^{-2}	e^{-3}	e^{-4}	e^{-5}
1000GtC	0.48	2010	2030	2120	2700	15000	2260	8500	780010	-	-
1000GtC	0.65	2010	2030	2120	2700	15000	2260	8500	620010	-	-
1000GtC	0.8	2010	2030	2120	2700	15000	2260	8500	500010	-	-
1000GtC	1.12	2010	2030	2120	2700	15000	2260	8500	370010	-	-
5000GtC	0.48	2030	2140	2800	8010	34010	3700	20010	-	-	-
5000GtC	0.65	2030	2140	2800	8010	32010	3700	19000	-	-	-
5000GtC	0.8	2030	2140	2800	8010	30010	3700	19000	-	-	-
5000GtC	1.12	2030	2140	2750	7500	30010	3700	19000	520010	-	-

variables		fraction									
emis.	k_run	90%	75%	50%	25%	10%	e^{-1}	e^{-2}	e^{-3}	e^{-4}	e^{-5}
1000GtC	0.012	2010	2030	2120	2700	16010	2260	8500	920010	-	-
1000GtC	0.024	2010	2030	2120	2700	15000	2260	8500	470010	-	-
1000GtC	0.028	2010	2030	2120	2700	15000	2260	8500	460010	-	-
1000GtC	0.045	2010	2030	2120	2700	14010	2260	8010	270010	960010	-
5000GtC	0.012	2030	2140	2800	8010	36010	3700	22010	-	-	-
5000GtC	0.024	2030	2140	2750	8010	32010	3700	19000	740010	-	-
5000GtC	0.028	2030	2140	2750	7500	30010	3700	19000	660010	-	-
5000GtC	0.045	2030	2140	2750	7500	26010	3700	17000	400010	-	-

variables			fraction									
emis.	P_Ca	P_Si	90%	75%	50%	25%	10%	e^{-1}	e^{-2}	e^{-3}	e^{-4}	e^{-5}
1000GtC	on	on	2010	2030	2120	2800	22000	2280	11000	360000	900000	-
1000GtC	on	off	2010	2030	2120	2800	28000	2280	12000	-	-	-
1000GtC	off	on	2010	2030	2120	2800	22000	2280	11000	360000	950000	-
1000GtC	off	off	2010	2030	2120	2800	34000	2280	12000	-	-	-
5000GtC	on	on	2030	2160	2800	9000	32000	3800	22000	360000	900000	-
5000GtC	on	off	2030	2160	2800	10000	44000	3900	26000	-	-	-
5000GtC	off	on	2030	2160	2800	9500	34000	3800	22000	380000	900000	-
5000GtC	off	off	2030	2160	2850	11000	55000	3900	28000	-	-	-

variables			fraction									
emis.	f_Ca	f_Si	90%	75%	50%	25%	10%	e^{-1}	e^{-2}	e^{-3}	e^{-4}	e^{-5}
1000GtC	on	on	2010	2030	2120	2700	14000	2260	8000	95000	340000	550000
1000GtC	on	off	2010	2030	2120	2800	24000	2280	11000	-	-	-
1000GtC	off	on	2010	2030	2120	2750	15000	2260	8500	100000	320000	550000
1000GtC	off	off	2010	2030	2120	2800	34000	2280	12000	-	-	-
5000GtC	on	on	2030	2160	2750	5800	17000	3500	13000	70000	300000	550000
5000GtC	on	off	2030	2160	2800	8500	36000	3800	22000	-	-	-
5000GtC	off	on	2030	2160	2750	6400	19000	3500	14000	75000	300000	550000
5000GtC	off	off	2030	2160	2850	11000	55000	3900	28000	-	-	-

variables		fraction									
emis.	Scheme	90%	75%	50%	25%	10%	e^{-1}	e^{-2}	e^{-3}	e^{-4}	e^{-5}
1000GtC	Globavg	2010	2030	2120	2600	9500	2240	6200	28010	170010	340010
1000GtC	GKWM	2010	2020	2100	2550	7500	2220	5200	18010	110010	230010
1000GtC	GEM-CO2	2010	2020	2100	2500	7500	2220	5000	16010	95000	210010
5000GtC	Globavg	2030	2140	2650	4700	13000	3300	9500	30010	170010	330010
5000GtC	GKWM	2030	2120	2600	4010	9000	3100	7000	20010	120010	230010
5000GtC	GEM-CO2	2030	2120	2550	3800	8500	3000	6400	18010	110010	210010

variables				fraction									
emis.	f_Ca	f_Si	Scheme	90%	75%	50%	25%	10%	e^{-1}	e^{-2}	e^{-3}	e^{-4}	e^{-5}
1000GtC	on	on	Globavg	2010	2030	2120	2600	9500	2240	6200	32010	210010	390010
1000GtC	on	on	GKWM	2010	2020	2100	2550	7500	2220	5200	18010	110010	230010
1000GtC	on	off	Globavg	2010	2030	2120	2650	14010	2260	8010	-	-	-
1000GtC	on	off	GKWM	2010	2030	2120	2700	15000	2260	8500	660010	-	-
1000GtC	off	on	Globavg	2010	2030	2120	2600	10010	2240	6600	36010	210010	410010
1000GtC	off	on	GKWM	2010	2020	2120	2550	8010	2220	5400	19000	110010	220010
1000GtC	off	off	Globavg	2010	2030	2120	2700	16010	2260	9000	-	-	-
1000GtC	off	off	GKWM	2010	2030	2120	2750	19000	2260	10010	-	-	-
5000GtC	on	on	Globavg	2030	2140	2650	4800	13000	3300	9500	38010	210010	410010
5000GtC	on	on	GKWM	2030	2120	2600	4010	9000	3100	7000	20010	120010	230010
5000GtC	on	off	Globavg	2030	2140	2750	7000	28010	3700	17000	-	-	-
5000GtC	on	off	GKWM	2030	2160	2800	8500	32010	3800	20010	-	-	-
5000GtC	off	on	Globavg	2030	2140	2700	5200	15000	3400	11000	44010	210010	390010
5000GtC	off	on	GKWM	2030	2140	2600	4100	9500	3100	7500	22010	110010	210010
5000GtC	off	off	Globavg	2030	2140	2800	8500	40010	3800	22010	-	-	-
5000GtC	off	off	GKWM	2030	2160	2850	12010	55000	4010	30010	-	-	-

variables		fraction									
emis.	routing	90%	75%	50%	25%	10%	e^{-1}	e^{-2}	e^{-3}	e^{-4}	e^{-5}
1000GtC	1	2010	2030	2120	2800	34000	2280	12000	-	-	-
1000GtC	2	2010	2030	2120	2800	34000	2280	12000	-	-	-
1000GtC	3	2010	2030	2140	2950	-	2300	-	-	-	-
5000GtC	1	2030	2160	2850	11000	55000	3900	28000	-	-	-
5000GtC	2	2030	2160	2850	11000	55000	3900	28000	-	-	-
5000GtC	3	2030	2160	2850	15000	-	4200	40000	-	-	-

variables		fraction									
emis.	lith.	90%	75%	50%	25%	10%	e^{-1}	e^{-2}	e^{-3}	e^{-4}	e^{-5}
1000GtC	GKWM	2010	2020	2100	2550	8010	2220	5200	18010	110010	230010
1000GtC	GEM-CO2	2010	2020	2100	2550	7500	2220	5200	18010	110010	230010
1000GtC	GKWM av.	2010	2030	2120	2550	8500	2240	5600	22010	120010	240010
1000GtC	GEM-CO2 av.	2010	2030	2120	2650	10010	2260	6600	32010	180010	320010
1000GtC	mono acid	2010	2030	2120	2600	8500	2240	5600	20010	110010	220010
1000GtC	mono basalt	2010	2020	2100	2500	6400	2220	4600	13000	60010	140010
1000GtC	mono carb	2010	2020	2080	2400	8010	2180	5000	20010	200010	410010
1000GtC	mono granite	2010	2030	2120	2600	8500	2240	5600	20010	110010	220010
1000GtC	mono sand	2010	2030	2140	2850	22010	2280	13000	95000	430010	740010
1000GtC	mono shale	2010	2020	2080	2400	5600	2180	3900	10010	28010	100010
1000GtC	mono shield	2010	2030	2120	2600	8500	2240	5600	20010	110010	220010
5000GtC	GKWM	2030	2120	2600	4010	9500	3100	7000	22010	120010	240010
5000GtC	GEM-CO2	2030	2120	2600	4010	9000	3100	7000	20010	120010	220010
5000GtC	GKWM av.	2030	2140	2600	4300	11000	3200	8010	24010	140010	260010
5000GtC	GEM-CO2 av.	2030	2140	2700	5400	15000	3400	11000	38010	190010	370010
5000GtC	mono acid	2030	2140	2600	4400	11000	3200	8010	22010	110010	220010
5000GtC	mono basalt	2030	2120	2500	3600	7500	2900	5800	14010	65000	150010
5000GtC	mono carb	2020	2100	2500	3700	9000	2850	6400	24010	230010	470010
5000GtC	mono granite	2030	2140	2600	4400	11000	3200	8010	22010	110010	220010
5000GtC	mono sand	2030	2160	2850	13000	34010	4400	26010	110010	430010	780010
5000GtC	mono shale	2020	2100	2400	3200	5800	2700	4600	10010	32010	110010
5000GtC	mono shield	2030	2140	2600	4400	11000	3200	8010	22010	110010	220010

variables		fraction									
emis.	clim. sens.	90%	75%	50%	25%	10%	e^{-1}	e^{-2}	e^{-3}	e^{-4}	e^{-5}
1000GtC	1.5	2010	2030	2120	2750	16000	2260	9000	170000	500000	850000
1000GtC	2.64	2010	2030	2120	2700	14000	2260	8000	95000	320000	550000
1000GtC	3	2010	2030	2120	2700	14000	2260	8500	90000	320000	550000
1000GtC	4.5	2010	2030	2140	2750	13000	2280	8500	60000	240000	400000
1000GtC	6.	2010	2030	2140	2750	12000	2300	8000	36000	180000	320000
5000GtC	1.5	2030	2140	2650	7500	24000	3500	17000	170000	550000	850000
5000GtC	2.64	2030	2160	2750	5800	17000	3500	13000	70000	320000	600000
5000GtC	3	2030	2160	2750	5800	17000	3500	12000	65000	280000	500000
5000GtC	4.5	2030	2180	2850	5600	15000	3600	11000	46000	190000	340000
5000GtC	6.	2030	2200	2900	5000	14000	3500	10000	36000	150000	300000

Table 31: **Timescale fitting** for excess **Atmospheric pCO_2** decay

variables		fit to $pCO_2(t) = b + h\sum_i w_i e^{-(t-t_0)/\tau_i}$									
emis.	short-circ.		pCO_2 (ppm)	i	1	2	3	4	5	6	7	R^2
1000GtC	yes	b	278.47±0.02	w_i (%)	12.6±0.2	17.5±0.1	36.6±0.2	9.9±0.6	10.7±0.6	7.3±0.7	5.38±0.04	0.99999998
		h	400±40	τ_i (yr)	5.7±0.1	29.0±0.6	156±2	440±20	3800±100	8800±400	179300±1000	
1000GtC	no	b	278.58±0.02	w_i (%)	12.7±0.2	17.6±0.1	36.4±0.2	10.0±0.6	11.0±0.6	7.1±0.8	5.26±0.04	0.99999998
		h	400±40	τ_i (yr)	5.71±0.1	28.9±0.6	154±2	430±20	3700±100	8600±400	169400±900	
5000GtC	yes	b	279.8±0.5	w_i (%)	7.2±0.2	11.3±0.2	44.8±0.2	29.6±0.3	1.3±0.5	5.7±0.1		0.9999992
		h	2170±217	τ_i (yr)	11.3±0.6	82±3	648±5	5230±100	21000±8000	177000±5000		
5000GtC	no	b	279.9±0.4	w_i (%)	7.3±0.2	11.6±0.2	44.5±0.2	29.0±0.4	2.0±0.7	5.6±0.1		0.9999992
		h	2170±217	τ_i (yr)	11.4±0.5	83±3	646±5	4700±100	16000±4000	166000±4000		

variables			fit to $pCO_2(t) = b + h\sum_i w_i e^{-(t-t_0)/\tau_i}$									
emis.	T_Ca	T_Si		pCO_2 (ppm)	i	1	2	3	4	5	6	7	R^2
1000GtC	on	on	b	272.8±0.2	w_i (%)	11.7±0.5	16.8±0.3	31±1	15±2	7±1	9±1	9.4±0.1	0.99999992
			h	408±40	τ_i (yr)	5.8±0.3	29±1	148±7	370±30	4100±400	9400±600	391000±6000	
1000GtC	on	off	b	315.06±0.07	w_i (%)	13.1±0.5	18.9±0.3	35.8±0.9	15±2	9.3±0.9	8±1		0.99999995
			h	365±36	τ_i (yr)	5.8±0.2	29±1	151±6	390±20	4800±300	11700±700		
1000GtC	off	on	b	277.5±0.2	w_i (%)	11.9±0.4	17.1±0.3	32.1±0.8	14±2	9.0±0.9	7±1	8.6±0.1	0.99999995
			h	403±40	τ_i (yr)	5.8±0.2	29±1	150±5	380±20	4600±300	10900±700	371000±5000	
1000GtC	off	off	b	316.02±0.07	w_i (%)	13.2±0.5	19.0±0.3	35.9±0.9	15±2	8.7±0.9	8±1		0.99999995
			h	364±36	τ_i (yr)	5.8±0.2	29±1	151±6	390±20	4600±300	11600±700		
5000GtC	on	on	b	2170±2170	w_i (%)	6.1±0.7	11.6±0.6	44.6±0.2	30.1±0.2	7.6±0.2			0.999995
			h	2170±217	τ_i (yr)	11±2	74±7	666±9	9200±100	350000±20000			
5000GtC	on	off	b	1980±1980	w_i (%)	7±1	13±1	48.6±0.3	31.6±0.3				0.99999
			h	1980±198	τ_i (yr)	11±3	80±10	680±10	12500±200				
5000GtC	off	on	b	2170±2170	w_i (%)	6.1±0.7	11.7±0.6	44.6±0.2	29.9±0.2	7.7±0.2			0.999995
			h	2170±217	τ_i (yr)	11±2	75±7	671±9	9700±100	360000±20000			
5000GtC	off	off	b	1970±1970	w_i (%)	7±2	13±1	48.7±0.3	31.4±0.3				0.99999
			h	1970±197	τ_i (yr)	11±3	80±10	680±10	13300±200				

variables		fit to $pCO_2(t) = b + h\sum_i w_i e^{-(t-t_0)/\tau_i}$									
emis.	E_a (kJ/mol)		pCO$_2$ (ppm)	i	1	2	3	4	5	6	7	R^2
1000GtC	45	b	277.88±0.07	w_i (%)	12.6±0.2	17.4±0.1	35.1±0.3	10.8±0.8	8.2±0.4	9.2±0.5	6.77±0.06	0.99999998
		h	400±40	τ_i (yr)	5.7±0.1	28.8±0.6	153±3	410±20	3600±100	9100±200	420000±3000	
1000GtC	63	b	278.04±0.04	w_i (%)	12.6±0.2	17.5±0.1	35.5±0.3	10.5±0.7	8.9±0.4	8.6±0.6	6.44±0.05	0.99999998
		h	400±40	τ_i (yr)	5.7±0.1	28.9±0.6	154±2	420±20	3700±100	9100±300	307000±2000	
1000GtC	74	b	278.29±0.04	w_i (%)	12.6±0.2	17.4±0.2	35.4±0.4	10.6±0.9	8.5±0.5	9.2±0.7	6.27±0.06	0.99999998
		h	400±40	τ_i (yr)	5.7±0.1	28.8±0.7	154±3	410±20	3500±200	8700±300	262000±1000	
1000GtC	103	b	278.60±0.04	w_i (%)	12.6±0.3	17.5±0.2	35.8±0.5	10±1	8.4±0.9	9±1	5.86±0.07	0.99999996
		h	400±40	τ_i (yr)	5.7±0.2	28.9±0.9	154±4	420±30	3500±300	8200±400	188000±1000	
5000GtC	45	b	2168±2168	w_i (%)	7.3±0.3	12.0±0.2	43.38±0.09	29.75±0.09	7.57±0.05			0.999999
		h	2168±216	τ_i (yr)	11.4±0.7	85±4	679±5	7910±50	368000±8000			
5000GtC	63	b	282.4±0.8	w_i (%)	7.4±0.3	11.9±0.2	43.58±0.08	29.97±0.09	7.20±0.04			0.999999
		h	2169±216	τ_i (yr)	11.5±0.7	85±3	675±5	7210±40	271000±4000			
5000GtC	74	b	2172±2172	w_i (%)	7.3±0.3	11.8±0.2	43.72±0.09	29.9±0.1	1.0±0.9	6.3±0.9		0.9999990
		h	2172±217	τ_i (yr)	11.4±0.6	85±3	671±5	6850±60	80000±60000	270000±30000		
5000GtC	103	b	279.9±0.6	w_i (%)	7.3±0.3	11.6±0.2	44.51±0.1	29.6±0.2	1.1±0.2	5.9±0.2		0.9999992
		h	2172±217	τ_i (yr)	11.4±0.6	84±3	660±5	5890±80	30000±10000	198000±7000		

variables				fit to $pCO_2(t) = b + h\sum_i w_i e^{-(t-t_0)/\tau_i}$									
emis.	R_Ca	R_Si	R_explicit		pCO_2 (ppm)	i	1	2	3	4	5	6	7	R^2
1000GtC	on	on	on	b	404±404	w_i (%)	11.9±0.4	17.1±0.3	32.2±0.8	14±2	7.8±0.7	7.6±0.9	9.6±0.8	0.99999996
				h	404±40	τ_i (yr)	5.8±0.2	29±1	151±5	390±20	4500±300	11000±500	1900000±200000	
1000GtC	on	on	off	b	403±403	w_i (%)	11.9±0.4	17.1±0.2	32.4±0.8	14±2	8.1±0.8	7.5±1	9.0±0.3	0.99999995
				h	403±40	τ_i (yr)	5.8±0.2	29±1	151±5	380±20	4500±300	10900±600	1110000±50000	
1000GtC	on	off	on	b	315.37±0.07	w_i (%)	13.2±0.5	18.9±0.3	35.9±0.9	15±2	9.2±0.9	8±1		0.99999995
				h	365±36	τ_i (yr)	5.8±0.2	29±1	152±6	390±20	4700±300	11900±700		
1000GtC	on	off	off	b	315.12±0.07	w_i (%)	13.1±0.5	18.9±0.3	35.8±0.9	15±2	9.4±1	8±1		0.99999995
				h	365±36	τ_i (yr)	5.8±0.2	29±1	151±6	390±20	4800±300	11900±800		
1000GtC	off	on	on	b	415±415	w_i (%)	11.6±0.4	16.6±0.3	31.5±0.8	13±1	7.7±0.7	7.3±0.9	12±1	0.99999995
				h	415±41	τ_i (yr)	5.8±0.2	29±1	151±5	390±20	4600±300	11300±600	2200000±200000	
1000GtC	off	on	off	b	405±405	w_i (%)	11.8±0.4	17.0±0.2	32.2±0.8	14±2	7.7±0.8	7.6±0.9	9.7±0.3	0.99999995
				h	405±40	τ_i (yr)	5.8±0.2	29±1	151±5	390±20	4600±300	11000±600	1090000±50000	
1000GtC	off	off	on	b	316.02±0.07	w_i (%)	13.2±0.5	19.0±0.3	35.9±0.9	15±2	8.7±0.9	8±1		0.99999995
				h	364±36	τ_i (yr)	5.8±0.2	29±1	151±6	390±20	4600±300	11600±700		
1000GtC	off	off	off	b	316.02±0.07	w_i (%)	13.2±0.5	19.0±0.3	35.9±0.9	15±2	8.7±0.9	8±1		0.99999995
				h	364±36	τ_i (yr)	5.8±0.2	29±1	151±6	390±20	4600±300	11600±700		
5000GtC	on	on	on	b	2000±2000	w_i (%)	7±4	13±3	48.0±0.8	31.8±0.8				0.9999
				h	2000±200	τ_i (yr)	12±8	80±40	710±40	13600±500				
5000GtC	on	on	off	b	2280±2280	w_i (%)	5.8±0.9	11.2±0.7	42±1	27.9±0.8	13±6			0.999992
				h	2280±228	τ_i (yr)	11±2	75±9	680±10	11400±200	2000000±1000000			
5000GtC	on	off	on	b	1940±1940	w_i (%)	16.9±0.7	50.9±0.3	32.2±0.4					0.99997
				h	1940±194	τ_i (yr)	43±4	650±10	12600±300					
5000GtC	on	off	off	b	1980±1980	w_i (%)	7±1	13±1	48.6±0.3	31.6±0.3				0.99999
				h	1980±198	τ_i (yr)	11±3	80±10	680±10	12700±200				
5000GtC	off	on	on	b	2000±2000	w_i (%)	7±4	13±3	48.0±0.8	31.8±0.8				0.9999
				h	2000±200	τ_i (yr)	12±9	80±40	710±40	14400±600				
5000GtC	off	on	off	b	2300±2300	w_i (%)	6±1	11.1±0.9	41±2	27±1	15±8			0.99999
				h	2300±230	τ_i (yr)	11±3	75±10	680±10	12400±200	2000000±1000000			
5000GtC	off	off	on	b	1970±1970	w_i (%)	7±2	13±1	48.7±0.3	31.4±0.3				0.99999
				h	1970±197	τ_i (yr)	11±3	80±10	680±10	13300±200				
5000GtC	off	off	off	b	1970±1970	w_i (%)	7±2	13±1	48.7±0.3	31.4±0.3				0.99999
				h	1970±197	τ_i (yr)	11±3	80±10	680±10	13300±200				

variables		fit to $pCO_2(t) = b + h\sum_i w_i e^{-(t-t_0)/\tau_i}$									
emis.	beta		pCO_2 (ppm)	i	1	2	3	4	5	6	7	R^2
1000GtC	0.48	b	401±401	w_i (%)	12.5±0.2	17.4±0.1	34.5±0.3	11.2±0.8	7.7±0.3	9.2±0.4	7.6±0.3	0.99999999
		h	401±40	τ_i (yr)	5.69±0.1	28.7±0.6	152±2	400±10	3600±100	9600±200	2000000±100000	
1000GtC	0.65	b	279.1±0.7	w_i (%)	12.6±0.2	17.5±0.1	34.7±0.3	11.1±0.8	7.7±0.3	9.2±0.4	7.1±0.2	0.99999999
		h	399±39	τ_i (yr)	5.7±0.1	28.7±0.6	152±3	400±20	3600±100	9500±200	1470000±50000	
1000GtC	0.8	b	279.0±0.5	w_i (%)	12.6±0.2	17.5±0.1	34.8±0.3	11.1±0.8	7.8±0.3	9.2±0.4	7.1±0.1	0.99999998
		h	399±39	τ_i (yr)	5.7±0.1	28.7±0.6	152±3	400±20	3600±100	9500±200	1240000±30000	
1000GtC	1.12	b	279.6±0.3	w_i (%)	12.6±0.2	17.5±0.2	34.8±0.4	11.2±0.9	7.6±0.4	9.5±0.5	6.90±0.08	0.99999998
		h	399±39	τ_i (yr)	5.7±0.1	28.7±0.6	152±3	400±20	3500±200	9300±200	890000±20000	
5000GtC	0.48	b	2220±2220	w_i (%)	7.2±0.4	11.9±0.3	42.1±0.5	28.0±0.4	11±3			0.999998
		h	2220±222	τ_i (yr)	11.4±1	86±5	696±6	9810±70	3000000±1000000			
5000GtC	0.65	b	1980±1980	w_i (%)	18±1	49.9±0.6	32.4±0.7					0.9999
		h	1980±198	τ_i (yr)	44±6	670±30	10700±400					
5000GtC	0.8	b	2010±2010	w_i (%)	9±3	14±3	46±1	31.1±0.9				0.9999
		h	2010±201	τ_i (yr)	13±7	110±40	750±50	11200±500				
5000GtC	1.12	b	2163±2163	w_i (%)	7.3±0.4	12.2±0.3	43.2±0.1	29.1±0.1	8.2±0.3			0.999998
		h	2163±216	τ_i (yr)	11.4±0.9	85±5	689±6	9270±60	850000±60000			

variables		fit to $pCO_2(t) = b + h\sum_i w_i e^{-(t-t_0)/\tau_i}$									
emis.	k_run		pCO_2 (ppm)	i	1	2	3	4	5	6	7	R^2
1000GtC	0.012	b	407±407	w_i (%)	12.3±0.2	17.1±0.1	34.0±0.3	11.0±0.8	7.8±0.3	8.7±0.4	9.0±0.6	0.99999998
		h	407±40	τ_i (yr)	5.7±0.1	28.7±0.6	152±3	410±20	3700±100	9900±200	2800000±200000	
1000GtC	0.024	b	275.9±0.6	w_i (%)	12.5±0.2	17.3±0.2	34.4±0.4	11.1±0.9	7.8±0.4	9.0±0.5	7.9±0.2	0.99999998
		h	402±40	τ_i (yr)	5.7±0.1	28.7±0.7	152±3	400±20	3600±100	9600±200	1270000±30000	
1000GtC	0.028	b	276.6±0.6	w_i (%)	12.5±0.2	17.4±0.1	34.8±0.3	10.8±0.8	8.5±0.4	8.3±0.4	7.7±0.1	0.99999998
		h	402±40	τ_i (yr)	5.7±0.1	28.8±0.6	153±3	410±20	3800±100	10100±200	1250000±30000	
1000GtC	0.045	b	276.3±0.2	w_i (%)	12.5±0.2	17.4±0.2	35.0±0.3	10.7±0.8	9.0±0.4	7.9±0.5	7.53±0.08	0.99999998
		h	402±40	τ_i (yr)	5.7±0.1	28.8±0.6	154±3	420±20	3900±100	10200±300	790000±10000	
5000GtC	0.012	b	1970±1970	w_i (%)	18±1	50.1±0.7	32.0±0.8					0.9998
		h	1970±197	τ_i (yr)	45±7	680±30	11400±500					
5000GtC	0.024	b	2175±2175	w_i (%)	7.3±0.4	12.1±0.3	43.0±0.2	28.7±0.1	8.8±0.7			0.999998
		h	2175±217	τ_i (yr)	11.4±0.9	86±5	692±6	9560±70	1300000±200000			
5000GtC	0.028	b	2177±2177	w_i (%)	7.3±0.4	12.1±0.3	42.9±0.1	28.7±0.1	8.9±0.6			0.999998
		h	2177±217	τ_i (yr)	11.5±0.9	86±5	692±6	9370±70	1200000±100000			
5000GtC	0.045	b	2171±2171	w_i (%)	7.3±0.4	12.1±0.3	43.1±0.1	29.16±0.1	8.3±0.2			0.999998
		h	2171±217	τ_i (yr)	11.4±0.8	85±4	686±5	8810±60	720000±30000			

variables			fit to $pCO_2(t) = b + h\sum_i w_i e^{-(t-t_0)/\tau_i}$									
emis.	P_Ca	P_Si		pCO_2 (ppm)	i	1	2	3	4	5	6	7	R^2
1000GtC	on	on	b	273.8±0.6	w_i (%)	11.8±0.5	16.9±0.3	32.0±0.9	14±2	8.8±1	7±1	9.6±0.2	0.99999994
			h	407±40	τ_i (yr)	5.8±0.2	29±1	150±6	380±20	4700±300	11200±800	710000±20000	
1000GtC	on	off	b	315.09±0.07	w_i (%)	13.2±0.5	18.9±0.3	35.8±0.9	15±2	9.1±0.9	8±1		0.99999995
			h	365±36	τ_i (yr)	5.8±0.2	29±1	151±6	390±20	4700±300	11500±700		
1000GtC	off	on	b	275.6±0.6	w_i (%)	11.8±0.5	17.0±0.3	32.1±1	14±2	8±1	7±1	9.5±0.2	0.99999993
			h	405±40	τ_i (yr)	5.8±0.3	29±1	150±6	380±20	4600±400	10900±800	660000±20000	
1000GtC	off	off	b	316.02±0.07	w_i (%)	13.2±0.5	19.0±0.3	35.9±0.9	15±2	8.7±0.9	8±1		0.99999995
			h	364±36	τ_i (yr)	5.8±0.2	29±1	151±6	390±20	4600±300	11600±700		
5000GtC	on	on	b	2260±2260	w_i (%)	5.8±0.9	11.4±0.7	42.6±0.4	28.5±0.3	12±2			0.999992
			h	2260±226	τ_i (yr)	10±2	74±9	670±10	11200±200	1100000±300000			
5000GtC	on	off	b	1980±1980	w_i (%)	7±1	13±1	48.6±0.3	31.6±0.3				0.99999
			h	1980±198	τ_i (yr)	11±3	80±10	680±10	12500±200				
5000GtC	off	on	b	2250±2250	w_i (%)	6±1	11.4±0.8	42.6±0.4	28.4±0.3	12±2			0.999990
			h	2250±225	τ_i (yr)	11±3	75±10	680±10	11900±200	1100000±300000			
5000GtC	off	off	b	1970±1970	w_i (%)	7±2	13±1	48.7±0.3	31.4±0.3				0.99999
			h	1970±197	τ_i (yr)	11±3	80±10	680±10	13300±200				

variables			fit to $pCO_2(t) = b + h\sum_i w_i e^{-(t-t_0)/\tau_i}$									
emis.	f_Ca	f_Si		pCO_2 (ppm)	i	1	2	3	4	5	6	7	R^2
1000GtC	on	on	b	277.56±0.09	w_i (%)	11.8±0.4	17.0±0.2	32.0±0.8	15±2	11±1	6±1	7.5±0.1	0.99999996
			h	403±40	τ_i (yr)	5.8±0.2	29±1	148±5	370±20	4500±300	10300±800	237000±2000	
1000GtC	on	off	b	313.89±0.07	w_i (%)	13.1±0.5	18.8±0.3	35.7±0.9	15±2	10±1	7±1		0.99999994
			h	367±36	τ_i (yr)	5.8±0.2	29±1	151±6	390±20	4700±300	11400±800		
1000GtC	off	on	b	277.42±0.09	w_i (%)	11.9±0.4	17.0±0.3	32.1±0.9	15±2	10.0±1	7±1	7.9±0.1	0.99999995
			h	403±40	τ_i (yr)	5.8±0.2	29±1	149±5	370±20	4600±300	10700±800	225000±2000	
1000GtC	off	off	b	316.02±0.07	w_i (%)	13.2±0.5	19.0±0.3	35.9±0.9	15±2	8.7±0.9	8±1		0.99999995
			h	364±36	τ_i (yr)	5.8±0.2	29±1	151±6	390±20	4600±300	11600±700		
5000GtC	on	on	b	2172±2172	w_i (%)	6.1±0.6	11.4±0.4	45.2±0.1	30.7±0.2	6.63±0.08			0.999997
			h	2172±217	τ_i (yr)	11±1	74±5	653±7	7180±70	223000±9000			
5000GtC	on	off	b	1980±1980	w_i (%)	7±1	12.9±0.9	48.4±0.2	32.0±0.3				0.999992
			h	1980±198	τ_i (yr)	11±3	75±10	670±10	10800±200				
5000GtC	off	on	b	2172±2172	w_i (%)	6.2±0.6	11.5±0.4	45.0±0.1	30.5±0.1	6.81±0.09			0.999997
			h	2172±217	τ_i (yr)	11±1	76±6	663±7	8020±80	215000±9000			
5000GtC	off	off	b	1970±1970	w_i (%)	7±2	13±1	48.7±0.3	31.4±0.3				0.99999
			h	1970±197	τ_i (yr)	11±3	80±10	680±10	13300±200				

variables		fit to $pCO_2(t) = b + h\sum_i w_i e^{-(t-t_0)/\tau_i}$									
emis.	Scheme		pCO_2 (ppm)	i	1	2	3	4	5	6	7	R^2
1000GtC	Globavg	b	278.64±0.02	w_i (%)	12.5±0.2	17.4±0.1	36.5±0.2	10.1±0.6	10.5±0.7	7.8±0.8	5.23±0.04	0.99999999
		h	400±40	τ_i (yr)	5.71±0.1	28.9±0.5	155±2	440±20	3700±100	8500±300	147800±800	
1000GtC	GKWM	b	278.37±0.04	w_i (%)	13.1±0.3	18.0±0.2	37.2±0.2	9.2±0.7	12±1	6±1	4.51±0.06	0.99999998
		h	399±39	τ_i (yr)	5.7±0.1	28.7±0.6	153±2	440±20	3600±200	7800±700	109000±1000	
1000GtC	GEM-CO2	b	278.38±0.04	w_i (%)	13.3±0.3	18.1±0.2	37.0±0.3	9.3±0.8	13±1	5±1	4.28±0.07	0.99999998
		h	398±39	τ_i (yr)	5.7±0.1	28.6±0.6	152±3	420±20	3600±200	7800±800	103000±1000	
5000GtC	Globavg	b	279.9±0.4	w_i (%)	7.1±0.3	11.2±0.2	45.3±0.2	29.8±0.3	1.3±0.5	5.3±0.2		0.9999992
		h	2170±217	τ_i (yr)	11.1±0.6	79±3	642±5	5110±100	20000±8000	147000±4000		
5000GtC	GKWM	b	279.1±0.1	w_i (%)	3.6±0.4	6.2±0.3	9.9±0.2	44.6±0.1	24.9±0.4	5.7±0.7	4.94±0.04	0.99999993
		h	2170±217	τ_i (yr)	6.5±0.6	24±2	105±3	632±3	3220±60	8300±500	108200±800	
5000GtC	GEM-CO2	b	279.17±0.09	w_i (%)	3.8±0.4	6.3±0.2	9.6±0.2	44.94±0.09	22.3±0.5	8.2±0.8	4.75±0.04	0.99999995
		h	2170±217	τ_i (yr)	6.8±0.5	26±2	107±3	616±4	2740±70	6700±300	101200±600	

variables				fit to $pCO_2(t) = b + h\sum_i w_i e^{-(t-t_0)/\tau_i}$									
emis.	f_Ca	f_Si	Scheme		pCO_2 (ppm)	i	1	2	3	4	5	6	7	R^2
1000GtC	on	on	Globavg	b	278.41±0.03	w_i (%)	12.6±0.3	17.5±0.2	36.5±0.3	10.0±0.8	10.1±0.9	8±1	5.42±0.06	0.99999997
				h	400±40	τ_i (yr)	5.7±0.1	28.9±0.7	155±3	440±20	3700±200	8400±400	178000±1000	
1000GtC	on	on	GKWM	b	278.37±0.04	w_i (%)	13.1±0.3	18.0±0.2	37.1±0.2	9.2±0.7	12±1	6±1	4.51±0.06	0.99999998
				h	399±39	τ_i (yr)	5.7±0.1	28.7±0.6	153±2	430±20	3600±200	7800±600	109000±1000	
1000GtC	on	off	Globavg	b	306.50±0.03	w_i (%)	6±6	10±4	17.2±1	38.1±0.6	10.4±0.9	9.4±0.5	8.8±0.6	0.99999999
				h	372±37	τ_i (yr)	4±2	9±3	33±2	159±4	440±20	3800±100	9900±300	
1000GtC	on	off	GKWM	b	403±403	w_i (%)	12.3±0.2	17.1±0.1	34.2±0.3	11.6±0.8	7.7±0.3	9.4±0.4	7.8±0.3	0.99999998
				h	403±40	τ_i (yr)	5.7±0.1	28.6±0.6	152±3	410±10	3600±100	9900±200	2000000±100000	
1000GtC	off	on	Globavg	b	278.61±0.02	w_i (%)	12.6±0.2	17.5±0.1	36.3±0.3	10.0±0.7	9.7±0.6	8.2±0.7	5.64±0.04	0.99999998
				h	400±40	τ_i (yr)	5.7±0.1	29.0±0.6	155±2	430±20	3700±200	8900±300	169900±900	
1000GtC	off	on	GKWM	b	278.37±0.04	w_i (%)	13.0±0.2	17.9±0.2	37.1±0.2	9.3±0.7	12.1±1	6±1	4.64±0.06	0.99999998
				h	399±39	τ_i (yr)	5.7±0.1	28.8±0.6	154±2	440±20	3700±200	8100±600	106000±1000	
1000GtC	off	off	Globavg	b	308.31±0.04	w_i (%)	13.6±0.3	18.9±0.2	37.5±0.5	12±1	8.7±0.4	9.4±0.6		0.99999998
				h	370±37	τ_i (yr)	5.7±0.1	28.7±0.8	153±3	410±20	3800±200	10200±300		
1000GtC	off	off	GKWM	b	308.69±0.04	w_i (%)	13.2±0.3	18.5±0.2	36.8±0.5	13±1	7.4±0.3	10.9±0.4		0.99999997
				h	370±37	τ_i (yr)	5.7±0.2	28.6±0.8	151±4	410±20	3600±200	11200±200		
5000GtC	on	on	Globavg	b	279.8±0.5	w_i (%)	7.2±0.2	11.3±0.2	44.8±0.2	29.6±0.3	1.3±0.5	5.7±0.1		0.9999992
				h	2170±217	τ_i (yr)	11.3±0.6	82±3	648±5	5230±100	20000±8000	176000±5000		
5000GtC	on	on	GKWM	b	279.1±0.1	w_i (%)	3.7±0.5	6.3±0.3	9.8±0.2	44.6±0.2	24.7±0.5	5.9±0.8	4.97±0.05	0.99999992
				h	2170±217	τ_i (yr)	6.6±0.6	25±2	107±4	631±4	3220±80	8000±500	107200±900	
5000GtC	on	off	Globavg	b	465.3±0.4	w_i (%)	8.0±0.4	13.2±0.3	47.0±0.1	31.8±0.1				0.999999
				h	1987±198	τ_i (yr)	11.5±0.9	86±4	685±6	8520±50				
5000GtC	on	off	GKWM	b	1990±1990	w_i (%)	17±1	49.8±0.7	33.1±0.8					0.9998
				h	1990±199	τ_i (yr)	43±7	660±30	11600±500					
5000GtC	off	on	Globavg	b	280.8±0.5	w_i (%)	7.4±0.3	11.6±0.2	44.60±0.09	30.1±0.1	6.26±0.04			0.999999
				h	2171±217	τ_i (yr)	11.6±0.7	86±4	667±5	6090±40	156000±3000			
5000GtC	off	on	GKWM	b	279.3±0.2	w_i (%)	3.6±0.7	6.2±0.4	10.0±0.3	44.5±0.3	25.2±0.9	5±1	5.19±0.09	0.9999998
				h	2170±217	τ_i (yr)	6.5±0.9	24±3	105±5	637±5	3500±100	8300±900	98000±1000	
5000GtC	off	off	Globavg	b	1480±1480	w_i (%)	100.0±0.4							0.99
				h	1480±148	τ_i (yr)	1900±200							
5000GtC	off	off	GKWM	b	1980±1980	w_i (%)	7±2	13±1	48.0±0.4	32.1±0.4				0.99998
				h	1980±198	τ_i (yr)	10±4	70±20	670±20	15500±400				

variables		fit to $pCO_2(t) = b + h\sum_i w_i e^{-(t-t_0)/\tau_i}$								
emis.	routing		pCO_2 (ppm)	i	1	2	3	4	5	6	R^2
1000GtC	1	b	315.96±0.07	w_i (%)	13.2±0.5	19.0±0.3	36.0±0.9	15±2	9.0±0.9	8±1	0.99999995
		h	365±36	τ_i (yr)	5.8±0.2	29±1	152±6	390±20	4700±300	11900±700	
1000GtC	2	b	316.02±0.07	w_i (%)	13.2±0.5	19.0±0.3	35.9±0.9	15±2	8.7±0.9	8±1	0.99999995
		h	364±36	τ_i (yr)	5.8±0.2	29±1	151±6	390±20	4600±300	11600±700	
1000GtC	3	b	336.86±0.09	w_i (%)	13.8±0.4	19.9±0.2	39.5±0.4	14±1	12.5±0.1		0.99999997
		h	347±34	τ_i (yr)	5.9±0.2	29.9±1	158±4	440±20	6140±50		
5000GtC	1	b	1970±1970	w_i (%)	7±2	13±1	48.7±0.3	31.5±0.3			0.99999
		h	1970±197	τ_i (yr)	11±3	70±10	680±20	13500±200			
5000GtC	2	b	1970±1970	w_i (%)	7±2	13±1	48.7±0.3	31.4±0.3			0.99999
		h	1970±197	τ_i (yr)	11±3	80±10	680±10	13300±200			
5000GtC	3	b	1940±1940	w_i (%)	17.0±0.8	51.3±0.3	31.7±0.4				0.99997
		h	1940±194	τ_i (yr)	44±4	670±20	19100±800				

variables		fit to $pCO_2(t) = b + h\sum_i w_i e^{-(t-t_0)/\tau_i}$										
emis.	lith.		pCO_2 (ppm)	i	1	2	3	4	5	6	7	R^2
1000GtC	GKWM	b	278.35±0.04	w_i (%)	13.1±0.2	17.9±0.2	37.2±0.2	9.2±0.7	12.3±1	6±1	4.55±0.06	0.99999998
		h	399±39	τ_i (yr)	5.7±0.1	28.8±0.6	153±2	440±20	3600±200	8000±600	112000±1000	
1000GtC	GEM-CO2	b	278.37±0.04	w_i (%)	13.1±0.3	18.0±0.2	37.2±0.2	9.2±0.7	12±1	6±1	4.51±0.06	0.99999998
		h	399±39	τ_i (yr)	5.7±0.1	28.7±0.6	153±2	440±20	3600±200	7800±700	109000±1000	
1000GtC	GKWM av.	b	277.40±0.04	w_i (%)	12.8±0.4	17.7±0.3	37.2±0.3	9±1	14.1±0.8	4.1±1	4.84±0.09	0.99999994
		h	400±40	τ_i (yr)	5.7±0.2	29±1	155±4	460±30	4100±200	11000±1000	133000±2000	
1000GtC	GEM-CO2 av.	b	277.43±0.03	w_i (%)	12.3±0.3	17.1±0.2	35.2±0.4	11±1	8.9±0.8	9.5±0.9	5.64±0.06	0.99999997
		h	401±40	τ_i (yr)	5.7±0.2	28.7±0.9	152±3	420±20	3600±200	8700±400	165000±1000	
1000GtC	mono acid	b	278.40±0.04	w_i (%)	12.5±0.2	17.3±0.2	36.4±0.2	10.4±0.7	11.8±0.9	7±1	4.59±0.05	0.99999998
		h	400±40	τ_i (yr)	5.7±0.1	28.8±0.6	153±2	430±20	3700±200	8300±500	105000±1000	
1000GtC	mono basalt	b	278.44±0.05	w_i (%)	13.1±0.3	18.0±0.2	37.2±0.3	9.6±0.9	14±1	4±1	3.56±0.09	0.99999998
		h	398±39	τ_i (yr)	5.7±0.1	28.3±0.7	150±3	410±20	3600±200	8000±1000	75000±2000	
1000GtC	mono carb	b	277.55±0.04	w_i (%)	14.7±0.4	19.4±0.2	31±1	15±2	7±3	9±3	4.59±0.07	0.99999996
		h	395±39	τ_i (yr)	5.6±0.1	27.2±0.9	133±6	300±20	4100±600	7200±700	229000±2000	
1000GtC	mono granite	b	278.40±0.04	w_i (%)	12.5±0.2	17.3±0.2	36.4±0.2	10.4±0.7	11.9±0.9	7±1	4.58±0.06	0.99999998
		h	400±40	τ_i (yr)	5.7±0.1	28.8±0.6	153±2	430±20	3700±200	8400±500	105000±1000	
1000GtC	mono sand	b	277.64±0.08	w_i (%)	11.2±0.4	15.9±0.2	31.5±0.6	17±1	2.7±0.2	15.2±0.3	6.67±0.04	0.99999996
		h	403±40	τ_i (yr)	5.6±0.2	27.5±1	142±4	380±10	3800±400	13300±200	339000±3000	
1000GtC	mono shale	b	278.57±0.06	w_i (%)	6±10	11±8	18±1	36±1	10±2	16.7±0.5	2.61±0.08	0.99999996
		h	390±39	τ_i (yr)	4±3	9±5	31±3	144±6	350±20	4230±20	60000±2000	
1000GtC	mono shield	b	278.40±0.04	w_i (%)	12.5±0.2	17.3±0.2	36.4±0.2	10.4±0.7	11.9±0.9	7±1	4.58±0.06	0.99999998
		h	400±40	τ_i (yr)	5.7±0.1	28.8±0.6	153±2	430±20	3700±200	8400±500	105000±1000	

variables		fit to $pCO_2(t) = b + h\sum_i w_i e^{-(t-t_0)/\tau_i}$									
emis.	lith.		pCO_2 (ppm)	i	1	2	3	4	5	6	7	R^2
5000GtC	GKWM	b	279.2±0.1	w_i (%)	3.7±0.5	6.3±0.3	10.0±0.2	44.5±0.2	25.2±0.5	5.4±0.7	4.98±0.05	0.99999992
		h	2170±217	τ_i (yr)	6.6±0.6	25±2	108±4	638±4	3320±70	8500±600	110200±900	
5000GtC	GEM-CO2	b	279.0±0.3	w_i (%)	7.6±0.2	11.2±0.2	44.6±0.4	23±2	9±3	5.1±0.1		0.9999995
		h	2170±217	τ_i (yr)	11.7±0.5	83±3	610±8	2900±200	6800±800	105000±2000		
5000GtC	GKWM av.	b	278.8±0.3	w_i (%)	7.5±0.2	11.4±0.2	44.9±0.4	27.3±1	4±2	5.2±0.1		0.9999994
		h	2170±217	τ_i (yr)	11.5±0.5	83±3	637±6	4000±200	11000±2000	124000±3000		
5000GtC	GEM-CO2 av.	b	279.5±0.6	w_i (%)	6.7±0.4	11.3±0.3	45.01±0.1	31.1±0.1	5.90±0.05			0.999998
		h	2173±217	τ_i (yr)	10.7±0.9	76±4	646±5	6470±50	155000±3000			
5000GtC	mono acid	b	279.1±0.3	w_i (%)	7.0±0.3	11.1±0.2	46.1±0.2	29.3±0.5	1.8±0.7	4.7±0.2		0.9999992
		h	2170±217	τ_i (yr)	11.1±0.6	79±3	634±5	4600±100	16000±6000	106000±4000		
5000GtC	mono basalt	b	279.22±0.1	w_i (%)	3.6±0.4	6.0±0.2	9.3±0.2	47.34±0.09	22.4±0.4	7.4±0.7	3.93±0.04	0.99999996
		h	2169±216	τ_i (yr)	6.6±0.5	24±2	97±3	594±3	2590±60	6300±300	74700±600	
5000GtC	mono carb	b	279.1±0.2	w_i (%)	3.8±0.7	6.5±0.4	9.1±0.4	45.1±0.1	19.0±0.2	11.7±0.5	4.71±0.02	0.9999999
		h	2144±214	τ_i (yr)	5.7±0.8	22±3	84±5	517±5	2120±60	6900±100	230000±2000	
5000GtC	mono granite	b	279.1±0.3	w_i (%)	7.0±0.3	11.1±0.2	46.1±0.2	29.3±0.5	1.8±0.7	4.7±0.2		0.9999992
		h	2170±217	τ_i (yr)	11.1±0.6	79±3	634±5	4600±100	16000±6000	106000±4000		
5000GtC	mono sand	b	2170±2170	w_i (%)	13.5±0.6	44.8±0.3	35.5±0.3	6.3±0.4				0.99996
		h	2170±217	τ_i (yr)	34±3	570±10	16600±400	430000±80000				
5000GtC	mono shale	b	279.0±0.3	w_i (%)	6.5±0.2	10.1±0.2	53.8±0.1	17.7±0.8	9±1	2.61±0.06		0.9999997
		h	2150±215	τ_i (yr)	8.8±0.4	53±1	479±4	2000±100	5300±300	71000±2000		
5000GtC	mono shield	b	279.1±0.3	w_i (%)	7.0±0.3	11.1±0.2	46.1±0.2	29.3±0.5	1.8±0.7	4.7±0.2		0.9999992
		h	2170±217	τ_i (yr)	11.1±0.6	79±3	634±5	4600±100	16000±6000	106000±4000		

variables		fit to $pCO_2(t) = b + h\sum_i w_i e^{-(t-t_0)/\tau_i}$									
emis.	clim. sens.		pCO_2 (ppm)	i	1	2	3	4	5	6	7	R^2
1000GtC	1.5	b	277.4±0.1	w_i (%)	11.9±0.3	17.6±0.2	31.2±0.6	15±1	6.5±0.4	10.1±0.5	8.06±0.07	0.99999998
		h	404±40	τ_i (yr)	5.9±0.1	29.7±0.9	146±4	380±20	3200±200	9200±200	353000±3000	
1000GtC	2.64	b	277.4±0.1	w_i (%)	11.8±0.6	17.0±0.3	32±1	15±3	8±2	9±2	7.6±0.1	0.99999990
		h	403±40	τ_i (yr)	5.8±0.3	29±2	147±8	360±30	4100±500	8800±900	227000±3000	
1000GtC	3	b	277.70±0.09	w_i (%)	12.0±0.4	17.0±0.3	33.9±0.6	13±1	12.7±1	4±1	7.4±0.1	0.99999995
		h	403±40	τ_i (yr)	5.8±0.2	29±1	156±5	400±20	5200±200	12000±1000	222000±3000	
1000GtC	4.5	b	277.7±0.1	w_i (%)	12.0±0.7	17.1±0.5	32±2	15±4	17.1±0.5	7.2±0.2		0.9999998
		h	404±40	τ_i (yr)	5.9±0.4	30±2	160±10	370±30	6680±60	166000±3000		
1000GtC	6.	b	277.7±0.2	w_i (%)	12±2	16±2	18±7	29±7	18.4±0.9	6.1±0.3		0.9999994
		h	400±40	τ_i (yr)	5.9±0.8	29±5	130±40	290±30	6900±90	152000±5000		
5000GtC	1.5	b	2180±2180	w_i (%)	6.5±0.6	11.5±0.4	43.8±0.1	30.1±0.1	8.0±0.1			0.999997
		h	2180±218	τ_i (yr)	12±1	75±6	569±6	9100±80	370000±20000			
5000GtC	2.64	b	2172±2172	w_i (%)	6.1±0.6	11.4±0.4	45.2±0.1	30.7±0.2	6.59±0.08			0.999997
		h	2172±217	τ_i (yr)	11±1	74±5	652±7	7180±70	224000±9000			
5000GtC	3	b	2174±2174	w_i (%)	6.0±0.7	11.2±0.5	45.3±0.2	30.9±0.2	6.56±0.1			0.999996
		h	2174±217	τ_i (yr)	11±2	74±7	680±9	6980±90	203000±9000			
5000GtC	4.5	b	2150±2150	w_i (%)	14.0±0.5	47.7±0.4	31.5±0.7	6.8±0.3				0.99997
		h	2150±215	τ_i (yr)	40±3	740±20	6300±200	140000±10000				
5000GtC	6.	b	2160±2160	w_i (%)	13.2±0.7	52.3±0.6	28±1	6.2±0.4				0.99995
		h	2160±216	τ_i (yr)	36±4	840±30	6300±400	120000±20000				

Table 32: **Surface warming** (°C) reached at specific calendar years

variables		year								
emis.	short-circ.	3000	5000	10000	20000	50000	100k	200k	500k	1000k
1000GtC	yes	1.010	0.769	0.479	0.306	0.218	0.166	0.098	0.022	0.006
1000GtC	no	1.010	0.760	0.466	0.297	0.212	0.159	0.092	0.021	0.007
5000GtC	yes	5.380	4.060	2.670	1.620	1.160	0.877	0.518	0.119	0.026
5000GtC	no	5.340	3.980	2.550	1.560	1.120	0.839	0.482	0.104	0.025

variables			year								
emis.	T_Ca	T_Si	3000	5000	10000	20000	50000	100k	200k	500k	1000k
1000GtC	on	on	1.090	0.892	0.645	0.466	0.364	0.314	0.230	0.073	0.000
1000GtC	on	off	1.110	0.929	0.714	0.545	0.470	0.463	0.459	0.448	0.427
1000GtC	off	on	1.090	0.902	0.666	0.483	0.382	0.331	0.254	0.112	0.020
1000GtC	off	off	1.110	0.935	0.724	0.557	0.481	0.475	0.472	0.465	0.452
5000GtC	on	on	5.590	4.590	3.640	2.430	1.650	1.440	1.140	0.518	0.142
5000GtC	on	off	5.670	4.780	4.090	3.070	2.150	2.100	2.100	2.090	2.070
5000GtC	off	on	5.600	4.620	3.710	2.510	1.670	1.460	1.140	0.516	0.137
5000GtC	off	off	5.680	4.820	4.170	3.200	2.210	2.150	2.140	2.140	2.130

variables		year								
emis.	E_a (kJ/mol)	3000	5000	10000	20000	50000	100k	200k	500k	1000k
1000GtC	45	1.060	0.829	0.563	0.393	0.308	0.272	0.216	0.106	0.030
1000GtC	63	1.040	0.816	0.544	0.372	0.283	0.240	0.174	0.066	0.012
1000GtC	74	1.040	0.810	0.535	0.361	0.272	0.225	0.155	0.052	0.009
1000GtC	103	1.030	0.792	0.508	0.333	0.241	0.188	0.113	0.029	0.007
5000GtC	45	5.560	4.490	3.430	2.290	1.660	1.480	1.190	0.599	0.205
5000GtC	63	5.520	4.400	3.250	2.110	1.520	1.300	0.944	0.376	0.089
5000GtC	74	5.500	4.350	3.160	2.020	1.440	1.200	0.838	0.298	0.064
5000GtC	103	5.430	4.180	2.880	1.770	1.250	0.971	0.604	0.159	0.032

variables				year								
emis.	R_Ca	R_Si	R_explicit	3000	5000	10000	20000	50000	100k	200k	500k	1000k
1000GtC	on	on	on	1.110	0.926	0.708	0.538	0.457	0.441	0.419	0.359	0.268
1000GtC	on	on	off	1.100	0.920	0.697	0.524	0.440	0.417	0.383	0.295	0.182
1000GtC	on	off	on	1.110	0.931	0.718	0.550	0.474	0.467	0.462	0.448	0.422
1000GtC	on	off	off	1.110	0.931	0.716	0.547	0.471	0.464	0.460	0.449	0.429
1000GtC	off	on	on	1.110	0.930	0.715	0.543	0.459	0.441	0.415	0.344	0.237
1000GtC	off	on	off	1.100	0.926	0.707	0.533	0.446	0.421	0.383	0.288	0.165
1000GtC	off	off	on	1.110	0.935	0.724	0.557	0.481	0.475	0.472	0.465	0.452
1000GtC	off	off	off	1.110	0.935	0.724	0.557	0.481	0.475	0.472	0.465	0.452
5000GtC	on	on	on	5.660	4.770	4.060	3.010	2.090	1.990	1.910	1.660	1.320
5000GtC	on	on	off	5.650	4.740	3.980	2.880	2.010	1.890	1.730	1.380	0.846
5000GtC	on	off	on	5.670	4.800	4.130	3.130	2.180	2.120	2.110	2.100	2.080
5000GtC	on	off	off	5.670	4.800	4.110	3.090	2.160	2.100	2.100	2.100	2.080
5000GtC	off	on	on	5.670	4.800	4.120	3.100	2.120	2.010	1.920	1.660	1.280
5000GtC	off	on	off	5.670	4.780	4.070	3.020	2.050	1.910	1.750	1.370	0.817
5000GtC	off	off	on	5.680	4.820	4.170	3.200	2.210	2.150	2.140	2.140	2.130
5000GtC	off	off	off	5.680	4.820	4.170	3.200	2.210	2.150	2.140	2.140	2.130

variables		year								
emis.	beta	3000	5000	10000	20000	50000	100k	200k	500k	1000k
1000GtC	0.48	1.070	0.856	0.606	0.442	0.369	0.356	0.340	0.293	0.228
1000GtC	0.65	1.070	0.853	0.602	0.438	0.364	0.350	0.329	0.273	0.199
1000GtC	0.8	1.070	0.852	0.600	0.436	0.360	0.344	0.319	0.255	0.175
1000GtC	1.12	1.070	0.849	0.595	0.430	0.352	0.332	0.301	0.222	0.133
5000GtC	0.48	5.620	4.660	3.800	2.730	2.030	1.970	1.870	1.670	1.370
5000GtC	0.65	5.620	4.650	3.770	2.690	2.010	1.930	1.820	1.560	-
5000GtC	0.8	5.620	4.640	3.750	2.670	1.980	1.880	1.770	1.460	-
5000GtC	1.12	5.610	4.630	3.720	2.610	1.940	1.820	1.660	1.270	0.796

variables		year								
emis.	k_run	3000	5000	10000	20000	50000	100k	200k	500k	1000k
1000GtC	0.012	1.070	0.859	0.611	0.448	0.374	0.363	0.348	0.306	0.245
1000GtC	0.024	1.070	0.853	0.602	0.438	0.361	0.344	0.317	0.247	0.159
1000GtC	0.028	1.070	0.852	0.601	0.436	0.359	0.342	0.315	0.246	0.160
1000GtC	0.045	1.070	0.845	0.589	0.423	0.343	0.318	0.279	0.186	0.089
5000GtC	0.012	5.630	4.680	3.830	2.780	2.070	2.000	1.940	1.750	1.480
5000GtC	0.024	5.620	4.640	3.760	2.670	1.990	1.890	1.760	1.460	1.030
5000GtC	0.028	5.610	4.630	3.730	2.640	1.970	1.860	1.730	1.400	0.947
5000GtC	0.045	5.590	4.590	3.630	2.520	1.860	1.740	1.560	1.110	0.598

variables			year								
emis.	P_Ca	P_Si	3000	5000	10000	20000	50000	100k	200k	500k	1000k
1000GtC	on	on	1.100	0.911	0.683	0.504	0.413	0.379	0.324	0.195	0.070
1000GtC	on	off	1.110	0.927	0.712	0.544	0.470	0.464	0.461	0.452	0.436
1000GtC	off	on	1.100	0.918	0.694	0.516	0.423	0.387	0.331	0.205	0.077
1000GtC	off	off	1.110	0.935	0.724	0.557	0.481	0.475	0.472	0.465	0.452
5000GtC	on	on	5.650	4.730	3.940	2.810	1.910	1.740	1.540	1.010	0.400
5000GtC	on	off	5.670	4.790	4.100	3.070	2.160	2.100	2.100	2.090	2.070
5000GtC	off	on	5.660	4.760	4.020	2.920	1.960	1.770	1.560	1.010	0.396
5000GtC	off	off	5.680	4.820	4.170	3.200	2.210	2.150	2.140	2.140	2.130

variables			year								
emis.	f_Ca	f_Si	3000	5000	10000	20000	50000	100k	200k	500k	1000k
1000GtC	on	on	1.070	0.861	0.596	0.415	0.313	0.251	0.165	0.043	0.000
1000GtC	on	off	1.100	0.918	0.696	0.527	0.455	0.450	0.446	0.437	0.422
1000GtC	off	on	1.080	0.876	0.617	0.434	0.323	0.256	0.163	0.039	0.000
1000GtC	off	off	1.110	0.935	0.724	0.557	0.481	0.475	0.472	0.465	0.451
5000GtC	on	on	5.510	4.370	3.190	1.980	1.370	1.120	0.749	0.227	0.038
5000GtC	on	off	5.650	4.720	3.930	2.840	2.070	2.040	2.040	2.030	2.020
5000GtC	off	on	5.540	4.460	3.370	2.130	1.400	1.130	0.738	0.215	0.032
5000GtC	off	off	5.680	4.820	4.170	3.200	2.210	2.150	2.140	2.140	2.130

variables		year								
emis.	Scheme	3000	5000	10000	20000	50000	100k	200k	500k	1000k
1000GtC	Globavg	1.020	0.770	0.473	0.297	0.204	0.147	0.079	0.017	0.007
1000GtC	GKWM	0.959	0.697	0.394	0.235	0.155	0.100	0.042	0.006	0.003
1000GtC	GEM-CO2	0.939	0.673	0.373	0.220	0.144	0.090	0.037	0.005	0.004
5000GtC	Globavg	5.360	4.020	2.590	1.530	1.040	0.751	0.401	0.075	0.023
5000GtC	GKWM	5.130	3.540	2.050	1.250	0.848	0.547	0.234	0.027	0.012
5000GtC	GEM-CO2	5.040	3.380	1.890	1.170	0.793	0.500	0.198	0.023	0.011

variables				year								
emis.	f_Ca	f_Si	Scheme	3000	5000	10000	20000	50000	100k	200k	500k	1000k
1000GtC	on	on	Globavg	1.010	0.769	0.479	0.306	0.218	0.166	0.098	0.021	0.006
1000GtC	on	on	GKWM	0.959	0.697	0.394	0.235	0.155	0.100	0.042	0.006	0.003
1000GtC	on	off	Globavg	1.070	0.843	0.589	0.428	0.363	0.358	0.355	0.345	0.328
1000GtC	on	off	GKWM	1.080	0.861	0.608	0.438	0.359	0.346	0.328	0.278	0.209
1000GtC	off	on	Globavg	1.030	0.789	0.503	0.324	0.228	0.171	0.099	0.022	0.007
1000GtC	off	on	GKWM	0.971	0.711	0.408	0.244	0.157	0.100	0.041	0.006	0.003
1000GtC	off	off	Globavg	1.080	0.863	0.619	0.457	0.386	0.380	0.376	0.365	0.345
1000GtC	off	off	GKWM	1.100	0.892	0.658	0.485	0.393	0.385	0.380	0.367	0.345
5000GtC	on	on	Globavg	5.380	4.060	2.670	1.620	1.160	0.877	0.518	0.119	0.025
5000GtC	on	on	GKWM	5.130	3.540	2.050	1.250	0.848	0.547	0.227	0.026	0.012
5000GtC	on	off	Globavg	5.590	4.580	3.610	2.540	2.000	1.970	1.970	1.960	1.950
5000GtC	on	off	GKWM	5.640	4.700	3.860	2.730	1.970	1.880	1.800	1.600	1.290
5000GtC	off	on	Globavg	5.430	4.180	2.860	1.730	1.190	0.887	0.511	0.111	0.026
5000GtC	off	on	GKWM	5.180	3.630	2.140	1.290	0.856	0.525	0.204	0.023	0.012
5000GtC	off	off	Globavg	5.640	4.700	3.900	2.870	2.140	2.100	2.100	2.090	2.070
5000GtC	off	off	GKWM	5.710	4.900	4.320	3.400	2.240	2.130	2.130	2.130	2.120

variables		year								
emis.	routing	3000	5000	10000	20000	50000	100k	200k	500k	1000k
1000GtC	1	1.110	0.936	0.725	0.558	0.481	0.474	0.471	0.462	0.446
1000GtC	2	1.110	0.935	0.724	0.557	0.481	0.475	0.472	0.465	0.452
1000GtC	3	1.150	1.020	0.840	0.734	0.745	0.879	1.140	1.960	3.270
5000GtC	1	5.680	4.830	4.190	3.220	2.220	2.150	2.140	2.140	2.120
5000GtC	2	5.680	4.820	4.170	3.200	2.210	2.150	2.140	2.140	2.130
5000GtC	3	5.730	4.960	4.480	3.710	2.550	2.510	2.750	3.500	4.610

variables		year								
emis.	lith.	3000	5000	10000	20000	50000	100k	200k	500k	1000k
1000GtC	GKWM	0.963	0.701	0.398	0.239	0.157	0.102	0.044	0.006	0.003
1000GtC	GEM-CO2	0.959	0.697	0.394	0.235	0.155	0.100	0.042	0.006	-
1000GtC	GKWM av.	0.986	0.730	0.427	0.257	0.169	0.112	0.048	0.000	0.000
1000GtC	GEM-CO2 av.	1.040	0.796	0.504	0.316	0.212	0.155	0.081	0.007	0.000
1000GtC	mono acid	1.000	0.737	0.426	0.249	0.156	0.098	0.040	0.006	0.004
1000GtC	mono basalt	0.919	0.630	0.323	0.175	0.103	0.055	0.018	0.005	0.005
1000GtC	mono carb	0.864	0.663	0.409	0.250	0.184	0.148	0.093	0.020	0.000
1000GtC	mono granite	1.000	0.737	0.426	0.249	0.156	0.098	0.040	0.006	0.004
1000GtC	mono sand	1.140	0.961	0.747	0.511	0.313	0.253	0.188	0.076	0.012
1000GtC	mono shale	0.809	0.547	0.256	0.119	0.067	0.034	0.011	0.005	0.005
1000GtC	mono shield	1.000	0.737	0.426	0.249	0.156	0.098	0.040	0.006	0.004
5000GtC	GKWM	5.150	3.570	2.080	1.270	0.862	0.560	0.244	0.029	0.012
5000GtC	GEM-CO2	5.130	3.540	2.050	1.250	0.848	0.547	0.219	0.025	0.012
5000GtC	GKWM av.	5.260	3.790	2.300	1.370	0.931	0.633	0.302	0.036	0.009
5000GtC	GEM-CO2 av.	5.450	4.240	2.940	1.710	1.130	0.835	0.460	0.089	0.012
5000GtC	mono acid	5.270	3.830	2.320	1.300	0.819	0.517	0.215	0.025	0.013
5000GtC	mono basalt	4.910	3.150	1.630	0.932	0.569	0.307	0.094	0.015	0.013
5000GtC	mono carb	4.790	3.260	2.000	1.310	0.984	0.816	0.540	0.166	0.024
5000GtC	mono granite	5.270	3.830	2.320	1.300	0.819	0.517	0.215	0.025	0.013
5000GtC	mono sand	5.740	5.050	4.440	3.310	1.630	1.260	0.940	0.397	0.095
5000GtC	mono shale	4.360	2.580	1.230	0.630	0.373	0.195	0.056	0.014	0.014
5000GtC	mono shield	5.270	3.830	2.320	1.300	0.819	0.517	0.215	0.025	0.013

variables		year								
emis.	clim. sens.	3000	5000	10000	20000	50000	100k	200k	500k	1000k
1000GtC	1.5	0.608	0.491	0.357	0.260	0.204	0.176	0.133	0.054	0.008
1000GtC	2.64	1.070	0.861	0.596	0.415	0.313	0.251	0.162	0.040	0.000
1000GtC	3	1.220	1.010	0.681	0.467	0.348	0.275	0.175	0.043	0.000
1000GtC	4.5	1.810	1.530	1.060	0.660	0.461	0.341	0.188	0.027	0.001
1000GtC	6.	2.360	2.020	1.350	0.774	0.499	0.351	0.182	0.019	0.000
5000GtC	1.5	3.120	2.600	2.080	1.390	0.948	0.828	0.640	0.293	0.055
5000GtC	2.64	5.510	4.370	3.200	1.980	1.370	1.120	0.748	0.234	0.041
5000GtC	3	6.310	4.970	3.580	2.200	1.510	1.210	0.772	0.208	0.020
5000GtC	4.5	9.800	7.520	5.180	3.070	2.090	1.510	0.773	0.121	0.001
5000GtC	6.	15.100	10.100	6.500	3.720	2.460	1.610	0.756	0.091	0.002

Table 33: **Percentages** of remaining excess **Surface warming** reached at specific calendar years

variables		year								
emis.	short-circ.	3000	5000	10000	20000	50000	100k	200k	500k	1000k
1000GtC	yes	56.4	42.8	26.7	17.0	12.1	9.2	5.5	1.2	0.3
1000GtC	no	56.2	42.4	26.0	16.6	11.8	8.9	5.1	1.2	0.4
5000GtC	yes	85.2	64.3	42.3	25.6	18.3	13.9	8.2	1.9	0.4
5000GtC	no	84.8	63.1	40.5	24.7	17.8	13.3	7.6	1.7	0.4

variables			year								
emis.	T_Ca	T_Si	3000	5000	10000	20000	50000	100k	200k	500k	1000k
1000GtC	on	on	60.9	49.9	36.1	26.1	20.4	17.6	12.9	4.1	0.0
1000GtC	on	off	61.9	52.0	39.9	30.5	26.3	25.9	25.7	25.1	23.9
1000GtC	off	on	61.2	50.5	37.3	27.0	21.4	18.5	14.2	6.3	1.1
1000GtC	off	off	62.0	52.3	40.5	31.2	26.9	26.6	26.4	26.0	25.3
5000GtC	on	on	88.0	72.1	57.2	38.2	25.9	22.7	17.9	8.1	2.2
5000GtC	on	off	89.0	75.1	64.3	48.1	33.8	33.0	32.9	32.8	32.5
5000GtC	off	on	88.1	72.6	58.3	39.5	26.3	22.9	17.9	8.1	2.2
5000GtC	off	off	89.2	75.6	65.5	50.2	34.7	33.7	33.6	33.5	33.4

variables		year								
emis.	E_a (kJ/mol)	3000	5000	10000	20000	50000	100k	200k	500k	1000k
1000GtC	45	59.0	46.1	31.3	21.9	17.1	15.1	12.0	5.9	1.7
1000GtC	63	58.0	45.4	30.3	20.7	15.7	13.4	9.7	3.7	0.7
1000GtC	74	57.8	45.1	29.8	20.1	15.1	12.5	8.6	2.9	0.5
1000GtC	103	57.2	44.1	28.3	18.5	13.4	10.5	6.3	1.6	0.4
5000GtC	45	87.7	70.9	54.1	36.1	26.2	23.3	18.8	9.4	3.2
5000GtC	63	87.2	69.5	51.3	33.4	24.0	20.4	14.9	5.9	1.4
5000GtC	74	86.9	68.7	49.9	32.0	22.8	19.0	13.2	4.7	1.0
5000GtC	103	85.8	66.1	45.5	28.0	19.8	15.4	9.6	2.5	0.5

variables				year								
emis.	R_Ca	R_Si	R_explicit	3000	5000	10000	20000	50000	100k	200k	500k	1000k
1000GtC	on	on	on	61.8	51.8	39.6	30.1	25.6	24.7	23.4	20.1	15.0
1000GtC	on	on	off	61.6	51.5	39.0	29.3	24.6	23.3	21.4	16.5	10.2
1000GtC	on	off	on	61.9	52.1	40.2	30.8	26.5	26.1	25.8	25.1	23.6
1000GtC	on	off	off	61.9	52.0	40.0	30.6	26.3	25.9	25.7	25.1	24.0
1000GtC	off	on	on	61.9	52.0	40.0	30.4	25.7	24.7	23.2	19.2	13.2
1000GtC	off	on	off	61.7	51.8	39.5	29.8	24.9	23.5	21.4	16.1	9.2
1000GtC	off	off	on	62.0	52.3	40.5	31.2	26.9	26.6	26.4	26.0	25.3
1000GtC	off	off	off	62.0	52.3	40.5	31.2	26.9	26.6	26.4	26.0	25.3
5000GtC	on	on	on	88.9	74.9	63.8	47.3	32.8	31.3	29.9	26.1	20.7
5000GtC	on	on	off	88.8	74.5	62.5	45.3	31.5	29.7	27.3	21.7	13.3
5000GtC	on	off	on	89.0	75.3	64.8	49.1	34.2	33.3	33.2	33.0	32.6
5000GtC	on	off	off	89.0	75.3	64.6	48.5	34.0	33.0	33.0	32.9	32.7
5000GtC	off	on	on	89.0	75.3	64.7	48.7	33.2	31.6	30.1	26.1	20.1
5000GtC	off	on	off	88.9	75.0	63.9	47.3	32.2	30.1	27.5	21.5	12.8
5000GtC	off	off	on	89.2	75.6	65.5	50.2	34.7	33.7	33.6	33.5	33.4
5000GtC	off	off	off	89.2	75.6	65.5	50.2	34.7	33.7	33.6	33.5	33.4

variables		year								
emis.	beta	3000	5000	10000	20000	50000	100k	200k	500k	1000k
1000GtC	0.48	59.7	47.6	33.7	24.6	20.5	19.8	18.9	16.3	12.7
1000GtC	0.65	59.6	47.4	33.5	24.3	20.2	19.5	18.3	15.2	11.1
1000GtC	0.8	59.6	47.4	33.4	24.2	20.0	19.1	17.7	14.2	9.7
1000GtC	1.12	59.5	47.2	33.1	23.9	19.6	18.5	16.7	12.3	7.4
5000GtC	0.48	88.5	73.3	59.7	42.9	32.0	31.0	29.4	26.3	21.5
5000GtC	0.65	88.5	73.3	59.3	42.3	31.6	30.4	28.6	24.5	-
5000GtC	0.8	88.4	73.1	59.1	42.0	31.2	29.6	27.8	22.9	-
5000GtC	1.12	88.3	72.8	58.5	41.2	30.5	28.6	26.1	20.0	12.5

variables		year								
emis.	k_run	3000	5000	10000	20000	50000	100k	200k	500k	1000k
1000GtC	0.012	59.8	47.7	34.0	24.9	20.8	20.2	19.3	17.0	13.6
1000GtC	0.024	59.6	47.4	33.5	24.3	20.1	19.1	17.6	13.7	8.8
1000GtC	0.028	59.6	47.4	33.4	24.2	20.0	19.0	17.5	13.7	8.9
1000GtC	0.045	59.4	47.0	32.8	23.5	19.1	17.7	15.5	10.3	4.9
5000GtC	0.012	88.6	73.6	60.4	43.7	32.6	31.6	30.6	27.5	23.3
5000GtC	0.024	88.4	73.1	59.2	42.1	31.3	29.7	27.7	23.0	16.2
5000GtC	0.028	88.3	72.9	58.7	41.6	31.0	29.3	27.3	22.0	14.9
5000GtC	0.045	88.1	72.3	57.2	39.7	29.3	27.4	24.5	17.4	9.4

variables			year								
emis.	P_Ca	P_Si	3000	5000	10000	20000	50000	100k	200k	500k	1000k
1000GtC	on	on	61.4	51.0	38.2	28.2	23.1	21.2	18.1	10.9	3.9
1000GtC	on	off	61.8	51.8	39.8	30.4	26.3	26.0	25.8	25.3	24.4
1000GtC	off	on	61.6	51.3	38.8	28.9	23.7	21.6	18.5	11.5	4.3
1000GtC	off	off	62.0	52.3	40.5	31.2	26.9	26.6	26.4	26.0	25.3
5000GtC	on	on	88.7	74.3	62.0	44.1	30.1	27.4	24.2	15.8	6.3
5000GtC	on	off	89.0	75.1	64.3	48.2	33.8	33.0	32.9	32.8	32.6
5000GtC	off	on	88.8	74.7	63.1	45.8	30.7	27.8	24.5	15.9	6.2
5000GtC	off	off	89.2	75.6	65.5	50.2	34.7	33.7	33.6	33.5	33.4

variables			year								
emis.	f_Ca	f_Si	3000	5000	10000	20000	50000	100k	200k	500k	1000k
1000GtC	on	on	60.0	48.2	33.4	23.2	17.5	14.1	9.2	2.4	0.0
1000GtC	on	off	61.6	51.3	38.9	29.5	25.4	25.2	24.9	24.4	23.6
1000GtC	off	on	60.4	49.0	34.5	24.3	18.1	14.3	9.1	2.2	0.0
1000GtC	off	off	62.0	52.3	40.5	31.2	26.9	26.6	26.4	26.0	25.2
5000GtC	on	on	86.8	68.9	50.3	31.2	21.5	17.6	11.8	3.6	0.6
5000GtC	on	off	88.7	74.2	61.8	44.6	32.6	32.1	32.0	31.9	31.7
5000GtC	off	on	87.3	70.2	53.0	33.5	22.1	17.8	11.6	3.4	0.5
5000GtC	off	off	89.2	75.6	65.5	50.2	34.7	33.7	33.6	33.5	33.3

variables		year								
emis.	Scheme	3000	5000	10000	20000	50000	100k	200k	500k	1000k
1000GtC	Globavg	56.6	42.7	26.2	16.5	11.3	8.2	4.4	0.9	0.4
1000GtC	GKWM	54.2	39.4	22.3	13.3	8.8	5.6	2.4	0.3	0.2
1000GtC	GEM-CO2	53.4	38.3	21.2	12.5	8.2	5.1	2.1	0.3	0.2
5000GtC	Globavg	84.8	63.6	41.0	24.2	16.4	11.9	6.3	1.2	0.4
5000GtC	GKWM	82.1	56.6	32.8	20.0	13.6	8.7	3.7	0.4	0.2
5000GtC	GEM-CO2	80.9	54.2	30.4	18.8	12.7	8.0	3.2	0.4	0.2

variables				year							
emis.	f_Ca	f_Si	Scheme	3000	5000	10000	20000	50000	100k	200k	500k	1000k
1000GtC	on	on	Globavg	56.4	42.8	26.7	17.0	12.1	9.2	5.5	1.2	0.3
1000GtC	on	on	GKWM	54.2	39.4	22.3	13.3	8.8	5.6	2.4	0.3	0.2
1000GtC	on	off	Globavg	59.3	46.9	32.8	23.8	20.2	19.9	19.7	19.2	18.2
1000GtC	on	off	GKWM	59.9	47.6	33.6	24.2	19.9	19.1	18.1	15.4	11.6
1000GtC	off	on	Globavg	57.1	43.9	28.0	18.0	12.7	9.5	5.5	1.2	0.4
1000GtC	off	on	GKWM	54.7	40.1	23.0	13.7	8.8	5.6	2.3	0.3	0.2
1000GtC	off	off	Globavg	59.9	48.0	34.4	25.4	21.5	21.1	20.9	20.3	19.2
1000GtC	off	off	GKWM	60.6	49.1	36.2	26.7	21.6	21.2	20.9	20.2	19.0
5000GtC	on	on	Globavg	85.2	64.3	42.3	25.6	18.3	13.9	8.2	1.9	0.4
5000GtC	on	on	GKWM	82.1	56.6	32.8	20.0	13.6	8.7	3.6	0.4	0.2
5000GtC	on	off	Globavg	88.1	72.1	56.9	40.0	31.5	31.1	31.0	30.9	30.7
5000GtC	on	off	GKWM	88.5	73.9	60.6	42.9	30.9	29.5	28.3	25.1	20.3
5000GtC	off	on	Globavg	85.9	66.1	45.3	27.4	18.8	14.0	8.1	1.8	0.4
5000GtC	off	on	GKWM	82.7	58.0	34.1	20.6	13.7	8.4	3.3	0.4	0.2
5000GtC	off	off	Globavg	88.7	74.0	61.3	45.1	33.7	33.1	33.0	32.9	32.6
5000GtC	off	off	GKWM	89.4	76.9	67.8	53.4	35.0	33.4	33.4	33.4	33.2

variables		year								
emis.	routing	3000	5000	10000	20000	50000	100k	200k	500k	1000k
1000GtC	1	62.0	52.3	40.5	31.2	26.9	26.5	26.3	25.8	24.9
1000GtC	2	62.0	52.3	40.5	31.2	26.9	26.6	26.4	26.0	25.3
1000GtC	3	63.7	56.3	46.6	40.7	41.3	48.7	63.4	109.0	181.0
5000GtC	1	89.2	75.8	65.8	50.6	34.8	33.7	33.6	33.5	33.3
5000GtC	2	89.2	75.6	65.5	50.2	34.7	33.7	33.6	33.5	33.4
5000GtC	3	89.8	77.7	70.2	58.1	39.9	39.3	43.1	54.9	72.2

variables		year								
emis.	lith.	3000	5000	10000	20000	50000	100k	200k	500k	1000k
1000GtC	GKWM	54.3	39.6	22.5	13.5	8.9	5.8	2.5	0.3	0.2
1000GtC	GEM-CO2	54.2	39.4	22.3	13.3	8.8	5.6	2.4	0.3	-
1000GtC	GKWM av.	55.3	40.9	23.9	14.4	9.5	6.3	2.7	-0.1	-0.1
1000GtC	GEM-CO2 av.	57.5	44.1	27.9	17.5	11.7	8.6	4.5	0.4	-0.1
1000GtC	mono acid	55.7	41.0	23.7	13.9	8.7	5.5	2.2	0.3	0.2
1000GtC	mono basalt	52.2	35.8	18.4	9.9	5.9	3.1	1.0	0.3	0.3
1000GtC	mono carb	51.2	39.3	24.2	14.8	10.9	8.8	5.5	1.2	-0.1
1000GtC	mono granite	55.7	41.0	23.7	13.9	8.7	5.5	2.2	0.3	0.2
1000GtC	mono sand	61.7	52.0	40.4	27.6	16.9	13.7	10.2	4.1	0.6
1000GtC	mono shale	47.8	32.3	15.1	7.0	4.0	2.0	0.7	0.3	0.3
1000GtC	mono shield	55.7	41.0	23.7	13.9	8.7	5.5	2.2	0.3	0.2
5000GtC	GKWM	82.3	57.0	33.2	20.3	13.8	8.9	3.9	0.5	0.2
5000GtC	GEM-CO2	82.1	56.6	32.8	20.0	13.6	8.7	3.5	0.4	0.2
5000GtC	GKWM av.	83.7	60.3	36.6	21.8	14.8	10.1	4.8	0.6	0.1
5000GtC	GEM-CO2 av.	86.0	67.0	46.4	27.1	17.8	13.2	7.3	1.4	0.2
5000GtC	mono acid	83.7	60.8	36.9	20.7	13.0	8.2	3.4	0.4	0.2
5000GtC	mono basalt	79.0	50.6	26.2	15.0	9.2	4.9	1.5	0.2	0.2
5000GtC	mono carb	78.5	53.5	32.7	21.5	16.1	13.4	8.8	2.7	0.4
5000GtC	mono granite	83.7	60.8	36.9	20.7	13.0	8.2	3.4	0.4	0.2
5000GtC	mono sand	89.5	78.7	69.2	51.6	25.4	19.7	14.7	6.2	1.5
5000GtC	mono shale	71.9	42.7	20.3	10.4	6.2	3.2	0.9	0.2	0.2
5000GtC	mono shield	83.7	60.8	36.9	20.7	13.0	8.2	3.4	0.4	0.2

variables		year								
emis.	clim. sens.	3000	5000	10000	20000	50000	100k	200k	500k	1000k
1000GtC	1.5	51.6	41.6	30.3	22.1	17.3	14.9	11.3	4.6	0.7
1000GtC	2.64	60.0	48.2	33.4	23.2	17.5	14.1	9.1	2.2	0.0
1000GtC	3	62.4	51.4	34.9	23.9	17.8	14.1	9.0	2.2	0.0
1000GtC	4.5	69.3	58.3	40.6	25.2	17.6	13.0	7.2	1.0	0.0
1000GtC	6.	73.6	62.9	42.1	24.1	15.6	10.9	5.7	0.6	0.0
5000GtC	1.5	83.3	69.4	55.4	37.0	25.3	22.1	17.1	7.8	1.5
5000GtC	2.64	86.8	68.9	50.4	31.2	21.5	17.6	11.8	3.7	0.6
5000GtC	3	88.2	69.5	50.1	30.7	21.1	16.9	10.8	2.9	0.3
5000GtC	4.5	92.4	70.9	48.8	28.9	19.7	14.2	7.3	1.1	0.0
5000GtC	6.	96.3	64.3	41.6	23.8	15.7	10.3	4.8	0.6	0.0

Table 34: **Years** that specific values of **Surface warming** are reached

variables		Surface warming (°C)									
emis.	short-circ.	peak	at year	5	4	3	2	1.5	1	0.5	0
1000GtC	yes	1.80	2060	-	-	-	-	2260	3100	9500	-
1000GtC	no	1.79	2060	-	-	-	-	2240	3100	9500	-
5000GtC	yes	6.32	2220	3400	5200	9000	15000	24010	75000	210010	-
5000GtC	no	6.30	2220	3400	5000	8500	14010	22010	70010	200010	-

variables			Surface warming (°C)									
emis.	T_Ca	T_Si	peak	at year	5	4	3	2	1.5	1	0.5	0
1000GtC	on	on	1.79	2060	-	-	-	-	2260	3700	17000	800000
1000GtC	on	off	1.79	2060	-	-	-	-	2260	4100	30000	-
1000GtC	off	on	1.79	2060	-	-	-	-	2260	3800	19000	-
1000GtC	off	off	1.79	2060	-	-	-	-	2260	4200	34000	-
5000GtC	on	on	6.36	2240	3900	8000	15000	28000	85000	260000	550000	-
5000GtC	on	off	6.37	2240	4200	11000	22000	-	-	-	-	-
5000GtC	off	on	6.36	2240	3900	8500	16000	30000	90000	260000	550000	-
5000GtC	off	off	6.37	2240	4300	12000	24000	-	-	-	-	-

variables		Surface warming (°C)									
emis.	E_a (kJ/mol)	peak	at year	5	4	3	2	1.5	1	0.5	0
1000GtC	45	1.80	2060	-	-	-	-	2260	3300	13000	-
1000GtC	63	1.80	2060	-	-	-	-	2260	3200	12010	-
1000GtC	74	1.80	2060	-	-	-	-	2260	3200	12010	-
1000GtC	103	1.80	2060	-	-	-	-	2260	3200	11000	-
5000GtC	45	6.34	2240	3800	7500	13000	28010	95000	270010	600010	-
5000GtC	63	6.33	2240	3700	6600	12010	24010	55000	190010	410010	-
5000GtC	74	6.33	2220	3600	6400	11000	22010	44010	150010	350010	-
5000GtC	103	6.32	2220	3500	5600	9500	17000	28010	95000	250010	-

variables				Surface warming (°C)									
emis.	R_Ca	R_Si	R_explicit	peak	at year	5	4	3	2	1.5	1	0.5	0
1000GtC	on	on	on	1.79	2060	-	-	-	-	2260	4100	28000	-
1000GtC	on	on	off	1.79	2060	-	-	-	-	2260	4000	24000	-
1000GtC	on	off	on	1.79	2060	-	-	-	-	2260	4100	30000	-
1000GtC	on	off	off	1.79	2060	-	-	-	-	2260	4100	30000	-
1000GtC	off	on	on	1.79	2060	-	-	-	-	2260	4100	28000	-
1000GtC	off	on	off	1.79	2060	-	-	-	-	2260	4100	26000	-
1000GtC	off	off	on	1.79	2060	-	-	-	-	2260	4200	34000	-
1000GtC	off	off	off	1.79	2060	-	-	-	-	2260	4200	34000	-
5000GtC	on	on	on	6.37	2240	4200	11000	22000	95000	750000	-	-	-
5000GtC	on	on	off	6.37	2240	4100	10000	19000	55000	400000	900000	-	-
5000GtC	on	off	on	6.37	2240	4200	12000	22000	-	-	-	-	-
5000GtC	on	off	off	6.37	2240	4200	11000	22000	-	-	-	-	-
5000GtC	off	on	on	6.37	2240	4200	12000	22000	120000	750000	-	-	-
5000GtC	off	on	off	6.37	2240	4200	11000	22000	60000	400000	850000	-	-
5000GtC	off	off	on	6.37	2240	4300	12000	24000	-	-	-	-	-
5000GtC	off	off	off	6.37	2240	4300	12000	24000	-	-	-	-	-

variables		Surface warming (°C)									
emis.	beta	peak	at year	5	4	3	2	1.5	1	0.5	0
1000GtC	0.48	1.80	2060	-	-	-	-	2260	3400	15000	-
1000GtC	0.65	1.80	2060	-	-	-	-	2260	3400	15000	-
1000GtC	0.8	1.80	2060	-	-	-	-	2260	3400	15000	-
1000GtC	1.12	1.80	2060	-	-	-	-	2260	3400	15000	-
5000GtC	0.48	6.35	2240	4010	9000	17000	70010	780010	-	-	-
5000GtC	0.65	6.35	2240	4010	9000	17000	55000	580010	-	-	-
5000GtC	0.8	6.35	2240	4010	8500	17000	48010	460010	-	-	-
5000GtC	1.12	6.35	2240	3900	8500	16010	42010	310010	760010	-	-

variables		Surface warming (°C)									
emis.	k_run	peak	at year	5	4	3	2	1.5	1	0.5	0
1000GtC	0.012	1.80	2060	-	-	-	-	2260	3400	16010	-
1000GtC	0.024	1.80	2060	-	-	-	-	2260	3400	15000	-
1000GtC	0.028	1.80	2060	-	-	-	-	2260	3400	15000	-
1000GtC	0.045	1.80	2060	-	-	-	-	2260	3400	14010	-
5000GtC	0.012	6.35	2240	4010	9000	18010	110010	980010	-	-	-
5000GtC	0.024	6.35	2240	4010	8500	17000	48010	460010	-	-	-
5000GtC	0.028	6.35	2240	4010	8500	16010	44010	400010	940010	-	-
5000GtC	0.045	6.35	2240	3900	8010	15000	36010	240010	580010	-	-

variables			Surface warming (°C)									
emis.	P_Ca	P_Si	peak	at year	5	4	3	2	1.5	1	0.5	0
1000GtC	on	on	1.79	2060	-	-	-	-	2260	3900	22000	-
1000GtC	on	off	1.79	2060	-	-	-	-	2260	4100	30000	-
1000GtC	off	on	1.79	2060	-	-	-	-	2260	4000	22000	-
1000GtC	off	off	1.79	2060	-	-	-	-	2260	4200	34000	-
5000GtC	on	on	6.37	2240	4100	10000	18000	42000	220000	550000	850000	-
5000GtC	on	off	6.37	2240	4200	11000	22000	-	-	-	-	-
5000GtC	off	on	6.37	2240	4100	11000	20000	46000	240000	550000	900000	-
5000GtC	off	off	6.37	2240	4300	12000	24000	-	-	-	-	-

variables			Surface warming (°C)									
emis.	f_Ca	f_Si	peak	at year	5	4	3	2	1.5	1	0.5	0
1000GtC	on	on	1.79	2060	-	-	-	-	2260	3500	14000	1000000
1000GtC	on	off	1.79	2060	-	-	-	-	2260	4000	26000	-
1000GtC	off	on	1.79	2060	-	-	-	-	2260	3600	15000	900000
1000GtC	off	off	1.79	2060	-	-	-	-	2260	4200	34000	-
5000GtC	on	on	6.35	2220	3600	6600	12000	20000	36000	130000	300000	-
5000GtC	on	off	6.37	2240	4100	10000	19000	-	-	-	-	-
5000GtC	off	on	6.35	2240	3700	7000	13000	22000	40000	130000	300000	-
5000GtC	off	off	6.37	2240	4300	12000	24000	-	-	-	-	-

variables		Surface warming (°C)								
emis.	Scheme	peak	at year	5	4	3	2	1.5	1	0.5	0
1000GtC	Globavg	1.80	2060	-	-	-	-	2260	3100	9500	-
1000GtC	GKWM	1.77	2060	-	-	-	-	2220	2850	8010	-
1000GtC	GEM-CO2	1.76	2060	-	-	-	-	2220	2800	7500	-
5000GtC	Globavg	6.32	2220	3400	5200	8500	14010	22010	60010	170010	-
5000GtC	GKWM	6.25	2200	3200	4200	6400	11000	15000	34010	120010	-
5000GtC	GEM-CO2	6.23	2200	3100	4010	6010	9500	14010	28010	100010	-

variables				Surface warming (°C)									
emis.	f_Ca	f_Si	Scheme	peak	at year	5	4	3	2	1.5	1	0.5	0
1000GtC	on	on	Globavg	1.80	2060	-	-	-	-	2260	3100	9500	-
1000GtC	on	on	GKWM	1.77	2060	-	-	-	-	2220	2850	8010	-
1000GtC	on	off	Globavg	1.80	2060	-	-	-	-	2260	3400	14010	-
1000GtC	on	off	GKWM	1.81	2060	-	-	-	-	2280	3500	15000	-
1000GtC	off	on	Globavg	1.80	2060	-	-	-	-	2260	3200	11000	-
1000GtC	off	on	GKWM	1.78	2060	-	-	-	-	2220	2900	8010	-
1000GtC	off	off	Globavg	1.80	2060	-	-	-	-	2260	3400	16010	-
1000GtC	off	off	GKWM	1.82	2060	-	-	-	-	2280	3700	19000	-
5000GtC	on	on	Globavg	6.32	2220	3400	5200	9000	15000	24010	75000	210010	-
5000GtC	on	on	GKWM	6.25	2200	3200	4200	6400	11000	15000	34010	120010	-
5000GtC	on	off	Globavg	6.35	2240	3900	8010	15000	50010	-	-	-	-
5000GtC	on	off	GKWM	6.36	2240	4010	9500	17000	44010	660010	-	-	-
5000GtC	off	on	Globavg	6.32	2220	3500	5600	9500	17000	28010	80010	210010	-
5000GtC	off	on	GKWM	6.26	2220	3200	4400	6600	11000	16010	36010	110010	-
5000GtC	off	off	Globavg	6.35	2240	4100	9500	19000	-	-	-	-	-
5000GtC	off	off	GKWM	6.38	2240	4500	14010	26010	-	-	-	-	-

variables		Surface warming (°C)									
emis.	routing	peak	at year	5	4	3	2	1.5	1	0.5	0
1000GtC	1	1.79	2060	-	-	-	-	2280	4200	34000	-
1000GtC	2	1.79	2060	-	-	-	-	2260	4200	34000	-
1000GtC	3	1.80	2070	-	-	-	-	2300	5400	-	-
5000GtC	1	6.37	2240	4300	12000	24000	-	-	-	-	-
5000GtC	2	6.37	2240	4300	12000	24000	-	-	-	-	-
5000GtC	3	6.38	2260	4800	16000	32000	-	-	-	-	-

variables		Surface warming (°C)									
emis.	lith.	peak	at year	5	4	3	2	1.5	1	0.5	0
1000GtC	GKWM	1.77	2060	-	-	-	-	2220	2900	8010	-
1000GtC	GEM-CO2	1.77	2060	-	-	-	-	2220	2850	8010	-
1000GtC	GKWM av.	1.78	2060	-	-	-	-	2240	2950	8500	470010
1000GtC	GEM-CO2 av.	1.81	2060	-	-	-	-	2260	3200	11000	600010
1000GtC	mono acid	1.80	2060	-	-	-	-	2240	3000	8500	-
1000GtC	mono basalt	1.76	2060	-	-	-	-	2220	2750	6600	-
1000GtC	mono carb	1.69	2050	-	-	-	-	2160	2600	8010	780010
1000GtC	mono granite	1.80	2060	-	-	-	-	2240	3000	8500	-
1000GtC	mono sand	1.85	2070	-	-	-	-	2350	4300	22010	-
1000GtC	mono shale	1.69	2050	-	-	-	-	2160	2550	5600	-
1000GtC	mono shield	1.80	2060	-	-	-	-	2240	3000	8500	-
5000GtC	GKWM	6.26	2200	3200	4300	6400	11000	16010	36010	120010	-
5000GtC	GEM-CO2	6.25	2200	3200	4200	6400	11000	15000	34010	120010	-
5000GtC	GKWM av.	6.28	2220	3300	4600	7500	12010	18010	42010	140010	-
5000GtC	GEM-CO2 av.	6.33	2220	3500	5800	10010	17000	26010	70010	190010	-
5000GtC	mono acid	6.30	2220	3300	4700	7500	12010	17000	32010	110010	-
5000GtC	mono basalt	6.21	2200	2950	3800	5400	8500	11000	18010	65000	-
5000GtC	mono carb	6.10	2180	2900	3800	5800	10010	16010	48010	220010	-
5000GtC	mono granite	6.30	2220	3300	4700	7500	12010	17000	32010	110010	-
5000GtC	mono sand	6.42	2240	5400	14010	24010	40010	60010	180010	430010	-
5000GtC	mono shale	6.06	2180	2700	3300	4300	6600	8500	12010	30010	-
5000GtC	mono shield	6.30	2220	3300	4700	7500	12010	17000	32010	110010	-

variables		Surface warming (°C)									
emis.	clim. sens.	peak	at year	5	4	3	2	1.5	1	0.5	0
1000GtC	1.5	1.18	2040	-	-	-	-	-	2160	4800	-
1000GtC	2.64	1.79	2060	-	-	-	-	2260	3500	14000	950000
1000GtC	3	1.95	2070	-	-	-	-	2400	5200	18000	1000000
1000GtC	4.5	2.62	2120	-	-	-	2650	5400	11000	40000	-
1000GtC	6.	3.21	2140	-	-	2350	5200	9000	15000	50000	750000
5000GtC	1.5	3.75	2140	-	-	3300	11000	18000	40000	300000	-
5000GtC	2.64	6.35	2220	3600	6600	12000	20000	36000	130000	320000	-
5000GtC	3	7.15	2260	5000	8500	13000	24000	55000	150000	300000	-
5000GtC	4.5	10.61	2400	11000	14000	22000	60000	110000	160000	260000	-
5000GtC	6.	15.64	2600	14000	18000	32000	80000	110000	170000	280000	-

Table 35: **Years** that specific fractions of remaining excess **Surface warming** are reached

variables		fraction									
emis.	short-circ.	90%	75%	50%	25%	10%	e^{-1}	e^{-2}	e^{-3}	e^{-4}	e^{-5}
1000GtC	yes	2180	2400	3800	11000	90010	6400	36010	220010	420010	660010
1000GtC	no	2180	2350	3700	11000	80010	6200	34010	210010	410010	660010
5000GtC	yes	2800	3700	8010	22010	170010	13000	110010	300010	520010	760010
5000GtC	no	2750	3700	7500	20010	160010	12010	100010	290010	480010	720010

variables			fraction									
emis.	T_Ca	T_Si	90%	75%	50%	25%	10%	e^{-1}	e^{-2}	e^{-3}	e^{-4}	e^{-5}
1000GtC	on	on	2200	2400	5000	24000	280000	10000	190000	460000	650000	750000
1000GtC	on	off	2200	2450	5800	550000	-	13000	-	-	-	-
1000GtC	off	on	2200	2400	5200	26000	340000	11000	220000	600000	950000	-
1000GtC	off	off	2200	2450	5800	-	-	13000	-	-	-	-
5000GtC	on	on	2900	4400	14000	65000	420000	22000	300000	750000	-	-
5000GtC	on	off	2950	5200	19000	-	-	36000	-	-	-	-
5000GtC	off	on	2900	4500	14000	70000	420000	24000	320000	700000	-	-
5000GtC	off	off	2950	5400	22000	-	-	40000	-	-	-	-

variables		fraction									
emis.	E_a (kJ/mol)	90%	75%	50%	25%	10%	e^{-1}	e^{-2}	e^{-3}	e^{-4}	e^{-5}
1000GtC	45	2180	2400	4200	16010	280010	8010	150010	580010	980010	-
1000GtC	63	2180	2400	4100	14010	200010	7500	95000	410010	720010	1000010
1000GtC	74	2180	2400	4010	14010	160010	7500	80010	350010	640010	900010
1000GtC	103	2180	2400	3900	13000	110010	6800	50010	250010	480010	740010
5000GtC	45	2900	4300	12010	70010	480010	20010	350010	800010	-	-
5000GtC	63	2850	4100	11000	42010	330010	18010	230010	560010	920010	-
5000GtC	74	2850	4010	10010	36010	280010	17000	200010	490010	800010	-
5000GtC	103	2800	3900	9000	26010	190010	14010	130010	350010	580010	880010

variables				fraction									
emis.	R_Ca	R_Si	R_explicit	90%	75%	50%	25%	10%	e^{-1}	e^{-2}	e^{-3}	e^{-4}	e^{-5}
1000GtC	on	on	on	2200	2400	5600	75000	-	12000	-	-	-	-
1000GtC	on	on	off	2200	2400	5600	44000	-	12000	750000	-	-	-
1000GtC	on	off	on	2200	2450	5800	550000	-	13000	-	-	-	-
1000GtC	on	off	off	2200	2450	5800	550000	-	13000	-	-	-	-
1000GtC	off	on	on	2200	2450	5800	80000	-	13000	1000000	-	-	-
1000GtC	off	on	off	2200	2400	5600	50000	1000000	12000	700000	-	-	-
1000GtC	off	off	on	2200	2450	5800	-	-	13000	-	-	-	-
1000GtC	off	off	off	2200	2450	5800	-	-	13000	-	-	-	-
5000GtC	on	on	on	2950	5000	19000	650000	-	34000	-	-	-	-
5000GtC	on	on	off	2950	4900	17000	320000	-	30000	1000000	-	-	-
5000GtC	on	off	on	2950	5200	20000	-	-	38000	-	-	-	-
5000GtC	on	off	off	2950	5200	19000	-	-	36000	-	-	-	-
5000GtC	off	on	on	2950	5200	20000	600000	-	36000	-	-	-	-
5000GtC	off	on	off	2950	5200	19000	340000	-	32000	1000000	-	-	-
5000GtC	off	off	on	2950	5400	22000	-	-	40000	-	-	-	-
5000GtC	off	off	off	2950	5400	22000	-	-	40000	-	-	-	-

variables		fraction									
emis.	beta	90%	75%	50%	25%	10%	e^{-1}	e^{-2}	e^{-3}	e^{-4}	e^{-5}
1000GtC	0.48	2200	2400	4500	20010	-	8500	880010	-	-	-
1000GtC	0.65	2200	2400	4400	19000	-	8500	700010	-	-	-
1000GtC	0.8	2200	2400	4400	19000	980010	8500	580010	-	-	-
1000GtC	1.12	2200	2400	4400	18010	720010	8500	410010	-	-	-
5000GtC	0.48	2950	4600	15000	640010	-	28010	-	-	-	-
5000GtC	0.65	2900	4600	15000	470010	-	28010	-	-	-	-
5000GtC	0.8	2900	4600	15000	370010	-	28010	-	-	-	-
5000GtC	1.12	2900	4600	15000	250010	-	26010	940010	-	-	-

variables		fraction									
emis.	k_run	90%	75%	50%	25%	10%	e^{-1}	e^{-2}	e^{-3}	e^{-4}	e^{-5}
1000GtC	0.012	2200	2400	4500	20010	-	9000	-	-	-	-
1000GtC	0.024	2200	2400	4400	19000	880010	8500	520010	-	-	-
1000GtC	0.028	2200	2400	4400	19000	880010	8500	520010	-	-	-
1000GtC	0.045	2200	2400	4400	18010	540010	8500	310010	1000010	-	-
5000GtC	0.012	2950	4700	16010	800010	-	30010	-	-	-	-
5000GtC	0.024	2900	4600	15000	370010	-	28010	-	-	-	-
5000GtC	0.028	2900	4600	15000	320010	-	26010	-	-	-	-
5000GtC	0.045	2900	4500	14010	190010	960010	24010	720010	-	-	-

variables			fraction									
emis.	P_Ca	P_Si	90%	75%	50%	25%	10%	e^{-1}	e^{-2}	e^{-3}	e^{-4}	e^{-5}
1000GtC	on	on	2200	2400	5400	32000	600000	11000	400000	950000	-	-
1000GtC	on	off	2200	2400	5600	700000	-	13000	-	-	-	-
1000GtC	off	on	2200	2400	5400	36000	600000	12000	400000	1000000	-	-
1000GtC	off	off	2200	2450	5800	-	-	13000	-	-	-	-
5000GtC	on	on	2950	4800	17000	180000	800000	28000	650000	-	-	-
5000GtC	on	off	2950	5200	19000	-	-	36000	-	-	-	-
5000GtC	off	on	2950	5000	18000	190000	750000	30000	600000	-	-	-
5000GtC	off	off	2950	5400	22000	-	-	40000	-	-	-	-

variables			fraction									
emis.	f_Ca	f_Si	90%	75%	50%	25%	10%	e^{-1}	e^{-2}	e^{-3}	e^{-4}	e^{-5}
1000GtC	on	on	2200	2400	4600	18000	190000	9000	110000	360000	600000	750000
1000GtC	on	off	2200	2400	5400	170000	-	12000	-	-	-	-
1000GtC	off	on	2200	2400	4800	19000	190000	9500	120000	340000	550000	700000
1000GtC	off	off	2200	2450	5800	-	-	13000	-	-	-	-
5000GtC	on	on	2850	4000	11000	30000	260000	16000	170000	420000	700000	1000000
5000GtC	on	off	2950	4800	17000	-	-	30000	-	-	-	-
5000GtC	off	on	2850	4200	12000	34000	240000	18000	170000	420000	700000	1000000
5000GtC	off	off	2950	5400	22000	-	-	40000	-	-	-	-

variables		fraction									
emis.	Scheme	90%	75%	50%	25%	10%	e^{-1}	e^{-2}	e^{-3}	e^{-4}	e^{-5}
1000GtC	Globavg	2180	2400	3800	11000	70010	6400	32010	180010	350010	580010
1000GtC	GKWM	2180	2350	3400	9000	38010	5600	20010	120010	240010	370010
1000GtC	GEM-CO2	2180	2350	3300	8500	32010	5400	18010	110010	220010	350010
5000GtC	Globavg	2750	3700	8010	19000	130010	12010	80010	250010	420010	660010
5000GtC	GKWM	2700	3400	6010	14010	85000	9000	55000	170010	290010	430010
5000GtC	GEM-CO2	2650	3300	5600	13000	80010	8500	44010	160010	270010	400010

variables				fraction									
emis.	f_Ca	f_Si	Scheme	90%	75%	50%	25%	10%	e^{-1}	e^{-2}	e^{-3}	e^{-4}	e^{-5}
1000GtC	on	on	Globavg	2180	2400	3800	11000	90010	6400	36010	220010	410010	640010
1000GtC	on	on	GKWM	2180	2350	3400	9000	38010	5600	20010	120010	240010	370010
1000GtC	on	off	Globavg	2180	2400	4300	18010	-	8500	-	-	-	-
1000GtC	on	off	GKWM	2200	2400	4500	19000	-	8500	740010	-	-	-
1000GtC	off	on	Globavg	2180	2400	3900	12010	95000	6800	42010	220010	420010	680010
1000GtC	off	on	GKWM	2180	2350	3500	9500	40010	5600	22010	120010	230010	370010
1000GtC	off	off	Globavg	2200	2400	4600	22010	-	9000	-	-	-	-
1000GtC	off	off	GKWM	2200	2400	4800	26010	-	10010	-	-	-	-
5000GtC	on	on	Globavg	2800	3700	8010	22010	170010	13000	110010	300010	520010	780010
5000GtC	on	on	GKWM	2700	3400	6010	14010	85000	9000	55000	170010	290010	420010
5000GtC	on	off	Globavg	2900	4400	14010	-	-	24010	-	-	-	-
5000GtC	on	off	GKWM	2950	4700	16010	520010	-	28010	-	-	-	-
5000GtC	off	on	Globavg	2800	3900	9000	24010	170010	14010	110010	300010	500010	760010
5000GtC	off	on	GKWM	2700	3500	6400	15000	80010	9500	55000	160010	270010	400010
5000GtC	off	off	Globavg	2950	4800	17000	-	-	32010	-	-	-	-
5000GtC	off	off	GKWM	3000	6010	24010	-	-	42010	-	-	-	-

variables		fraction									
emis.	routing	90%	75%	50%	25%	10%	e^{-1}	e^{-2}	e^{-3}	e^{-4}	e^{-5}
1000GtC	1	2200	2450	5800	1000000	-	13000	-	-	-	-
1000GtC	2	2200	2450	5800	-	-	13000	-	-	-	-
1000GtC	3	2200	2450	8000	-	-	-	-	-	-	-
5000GtC	1	2950	5400	22000	-	-	40000	-	-	-	-
5000GtC	2	2950	5400	22000	-	-	40000	-	-	-	-
5000GtC	3	3000	6800	30000	-	-	-	-	-	-	-

variables		fraction									
emis.	lith.	90%	75%	50%	25%	10%	e^{-1}	e^{-2}	e^{-3}	e^{-4}	e^{-5}
1000GtC	GKWM	2180	2350	3400	9000	38010	5600	20010	120010	240010	380010
1000GtC	GEM-CO2	2180	2350	3400	9000	38010	5600	20010	120010	240010	370010
1000GtC	GKWM av.	2180	2350	3600	9500	46010	5800	24010	130010	250010	340010
1000GtC	GEM-CO2 av.	2180	2400	3900	12010	75000	6800	34010	190010	330010	450010
1000GtC	mono acid	2180	2350	3600	9500	38010	5800	22010	110010	230010	350010
1000GtC	mono basalt	2180	2350	3200	7500	20010	4900	14010	65000	150010	250010
1000GtC	mono carb	2160	2300	3200	10010	75000	5600	24010	220010	430010	600010
1000GtC	mono granite	2180	2350	3600	9500	38010	5800	22010	110010	230010	350010
1000GtC	mono sand	2200	2450	5800	24010	210010	13000	110010	440010	760010	1000010
1000GtC	mono shale	2160	2280	2900	6600	15000	4300	11000	34010	110010	200010
1000GtC	mono shield	2180	2350	3600	9500	38010	5800	22010	110010	230010	350010
5000GtC	GKWM	2700	3400	6200	15000	90010	9000	55000	180010	300010	440010
5000GtC	GEM-CO2	2700	3400	6010	14010	85000	9000	55000	160010	280010	410010
5000GtC	GKWM av.	2750	3600	6800	17000	110010	10010	65000	200010	330010	480010
5000GtC	GEM-CO2 av.	2800	3900	9000	24010	150010	14010	100010	270010	460010	660010
5000GtC	mono acid	2750	3600	7000	16010	80010	11000	46010	160010	280010	410010
5000GtC	mono basalt	2650	3200	5200	11000	44010	7500	26010	100010	190010	290010
5000GtC	mono carb	2600	3200	5600	15000	170010	8500	100010	350010	620010	860010
5000GtC	mono granite	2750	3600	7000	16010	80010	11000	46010	160010	280010	410010
5000GtC	mono sand	3000	7500	22010	55000	340010	32010	230010	580010	940010	-
5000GtC	mono shale	2500	2900	4300	8500	22010	6010	15000	70010	150010	230010
5000GtC	mono shield	2750	3600	7000	16010	80010	11000	46010	160010	280010	410010

variables		fraction									
emis.	clim. sens.	90%	75%	50%	25%	10%	e^{-1}	e^{-2}	e^{-3}	e^{-4}	e^{-5}
1000GtC	1.5	2120	2260	3200	15000	260000	6800	140000	480000	800000	-
1000GtC	2.64	2200	2400	4600	18000	180000	9000	110000	340000	550000	700000
1000GtC	3	2220	2450	5400	19000	180000	9500	110000	340000	550000	700000
1000GtC	4.5	2350	2700	7500	22000	150000	12000	95000	280000	420000	600000
1000GtC	6.	2400	2900	8000	19000	120000	12000	70000	220000	360000	500000
5000GtC	1.5	2650	3900	13000	55000	420000	22000	300000	650000	1000000	-
5000GtC	2.64	2850	4000	11000	30000	260000	16000	170000	440000	700000	1000000
5000GtC	3	2900	4200	11000	30000	220000	16000	150000	380000	650000	850000
5000GtC	4.5	3200	4400	10000	28000	160000	15000	110000	260000	440000	600000
5000GtC	6.	3400	4100	8000	19000	110000	12000	70000	200000	360000	480000

Table 36: **Timescale fitting** for excess **Surface warming** decay

variables		fit to $T(t) = b + h\sum_i w_i e^{-(t-t_0)/\tau_i}$					
emis.	short-circ.		warming (°C)	i	1	2	3	R^2
1000GtC	yes	b	0.11±0.01	w_i (%)	51±2	49±2		0.996
		h	1.69±0.02	τ_i (yr)	460±60	12000±1000		
1000GtC	no	b	0.012±0.007	w_i (%)	40.4±0.4	44.3±0.4	15.3±0.3	0.99994
		h	1.817±0.007	τ_i (yr)	324±8	5500±100	160000±10000	
5000GtC	yes	b	0.02±0.01	w_i (%)	18±1	59.0±0.5	22.6±0.3	0.99993
		h	6.41±0.05	τ_i (yr)	950±80	7100±200	187000±7000	
5000GtC	no	b	0.02±0.01	w_i (%)	19±1	58.8±0.6	22.4±0.3	0.99994
		h	6.39±0.06	τ_i (yr)	990±80	6700±200	175000±6000	

variables			fit to $T(t) = b + h\sum_i w_i e^{-(t-t_0)/\tau_i}$					
emis.	T_Ca	T_Si		warming (°C)	i	1	2	R^2
1000GtC	on	on	b	0.375±0.006	w_i (%)	48.4±0.7	51.6±0.6	0.99990
			h	1.452±0.006	τ_i (yr)	330±10	8000±300	
1000GtC	on	off	b	0.472±0.004	w_i (%)	50.6±0.6	49.4±0.5	0.99994
			h	1.358±0.005	τ_i (yr)	320±10	7800±200	
1000GtC	off	on	b	0.30±0.04	w_i (%)	100±4		0.97
			h	1.19±0.01	τ_i (yr)	4600±700		
1000GtC	off	off	b	0.484±0.005	w_i (%)	50.9±0.6	49.1±0.5	0.99994
			h	1.346±0.006	τ_i (yr)	320±10	7900±200	
5000GtC	on	on	b	1.1±0.1	w_i (%)	100±3		0.990
			h	4.76±0.04	τ_i (yr)	13000±2000		
5000GtC	on	off	-	-	-	-	-	-
5000GtC	off	on	b	1.0±0.1	w_i (%)	100±2		0.990
			h	4.74±0.06	τ_i (yr)	14000±2000		
5000GtC	off	off	-	-	-	-	-	-

variables		fit to $T(t) = b + h\sum_i w_i e^{-(t-t_0)/\tau_i}$						
emis.	E_a (kJ/mol)		warming (°C)	i	1	2	3	4	R^2
1000GtC	45	b	-0.007±0.01	w_i (%)	39±3	32±9	10±10	19±2	0.99995
		h	1.8±0.2	τ_i (yr)	325±9	5000±1000	12000±7000	440000±30000	
1000GtC	63	b	0.17±0.03	w_i (%)	100±4				0.97
		h	1.32±0.01	τ_i (yr)	4200±500				
1000GtC	74	b	0.11±0.01	w_i (%)	53±2	47±3			0.993
		h	1.68±0.04	τ_i (yr)	550±80	18000±2000			
1000GtC	103	b	0.010±0.004	w_i (%)	40.3±0.4	42.9±0.3	16.8±0.3		0.99994
		h	1.825±0.007	τ_i (yr)	332±8	6000±100	179000±9000		
5000GtC	45	b	0.1±0.1	w_i (%)	68.9±0.8	31±2			0.999
		h	5.91±0.09	τ_i (yr)	6700±400	340000±60000			
5000GtC	63	b	0.10±0.08	w_i (%)	69.6±0.7	30±1			0.999
		h	5.98±0.08	τ_i (yr)	6200±300	260000±40000			
5000GtC	74	b	0.09±0.07	w_i (%)	70.3±0.7	30±1			0.999
		h	6.02±0.08	τ_i (yr)	5900±300	220000±30000			
5000GtC	103	b	0.02±0.01	w_i (%)	19±1	57.7±0.5	23.7±0.3		0.99993
		h	6.42±0.05	τ_i (yr)	950±80	7900±200	208000±8000		

variables				fit to $T(t) = b + h\sum_i w_i e^{-(t-t_0)/\tau_i}$						
emis.	R_Ca	R_Si	R_explicit	warming (°C)		i	1	2	3	R^2
1000GtC	on	on	on	b	0.408±0.009	w_i (%)	51±2	49±2		0.999
				h	1.42±0.02	τ_i (yr)	350±40	10200±900		
1000GtC	on	on	off	b	0.06±0.06	w_i (%)	38.8±0.7	38.4±0.7	23±3	0.99994
				h	1.77±0.03	τ_i (yr)	322±9	7600±200	900000±200000	
1000GtC	on	off	on	b	0.476±0.004	w_i (%)	50.7±0.6	49.3±0.5		0.99994
				h	1.353±0.007	τ_i (yr)	320±10	7900±200		
1000GtC	on	off	off	b	0.473±0.004	w_i (%)	50.6±0.6	49.4±0.5		0.99994
				h	1.358±0.005	τ_i (yr)	320±10	7900±200		
1000GtC	off	on	on	b	0.40±0.01	w_i (%)	51±2	49±2		0.998
				h	1.42±0.02	τ_i (yr)	360±40	11000±1000		
1000GtC	off	on	off	b	0.36±0.01	w_i (%)	51±3	49±2		0.997
				h	1.46±0.03	τ_i (yr)	380±60	13000±2000		
1000GtC	off	off	on	b	0.484±0.005	w_i (%)	50.9±0.6	49.1±0.5		0.99994
				h	1.346±0.006	τ_i (yr)	320±10	7900±200		
1000GtC	off	off	off	b	0.484±0.005	w_i (%)	50.9±0.6	49.1±0.5		0.99994
				h	1.346±0.006	τ_i (yr)	320±10	7900±200		
5000GtC	on	on	on	-	-	-	-	-	-	-
5000GtC	on	on	off	-	-	-	-	-	-	-
5000GtC	on	off	on	-	-	-	-	-	-	-
5000GtC	on	off	off	-	-	-	-	-	-	-
5000GtC	off	on	on	-	-	-	-	-	-	-
5000GtC	off	on	off	-	-	-	-	-	-	-
5000GtC	off	off	on	-	-	-	-	-	-	-
5000GtC	off	off	off	-	-	-	-	-	-	-

variables		fit to $T(t) = b + h\sum_i w_i e^{-(t-t_0)/\tau_i}$					
emis.	beta	warming (°C)	i	1	2	3	R^2
1000GtC	0.48	b 0.11±0.06	w_i (%)	42.2±0.5	42.2±0.5	16±3	0.99993
		h 1.72±0.02	τ_i (yr)	339±8	6900±100	1200000±400000	
1000GtC	0.65	b 0.09±0.05	w_i (%)	41.6±0.5	41.7±0.5	17±2	0.99994
		h 1.75±0.02	τ_i (yr)	339±8	6900±100	1100000±300000	
1000GtC	0.8	b 0.32±0.02	w_i (%)	100.0±0.3			0.98
		h 1.21±0.05	τ_i (yr)	3500±400			
1000GtC	1.12	b 0.29±0.02	w_i (%)	100±4			0.98
		h 1.2282±0.0004	τ_i (yr)	3600±400			
5000GtC	0.48	b 1.78±0.05	w_i (%)	100.0±0.8			0.996
		h 4.14±0.06	τ_i (yr)	10200±800			
5000GtC	0.65	b 1.82±0.05	w_i (%)	100.0±0.8			0.997
		h 4.12±0.06	τ_i (yr)	9700±700			
5000GtC	0.8	b 1.76±0.05	w_i (%)	100±2			0.997
		h 4.17±0.03	τ_i (yr)	9900±700			
5000GtC	1.12	b -0.4±0.5	w_i (%)	16.6±1	49±2	34±5	0.99993
		h 6.9±0.4	τ_i (yr)	890±70	11700±300	1500000±400000	

variables		fit to $T(t) = b + h\sum_i w_i e^{-(t-t_0)/\tau_i}$					
emis.	k_run		warming (°C)	i	1	2	3	R^2
1000GtC	0.012	b	0.364±0.008	w_i (%)	48±2	40±8	10±10	0.99995
		h	1.47±0.08	τ_i (yr)	330±10	5600±1000	17000±10000	
1000GtC	0.024	b	0.31±0.02	w_i (%)	100±1			0.98
		h	1.21±0.04	τ_i (yr)	3500±400			
1000GtC	0.028	b	0.31±0.02	w_i (%)	100±1			0.98
		h	1.22±0.04	τ_i (yr)	3500±400			
1000GtC	0.045	b	0.27±0.02	w_i (%)	100±3			0.98
		h	1.25±0.02	τ_i (yr)	3800±500			
5000GtC	0.012	b	1.85±0.04	w_i (%)	100±2			0.997
		h	4.07±0.03	τ_i (yr)	10200±700			
5000GtC	0.024	b	7.±7.	w_i (%)	16±2	47±6	40±10	0.99992
		h	7.2±7.	τ_i (yr)	890±70	11900±300	2000000±1000000	
5000GtC	0.028	b	1.56±0.06	w_i (%)	100±2			0.994
		h	4.31±0.04	τ_i (yr)	11000±1000			
5000GtC	0.045	b	0.3±0.3	w_i (%)	69±1	31±5		0.998
		h	5.7±0.2	τ_i (yr)	7400±500	600000±200000		

variables			fit to $T(t) = b + h\sum_i w_i e^{-(t-t_0)/\tau_i}$					
emis.	P_Ca	P_Si		warming (°C)	i	1	2	R^2
1000GtC	on	on	b	0.35±0.03	w_i (%)	100±3		0.98
			h	1.15±0.03	τ_i (yr)	4200±600		
1000GtC	on	off	b	0.473±0.005	w_i (%)	50.6±0.6	49.4±0.5	0.99994
			h	1.357±0.006	τ_i (yr)	320±10	7700±200	
1000GtC	off	on	b	0.30±0.02	w_i (%)	51±3	49±3	0.995
			h	1.51±0.04	τ_i (yr)	430±80	16000±2000	
1000GtC	off	off	b	0.484±0.005	w_i (%)	50.9±0.6	49.1±0.5	0.99994
			h	1.346±0.006	τ_i (yr)	320±10	7900±200	
5000GtC	on	on	b	1.42±0.1	w_i (%)	100±2		0.993
			h	4.41±0.06	τ_i (yr)	14000±2000		
5000GtC	on	off	-	-	-	-	-	-
5000GtC	off	on	-	-	-	-	-	-
5000GtC	off	off	-	-	-	-	-	-

variables			fit to $T(t) = b + h\sum_i w_i e^{-(t-t_0)/\tau_i}$					
emis.	f_Ca	f_Si		warming (°C)	i	1	2	R^2
1000GtC	on	on	b	0.14±0.02	w_i (%)	51±3	49±3	0.994
			h	1.64±0.04	τ_i (yr)	520±90	19000±3000	
1000GtC	on	off	b	0.458±0.004	w_i (%)	50.2±0.6	49.8±0.5	0.99994
			h	1.371±0.005	τ_i (yr)	320±10	7500±200	
1000GtC	off	on	b	0.23±0.04	w_i (%)	100.00±0.06		0.97
			h	1.25±0.07	τ_i (yr)	4900±800		
1000GtC	off	off	b	0.484±0.005	w_i (%)	50.9±0.6	49.1±0.5	0.99994
			h	1.346±0.006	τ_i (yr)	320±10	7900±200	
5000GtC	on	on	b	0.1±0.1	w_i (%)	71±1	29±2	0.998
			h	6.01±0.1	τ_i (yr)	6100±400	190000±40000	
5000GtC	on	off	-	-	-	-	-	-
5000GtC	off	on	b	0.8±0.1	w_i (%)	100.0±0.4		0.99
			h	5.0±0.1	τ_i (yr)	12000±1000		
5000GtC	off	off	-	-	-	-	-	-

variables		fit to $T(t) = b + h\sum_i w_i e^{-(t-t_0)/\tau_i}$						
emis.	Scheme		warming (°C)	i	1	2	3	4	R^2
1000GtC	Globavg	b	0.005±0.01	w_i (%)	40±3	40±6	6±10	15±2	0.99994
		h	1.8±0.2	τ_i (yr)	324±10	5100±700	10000±20000	150000±20000	
1000GtC	GKWM	b	0.007±0.005	w_i (%)	41.1±0.4	45.4±0.4	13.5±0.4		0.99994
		h	1.802±0.007	τ_i (yr)	310±8	4900±100	101000±9000		
1000GtC	GEM-CO2	b	0.13±0.03	w_i (%)	100±2				0.98
		h	1.36±0.03	τ_i (yr)	2900±300				
5000GtC	Globavg	b	0.02±0.01	w_i (%)	19±1	59.9±0.5	21.4±0.4		0.99993
		h	6.41±0.06	τ_i (yr)	950±80	7000±200	155000±7000		
5000GtC	GKWM	b	0.01±0.01	w_i (%)	25±3	55±1	20.1±0.4		0.99994
		h	6.36±0.09	τ_i (yr)	1200±100	5500±300	113000±5000		
5000GtC	GEM-CO2	b	0.01±0.01	w_i (%)	28±3	53±2	19.3±0.4		0.99994
		h	6.34±0.09	τ_i (yr)	1300±100	5300±300	106000±5000		

variables				fit to $T(t) = b + h\sum_i w_i e^{-(t-t_0)/\tau_i}$						
emis.	f_Ca	f_Si	Scheme		warming (°C)	i	1	2	3	R^2
1000GtC	on	on	Globavg	b	0.008±0.007	w_i (%)	40.5±0.4	43.8±0.4	15.7±0.3	0.99993
				h	1.827±0.007	τ_i (yr)	329±8	5700±100	170000±10000	
1000GtC	on	on	GKWM	b	0.13±0.03	w_i (%)	100±2			0.98
				h	1.36±0.03	τ_i (yr)	3100±400			
1000GtC	on	off	Globavg	b	0.36±0.02	w_i (%)	48±5	40±20	10±20	0.99995
				h	1.5±0.2	τ_i (yr)	330±10	6000±1000	10000±20000	
1000GtC	on	off	GKWM	b	0.35±0.01	w_i (%)	48±3	40±10	10±10	0.99995
				h	1.50±0.1	τ_i (yr)	330±10	6000±1000	20000±10000	
1000GtC	off	on	Globavg	b	0.15±0.03	w_i (%)	100±3			0.97
				h	1.35±0.02	τ_i (yr)	4000±500			
1000GtC	off	on	GKWM	b	0.008±0.006	w_i (%)	40.9±0.4	45.2±0.4	13.9±0.4	0.99994
				h	1.805±0.007	τ_i (yr)	313±8	5100±100	95000±9000	
1000GtC	off	off	Globavg	b	0.38±0.01	w_i (%)	49±4	40±20	10±20	0.99995
				h	1.5±0.1	τ_i (yr)	330±10	6000±2000	10000±10000	
1000GtC	off	off	GKWM	b	0.385±0.009	w_i (%)	48.7±0.8	30±20	30±20	0.99995
				h	1.471±0.008	τ_i (yr)	340±10	5000±2000	12000±5000	
5000GtC	on	on	Globavg	b	0.06±0.04	w_i (%)	73.3±0.6	27±1		0.999
				h	6.09±0.07	τ_i (yr)	4800±200	150000±20000		
5000GtC	on	on	GKWM	b	0.01±0.01	w_i (%)	25±3	55±1	20.1±0.4	0.99994
				h	6.36±0.09	τ_i (yr)	1200±100	5500±300	112000±5000	
5000GtC	on	off	Globavg	-	-	-	-	-	-	-
5000GtC	on	off	GKWM	b	1.70±0.05	w_i (%)	100±2			0.996
				h	4.21±0.03	τ_i (yr)	11000±800			
5000GtC	off	on	Globavg	b	0.06±0.04	w_i (%)	71.7±0.9	28±1		0.999
				h	6.07±0.06	τ_i (yr)	5200±300	140000±20000		
5000GtC	off	on	GKWM	b	0.01±0.01	w_i (%)	22±2	56.9±1	20.9±0.4	0.99995
				h	6.36±0.08	τ_i (yr)	1120±90	5600±200	104000±5000	
5000GtC	off	off	Globavg	-	-	-	-	-	-	-
5000GtC	off	off	GKWM	-	-	-	-	-	-	-

variables		fit to $T(t) = b + h\sum_i w_i e^{-(t-t_0)/\tau_i}$					
emis.	routing		warming (°C)	i	1	2	R^2
1000GtC	1	b	0.483±0.004	w_i (%)	50.9±0.6	49.1±0.5	0.99994
		h	1.348±0.005	τ_i (yr)	320±10	8000±200	
1000GtC	2	b	0.484±0.005	w_i (%)	50.9±0.6	49.1±0.5	0.99994
		h	1.346±0.006	τ_i (yr)	320±10	7900±200	
1000GtC	3	b	0.703±0.008	w_i (%)	57.7±0.6	42.3±0.7	0.99996
		h	1.134±0.006	τ_i (yr)	310±10	6500±400	
5000GtC	1	-	-	-	-	-	-
5000GtC	2	-	-	-	-	-	-
5000GtC	3	-	-	-	-	-	-

variables		fit to $T(t) = b + h\sum_i w_i e^{-(t-t_0)/\tau_i}$						
emis.	lith.		warming (°C)	i	1	2	3	4	R^2
1000GtC	GKWM	b	0.08±0.01	w_i (%)	50±2	50±2			0.997
		h	1.71±0.02	τ_i (yr)	410±50	9000±900			
1000GtC	GEM-CO2	b	0.007±0.005	w_i (%)	41.1±0.4	45.4±0.4	13.5±0.4		0.99994
		h	1.802±0.007	τ_i (yr)	310±8	4900±100	101000±9000		
1000GtC	GKWM av.	b	0.14±0.03	w_i (%)	100.0±0.5				0.98
		h	1.37±0.05	τ_i (yr)	3300±400				
1000GtC	GEM-CO2 av.	b	-0.009±0.009	w_i (%)	39±4	30±10	10±20	16±2	0.99994
		h	1.9±0.2	τ_i (yr)	330±10	5000±1000	10000±10000	170000±20000	
1000GtC	mono acid	b	0.010±0.007	w_i (%)	40.3±0.5	45.9±0.4	13.8±0.4		0.99994
		h	1.825±0.008	τ_i (yr)	325±9	5300±100	91000±10000		
1000GtC	mono basalt	b	0.12±0.03	w_i (%)	100±2				0.98
		h	1.38±0.02	τ_i (yr)	2600±300				
1000GtC	mono carb	b	-0.007±0.006	w_i (%)	45.6±0.4	40.8±0.4	13.5±0.3		0.9999
		h	1.743±0.008	τ_i (yr)	283±7	6100±200	230000±20000		
1000GtC	mono granite	b	0.010±0.007	w_i (%)	40.4±0.4	45.9±0.4	13.8±0.4		0.99994
		h	1.825±0.009	τ_i (yr)	325±9	5300±100	91000±10000		
1000GtC	mono sand	b	-0.007±0.006	w_i (%)	38±1	3±2	40±1	18.3±0.3	0.99996
		h	1.89±0.03	τ_i (yr)	340±10	3000±2000	13000±600	350000±20000	
1000GtC	mono shale	b	0.10±0.03	w_i (%)	100±2				0.98
		h	1.33±0.03	τ_i (yr)	2200±300				
1000GtC	mono shield	b	0.010±0.007	w_i (%)	40.4±0.4	45.9±0.4	13.8±0.4		0.99994
		h	1.825±0.009	τ_i (yr)	325±9	5300±100	91000±10000		
5000GtC	GKWM	b	0.01±0.01	w_i (%)	25±3	55±1	20.2±0.4		0.99994
		h	6.37±0.09	τ_i (yr)	1200±100	5600±300	115000±5000		
5000GtC	GEM-CO2	b	0.01±0.01	w_i (%)	24±3	55±1	20.3±0.4		0.99994
		h	6.37±0.1	τ_i (yr)	1200±100	5500±300	111000±5000		
5000GtC	GKWM av.	b	0.01±0.01	w_i (%)	20±2	58.7±0.7	20.8±0.4		0.99994
		h	6.38±0.07	τ_i (yr)	1050±90	6100±200	131000±6000		
5000GtC	GEM-CO2 av.	b	0.05±0.05	w_i (%)	72.6±0.8	27±2			0.999
		h	6.07±0.08	τ_i (yr)	5600±300	130000±20000			
5000GtC	mono acid	b	0.01±0.01	w_i (%)	20±2	61.1±0.6	19.2±0.5		0.99993
		h	6.40±0.07	τ_i (yr)	980±90	6500±200	111000±6000		
5000GtC	mono basalt	b	0.01±0.02	w_i (%)	31±4	53±2	16.3±0.6		0.99993
		h	6.32±0.1	τ_i (yr)	1200±100	5000±300	78000±7000		
5000GtC	mono carb	b	0.01±0.02	w_i (%)	34±2	47±1	19.2±0.3		0.99993
		h	6.22±0.03	τ_i (yr)	1180±60	6300±200	240000±10000		
5000GtC	mono granite	b	0.01±0.01	w_i (%)	20±2	61.1±0.6	19.2±0.5		0.99993
		h	6.40±0.07	τ_i (yr)	980±90	6500±200	111000±6000		
5000GtC	mono sand	b	-0.2±0.1	w_i (%)	14±1	62.4±0.5	23±1		0.9997
		h	6.7±0.1	τ_i (yr)	600±100	22200±1000	500000±100000		
5000GtC	mono shale	b	0.12±0.03	w_i (%)	72±1	28±3			0.999
		h	6.0±0.1	τ_i (yr)	1800±100	18000±3000			
5000GtC	mono shield	b	0.01±0.01	w_i (%)	20±2	61.1±0.6	19.2±0.5		0.99993
		h	6.40±0.07	τ_i (yr)	980±90	6500±200	111000±6000		

variables		fit to $T(t) = b + h\sum_i w_i e^{-(t-t_0)/\tau_i}$							
emis.	clim. sens.		warming (°C)	i	1	2	3	4	R^2
1000GtC	1.5	b	-0.007±0.004	w_i (%)	44.6±0.8	11±3	25±3	19.9±0.3	0.99999
		h	1.20±0.01	τ_i (yr)	268±4	2900±600	8900±700	370000±10000	
1000GtC	2.64	b	-0.006±0.007	w_i (%)	38.1±0.4	40.3±0.4	21.6±0.3		0.99994
		h	1.834±0.007	τ_i (yr)	322±9	6700±200	230000±10000		
1000GtC	3	b	0.16±0.02	w_i (%)	47±3	53±3			0.994
		h	1.80±0.04	τ_i (yr)	500±100	18000±3000			
1000GtC	4.5	b	0.27±0.05	w_i (%)	100±2				0.98
		h	1.92±0.05	τ_i (yr)	8000±1000				
1000GtC	6.	b	-0.02±0.02	w_i (%)	23.4±0.9	57.0±0.5	19.6±0.9		0.9998
		h	3.33±0.03	τ_i (yr)	320±30	8600±300	170000±20000		
5000GtC	1.5	b	0.1±0.1	w_i (%)	68±2	32±3			0.997
		h	3.41±0.07	τ_i (yr)	6900±600	270000±90000			
5000GtC	2.64	b	0.1±0.1	w_i (%)	71±1	29±2			0.998
		h	6.00±0.1	τ_i (yr)	6100±400	190000±40000			
5000GtC	3	b	0.1±0.1	w_i (%)	71.0±0.8	29±2			0.999
		h	6.8±0.1	τ_i (yr)	6200±400	180000±30000			
5000GtC	4.5	-	-	-	-	-	-	-	-
5000GtC	6.	-	-	-	-	-	-	-	-

Table 37: **Surface ocean acidification** (pH units below 8.15 baseline) reached at specific calendar years

variables		**year**								
emis.	short-circ.	3000	5000	10000	20000	50000	100k	200k	500k	1000k
1000GtC	yes	0.092	0.063	0.033	0.015	0.008	0.005	0.002	0.000	0.000
1000GtC	no	0.091	0.062	0.032	0.014	0.007	0.005	0.001	0.000	0.000
5000GtC	yes	0.520	0.352	0.196	0.088	0.050	0.036	0.018	0.000	0.000
5000GtC	no	0.515	0.342	0.183	0.083	0.047	0.034	0.016	0.000	0.000

variables			**year**								
emis.	T_Ca	T_Si	3000	5000	10000	20000	50000	100k	200k	500k	1000k
1000GtC	on	on	0.100	0.076	0.049	0.030	0.021	0.018	0.013	0.004	0.000
1000GtC	on	off	0.102	0.079	0.055	0.037	0.029	0.028	0.028	0.027	0.026
1000GtC	off	on	0.100	0.077	0.050	0.032	0.022	0.019	0.015	0.006	0.001
1000GtC	off	off	0.102	0.080	0.056	0.039	0.030	0.030	0.029	0.029	0.028
5000GtC	on	on	0.550	0.415	0.302	0.167	0.089	0.076	0.058	0.024	0.003
5000GtC	on	off	0.560	0.438	0.351	0.232	0.129	0.122	0.122	0.122	0.121
5000GtC	off	on	0.552	0.419	0.311	0.177	0.093	0.078	0.059	0.025	0.002
5000GtC	off	off	0.562	0.443	0.362	0.248	0.135	0.128	0.128	0.127	0.127

variables		**year**								
emis.	E_a (kJ/mol)	3000	5000	10000	20000	50000	100k	200k	500k	1000k
1000GtC	45	0.095	0.069	0.041	0.023	0.015	0.013	0.009	0.003	0.000
1000GtC	63	0.095	0.068	0.040	0.021	0.013	0.010	0.007	0.000	0.000
1000GtC	74	0.094	0.067	0.039	0.020	0.012	0.009	0.005	0.000	0.000
1000GtC	103	0.093	0.066	0.036	0.018	0.010	0.007	0.003	0.000	0.000
5000GtC	45	0.545	0.403	0.278	0.151	0.089	0.077	0.060	0.027	0.004
5000GtC	63	0.540	0.392	0.258	0.134	0.078	0.064	0.045	0.013	0.000
5000GtC	74	0.537	0.386	0.249	0.126	0.073	0.058	0.038	0.008	0.000
5000GtC	103	0.527	0.367	0.219	0.104	0.059	0.044	0.024	0.000	0.000

variables				**year**								
emis.	R_Ca	R_Si	R_explicit	3000	5000	10000	20000	50000	100k	200k	500k	1000k
1000GtC	on	on	on	0.102	0.079	0.054	0.037	0.028	0.027	0.026	0.022	0.016
1000GtC	on	on	off	0.101	0.078	0.053	0.035	0.027	0.025	0.023	0.018	0.011
1000GtC	on	off	on	0.102	0.080	0.055	0.038	0.029	0.029	0.028	0.028	0.026
1000GtC	on	off	off	0.102	0.079	0.055	0.037	0.029	0.028	0.028	0.027	0.026
1000GtC	off	on	on	0.102	0.080	0.055	0.037	0.028	0.027	0.025	0.021	0.015
1000GtC	off	on	off	0.102	0.079	0.054	0.036	0.027	0.026	0.023	0.017	0.010
1000GtC	off	off	on	0.102	0.080	0.056	0.039	0.030	0.030	0.029	0.029	0.028
1000GtC	off	off	off	0.102	0.080	0.056	0.039	0.030	0.030	0.029	0.029	0.028
5000GtC	on	on	on	0.559	0.437	0.348	0.227	0.124	0.115	0.110	0.095	0.074
5000GtC	on	on	off	0.558	0.433	0.339	0.213	0.117	0.107	0.099	0.077	0.045
5000GtC	on	off	on	0.561	0.440	0.356	0.239	0.132	0.125	0.124	0.124	0.122
5000GtC	on	off	off	0.560	0.440	0.354	0.235	0.129	0.123	0.123	0.122	0.122
5000GtC	off	on	on	0.561	0.441	0.356	0.238	0.127	0.118	0.112	0.096	0.072
5000GtC	off	on	off	0.560	0.438	0.350	0.229	0.122	0.110	0.101	0.077	0.044
5000GtC	off	off	on	0.562	0.443	0.362	0.248	0.135	0.128	0.128	0.127	0.127
5000GtC	off	off	off	0.562	0.443	0.362	0.248	0.135	0.128	0.128	0.127	0.127

variables		year								
emis.	beta	3000	5000	10000	20000	50000	100k	200k	500k	1000k
1000GtC	0.48	0.097	0.072	0.046	0.028	0.020	0.019	0.018	0.015	0.011
1000GtC	0.65	0.097	0.072	0.045	0.027	0.019	0.018	0.017	0.013	0.009
1000GtC	0.8	0.097	0.072	0.045	0.027	0.019	0.018	0.016	0.012	0.007
1000GtC	1.12	0.097	0.072	0.045	0.026	0.018	0.017	0.015	0.010	0.005
5000GtC	0.48	0.554	0.422	0.317	0.195	0.119	0.113	0.108	0.095	0.075
5000GtC	0.65	0.553	0.422	0.314	0.191	0.116	0.110	0.104	0.087	-
5000GtC	0.8	0.552	0.420	0.313	0.189	0.115	0.108	0.100	0.081	-
5000GtC	1.12	0.552	0.418	0.309	0.184	0.111	0.103	0.093	0.068	0.040

variables		year								
emis.	k_run	3000	5000	10000	20000	50000	100k	200k	500k	1000k
1000GtC	0.012	0.097	0.073	0.046	0.028	0.020	0.019	0.018	0.016	0.012
1000GtC	0.024	0.097	0.072	0.045	0.027	0.019	0.018	0.016	0.012	0.006
1000GtC	0.028	0.097	0.072	0.045	0.027	0.019	0.018	0.016	0.012	0.007
1000GtC	0.045	0.096	0.071	0.044	0.026	0.017	0.016	0.013	0.008	0.002
5000GtC	0.012	0.554	0.424	0.322	0.200	0.122	0.116	0.112	0.101	0.083
5000GtC	0.024	0.552	0.420	0.313	0.190	0.115	0.108	0.100	0.081	0.055
5000GtC	0.028	0.552	0.419	0.310	0.186	0.113	0.106	0.098	0.077	0.050
5000GtC	0.045	0.549	0.414	0.299	0.174	0.105	0.097	0.085	0.057	0.028

variables			year								
emis.	P_Ca	P_Si	3000	5000	10000	20000	50000	100k	200k	500k	1000k
1000GtC	on	on	0.101	0.077	0.052	0.034	0.024	0.022	0.019	0.011	0.004
1000GtC	on	off	0.102	0.079	0.055	0.037	0.029	0.028	0.028	0.028	0.027
1000GtC	off	on	0.101	0.078	0.053	0.035	0.026	0.023	0.020	0.012	0.005
1000GtC	off	off	0.102	0.080	0.056	0.039	0.030	0.030	0.029	0.029	0.028
5000GtC	on	on	0.557	0.432	0.335	0.206	0.109	0.097	0.085	0.054	0.018
5000GtC	on	off	0.560	0.439	0.352	0.232	0.129	0.123	0.122	0.122	0.121
5000GtC	off	on	0.559	0.436	0.344	0.218	0.114	0.101	0.088	0.055	0.018
5000GtC	off	off	0.562	0.443	0.362	0.248	0.135	0.128	0.128	0.127	0.127

variables			year								
emis.	f_Ca	f_Si	3000	5000	10000	20000	50000	100k	200k	500k	1000k
1000GtC	on	on	0.098	0.072	0.044	0.025	0.016	0.013	0.008	0.002	0.000
1000GtC	on	off	0.101	0.078	0.053	0.035	0.027	0.027	0.026	0.026	0.025
1000GtC	off	on	0.099	0.074	0.047	0.028	0.018	0.014	0.009	0.002	0.000
1000GtC	off	off	0.102	0.080	0.056	0.039	0.030	0.030	0.029	0.029	0.028
5000GtC	on	on	0.538	0.389	0.253	0.122	0.066	0.052	0.033	0.006	0.000
5000GtC	on	off	0.556	0.430	0.332	0.205	0.119	0.116	0.115	0.115	0.114
5000GtC	off	on	0.543	0.400	0.274	0.139	0.072	0.055	0.035	0.006	0.000
5000GtC	off	off	0.562	0.443	0.362	0.248	0.135	0.128	0.128	0.127	0.127

variables		year								
emis.	Scheme	3000	5000	10000	20000	50000	100k	200k	500k	1000k
1000GtC	Globavg	0.092	0.063	0.032	0.014	0.007	0.004	0.001	0.000	0.000
1000GtC	GKWM	0.085	0.055	0.025	0.009	0.004	0.001	0.000	0.000	0.000
1000GtC	GEM-CO2	0.083	0.053	0.023	0.008	0.003	0.000	0.000	0.000	0.000
5000GtC	Globavg	0.517	0.347	0.188	0.081	0.043	0.028	0.012	0.000	0.000
5000GtC	GKWM	0.487	0.291	0.133	0.057	0.031	0.018	0.003	0.000	0.000
5000GtC	GEM-CO2	0.475	0.273	0.119	0.051	0.027	0.015	0.001	0.000	0.000

variables				year								
emis.	f_Ca	f_Si	Scheme	3000	5000	10000	20000	50000	100k	200k	500k	1000k
1000GtC	on	on	Globavg	0.092	0.063	0.033	0.015	0.008	0.005	0.002	0.000	0.000
1000GtC	on	on	GKWM	0.085	0.055	0.025	0.009	0.004	0.001	0.000	0.000	0.000
1000GtC	on	off	Globavg	0.096	0.071	0.044	0.026	0.019	0.018	0.018	0.017	0.016
1000GtC	on	off	GKWM	0.098	0.073	0.046	0.027	0.018	0.017	0.016	0.013	0.009
1000GtC	off	on	Globavg	0.093	0.065	0.036	0.017	0.009	0.006	0.002	0.000	0.000
1000GtC	off	on	GKWM	0.087	0.057	0.027	0.010	0.004	0.001	0.000	0.000	0.000
1000GtC	off	off	Globavg	0.097	0.073	0.047	0.029	0.021	0.021	0.020	0.020	0.018
1000GtC	off	off	GKWM	0.100	0.076	0.051	0.032	0.022	0.021	0.021	0.020	0.019
5000GtC	on	on	Globavg	0.520	0.352	0.196	0.088	0.050	0.036	0.018	0.000	0.000
5000GtC	on	on	GKWM	0.487	0.291	0.133	0.057	0.031	0.018	0.003	0.000	0.000
5000GtC	on	off	Globavg	0.548	0.411	0.295	0.172	0.112	0.109	0.109	0.109	0.108
5000GtC	on	off	GKWM	0.554	0.427	0.324	0.194	0.110	0.104	0.099	0.086	0.068
5000GtC	off	on	Globavg	0.528	0.367	0.218	0.102	0.055	0.039	0.019	0.000	0.000
5000GtC	off	on	GKWM	0.494	0.303	0.143	0.062	0.033	0.017	0.002	0.000	0.000
5000GtC	off	off	Globavg	0.555	0.428	0.329	0.210	0.128	0.124	0.124	0.123	0.122
5000GtC	off	off	GKWM	0.565	0.453	0.380	0.271	0.137	0.126	0.126	0.125	0.125

variables		year								
emis.	routing	3000	5000	10000	20000	50000	100k	200k	500k	1000k
1000GtC	1	0.102	0.080	0.056	0.039	0.030	0.029	0.029	0.029	0.028
1000GtC	2	0.102	0.080	0.056	0.039	0.030	0.030	0.029	0.029	0.028
1000GtC	3	0.106	0.087	0.068	0.055	0.052	0.060	0.077	0.129	0.216
5000GtC	1	0.562	0.444	0.364	0.250	0.136	0.128	0.128	0.127	0.126
5000GtC	2	0.562	0.443	0.362	0.248	0.135	0.128	0.128	0.127	0.127
5000GtC	3	0.568	0.460	0.397	0.304	0.167	0.158	0.174	0.225	0.302

variables		year								
emis.	lith.	3000	5000	10000	20000	50000	100k	200k	500k	1000k
1000GtC	GKWM	0.086	0.056	0.025	0.010	0.004	0.001	0.000	0.000	0.000
1000GtC	GEM-CO2	0.085	0.055	0.025	0.009	0.004	0.001	0.000	0.000	-
1000GtC	GKWM av.	0.089	0.059	0.028	0.011	0.004	0.002	0.000	0.000	0.000
1000GtC	GEM-CO2 av.	0.094	0.066	0.036	0.016	0.007	0.004	0.001	0.000	0.000
1000GtC	mono acid	0.090	0.060	0.028	0.011	0.004	0.001	0.000	0.000	0.000
1000GtC	mono basalt	0.081	0.050	0.019	0.005	0.000	0.000	0.000	0.000	0.000
1000GtC	mono carb	0.076	0.054	0.027	0.010	0.005	0.003	0.000	0.000	0.000
1000GtC	mono granite	0.090	0.060	0.028	0.011	0.004	0.001	0.000	0.000	0.000
1000GtC	mono sand	0.104	0.085	0.061	0.036	0.016	0.011	0.008	0.002	0.000
1000GtC	mono shale	0.070	0.043	0.014	0.001	0.000	0.000	0.000	0.000	0.000
1000GtC	mono shield	0.090	0.060	0.028	0.011	0.004	0.001	0.000	0.000	0.000
5000GtC	GKWM	0.490	0.294	0.135	0.059	0.032	0.018	0.004	0.000	0.000
5000GtC	GEM-CO2	0.487	0.291	0.133	0.057	0.031	0.018	0.002	0.000	0.000
5000GtC	GKWM av.	0.505	0.321	0.158	0.067	0.036	0.022	0.006	0.000	0.000
5000GtC	GEM-CO2 av.	0.530	0.375	0.227	0.100	0.049	0.034	0.015	0.000	0.000
5000GtC	mono acid	0.506	0.327	0.163	0.063	0.029	0.015	0.002	0.000	0.000
5000GtC	mono basalt	0.459	0.249	0.096	0.034	0.014	0.004	0.000	0.000	0.000
5000GtC	mono carb	0.443	0.261	0.126	0.058	0.033	0.025	0.015	0.000	0.000
5000GtC	mono granite	0.506	0.327	0.163	0.063	0.029	0.015	0.002	0.000	0.000
5000GtC	mono sand	0.570	0.475	0.399	0.272	0.092	0.061	0.044	0.015	0.000
5000GtC	mono shale	0.392	0.193	0.062	0.011	0.000	0.000	0.000	0.000	0.000
5000GtC	mono shield	0.506	0.327	0.163	0.063	0.029	0.015	0.002	0.000	0.000

variables		year								
emis.	clim. sens.	3000	5000	10000	20000	50000	100k	200k	500k	1000k
1000GtC	1.5	0.098	0.073	0.047	0.029	0.019	0.017	0.013	0.005	0.001
1000GtC	2.64	0.098	0.072	0.044	0.025	0.016	0.013	0.008	0.002	0.000
1000GtC	3	0.098	0.073	0.044	0.025	0.016	0.013	0.008	0.002	0.000
1000GtC	4.5	0.100	0.074	0.044	0.023	0.014	0.010	0.005	0.000	0.000
1000GtC	6.	0.100	0.074	0.042	0.019	0.010	0.007	0.003	0.000	0.000
5000GtC	1.5	0.534	0.415	0.304	0.169	0.091	0.078	0.061	0.028	0.005
5000GtC	2.64	0.538	0.390	0.253	0.122	0.066	0.052	0.033	0.007	0.000
5000GtC	3	0.541	0.387	0.246	0.117	0.064	0.049	0.030	0.004	0.000
5000GtC	4.5	0.550	0.378	0.228	0.108	0.060	0.042	0.020	0.001	0.000
5000GtC	6.	0.540	0.355	0.206	0.099	0.056	0.035	0.016	0.001	0.000

Table 38: **Percentages** of remaining excess **Surface ocean acidification** reached at specific calendar years

variables		year								
emis.	short-circ.	3000	5000	10000	20000	50000	100k	200k	500k	1000k
1000GtC	yes	36.0	24.8	13.0	6.0	3.1	2.0	0.6	-0.9	-1.2
1000GtC	no	35.8	24.4	12.5	5.6	2.9	1.8	0.5	-0.9	-1.2
5000GtC	yes	66.5	45.0	25.1	11.3	6.4	4.6	2.4	-0.2	-0.8
5000GtC	no	66.0	43.8	23.4	10.6	6.1	4.3	2.1	-0.4	-0.8

variables			year								
emis.	T_Ca	T_Si	3000	5000	10000	20000	50000	100k	200k	500k	1000k
1000GtC	on	on	38.6	29.3	19.0	11.7	8.0	6.8	4.9	1.5	-1.2
1000GtC	on	off	39.4	30.7	21.3	14.5	11.2	11.0	10.9	10.6	10.2
1000GtC	off	on	38.9	29.7	19.6	12.4	8.7	7.5	5.7	2.5	0.4
1000GtC	off	off	39.6	31.0	21.7	15.0	11.7	11.5	11.4	11.3	11.0
5000GtC	on	on	70.4	53.2	38.6	21.4	11.4	9.7	7.4	3.1	0.3
5000GtC	on	off	71.6	56.1	45.0	29.7	16.5	15.7	15.6	15.6	15.4
5000GtC	off	on	70.6	53.7	39.8	22.7	11.9	10.0	7.6	3.1	0.3
5000GtC	off	off	71.9	56.7	46.3	31.7	17.3	16.4	16.3	16.3	16.2

variables		year								
emis.	E_a (kJ/mol)	3000	5000	10000	20000	50000	100k	200k	500k	1000k
1000GtC	45	37.4	27.2	16.3	9.1	5.8	4.9	3.6	1.1	-0.6
1000GtC	63	37.2	26.7	15.6	8.3	5.1	4.1	2.6	0.2	-1.0
1000GtC	74	37.0	26.5	15.2	8.0	4.8	3.7	2.1	-0.2	-1.1
1000GtC	103	36.6	25.7	14.2	7.0	3.9	2.7	1.1	-0.7	-1.1
5000GtC	45	69.6	51.5	35.5	19.3	11.4	9.9	7.7	3.4	0.5
5000GtC	63	69.0	50.1	33.0	17.1	10.0	8.2	5.8	1.7	-0.4
5000GtC	74	68.7	49.4	31.8	16.1	9.3	7.4	4.9	1.1	-0.6
5000GtC	103	67.4	46.9	28.0	13.3	7.5	5.6	3.1	0.0	-0.8

variables				year								
emis.	R_Ca	R_Si	R_explicit	3000	5000	10000	20000	50000	100k	200k	500k	1000k
1000GtC	on	on	on	39.4	30.6	21.1	14.3	10.9	10.4	9.9	8.5	6.4
1000GtC	on	on	off	39.2	30.3	20.6	13.7	10.3	9.7	8.9	6.9	4.2
1000GtC	on	off	on	39.5	30.9	21.5	14.7	11.4	11.1	11.0	10.7	10.1
1000GtC	on	off	off	39.5	30.8	21.4	14.5	11.2	11.0	10.9	10.6	10.2
1000GtC	off	on	on	39.5	30.8	21.4	14.5	11.0	10.5	9.9	8.2	5.6
1000GtC	off	on	off	39.4	30.6	21.1	14.1	10.6	9.9	9.0	6.8	3.9
1000GtC	off	off	on	39.6	31.0	21.7	15.0	11.7	11.5	11.4	11.3	11.0
1000GtC	off	off	off	39.6	31.0	21.7	15.0	11.7	11.5	11.4	11.3	11.0
5000GtC	on	on	on	71.6	56.0	44.6	29.1	15.9	14.8	14.1	12.2	9.4
5000GtC	on	on	off	71.4	55.4	43.4	27.2	14.9	13.7	12.6	9.8	5.8
5000GtC	on	off	on	71.8	56.3	45.6	30.6	16.9	16.0	15.9	15.8	15.7
5000GtC	on	off	off	71.7	56.3	45.3	30.1	16.6	15.7	15.7	15.7	15.6
5000GtC	off	on	on	71.8	56.4	45.5	30.4	16.3	15.0	14.3	12.3	9.2
5000GtC	off	on	off	71.7	56.1	44.8	29.3	15.6	14.1	13.0	9.8	5.6
5000GtC	off	off	on	71.9	56.7	46.3	31.7	17.3	16.4	16.3	16.3	16.2
5000GtC	off	off	off	71.9	56.7	46.3	31.7	17.3	16.4	16.3	16.3	16.2

variables		year								
emis.	beta	3000	5000	10000	20000	50000	100k	200k	500k	1000k
1000GtC	0.48	38.1	28.4	17.9	10.8	7.7	7.3	6.9	5.8	4.2
1000GtC	0.65	38.0	28.3	17.8	10.7	7.6	7.2	6.7	5.3	3.5
1000GtC	0.8	38.0	28.2	17.7	10.6	7.5	7.0	6.4	4.8	2.9
1000GtC	1.12	37.9	28.1	17.5	10.4	7.2	6.7	5.9	4.0	1.9
5000GtC	0.48	70.8	54.0	40.6	24.9	15.2	14.4	13.8	12.1	9.6
5000GtC	0.65	70.7	53.9	40.2	24.4	14.9	14.1	13.3	11.2	-
5000GtC	0.8	70.6	53.7	40.0	24.1	14.6	13.8	12.8	10.3	-
5000GtC	1.12	70.5	53.5	39.4	23.5	14.2	13.2	11.9	8.7	5.1

variables		year								
emis.	k_run	3000	5000	10000	20000	50000	100k	200k	500k	1000k
1000GtC	0.012	38.2	28.5	18.1	11.1	7.9	7.6	7.2	6.2	4.7
1000GtC	0.024	38.0	28.3	17.8	10.7	7.5	7.0	6.3	4.6	2.5
1000GtC	0.028	38.0	28.2	17.7	10.6	7.4	6.9	6.3	4.6	2.6
1000GtC	0.045	37.8	27.9	17.2	10.1	6.9	6.2	5.3	3.1	0.8
5000GtC	0.012	70.8	54.3	41.1	25.6	15.6	14.9	14.3	12.9	10.7
5000GtC	0.024	70.6	53.7	40.0	24.2	14.7	13.8	12.8	10.3	7.0
5000GtC	0.028	70.5	53.5	39.6	23.8	14.5	13.6	12.5	9.8	6.3
5000GtC	0.045	70.2	52.9	38.2	22.2	13.5	12.4	10.9	7.3	3.6

variables			year								
emis.	P_Ca	P_Si	3000	5000	10000	20000	50000	100k	200k	500k	1000k
1000GtC	on	on	39.0	30.0	20.1	13.0	9.5	8.6	7.3	4.4	1.6
1000GtC	on	off	39.4	30.7	21.2	14.4	11.2	11.0	10.9	10.7	10.4
1000GtC	off	on	39.2	30.3	20.6	13.5	9.9	9.0	7.7	4.7	1.8
1000GtC	off	off	39.6	31.0	21.7	15.0	11.7	11.5	11.4	11.3	11.0
5000GtC	on	on	71.3	55.3	42.9	26.4	14.0	12.5	10.8	6.9	2.3
5000GtC	on	off	71.7	56.1	45.0	29.7	16.5	15.7	15.7	15.6	15.5
5000GtC	off	on	71.5	55.8	44.0	27.9	14.6	12.9	11.2	7.0	2.3
5000GtC	off	off	71.9	56.7	46.3	31.7	17.3	16.4	16.3	16.3	16.2

variables			year								
emis.	f_Ca	f_Si	3000	5000	10000	20000	50000	100k	200k	500k	1000k
1000GtC	on	on	37.8	27.9	17.1	9.8	6.4	5.0	3.3	0.8	-0.1
1000GtC	on	off	39.1	30.2	20.5	13.6	10.5	10.3	10.3	10.1	9.7
1000GtC	off	on	38.3	28.6	18.0	10.7	7.0	5.4	3.4	0.8	-0.1
1000GtC	off	off	39.6	31.0	21.7	15.0	11.7	11.5	11.4	11.2	11.0
5000GtC	on	on	68.8	49.8	32.3	15.6	8.4	6.6	4.3	0.8	-0.5
5000GtC	on	off	71.2	55.0	42.5	26.3	15.3	14.8	14.8	14.7	14.6
5000GtC	off	on	69.5	51.3	35.1	17.8	9.2	7.1	4.4	0.8	-0.5
5000GtC	off	off	71.9	56.7	46.3	31.7	17.3	16.4	16.3	16.3	16.2

variables		year								
emis.	Scheme	3000	5000	10000	20000	50000	100k	200k	500k	1000k
1000GtC	Globavg	36.0	24.6	12.7	5.6	2.7	1.5	0.2	-1.0	-1.1
1000GtC	GKWM	34.1	22.1	10.0	3.7	1.4	0.4	-0.7	-1.4	-1.5
1000GtC	GEM-CO2	33.5	21.4	9.2	3.2	1.1	0.1	-0.8	-1.4	-1.6
5000GtC	Globavg	66.2	44.4	24.1	10.4	5.5	3.6	1.5	-0.6	-0.9
5000GtC	GKWM	62.7	37.4	17.0	7.4	4.0	2.3	0.4	-0.8	-1.0
5000GtC	GEM-CO2	61.2	35.1	15.3	6.5	3.5	1.9	0.2	-0.8	-0.9

variables				year								
emis.	f_Ca	f_Si	Scheme	3000	5000	10000	20000	50000	100k	200k	500k	1000k
1000GtC	on	on	Globavg	36.0	24.8	13.0	6.0	3.1	2.0	0.6	-0.9	-1.2
1000GtC	on	on	GKWM	34.1	22.1	10.0	3.7	1.4	0.4	-0.7	-1.4	-1.5
1000GtC	on	off	Globavg	37.7	27.8	17.1	10.1	7.3	7.1	7.0	6.8	6.4
1000GtC	on	off	GKWM	38.2	28.3	17.8	10.5	7.2	6.7	6.3	5.2	3.6
1000GtC	off	on	Globavg	36.6	25.7	14.1	6.8	3.6	2.3	0.8	-0.8	-1.1
1000GtC	off	on	GKWM	34.6	22.7	10.6	4.1	1.6	0.5	-0.7	-1.4	-1.4
1000GtC	off	off	Globavg	38.3	28.7	18.5	11.4	8.3	8.1	8.0	7.7	7.3
1000GtC	off	off	GKWM	38.9	29.7	19.9	12.4	8.4	8.1	8.0	7.7	7.2
5000GtC	on	on	Globavg	66.5	45.0	25.1	11.3	6.4	4.6	2.4	-0.2	-0.8
5000GtC	on	on	GKWM	62.7	37.5	17.1	7.4	4.0	2.3	0.4	-0.8	-1.0
5000GtC	on	off	Globavg	70.1	52.6	37.7	22.0	14.3	14.0	14.0	13.9	13.8
5000GtC	on	off	GKWM	70.8	54.5	41.4	24.8	14.0	13.2	12.7	11.0	8.6
5000GtC	off	on	Globavg	67.5	47.0	27.9	13.1	7.0	5.0	2.5	-0.3	-0.9
5000GtC	off	on	GKWM	63.5	38.9	18.3	8.0	4.2	2.2	0.3	-0.8	-0.9
5000GtC	off	off	Globavg	71.0	54.7	42.1	26.8	16.3	15.9	15.8	15.7	15.6
5000GtC	off	off	GKWM	72.0	57.8	48.4	34.6	17.5	16.0	16.0	16.0	15.9

variables		year								
emis.	routing	3000	5000	10000	20000	50000	100k	200k	500k	1000k
1000GtC	1	39.6	31.1	21.8	15.0	11.7	11.4	11.3	11.2	10.8
1000GtC	2	39.6	31.0	21.7	15.0	11.7	11.5	11.4	11.3	11.0
1000GtC	3	41.0	33.4	26.1	21.0	19.9	23.1	29.6	49.8	83.2
5000GtC	1	71.9	56.8	46.5	32.0	17.4	16.4	16.3	16.3	16.2
5000GtC	2	71.9	56.7	46.3	31.7	17.3	16.4	16.3	16.3	16.2
5000GtC	3	72.7	58.9	50.8	38.9	21.4	20.2	22.2	28.8	38.6

variables		year								
emis.	lith.	3000	5000	10000	20000	50000	100k	200k	500k	1000k
1000GtC	GKWM	34.3	22.3	10.1	3.8	1.5	0.4	-0.6	-1.4	-1.5
1000GtC	GEM-CO2	34.1	22.1	10.0	3.7	1.4	0.4	-0.7	-1.4	-
1000GtC	GKWM av.	35.1	23.3	11.1	4.4	1.8	0.6	-0.6	-1.5	-1.8
1000GtC	GEM-CO2 av.	36.7	25.7	14.0	6.4	2.9	1.7	0.2	-1.2	-1.6
1000GtC	mono acid	35.3	23.4	11.1	4.2	1.5	0.4	-0.6	-1.2	-1.2
1000GtC	mono basalt	32.6	20.0	7.5	1.9	0.1	-0.6	-1.2	-1.5	-1.6
1000GtC	mono carb	32.0	22.7	11.3	4.3	2.0	1.3	0.2	-1.5	-2.5
1000GtC	mono granite	35.3	23.4	11.2	4.2	1.5	0.4	-0.6	-1.2	-1.2
1000GtC	mono sand	39.8	32.3	23.3	13.9	6.1	4.4	3.0	0.7	-0.5
1000GtC	mono shale	29.2	17.9	5.7	0.3	-0.7	-1.1	-1.4	-1.7	-2.1
1000GtC	mono shield	35.3	23.4	11.2	4.2	1.5	0.4	-0.6	-1.2	-1.2
5000GtC	GKWM	62.9	37.9	17.4	7.6	4.1	2.4	0.5	-0.8	-0.9
5000GtC	GEM-CO2	62.7	37.5	17.1	7.4	4.0	2.3	0.3	-0.8	-1.0
5000GtC	GKWM av.	64.7	41.1	20.3	8.6	4.6	2.8	0.8	-0.9	-1.0
5000GtC	GEM-CO2 av.	67.7	47.9	29.0	12.7	6.2	4.3	1.9	-0.5	-1.0
5000GtC	mono acid	64.7	41.8	20.8	8.1	3.7	2.0	0.2	-0.9	-1.0
5000GtC	mono basalt	59.1	32.1	12.4	4.4	1.8	0.5	-0.5	-0.9	-1.0
5000GtC	mono carb	58.0	34.1	16.5	7.6	4.3	3.3	1.9	-0.2	-1.1
5000GtC	mono granite	64.7	41.8	20.8	8.1	3.7	2.0	0.2	-0.9	-1.0
5000GtC	mono sand	72.2	60.2	50.6	34.5	11.7	7.8	5.6	1.9	-0.2
5000GtC	mono shale	51.2	25.2	8.0	1.5	0.0	-0.4	-0.8	-1.0	-1.1
5000GtC	mono shield	64.7	41.8	20.8	8.1	3.7	2.0	0.2	-0.9	-1.0

variables		year								
emis.	clim. sens.	3000	5000	10000	20000	50000	100k	200k	500k	1000k
1000GtC	1.5	38.1	28.4	18.3	11.1	7.6	6.4	4.9	2.1	0.4
1000GtC	2.64	37.8	27.9	17.1	9.8	6.4	5.0	3.2	0.7	-0.1
1000GtC	3	38.1	28.1	17.2	9.7	6.2	4.9	3.1	0.7	-0.0
1000GtC	4.5	38.5	28.6	17.1	9.0	5.4	3.9	2.1	0.2	-0.2
1000GtC	6.	38.3	28.3	16.1	7.3	3.9	2.5	1.0	-0.5	-0.6
5000GtC	1.5	68.5	53.2	39.0	21.7	11.7	10.0	7.8	3.5	0.7
5000GtC	2.64	68.8	49.9	32.4	15.6	8.4	6.6	4.2	0.9	-0.4
5000GtC	3	69.4	49.6	31.6	15.0	8.2	6.2	3.8	0.5	-0.6
5000GtC	4.5	70.3	48.4	29.2	13.8	7.7	5.3	2.5	0.1	-0.4
5000GtC	6.	69.0	45.3	26.3	12.6	7.2	4.5	2.0	0.1	-0.2

Table 39: **Years** that specific values of **Surface ocean acidification** are reached

variables		**Surface ocean acidification (pH units below 8.15 baseline)**									
emis.	short-circ.	peak	at year	0.7	0.6	0.5	0.4	0.3	0.2	0.1	0.
1000GtC	yes	0.25	2010	-	-	-	-	-	2090	2750	280010
1000GtC	no	0.25	2010	-	-	-	-	-	2090	2750	260010
5000GtC	yes	0.78	2010	2180	2600	3200	4200	6400	10010	18010	450010
5000GtC	no	0.78	2010	2180	2550	3200	4100	6010	9500	17000	420010

variables			**Surface ocean acidification (pH units below 8.15 baseline)**									
emis.	T_Ca	T_Si	peak	at year	0.7	0.6	0.5	0.4	0.3	0.2	0.1	0.
1000GtC	on	on	0.26	2010	-	-	-	-	-	2100	3000	800000
1000GtC	on	off	0.26	2010	-	-	-	-	-	2100	3100	-
1000GtC	off	on	0.26	2010	-	-	-	-	-	2100	3100	-
1000GtC	off	off	0.26	2010	-	-	-	-	-	2100	3100	-
5000GtC	on	on	0.78	2010	2220	2700	3500	5600	11000	17000	38000	-
5000GtC	on	off	0.78	2010	2220	2750	3700	7000	14000	24000	-	-
5000GtC	off	on	0.78	2010	2220	2700	3500	5800	11000	18000	42000	-
5000GtC	off	off	0.78	2010	2220	2750	3700	7500	16000	28000	-	-

variables		**Surface ocean acidification (pH units below 8.15 baseline)**									
emis.	E_a (kJ/mol)	peak	at year	0.7	0.6	0.5	0.4	0.3	0.2	0.1	0.
1000GtC	45	0.25	2010	-	-	-	-	-	2090	2850	760010
1000GtC	63	0.25	2010	-	-	-	-	-	2090	2850	540010
1000GtC	74	0.25	2010	-	-	-	-	-	2090	2800	470010
1000GtC	103	0.25	2010	-	-	-	-	-	2090	2800	330010
5000GtC	45	0.78	2010	2200	2650	3400	5200	9000	15000	36010	-
5000GtC	63	0.78	2010	2200	2650	3400	4900	8500	14010	30010	840010
5000GtC	74	0.78	2010	2200	2650	3300	4700	8010	13000	26010	720010
5000GtC	103	0.78	2010	2200	2600	3200	4400	7000	11000	22010	520010

variables				Surface ocean acidification (pH units below 8.15 baseline)									
emis.	R_Ca	R_Si	R_explicit	peak	at year	0.7	0.6	0.5	0.4	0.3	0.2	0.1	0.
1000GtC	on	on	on	0.26	2010	-	-	-	-	-	2100	3100	-
1000GtC	on	on	off	0.26	2010	-	-	-	-	-	2100	3100	-
1000GtC	on	off	on	0.26	2010	-	-	-	-	-	2100	3100	-
1000GtC	on	off	off	0.26	2010	-	-	-	-	-	2100	3100	-
1000GtC	off	on	on	0.26	2010	-	-	-	-	-	2100	3100	-
1000GtC	off	on	off	0.26	2010	-	-	-	-	-	2100	3100	-
1000GtC	off	off	on	0.26	2010	-	-	-	-	-	2100	3100	-
1000GtC	off	off	off	0.26	2010	-	-	-	-	-	2100	3100	-
5000GtC	on	on	on	0.78	2010	2220	2750	3600	7000	14000	24000	400000	-
5000GtC	on	on	off	0.78	2010	2220	2700	3600	6600	13000	22000	190000	-
5000GtC	on	off	on	0.78	2010	2220	2750	3700	7500	15000	26000	-	-
5000GtC	on	off	off	0.78	2010	2220	2750	3700	7500	15000	26000	-	-
5000GtC	off	on	on	0.78	2010	2220	2750	3700	7500	15000	26000	440000	-
5000GtC	off	on	off	0.78	2010	2220	2750	3700	7000	14000	24000	220000	-
5000GtC	off	off	on	0.78	2010	2220	2750	3700	7500	16000	28000	-	-
5000GtC	off	off	off	0.78	2010	2220	2750	3700	7500	16000	28000	-	-

variables		Surface ocean acidification (pH units below 8.15 baseline)									
emis.	beta	peak	at year	0.7	0.6	0.5	0.4	0.3	0.2	0.1	0.
1000GtC	0.48	0.25	2010	-	-	-	-	-	2090	2900	-
1000GtC	0.65	0.25	2010	-	-	-	-	-	2090	2900	-
1000GtC	0.8	0.25	2010	-	-	-	-	-	2090	2900	-
1000GtC	1.12	0.25	2010	-	-	-	-	-	2090	2900	-
5000GtC	0.48	0.78	2010	2220	2700	3600	6010	12010	20010	380010	-
5000GtC	0.65	0.78	2010	2200	2700	3500	5800	11000	19000	270010	-
5000GtC	0.8	0.78	2010	2200	2700	3500	5800	11000	19000	210010	-
5000GtC	1.12	0.78	2010	2200	2700	3500	5800	11000	19000	130010	-

variables		Surface ocean acidification (pH units below 8.15 baseline)									
emis.	k_run	peak	at year	0.7	0.6	0.5	0.4	0.3	0.2	0.1	0.
1000GtC	0.012	0.25	2010	-	-	-	-	-	2090	2900	-
1000GtC	0.024	0.25	2010	-	-	-	-	-	2090	2900	-
1000GtC	0.028	0.25	2010	-	-	-	-	-	2090	2900	-
1000GtC	0.045	0.25	2010	-	-	-	-	-	2090	2900	-
5000GtC	0.012	0.78	2010	2220	2700	3600	6010	12010	22010	520010	-
5000GtC	0.024	0.78	2010	2200	2700	3500	5800	11000	19000	210010	-
5000GtC	0.028	0.78	2010	2200	2700	3500	5800	11000	19000	180010	-
5000GtC	0.045	0.78	2010	2200	2700	3500	5600	10010	18010	80010	-

variables			Surface ocean acidification (pH units below 8.15 baseline)									
emis.	P_Ca	P_Si	peak	at year	0.7	0.6	0.5	0.4	0.3	0.2	0.1	0.
1000GtC	on	on	0.26	2010	-	-	-	-	-	2100	3100	-
1000GtC	on	off	0.26	2010	-	-	-	-	-	2100	3100	-
1000GtC	off	on	0.26	2010	-	-	-	-	-	2100	3100	-
1000GtC	off	off	0.26	2010	-	-	-	-	-	2100	3100	-
5000GtC	on	on	0.78	2010	2220	2700	3600	6400	13000	22000	85000	-
5000GtC	on	off	0.78	2010	2220	2750	3700	7000	14000	24000	-	-
5000GtC	off	on	0.78	2010	2220	2750	3600	6800	14000	24000	110000	-
5000GtC	off	off	0.78	2010	2220	2750	3700	7500	16000	28000	-	-

variables			Surface ocean acidification (pH units below 8.15 baseline)									
emis.	f_Ca	f_Si	peak	at year	0.7	0.6	0.5	0.4	0.3	0.2	0.1	0.
1000GtC	on	on	0.26	2010	-	-	-	-	-	2100	2950	950000
1000GtC	on	off	0.26	2010	-	-	-	-	-	2100	3100	-
1000GtC	off	on	0.26	2010	-	-	-	-	-	2100	2950	850000
1000GtC	off	off	0.26	2010	-	-	-	-	-	2100	3100	-
5000GtC	on	on	0.78	2010	2200	2650	3300	4800	8000	13000	26000	750000
5000GtC	on	off	0.78	2010	2220	2700	3600	6400	13000	22000	-	-
5000GtC	off	on	0.78	2010	2200	2650	3400	5200	9000	15000	28000	700000
5000GtC	off	off	0.78	2010	2220	2750	3700	7500	16000	28000	-	-

variables		Surface ocean acidification (pH units below 8.15 baseline)									
emis.	Scheme	peak	at year	0.7	0.6	0.5	0.4	0.3	0.2	0.1	0.
1000GtC	Globavg	0.25	2010	-	-	-	-	-	2090	2750	230010
1000GtC	GKWM	0.25	2010	-	-	-	-	-	2080	2600	130010
1000GtC	GEM-CO2	0.25	2010	-	-	-	-	-	2080	2600	110010
5000GtC	Globavg	0.78	2010	2180	2550	3200	4100	6200	9500	17000	350010
5000GtC	GKWM	0.78	2010	2160	2500	2950	3700	4900	7500	13000	250010
5000GtC	GEM-CO2	0.78	2010	2160	2450	2900	3500	4600	6800	12010	220010

variables				Surface ocean acidification (pH units below 8.15 baseline)									
emis.	f_Ca	f_Si	Scheme	peak	at year	0.7	0.6	0.5	0.4	0.3	0.2	0.1	0.
1000GtC	on	on	Globavg	0.25	2010	-	-	-	-	-	2090	2750	280010
1000GtC	on	on	GKWM	0.25	2010	-	-	-	-	-	2080	2600	130010
1000GtC	on	off	Globavg	0.25	2010	-	-	-	-	-	2090	2850	-
1000GtC	on	off	GKWM	0.26	2010	-	-	-	-	-	2090	2950	-
1000GtC	off	on	Globavg	0.25	2010	-	-	-	-	-	2090	2800	290010
1000GtC	off	on	GKWM	0.25	2010	-	-	-	-	-	2080	2650	140010
1000GtC	off	off	Globavg	0.25	2010	-	-	-	-	-	2090	2900	-
1000GtC	off	off	GKWM	0.26	2010	-	-	-	-	-	2100	3000	-
5000GtC	on	on	Globavg	0.78	2010	2180	2600	3200	4200	6400	10010	18010	450010
5000GtC	on	on	GKWM	0.78	2010	2160	2500	2950	3700	4900	7500	13000	240010
5000GtC	on	off	Globavg	0.78	2010	2200	2700	3500	5400	10010	17000	-	-
5000GtC	on	off	GKWM	0.78	2010	2220	2700	3600	6200	12010	20010	190010	-
5000GtC	off	on	Globavg	0.78	2010	2200	2600	3300	4400	7000	11000	22010	430010
5000GtC	off	on	GKWM	0.78	2010	2160	2500	3000	3800	5200	8010	14010	230010
5000GtC	off	off	Globavg	0.78	2010	2220	2700	3600	6200	12010	22010	-	-
5000GtC	off	off	GKWM	0.78	2010	2220	2750	3800	8500	18010	30010	-	-

variables		Surface ocean acidification (pH units below 8.15 baseline)									
emis.	routing	peak	at year	0.7	0.6	0.5	0.4	0.3	0.2	0.1	0.
1000GtC	1	0.26	2010	-	-	-	-	-	2100	3200	-
1000GtC	2	0.26	2010	-	-	-	-	-	2100	3100	-
1000GtC	3	0.26	2010	-	-	-	-	-	2120	3400	-
5000GtC	1	0.78	2010	2220	2750	3700	7500	16000	28000	-	-
5000GtC	2	0.78	2010	2220	2750	3700	7500	16000	28000	-	-
5000GtC	3	0.78	2010	2220	2800	3900	10000	22000	38000	-	-

variables		Surface ocean acidification (pH units below 8.15 baseline)									
emis.	lith.	peak	at year	0.7	0.6	0.5	0.4	0.3	0.2	0.1	0.
1000GtC	GKWM	0.25	2010	-	-	-	-	-	2080	2650	140010
1000GtC	GEM-CO2	0.25	2010	-	-	-	-	-	2080	2600	130010
1000GtC	GKWM av.	0.25	2010	-	-	-	-	-	2080	2700	150010
1000GtC	GEM-CO2 av.	0.26	2010	-	-	-	-	-	2090	2800	230010
1000GtC	mono acid	0.25	2010	-	-	-	-	-	2090	2700	140010
1000GtC	mono basalt	0.25	2010	-	-	-	-	-	2070	2550	60010
1000GtC	mono carb	0.24	2010	-	-	-	-	-	2060	2450	220010
1000GtC	mono granite	0.25	2010	-	-	-	-	-	2090	2700	140010
1000GtC	mono sand	0.26	2010	-	-	-	-	-	2120	3300	700010
1000GtC	mono shale	0.24	2010	-	-	-	-	-	2060	2400	24010
1000GtC	mono shield	0.25	2010	-	-	-	-	-	2090	2700	140010
5000GtC	GKWM	0.78	2010	2160	2500	2950	3700	5000	7500	13000	250010
5000GtC	GEM-CO2	0.78	2010	2160	2500	2950	3700	4900	7500	13000	240010
5000GtC	GKWM av.	0.78	2010	2180	2550	3100	3900	5600	8500	15000	280010
5000GtC	GEM-CO2 av.	0.78	2010	2200	2600	3300	4500	7500	12010	20010	390010
5000GtC	mono acid	0.78	2010	2180	2550	3100	3900	5600	8500	15000	230010
5000GtC	mono basalt	0.78	2010	2140	2450	2800	3400	4300	6010	10010	140010
5000GtC	mono carb	0.76	2010	2120	2350	2750	3300	4400	6600	13000	460010
5000GtC	mono granite	0.78	2010	2180	2550	3100	3900	5600	8500	15000	230010
5000GtC	mono sand	0.79	2010	2240	2800	4100	10010	18010	28010	48010	940010
5000GtC	mono shale	0.77	2010	2100	2300	2600	3000	3700	4900	8010	55000
5000GtC	mono shield	0.78	2010	2180	2550	3100	3900	5600	8500	15000	230010

variables		Surface ocean acidification (pH units below 8.15 baseline)									
emis.	clim. sens.	peak	at year	0.7	0.6	0.5	0.4	0.3	0.2	0.1	0.
1000GtC	1.5	0.26	2010	-	-	-	-	-	2100	2950	-
1000GtC	2.64	0.26	2010	-	-	-	-	-	2100	2950	900000
1000GtC	3	0.26	2010	-	-	-	-	-	2100	2950	1000000
1000GtC	4.5	0.26	2010	-	-	-	-	-	2120	3000	650000
1000GtC	6.	0.26	2010	-	-	-	-	-	2120	3000	340000
5000GtC	1.5	0.78	2010	2200	2600	3400	5600	11000	17000	40000	-
5000GtC	2.64	0.78	2010	2200	2650	3300	4800	8000	13000	26000	750000
5000GtC	3	0.78	2010	2200	2650	3400	4700	8000	13000	24000	650000
5000GtC	4.5	0.78	2010	2220	2700	3400	4600	7500	12000	22000	550000
5000GtC	6.	0.78	2010	2220	2700	3300	4200	6600	11000	20000	600000

Table 40: **Years** that specific fractions of remaining excess **Surface ocean acidification** are reached

variables		fraction									
emis.	short-circ.	90%	75%	50%	25%	10%	e^{-1}	e^{-2}	e^{-3}	e^{-4}	e^{-5}
1000GtC	yes	2040	2120	2400	5000	13000	2950	10010	26010	110010	200010
1000GtC	no	2040	2120	2350	4900	13000	2950	9500	24010	100010	190010
5000GtC	yes	2180	2650	4300	11000	24010	6800	18010	90010	240010	340010
5000GtC	no	2180	2650	4200	9500	22010	6400	16010	80010	220010	320010

variables			fraction									
emis.	T_Ca	T_Si	90%	75%	50%	25%	10%	e^{-1}	e^{-2}	e^{-3}	e^{-4}	e^{-5}
1000GtC	on	on	2050	2120	2400	6600	28000	3300	17000	200000	460000	650000
1000GtC	on	off	2050	2120	2450	8000	-	3400	24000	-	-	-
1000GtC	off	on	2050	2120	2450	7000	32000	3300	18000	260000	650000	950000
1000GtC	off	off	2050	2120	2450	8000	-	3400	26000	-	-	-
5000GtC	on	on	2200	2800	6000	18000	90000	11000	34000	340000	700000	950000
5000GtC	on	off	2200	2850	7500	26000	-	15000	-	-	-	-
5000GtC	off	on	2200	2800	6200	19000	110000	12000	38000	360000	700000	950000
5000GtC	off	off	2200	2850	8000	28000	-	17000	-	-	-	-

variables		fraction									
emis.	E_a (kJ/mol)	90%	75%	50%	25%	10%	e^{-1}	e^{-2}	e^{-3}	e^{-4}	e^{-5}
1000GtC	45	2040	2120	2400	5800	18010	3100	13000	100010	390010	600010
1000GtC	63	2040	2120	2400	5600	17000	3100	12010	55000	270010	410010
1000GtC	74	2040	2120	2400	5600	16010	3100	12010	46010	230010	350010
1000GtC	103	2040	2120	2400	5400	15000	3000	11000	32010	150010	240010
5000GtC	45	2200	2750	5400	16010	95000	9500	32010	370010	720010	960010
5000GtC	63	2180	2700	5200	14010	55000	9000	28010	240010	490010	660010
5000GtC	74	2180	2700	4900	14010	42010	8500	26010	200010	420010	580010
5000GtC	103	2180	2650	4500	12010	28010	7500	20010	130010	290010	400010

variables				fraction									
emis.	R_Ca	R_Si	R_explicit	90%	75%	50%	25%	10%	e^{-1}	e^{-2}	e^{-3}	e^{-4}	e^{-5}
1000GtC	on	on	on	2050	2120	2450	7500	190000	3400	24000	-	-	-
1000GtC	on	on	off	2050	2120	2450	7500	70000	3400	22000	900000	-	-
1000GtC	on	off	on	2050	2120	2450	8000	-	3400	26000	-	-	-
1000GtC	on	off	off	2050	2120	2450	8000	-	3400	24000	-	-	-
1000GtC	off	on	on	2050	2120	2450	8000	180000	3400	24000	-	-	-
1000GtC	off	on	off	2050	2120	2450	7500	95000	3400	22000	850000	-	-
1000GtC	off	off	on	2050	2120	2450	8000	-	3400	26000	-	-	-
1000GtC	off	off	off	2050	2120	2450	8000	-	3400	26000	-	-	-
5000GtC	on	on	on	2200	2850	7500	24000	950000	15000	300000	-	-	-
5000GtC	on	on	off	2200	2800	7000	24000	480000	14000	120000	-	-	-
5000GtC	on	off	on	2200	2850	8000	26000	-	16000	-	-	-	-
5000GtC	on	off	off	2200	2850	8000	26000	-	16000	-	-	-	-
5000GtC	off	on	on	2200	2850	8000	26000	900000	16000	320000	-	-	-
5000GtC	off	on	off	2200	2850	7500	24000	500000	15000	150000	-	-	-
5000GtC	off	off	on	2200	2850	8000	28000	-	17000	-	-	-	-
5000GtC	off	off	off	2200	2850	8000	28000	-	17000	-	-	-	-

variables		fraction									
emis.	beta	90%	75%	50%	25%	10%	e^{-1}	e^{-2}	e^{-3}	e^{-4}	e^{-5}
1000GtC	0.48	2040	2120	2400	6200	24010	3200	15000	760010	-	-
1000GtC	0.65	2040	2120	2400	6200	24010	3200	15000	580010	-	-
1000GtC	0.8	2040	2120	2400	6200	22010	3200	15000	480010	-	-
1000GtC	1.12	2040	2120	2400	6200	22010	3200	14010	340010	-	-
5000GtC	0.48	2200	2800	6400	20010	940010	12010	250010	-	-	-
5000GtC	0.65	2200	2800	6200	20010	-	12010	170010	-	-	-
5000GtC	0.8	2200	2800	6200	20010	560010	12010	130010	-	-	-
5000GtC	1.12	2200	2800	6010	19000	370010	12010	75000	-	-	-

variables		fraction									
emis.	k_run	90%	75%	50%	25%	10%	e^{-1}	e^{-2}	e^{-3}	e^{-4}	e^{-5}
1000GtC	0.012	2040	2120	2400	6400	24010	3200	15000	900010	-	-
1000GtC	0.024	2040	2120	2400	6200	24010	3200	15000	440010	-	-
1000GtC	0.028	2040	2120	2400	6200	24010	3200	15000	430010	-	-
1000GtC	0.045	2040	2120	2400	6010	22010	3200	14010	240010	740010	-
5000GtC	0.012	2200	2800	6400	22010	-	13000	360010	-	-	-
5000GtC	0.024	2200	2800	6200	20010	560010	12010	130010	-	-	-
5000GtC	0.028	2200	2800	6200	19000	480010	12010	110010	-	-	-
5000GtC	0.045	2200	2750	5800	18010	270010	11000	50010	780010	-	-

variables			fraction									
emis.	P_Ca	P_Si	90%	75%	50%	25%	10%	e^{-1}	e^{-2}	e^{-3}	e^{-4}	e^{-5}
1000GtC	on	on	2050	2120	2450	7500	40000	3300	19000	440000	1000000	-
1000GtC	on	off	2050	2120	2450	7500	-	3400	24000	-	-	-
1000GtC	off	on	2050	2120	2450	7500	48000	3400	22000	480000	1000000	-
1000GtC	off	off	2050	2120	2450	8000	-	3400	26000	-	-	-
5000GtC	on	on	2200	2800	7000	22000	260000	14000	60000	700000	-	-
5000GtC	on	off	2200	2850	7500	26000	-	15000	-	-	-	-
5000GtC	off	on	2200	2800	7500	24000	280000	14000	75000	650000	-	-
5000GtC	off	off	2200	2850	8000	28000	-	17000	-	-	-	-

variables			fraction									
emis.	f_Ca	f_Si	90%	75%	50%	25%	10%	e^{-1}	e^{-2}	e^{-3}	e^{-4}	e^{-5}
1000GtC	on	on	2050	2120	2400	6000	20000	3200	14000	110000	340000	550000
1000GtC	on	off	2050	2120	2450	7500	650000	3400	22000	-	-	-
1000GtC	off	on	2050	2120	2400	6400	24000	3200	15000	120000	340000	550000
1000GtC	off	off	2050	2120	2450	8000	-	3400	26000	-	-	-
5000GtC	on	on	2200	2700	5000	14000	34000	8500	24000	170000	380000	550000
5000GtC	on	off	2200	2800	6800	22000	-	13000	-	-	-	-
5000GtC	off	on	2200	2750	5400	15000	42000	9500	28000	180000	380000	550000
5000GtC	off	off	2200	2850	8000	28000	-	17000	-	-	-	-

variables		fraction									
emis.	Scheme	90%	75%	50%	25%	10%	e^{-1}	e^{-2}	e^{-3}	e^{-4}	e^{-5}
1000GtC	Globavg	2040	2120	2400	4900	13000	2950	9500	24010	85000	160010
1000GtC	GKWM	2040	2100	2350	4400	10010	2800	8010	17000	40010	85000
1000GtC	GEM-CO2	2040	2100	2350	4300	9500	2750	8010	15000	32010	70010
5000GtC	Globavg	2180	2650	4300	10010	22010	6600	17000	65000	180010	270010
5000GtC	GKWM	2160	2550	3800	7500	16010	5200	12010	34010	120010	180010
5000GtC	GEM-CO2	2160	2550	3600	7000	14010	4800	11000	28010	110010	170010

variables				fraction									
emis.	f_Ca	f_Si	Scheme	90%	75%	50%	25%	10%	e^{-1}	e^{-2}	e^{-3}	e^{-4}	e^{-5}
1000GtC	on	on	Globavg	2040	2120	2400	5000	13000	2950	10010	26010	110010	200010
1000GtC	on	on	GKWM	2040	2100	2350	4400	10010	2800	8010	17000	40010	85000
1000GtC	on	off	Globavg	2040	2120	2400	6010	22010	3200	14010	-	-	-
1000GtC	on	off	GKWM	2050	2120	2400	6200	22010	3200	15000	580010	-	-
1000GtC	off	on	Globavg	2040	2120	2400	5200	14010	3000	11000	30010	130010	220010
1000GtC	off	on	GKWM	2040	2100	2350	4500	11000	2850	8500	18010	44010	90010
1000GtC	off	off	Globavg	2040	2120	2400	6400	26010	3200	16010	-	-	-
1000GtC	off	off	GKWM	2050	2120	2400	7000	30010	3300	18010	-	-	-
5000GtC	on	on	Globavg	2180	2650	4300	11000	24010	6800	18010	90010	240010	340010
5000GtC	on	on	GKWM	2160	2550	3800	7500	16010	5200	12010	34010	120010	180010
5000GtC	on	off	Globavg	2200	2750	5800	18010	-	11000	-	-	-	-
5000GtC	on	off	GKWM	2200	2800	6600	20010	720010	13000	70010	-	-	-
5000GtC	off	on	Globavg	2180	2700	4600	12010	28010	7500	20010	110010	240010	340010
5000GtC	off	on	GKWM	2160	2550	3900	8010	17000	5400	13000	38010	120010	180010
5000GtC	off	off	Globavg	2200	2800	6600	22010	-	13000	-	-	-	-
5000GtC	off	off	GKWM	2200	2850	9500	30010	-	19000	-	-	-	-

variables		fraction									
emis.	routing	90%	75%	50%	25%	10%	e^{-1}	e^{-2}	e^{-3}	e^{-4}	e^{-5}
1000GtC	1	2050	2120	2450	8000	-	3500	26000	-	-	-
1000GtC	2	2050	2120	2450	8000	-	3400	26000	-	-	-
1000GtC	3	2050	2120	2450	12000	-	3800	-	-	-	-
5000GtC	1	2200	2850	8500	28000	-	17000	-	-	-	-
5000GtC	2	2200	2850	8000	28000	-	17000	-	-	-	-
5000GtC	3	2220	2900	11000	38000	-	24000	-	-	-	-

variables		fraction									
emis.	lith.	90%	75%	50%	25%	10%	e^{-1}	e^{-2}	e^{-3}	e^{-4}	e^{-5}
1000GtC	GKWM	2040	2100	2350	4400	11000	2800	8010	17000	40010	90010
1000GtC	GEM-CO2	2040	2100	2350	4400	10010	2800	8010	17000	40010	85000
1000GtC	GKWM av.	2040	2100	2350	4700	11000	2900	9000	19000	48010	100010
1000GtC	GEM-CO2 av.	2040	2120	2400	5200	14010	3000	11000	26010	95000	170010
1000GtC	mono acid	2040	2120	2350	4700	11000	2900	9000	18010	42010	90010
1000GtC	mono basalt	2040	2100	2350	4010	8500	2700	7000	13000	22010	34010
1000GtC	mono carb	2040	2090	2280	4400	12010	2600	9000	19000	60010	150010
1000GtC	mono granite	2040	2120	2350	4700	11000	2900	9000	18010	42010	90010
1000GtC	mono sand	2050	2120	2450	9000	30010	3500	22010	75000	330010	520010
1000GtC	mono shale	2040	2090	2260	3600	8010	2550	6400	11000	15000	19000
1000GtC	mono shield	2040	2120	2350	4700	11000	2900	9000	18010	42010	90010
5000GtC	GKWM	2160	2550	3800	7500	16010	5200	13000	36010	130010	190010
5000GtC	GEM-CO2	2160	2550	3800	7500	16010	5200	12010	34010	120010	180010
5000GtC	GKWM av.	2180	2600	4010	8500	18010	5800	14010	44010	140010	210010
5000GtC	GEM-CO2 av.	2180	2700	4700	12010	26010	8010	20010	80010	210010	300010
5000GtC	mono acid	2180	2600	4010	9000	18010	6010	14010	34010	110010	170010
5000GtC	mono basalt	2160	2500	3500	6200	12010	4500	9500	19000	55000	95000
5000GtC	mono carb	2140	2450	3500	7000	16010	4700	12010	34010	220010	340010
5000GtC	mono granite	2180	2600	4010	9000	18010	6010	14010	34010	110010	170010
5000GtC	mono sand	2220	2850	11000	28010	60010	19000	46010	240010	520010	740010
5000GtC	mono shale	2120	2400	3100	5200	9000	3800	8010	13000	19000	26010
5000GtC	mono shield	2180	2600	4010	9000	18010	6010	14010	34010	110010	170010

variables		fraction									
emis.	clim. sens.	90%	75%	50%	25%	10%	e^{-1}	e^{-2}	e^{-3}	e^{-4}	e^{-5}
1000GtC	1.5	2040	2120	2400	6400	24000	3200	16000	200000	550000	900000
1000GtC	2.64	2050	2120	2400	6000	20000	3200	14000	110000	320000	550000
1000GtC	3	2050	2120	2400	6200	20000	3200	14000	100000	320000	550000
1000GtC	4.5	2050	2120	2450	6400	18000	3300	13000	65000	220000	380000
1000GtC	6.	2050	2120	2450	6200	16000	3200	12000	32000	150000	240000
5000GtC	1.5	2180	2700	6000	18000	110000	11000	36000	380000	750000	-
5000GtC	2.64	2200	2700	5000	14000	34000	8500	24000	170000	380000	550000
5000GtC	3	2200	2750	5000	13000	32000	8500	24000	150000	340000	480000
5000GtC	4.5	2220	2800	4800	12000	30000	8000	22000	110000	240000	380000
5000GtC	6.	2200	2750	4400	11000	28000	7000	19000	90000	220000	360000

Table 41: **Timescale fitting** for excess **Surface ocean acidification** decay

variables		fit to $pH(t) = b + h\sum_i w_i e^{-(t-t_0)/\tau_i}$						
emis.	short-circ.	acidification (pH)	i	1	2	3	4	R^2
1000GtC	yes	b 0.007±0.003	w_i (%)	100±4				0.95
		h 0.180±0.001	τ_i (yr)	1900±200				
1000GtC	no	b 0.006±0.003	w_i (%)	100±3				0.95
		h 0.179±0.004	τ_i (yr)	1900±200				
5000GtC	yes	b -0.0070±0.0005	w_i (%)	3.5±0.3	32.0±0.3	55.4±0.3	9.1±0.1	0.999990
		h 0.7916±0.0006	τ_i (yr)	70±10	810±20	6750±70	190000±6000	
5000GtC	no	b -0.007±0.001	w_i (%)	32.8±0.7	57.9±0.6	9.3±0.2		0.99995
		h 0.777±0.001	τ_i (yr)	710±20	6100±100	170000±10000		

variables			fit to $pH(t) = b + h\sum_i w_i e^{-(t-t_0)/\tau_i}$								
emis.	T_Ca	T_Si	acidification (pH)	i	1	2	3	4	5	6	R^2
1000GtC	on	on	b -0.0042±0.0006	w_i (%)	14±2	41±1	8.4±0.7	26.2±0.9	10.7±0.2		0.999991
			h 0.2629±0.0001	τ_i (yr)	68±7	240±10	1800±300	8100±200	390000±20000		
1000GtC	on	off	b 0.0272±0.0002	w_i (%)	9±3	42±5	14±6	11±4	22±5	0.8±0.1	0.999994
			h 0.2319±0.0002	τ_i (yr)	50±10	190±30	500±200	4000±1000	10000±1000	200000±100000	
1000GtC	off	on	b 0.024±0.005	w_i (%)	100±2						0.95
			h 0.168±0.007	τ_i (yr)	1800±300						
1000GtC	off	off	b 0.02922±0.00009	w_i (%)	9±3	44±3	13±5	20±4	13±4		0.999992
			h 0.2298±0.0002	τ_i (yr)	50±10	190±20	600±100	5300±800	13000±2000		
5000GtC	on	on	b 0.048±0.005	w_i (%)	40±2	60±2					0.999
			h 0.723±0.005	τ_i (yr)	900±100	15000±1000					
5000GtC	on	off	b 0.120±0.002	w_i (%)	39.8±0.7	60.2±0.6					0.9999
			h 0.6539±0.001	τ_i (yr)	740±30	14200±400					
5000GtC	off	on	b -0.012±0.009	w_i (%)	33.1±0.5	53.3±0.5	13.7±0.9				0.99992
			h 0.786±0.001	τ_i (yr)	730±30	11700±300	480000±90000				
5000GtC	off	off	b 0.123±0.002	w_i (%)	40.3±0.8	59.7±0.6					0.9999
			h 0.650±0.003	τ_i (yr)	750±40	15500±500					

variables		fit to $pH(t) = b + h\sum_i w_i e^{-(t-t_0)/\tau_i}$						
emis.	E_a (kJ/mol)	acidification (pH)	i	1	2	3	4	R^2
1000GtC	45	b 0.013±0.004	w_i (%)	100±3				0.95
		h 0.173±0.004	τ_i (yr)	2000±300				
1000GtC	63	b 0.010±0.004	w_i (%)	100±3				0.95
		h 0.175±0.004	τ_i (yr)	2000±300				
1000GtC	74	b 0.009±0.004	w_i (%)	100±3				0.95
		h 0.176±0.003	τ_i (yr)	2000±300				
1000GtC	103	b 0.008±0.003	w_i (%)	100±3				0.95
		h 0.178±0.004	τ_i (yr)	2000±300				
5000GtC	45	b -0.009±0.003	w_i (%)	3.4±0.5	31.2±0.4	52.2±0.3	13.2±0.3	0.99998
		h 0.794±0.001	τ_i (yr)	60±20	810±20	9600±100	470000±30000	
5000GtC	63	b -0.008±0.002	w_i (%)	32.7±0.5	54.9±0.3	12.4±0.3		0.99995
		h 0.779±0.003	τ_i (yr)	720±20	8600±200	320000±20000		
5000GtC	74	b 0.039±0.008	w_i (%)	100±1				0.99
		h 0.658±0.009	τ_i (yr)	5400±400				
5000GtC	103	b -0.0074±0.0007	w_i (%)	3.5±0.3	32.1±0.3	54.2±0.3	10.2±0.1	0.99999
		h 0.7922±0.0008	τ_i (yr)	70±10	820±20	7480±80	212000±7000	

variables				fit to $pH(t) = b + h \sum_i w_i e^{-(t-t_0)/\tau_i}$								
emis.	R_Ca	R_Si	R_explicit		acidification (pH)	i	1	2	3	4	5	6	R^2
1000GtC	on	on	on	b	0.006±0.006	w_i (%)	15±2	42±2	9.1±0.7	25±1	9±2		0.999991
				h	0.253±0.006	τ_i (yr)	70±6	250±10	2000±300	8900±300	1400000±500000		
1000GtC	on	on	off	b	0.003±0.003	w_i (%)	15±2	41±2	9.0±0.8	25.1±1	10±1		0.999991
				h	0.256±0.002	τ_i (yr)	70±7	250±10	2000±300	8700±300	1000000±200000		
1000GtC	on	off	on	b	0.024±0.005	w_i (%)	17±6	40±10	10±3	27±9	2±1		0.999991
				h	0.23±0.08	τ_i (yr)	71±6	250±10	2000±300	9100±300	1000000±2000000		
1000GtC	on	off	off	b	0.0272±0.0002	w_i (%)	9±3	42±5	15±6	11±4	22±5	0.8±0.1	0.999994
				h	0.2319±0.0006	τ_i (yr)	50±10	190±30	500±200	4000±1000	10000±1000	200000±100000	
1000GtC	off	on	on	b	0.034±0.004	w_i (%)	100±3						0.96
				h	0.163±0.004	τ_i (yr)	1500±200						
1000GtC	off	on	off	b	-0.002±0.003	w_i (%)	8±2	38±3	13±4	13±3	17±4	12±1	0.999995
				h	0.261±0.001	τ_i (yr)	49±9	190±20	500±100	4300±900	11000±1000	1100000±200000	
1000GtC	off	off	on	b	0.02922±0.00009	w_i (%)	9±3	44±3	13±4	20±4	13±4		0.999992
				h	0.2298±0.0002	τ_i (yr)	50±10	190±20	600±100	5300±800	13000±2000		
1000GtC	off	off	off	b	0.02922±0.00009	w_i (%)	9±3	44±3	13±4	20±4	13±4		0.999992
				h	0.2298±0.0002	τ_i (yr)	50±10	190±20	600±100	5300±800	13000±2000		
5000GtC	on	on	on	b	0.12±0.01	w_i (%)	100±2						0.99
				h	0.566±0.006	τ_i (yr)	6600±700						
5000GtC	on	on	off	b	0.088±0.003	w_i (%)	4±3	38±2	59±1				0.9994
				h	0.697±0.004	τ_i (yr)	100±100	900±100	15800±900				
5000GtC	on	off	on	b	0.14±0.01	w_i (%)	100±1						0.990
				h	0.55±0.01	τ_i (yr)	6200±700						
5000GtC	on	off	off	b	0.119±0.002	w_i (%)	39.9±0.8	60.1±0.6					0.9999
				h	0.655±0.002	τ_i (yr)	740±30	14600±400					
5000GtC	off	on	on	b	0.12±0.01	w_i (%)	100±1						0.99
				h	0.56±0.01	τ_i (yr)	6900±800						
5000GtC	off	on	off	b	0.11±0.01	w_i (%)	100±2						0.99
				h	0.574±0.008	τ_i (yr)	7100±800						
5000GtC	off	off	on	b	0.123±0.002	w_i (%)	40.3±0.8	59.7±0.6					0.9999
				h	0.650±0.003	τ_i (yr)	750±40	15500±500					
5000GtC	off	off	off	b	0.123±0.002	w_i (%)	40.3±0.8	59.7±0.6					0.9999
				h	0.650±0.003	τ_i (yr)	750±40	15500±500					

variables		fit to $pH(t) = b + h\sum_i w_i e^{-(t-t_0)/\tau_i}$						
emis.	beta		acidification (pH)	i	1	2	3	4	R^2
1000GtC	0.48	b	0.022±0.003	w_i (%)	100±2				0.96
		h	0.168±0.006	τ_i (yr)	1700±200				
1000GtC	0.65	b	0.021±0.003	w_i (%)	100±1				0.96
		h	0.168±0.006	τ_i (yr)	1800±200				
1000GtC	0.8	b	0.020±0.003	w_i (%)	100±3				0.96
		h	0.169±0.003	τ_i (yr)	1800±200				
1000GtC	1.12	b	0.018±0.003	w_i (%)	100±2				0.95
		h	0.170±0.005	τ_i (yr)	1900±200				
5000GtC	0.48	b	0.110±0.008	w_i (%)	100±2				0.990
		h	0.585±0.005	τ_i (yr)	5700±500				
5000GtC	0.65	b	0.114±0.009	w_i (%)	100±2				0.991
		h	0.583±0.006	τ_i (yr)	5500±500				
5000GtC	0.8	b	0.110±0.009	w_i (%)	100±2				0.991
		h	0.586±0.007	τ_i (yr)	5500±500				
5000GtC	1.12	b	-0.03±0.03	w_i (%)	3.3±0.5	30.5±0.5	48.7±0.5	18±3	0.99997
		h	0.819±0.007	τ_i (yr)	60±20	820±30	11100±200	1500000±400000	

variables		fit to $pH(t) = b + h\sum_i w_i e^{-(t-t_0)/\tau_i}$						
emis.	k_run		acidification (pH)	i	1	2	3	4	R^2
1000GtC	0.012	b	0.023±0.003	w_i (%)	100±3				0.96
		h	0.167±0.003	τ_i (yr)	1700±200				
1000GtC	0.024	b	0.020±0.003	w_i (%)	100±2				0.96
		h	0.169±0.006	τ_i (yr)	1800±200				
1000GtC	0.028	b	0.020±0.003	w_i (%)	100±3				0.96
		h	0.169±0.003	τ_i (yr)	1800±200				
1000GtC	0.045	b	0.017±0.003	w_i (%)	100±5				0.95
		h	0.1705±0.0008	τ_i (yr)	1900±300				
5000GtC	0.012	b	0.115±0.008	w_i (%)	100±2				0.990
		h	0.579±0.005	τ_i (yr)	5700±500				
5000GtC	0.024	b	-0.1±0.2	w_i (%)	29±3	45±5	30±20		0.99993
		h	0.88±0.09	τ_i (yr)	740±20	11300±200	3000000±4000000		
5000GtC	0.028	b	-0.1±0.1	w_i (%)	3.1±0.6	28±2	45±3	20±10	0.99997
		h	0.88±0.06	τ_i (yr)	60±20	820±30	11200±200	3000000±2000000	
5000GtC	0.045	b	-0.03±0.02	w_i (%)	3.3±0.5	30.6±0.4	49.6±0.3	17±2	0.99997
		h	0.814±0.002	τ_i (yr)	60±20	810±30	10600±200	1100000±200000	

variables			fit to $pH(t) = b + h\sum_i w_i e^{-(t-t_0)/\tau_i}$							
emis.	P_Ca	P_Si	acidification (pH)	i	1	2	3	4	5	R^2
1000GtC	on	on	b -0.002±0.002	w_i (%)	15±2	41±2	8.7±0.8	25±1	10.9±0.6	0.999990
			h 0.2610±0.0002	τ_i (yr)	70±7	250±10	2000±300	8600±300	680000±70000	
1000GtC	on	off	b 0.02787±0.0001	w_i (%)	9±3	44±3	13±4	23±4	10±4	0.999990
			h 0.2311±0.0002	τ_i (yr)	50±10	190±20	600±200	5700±700	15000±3000	
1000GtC	off	on	b -0.001±0.001	w_i (%)	15±2	41±2	8.7±0.7	25.0±0.9	10.9±0.5	0.999990
			h 0.2598±0.0005	τ_i (yr)	70±7	250±10	1900±300	8700±300	640000±60000	
1000GtC	off	off	b 0.02921±0.00009	w_i (%)	9±3	44±3	13±5	20±4	13±4	0.999992
			h 0.2298±0.0002	τ_i (yr)	50±10	190±20	600±100	5300±800	13000±2000	
5000GtC	on	on	b 0.071±0.004	w_i (%)	39±2	61±2				0.999
			h 0.701±0.003	τ_i (yr)	810±100	17000±1000				
5000GtC	on	off	b 0.119±0.002	w_i (%)	39.8±0.8	60.2±0.6				0.9999
			h 0.655±0.002	τ_i (yr)	740±30	14400±400				
5000GtC	off	on	b 0.09±0.01	w_i (%)	100±2					0.99
			h 0.587±0.007	τ_i (yr)	7400±800					
5000GtC	off	off	b 0.123±0.002	w_i (%)	40.3±0.8	59.7±0.6				0.9999
			h 0.650±0.003	τ_i (yr)	750±40	15500±500				

variables			fit to $pH(t) = b + h\sum_i w_i e^{-(t-t_0)/\tau_i}$								
emis.	f_Ca	f_Si	acidification (pH)	i	1	2	3	4	5	6	R^2
1000GtC	on	on	b -0.0005±0.0002	w_i (%)	8±2	38±4	13±5	17±6	16±7	7.8±0.1	0.999995
			h 0.2594±0.0003	τ_i (yr)	50±9	190±20	500±100	4400±900	10000±2000	240000±10000	
1000GtC	on	off	b 0.02621±0.0001	w_i (%)	9±3	44±3	13±4	25±3	9±4		0.999990
			h 0.2328±0.0003	τ_i (yr)	50±10	190±20	600±200	5800±700	15000±3000		
1000GtC	off	on	b -0.0006±0.0002	w_i (%)	8±2	38±4	13±5	16±5	16±6	8.6±0.1	0.999995
			h 0.2594±0.0004	τ_i (yr)	50±9	190±20	500±100	4300±900	10000±1000	228000±9000	
1000GtC	off	off	b 0.02921±0.00009	w_i (%)	9±3	44±3	13±5	20±4	13±4		0.999992
			h 0.2298±0.0002	τ_i (yr)	50±10	190±20	600±100	5300±800	13000±2000		
5000GtC	on	on	b 0.05±0.01	w_i (%)	100.0±0.8						0.99
			h 0.65±0.01	τ_i (yr)	5200±400						
5000GtC	on	off	b 0.113±0.002	w_i (%)	39.0±0.8	61.0±0.6					0.99990
			h 0.661±0.001	τ_i (yr)	730±30	12400±300					
5000GtC	off	on	b -0.007±0.003	w_i (%)	33.1±0.6	55.6±0.5	11.3±0.4				0.99994
			h 0.780±0.001	τ_i (yr)	720±20	9700±200	260000±30000				
5000GtC	off	off	b 0.123±0.002	w_i (%)	40.3±0.8	59.7±0.6					0.9999
			h 0.650±0.003	τ_i (yr)	750±40	15500±500					

variables		fit to $pH(t) = b + h\sum_i w_i e^{-(t-t_0)/\tau_i}$						
emis.	Scheme	acidification (pH)		i	1	2	3	4	R^2
1000GtC	Globavg	b	0.006±0.003	w_i (%)	100.0±0.3				0.95
		h	0.181±0.008	τ_i (yr)	1900±200				
1000GtC	GKWM	b	0.004±0.003	w_i (%)	100±1				0.95
		h	0.180±0.006	τ_i (yr)	1700±200				
1000GtC	GEM-CO2	b	0.007±0.004	w_i (%)	100±3				0.95
		h	0.179±0.003	τ_i (yr)	1500±200				
5000GtC	Globavg	b	-0.0071±0.0009	w_i (%)	33.1±0.6	58.1±0.4	8.8±0.3		0.99996
		h	0.779±0.002	τ_i (yr)	710±20	6400±100	150000±10000		
5000GtC	GKWM	b	-0.0070±0.0003	w_i (%)	4.7±0.2	35.5±0.4	52.1±0.4	7.67±0.08	0.999997
		h	0.7873±0.0006	τ_i (yr)	91±7	930±20	5080±50	109000±3000	
5000GtC	GEM-CO2	b	-0.0067±0.0002	w_i (%)	5.0±0.2	37.9±0.4	50.0±0.3	7.09±0.08	0.999997
		h	0.785±0.002	τ_i (yr)	95±7	960±20	4840±50	102000±2000	

variables				fit to $pH(t) = b + h\sum_i w_i e^{-(t-t_0)/\tau_i}$								
emis.	f_Ca	f_Si	Scheme		acidification (pH)	i	1	2	3	4	5	R^2
1000GtC	on	on	Globavg	b	0.007±0.003	w_i (%)	100±4					0.95
				h	0.1796±0.0006	τ_i (yr)	1900±200					
1000GtC	on	on	GKWM	b	0.004±0.003	w_i (%)	100±3					0.95
				h	0.180±0.003	τ_i (yr)	1700±200					
1000GtC	on	off	Globavg	b	0.023±0.003	w_i (%)	100±3					0.96
				h	0.169±0.003	τ_i (yr)	1600±200					
1000GtC	on	off	GKWM	b	0.020±0.003	w_i (%)	100±3					0.96
				h	0.170±0.003	τ_i (yr)	1800±200					
1000GtC	off	on	Globavg	b	0.007±0.003	w_i (%)	100±3					0.95
				h	0.178±0.004	τ_i (yr)	2000±300					
1000GtC	off	on	GKWM	b	0.007±0.004	w_i (%)	100±3					0.95
				h	0.179±0.004	τ_i (yr)	1600±200					
1000GtC	off	off	Globavg	b	0.026±0.003	w_i (%)	100±4					0.96
				h	0.166±0.002	τ_i (yr)	1600±200					
1000GtC	off	off	GKWM	b	0.026±0.003	w_i (%)	100±1					0.96
				h	0.166±0.006	τ_i (yr)	1700±200					
5000GtC	on	on	Globavg	b	-0.007±0.001	w_i (%)	33.0±0.7	57.6±0.4	9.4±0.2			0.99996
				h	0.779±0.003	τ_i (yr)	710±20	6600±100	190000±10000			
5000GtC	on	on	GKWM	b	-0.0073±0.0003	w_i (%)	4.5±0.2	33.9±0.5	50±3	4±4	7.3±0.3	0.999998
				h	0.788±0.009	τ_i (yr)	87±7	890±20	4700±300	11000±6000	116000±4000	
5000GtC	on	off	Globavg	b	0.117±0.006	w_i (%)	100.0±0.9					0.993
				h	0.586±0.008	τ_i (yr)	4800±300					
5000GtC	on	off	GKWM	b	0.101±0.008	w_i (%)	100±2					0.990
				h	0.590±0.006	τ_i (yr)	6200±500					
5000GtC	off	on	Globavg	b	-0.0074±0.0006	w_i (%)	3.4±0.3	31.9±0.3	54.6±0.3	10.0±0.1		0.99999
				h	0.7922±0.0008	τ_i (yr)	70±10	810±20	7500±80	181000±6000		
5000GtC	off	on	GKWM	b	-0.0069±0.0003	w_i (%)	4.5±0.2	34.2±0.4	53.1±0.2	8.26±0.1		0.999997
				h	0.788±0.002	τ_i (yr)	87±8	900±20	5240±50	100000±3000		
5000GtC	off	off	Globavg	b	0.133±0.007	w_i (%)	100±1					0.992
				h	0.564±0.006	τ_i (yr)	5400±400					
5000GtC	off	off	GKWM	b	0.118±0.004	w_i (%)	39.5±0.8	60.5±0.6				0.9998
				h	0.657±0.003	τ_i (yr)	720±40	18000±700				

variables		fit to $pH(t) = b + h\sum_i w_i e^{-(t-t_0)/\tau_i}$							
emis.	routing	acidification (pH)	i	1	2	3	4	5	R^2
1000GtC	1	b 0.02903±0.0001	w_i (%)	9±3	44±3	13±4	23±4	10±4	0.999990
		h 0.2301±0.0002	τ_i (yr)	50±10	190±20	600±200	5800±800	15000±3000	
1000GtC	2	b 0.02922±0.00009	w_i (%)	9±3	44±3	13±5	20±4	13±4	0.999992
		h 0.2298±0.0002	τ_i (yr)	50±10	190±20	600±100	5300±800	13000±2000	
1000GtC	3	b 0.075±0.004	w_i (%)	100±5					0.99
		h 0.159±0.003	τ_i (yr)	450±70					
5000GtC	1	b 0.125±0.002	w_i (%)	40.2±0.8	59.8±0.6				0.9999
		h 0.649±0.001	τ_i (yr)	740±30	15500±400				
5000GtC	2	b 0.123±0.002	w_i (%)	40.3±0.8	59.7±0.6				0.9999
		h 0.650±0.003	τ_i (yr)	750±40	15500±500				
5000GtC	3	b 0.129±0.007	w_i (%)	41.5±0.7	58.5±0.7				0.9999
		h 0.644±0.003	τ_i (yr)	760±40	22000±1000				

variables		fit to $pH(t) = b + h\sum_i w_i e^{-(t-t_0)/\tau_i}$								
emis.	lith.	acidification (pH)	i	1	2	3	4	5	6	R^2
1000GtC	GKWM	b 0.007±0.004	w_i (%)	100±2						0.95
		h 0.179±0.005	τ_i (yr)	1600±200						
1000GtC	GEM-CO2	b -0.0035±0.0001	w_i (%)	10±2	45±1	9.7±0.6	31.1±0.8	4.5±0.1		0.999993
		h 0.2550±0.0001	τ_i (yr)	53±6	197±8	1200±200	5400±100	103000±6000		
1000GtC	GKWM av.	b 0.004±0.003	w_i (%)	100±2						0.95
		h 0.181±0.005	τ_i (yr)	1800±200						
1000GtC	GEM-CO2 av.	b 0.006±0.004	w_i (%)	100±2						0.95
		h 0.180±0.006	τ_i (yr)	2100±300						
1000GtC	mono acid	b -0.0032±0.0001	w_i (%)	8±2	42±2	10±2	24±8	12±9	4.2±0.2	0.999996
		h 0.2587±0.0004	τ_i (yr)	49±7	180±10	600±100	4200±800	9000±3000	105000±9000	
1000GtC	mono basalt	b 0.007±0.004	w_i (%)	100±2						0.96
		h 0.181±0.006	τ_i (yr)	1300±200						
1000GtC	mono carb	b 0.005±0.003	w_i (%)	100±4						0.94
		h 0.162±0.002	τ_i (yr)	1700±200						
1000GtC	mono granite	b -0.0032±0.0002	w_i (%)	8±2	42±2	10±2	24±8	12±9	4.2±0.2	0.999996
		h 0.2588±0.0004	τ_i (yr)	49±7	180±10	600±100	4200±800	9000±3000	106000±9000	
1000GtC	mono sand	b 0.013±0.004	w_i (%)	100±2						0.94
		h 0.171±0.006	τ_i (yr)	3100±500						
1000GtC	mono shale	b 0.002±0.003	w_i (%)	100±1						0.94
		h 0.174±0.006	τ_i (yr)	1300±200						
1000GtC	mono shield	b -0.0030±0.0001	w_i (%)	10±2	44±1	10.2±0.6	31.7±0.7	4.6±0.1		0.999993
		h 0.2585±0.0001	τ_i (yr)	55±7	202±9	1100±100	5800±100	91000±6000		

variables		fit to $pH(t) = b + h\sum_i w_i e^{-(t-t_0)/\tau_i}$								
emis.	lith.		acidification (pH)	i	1	2	3	4	5	6	R^2
5000GtC	GKWM	b	-0.007±0.001	w_i (%)	34±1	57.5±1	8.3±0.4				0.99994
		h	0.773±0.002	τ_i (yr)	720±30	4700±100	100000±10000				
5000GtC	GEM-CO2	b	-0.0071±0.0003	w_i (%)	4.7±0.2	35.3±0.4	52.3±0.3	7.76±0.09			0.999997
		h	0.787±0.002	τ_i (yr)	91±7	920±20	5050±50	106000±3000			
5000GtC	GKWM av.	b	-0.0080±0.0003	w_i (%)	4.1±0.2	33.0±0.4	54.8±0.2	8.12±0.1			0.999995
		h	0.791±0.002	τ_i (yr)	77±9	870±20	5740±50	129000±3000			
5000GtC	GEM-CO2 av.	b	-0.008±0.001	w_i (%)	32.7±0.6	58.2±0.3	9.2±0.3				0.99995
		h	0.782±0.003	τ_i (yr)	700±20	7900±200	180000±10000				
5000GtC	mono acid	b	-0.0076±0.0009	w_i (%)	33.6±0.8	58.9±0.5	7.6±0.4				0.99995
		h	0.779±0.003	τ_i (yr)	700±20	5800±100	105000±10000				
5000GtC	mono basalt	b	-0.0069±0.0003	w_i (%)	4.6±0.2	39.9±0.5	50.1±0.4	5.4±0.1			0.999997
		h	0.786±0.002	τ_i (yr)	88±7	930±10	4470±50	71000±3000			
5000GtC	mono carb	b	-0.008±0.002	w_i (%)	43±1	50±1	7.0±0.3				0.9999
		h	0.7577±0.0009	τ_i (yr)	720±30	5200±200	230000±30000				
5000GtC	mono granite	b	0.014±0.007	w_i (%)	100.0±0.9						0.992
		h	0.696±0.008	τ_i (yr)	3800±200						
5000GtC	mono sand	b	-0.03±0.02	w_i (%)	29.7±0.7	59.4±0.4	11±2				0.9998
		h	0.81±0.01	τ_i (yr)	600±30	21000±700	700000±400000				
5000GtC	mono shale	b	-0.0077±0.0002	w_i (%)	3.6±0.2	48.2±0.4	46.1±0.4	2.1±0.1			0.999994
		h	0.775±0.001	τ_i (yr)	62±7	760±10	4250±50	72000±7000			
5000GtC	mono shield	b	0.014±0.007	w_i (%)	100±1						0.992
		h	0.696±0.006	τ_i (yr)	3800±200						

variables		fit to $pH(t) = b + h\sum_i w_i e^{-(t-t_0)/\tau_i}$								
emis.	clim. sens.	acidification (pH)	i	1	2	3	4	5	6	R^2
1000GtC	1.5	b 0.022±0.005	w_i (%)	100±3						0.96
		h 0.170±0.004	τ_i (yr)	1800±300						
1000GtC	2.64	b -0.0005±0.0002	w_i (%)	8±2	38±5	13±6	14±7	19±7	8.0±0.1	0.999995
		h 0.2594±0.0002	τ_i (yr)	49±10	180±30	500±100	4000±1000	9000±1000	229000±9000	
1000GtC	3	b -0.0003±0.0002	w_i (%)	8±2	40±3	12±3	22±8	11±8	7.7±0.1	0.999995
		h 0.2595±0.0006	τ_i (yr)	48±8	190±20	600±100	5100±900	11000±3000	225000±10000	
1000GtC	4.5	b -0.0004±0.0002	w_i (%)	8±2	40±3	12±4	32.9±0.3	7.46±0.1		0.999993
		h 0.2609±0.0003	τ_i (yr)	48±8	200±20	600±100	6800±90	163000±6000		
1000GtC	6.	b 0.013±0.005	w_i (%)	100±2						0.95
		h 0.182±0.007	τ_i (yr)	2100±300						
5000GtC	1.5	b -0.012±0.008	w_i (%)	2.4±0.9	31.5±0.7	52.8±0.4	13.3±0.9			0.99995
		h 0.796±0.002	τ_i (yr)	60±40	650±30	11200±200	530000±80000			
5000GtC	2.64	b -0.006±0.003	w_i (%)	2.8±0.6	31.5±0.6	55.3±0.4	10.3±0.3			0.99997
		h 0.792±0.001	τ_i (yr)	60±30	770±30	8800±200	280000±30000			
5000GtC	3	b 0.046±0.01	w_i (%)	100.0±0.8						0.990
		h 0.66±0.01	τ_i (yr)	5100±400						
5000GtC	4.5	b -0.003±0.002	w_i (%)	32.2±0.9	57.0±0.8	10.8±0.5				0.99993
		h 0.776±0.002	τ_i (yr)	840±40	7400±200	150000±20000				
5000GtC	6.	b 0.020±0.004	w_i (%)	50±3	50±3					0.999
		h 0.749±0.003	τ_i (yr)	1300±100	13000±1000					

A.4 Percentages of key variables remaining

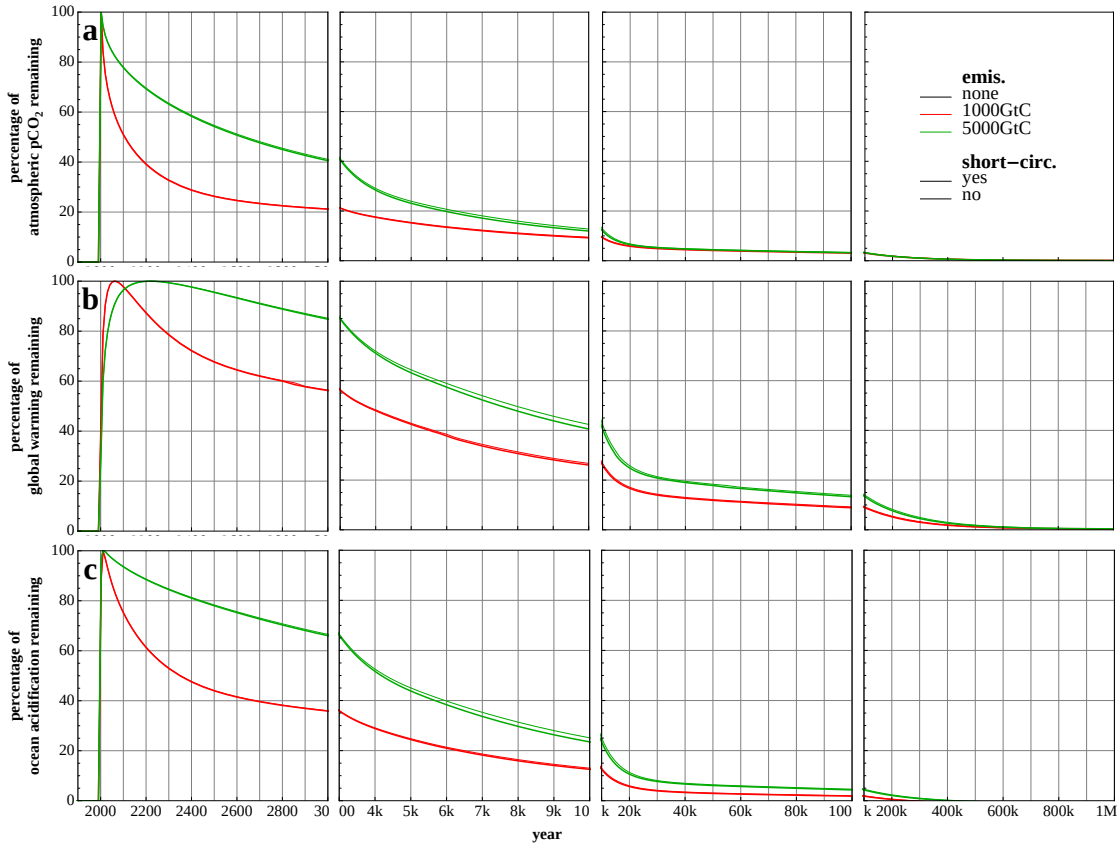

Figure 57: Percentages of key variables remaining for short-circuit test ensemble

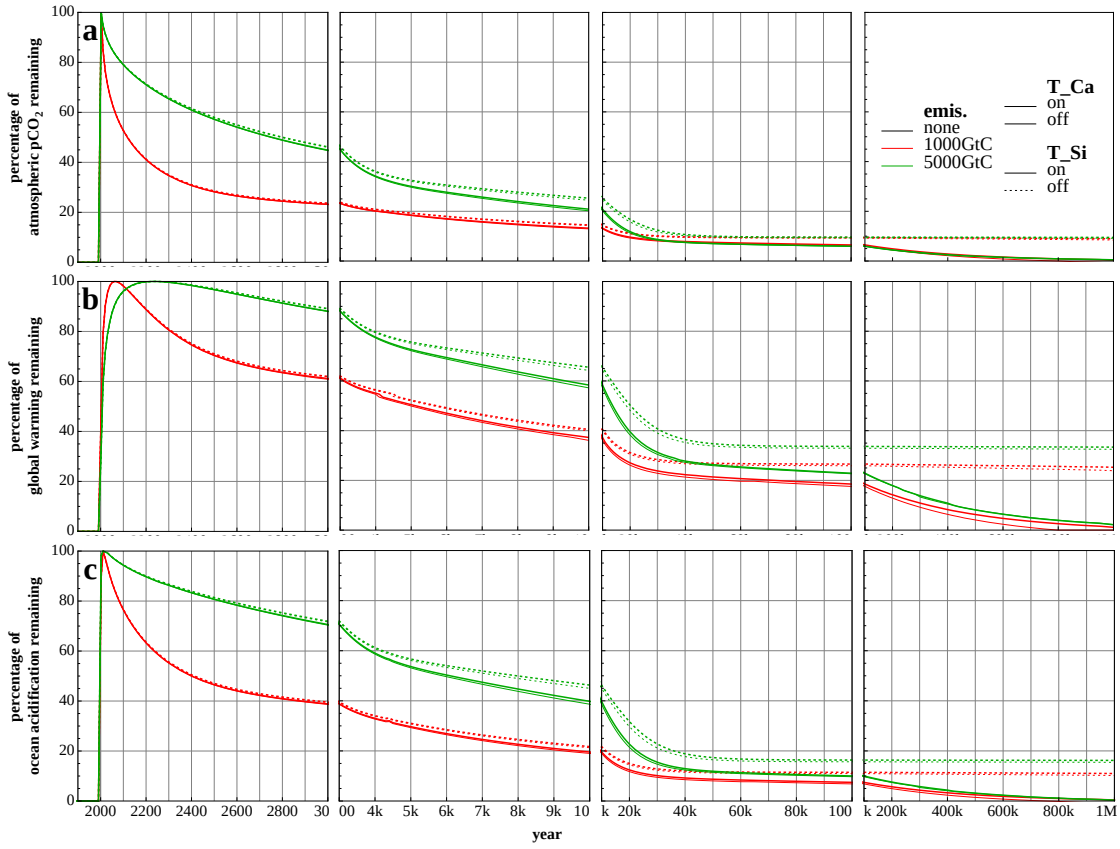

Figure 58: Percentages of key variables remaining for weathering-temperature feedbacks ensemble

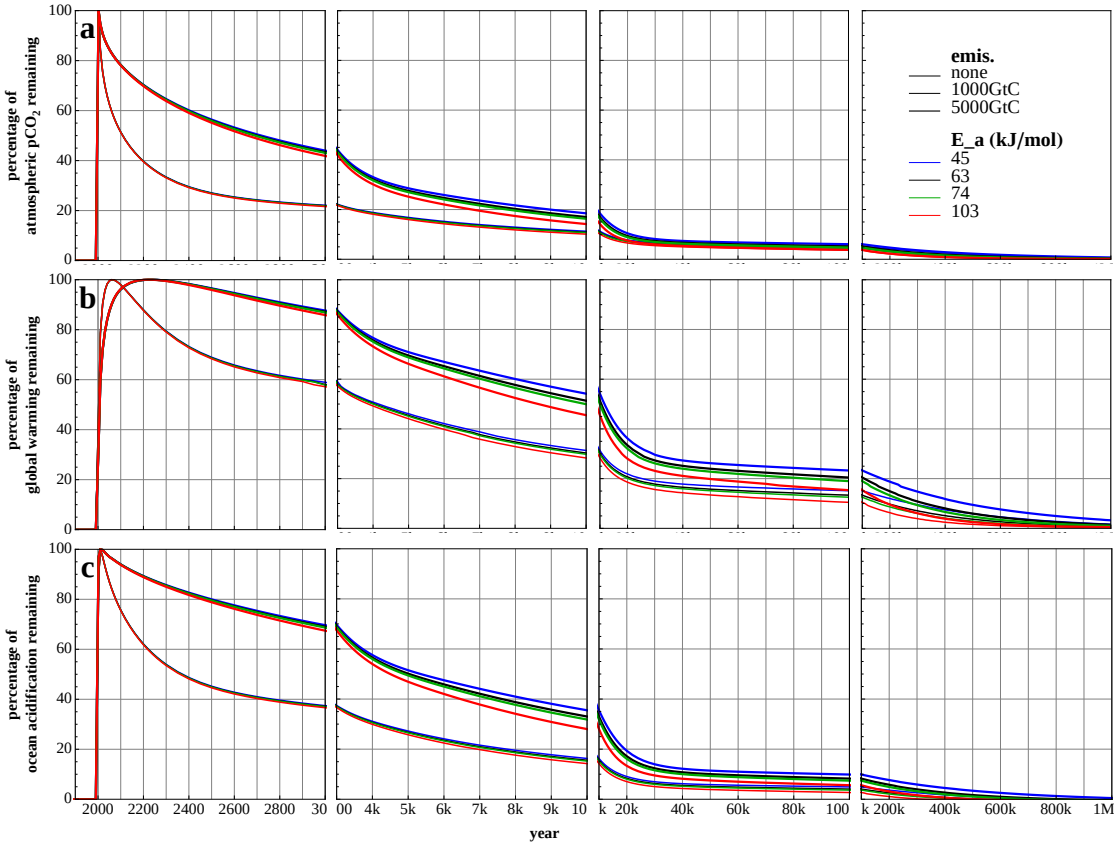

Figure 59: Percentages of key variables remaining for weathering activation energy ensemble

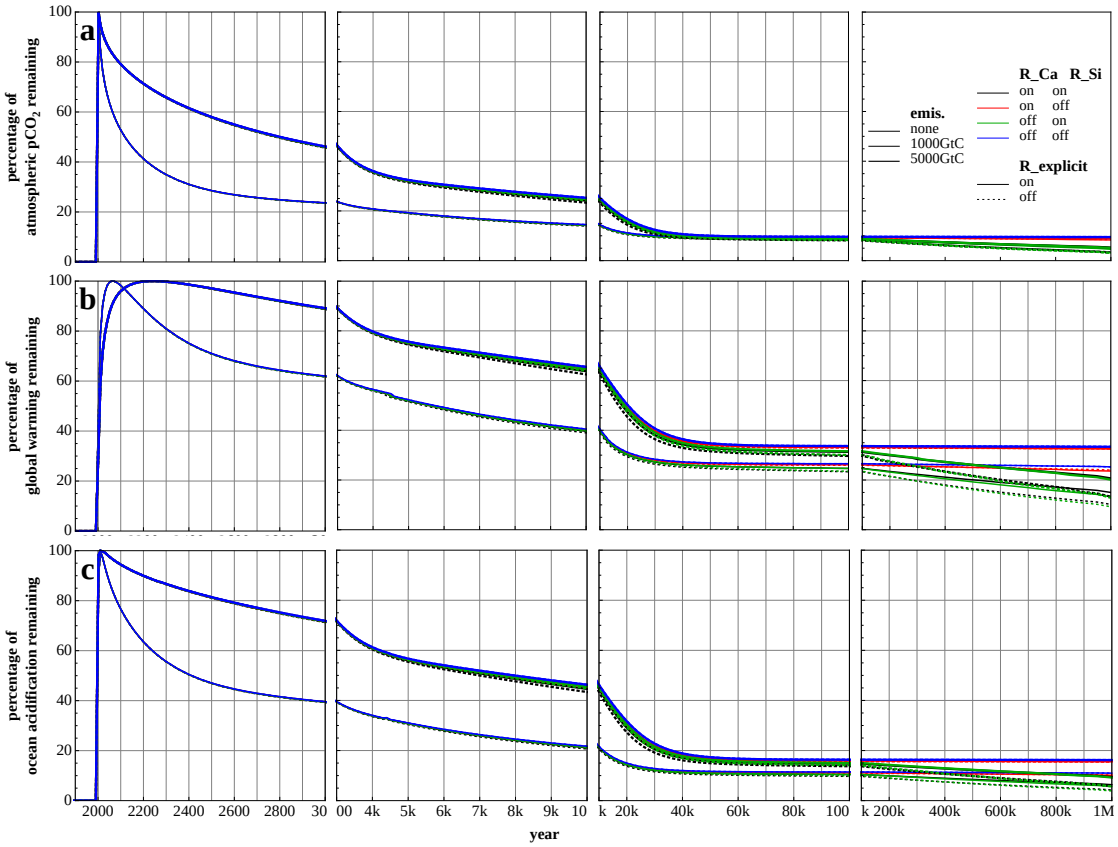

Figure 60: Percentages of key variables remaining for weathering-runoff feedbacks ensemble

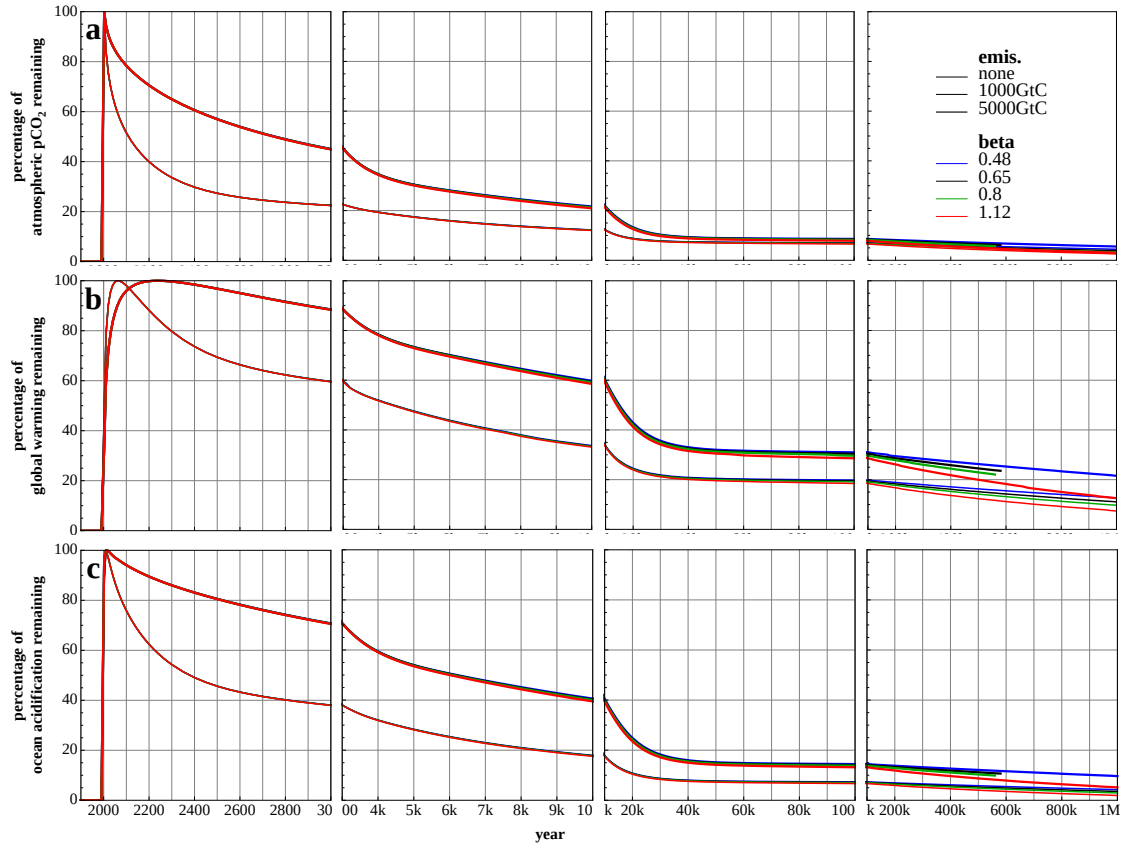

Figure 61: Percentages of key variables remaining for fractional power of explicit weathering-runoff dependence ensemble

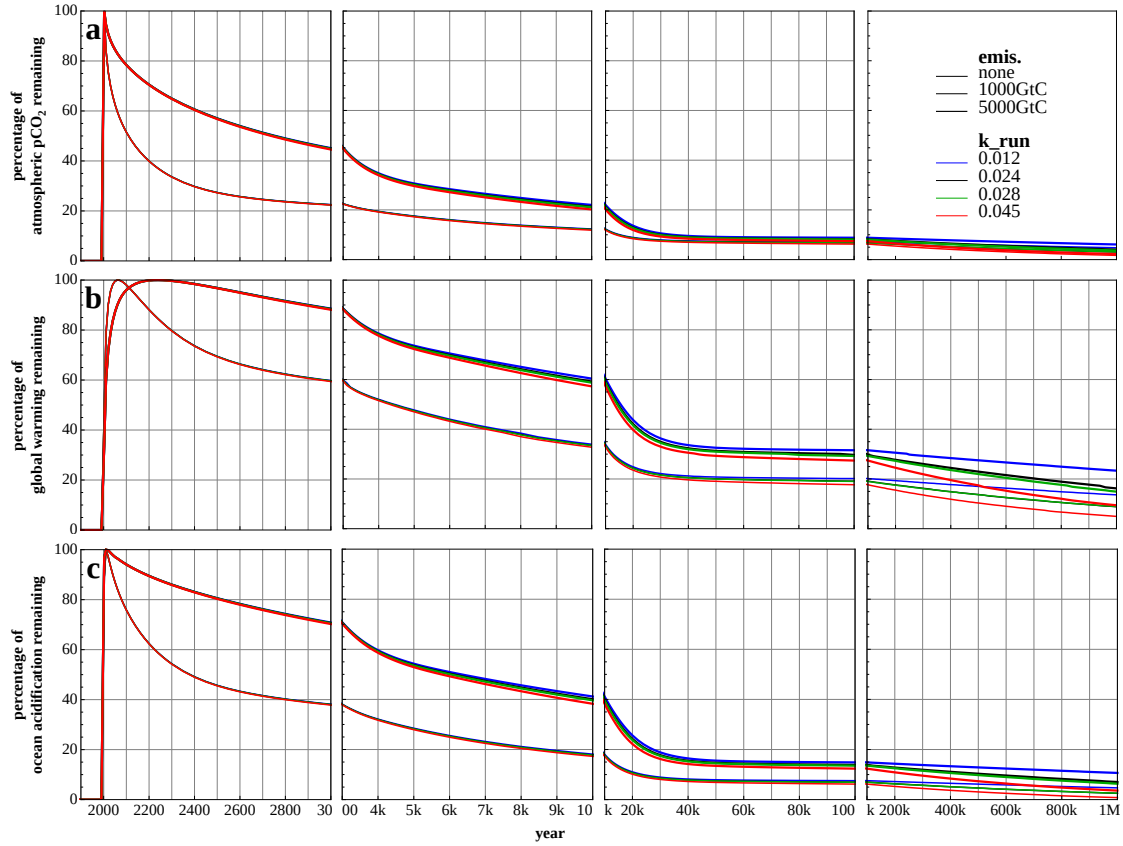

Figure 62: Percentages of key variables remaining for runoff-temperature correlation constant ensemble

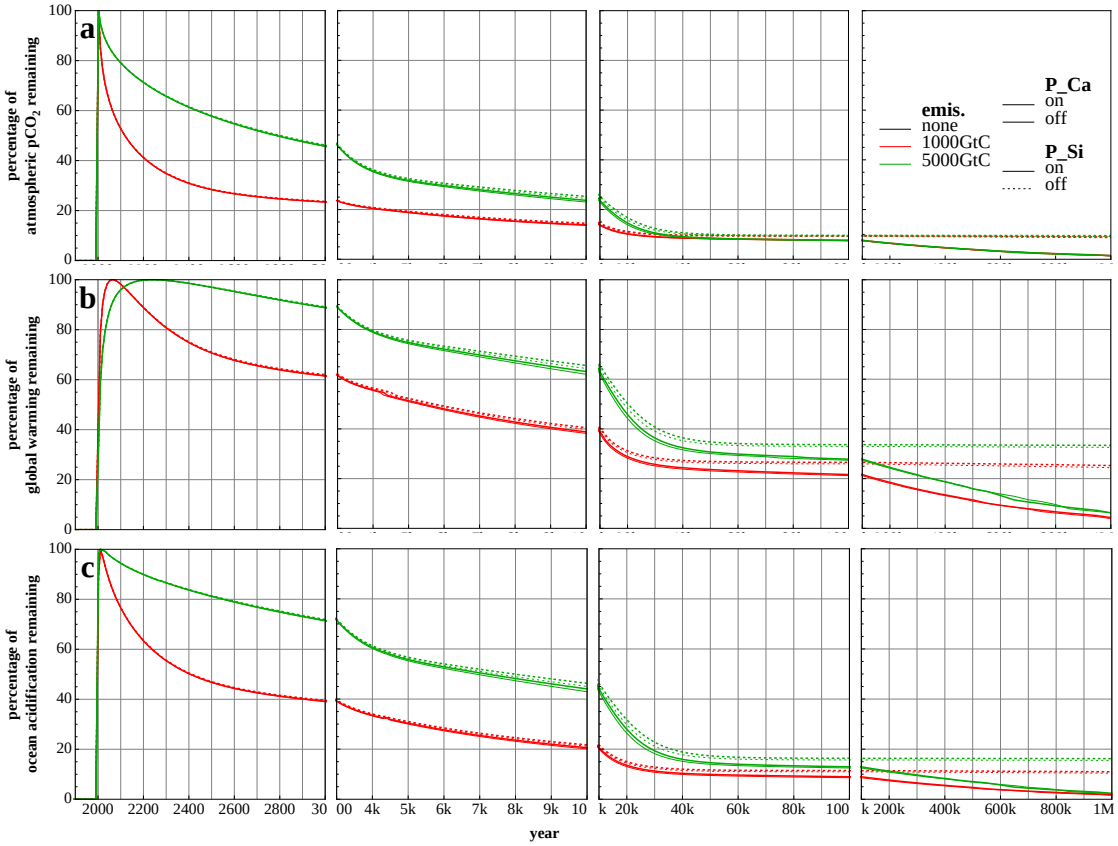

Figure 63: Percentages of key variables remaining for weathering-productivity feedbacks ensemble

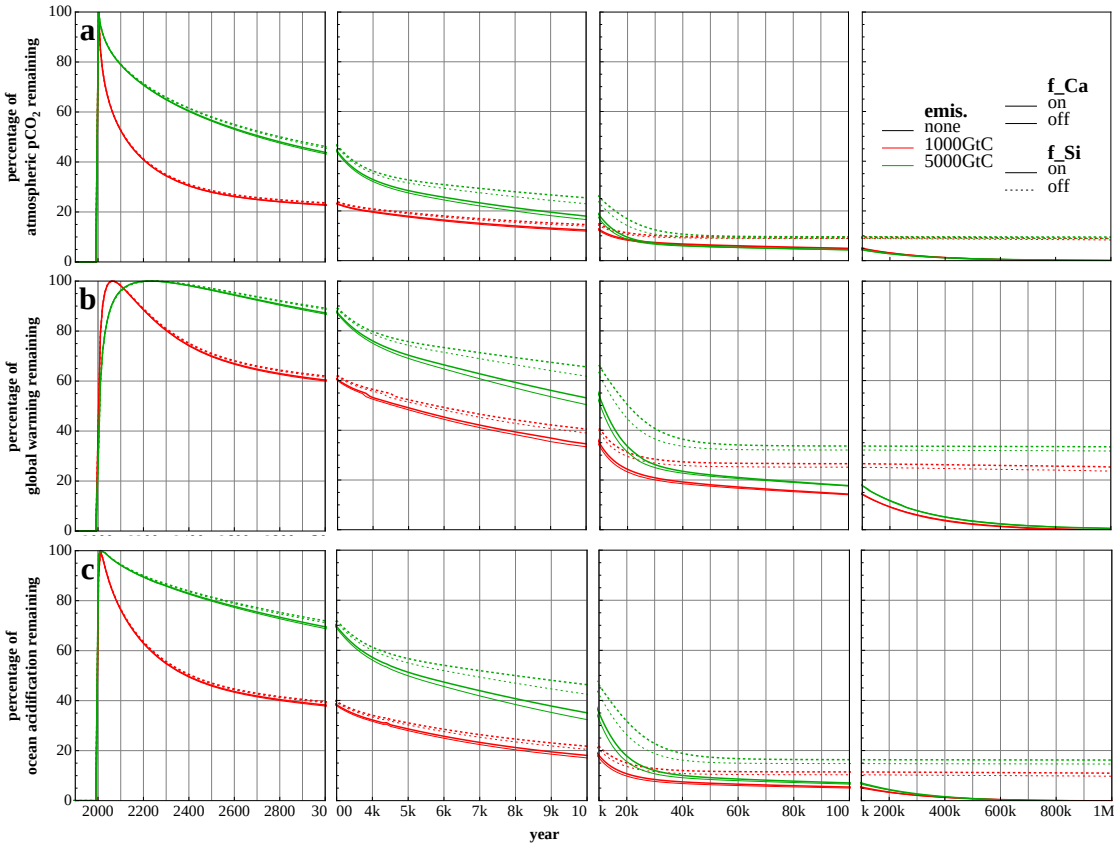

Figure 64: Percentages of key variables remaining for calcite and silicate weathering feedbacks ensemble

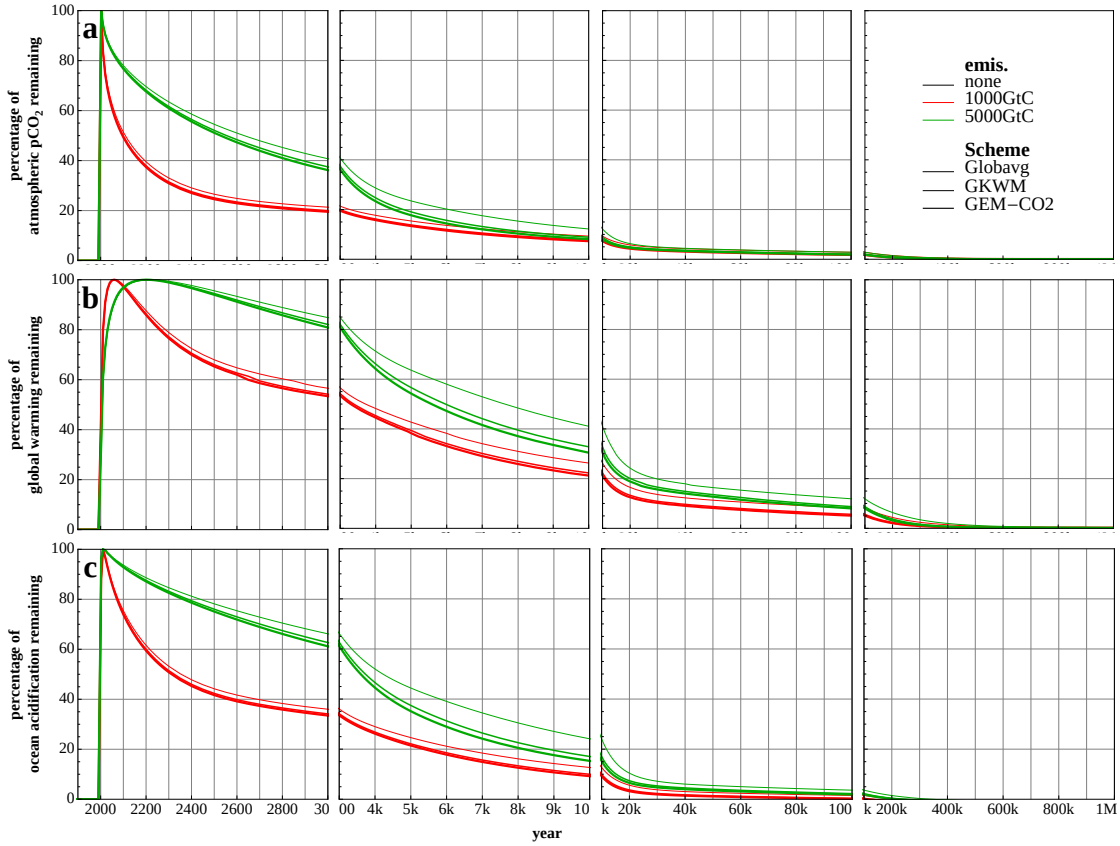

Figure 65: Percentages of key variables remaining for weathering schemes ensemble

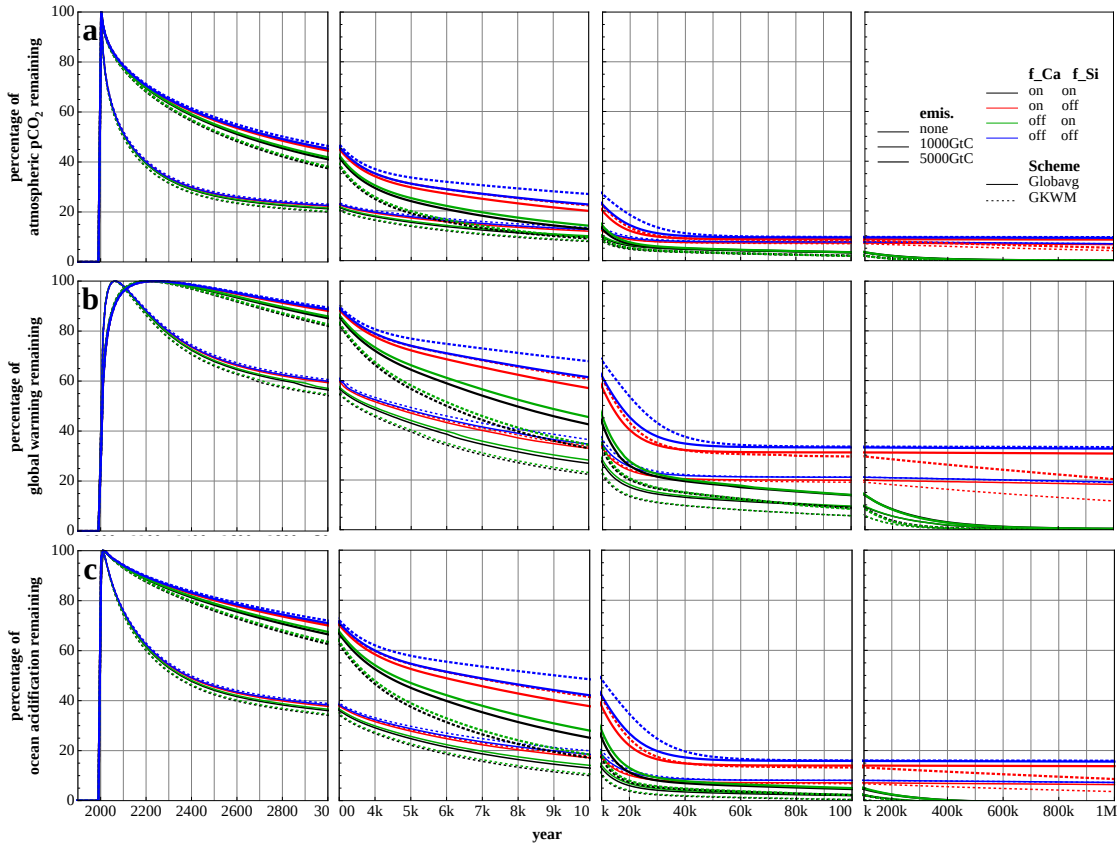

Figure 66: Percentages of key variables remaining for weathering schemes with f_Ca and f_Si on/off ensemble

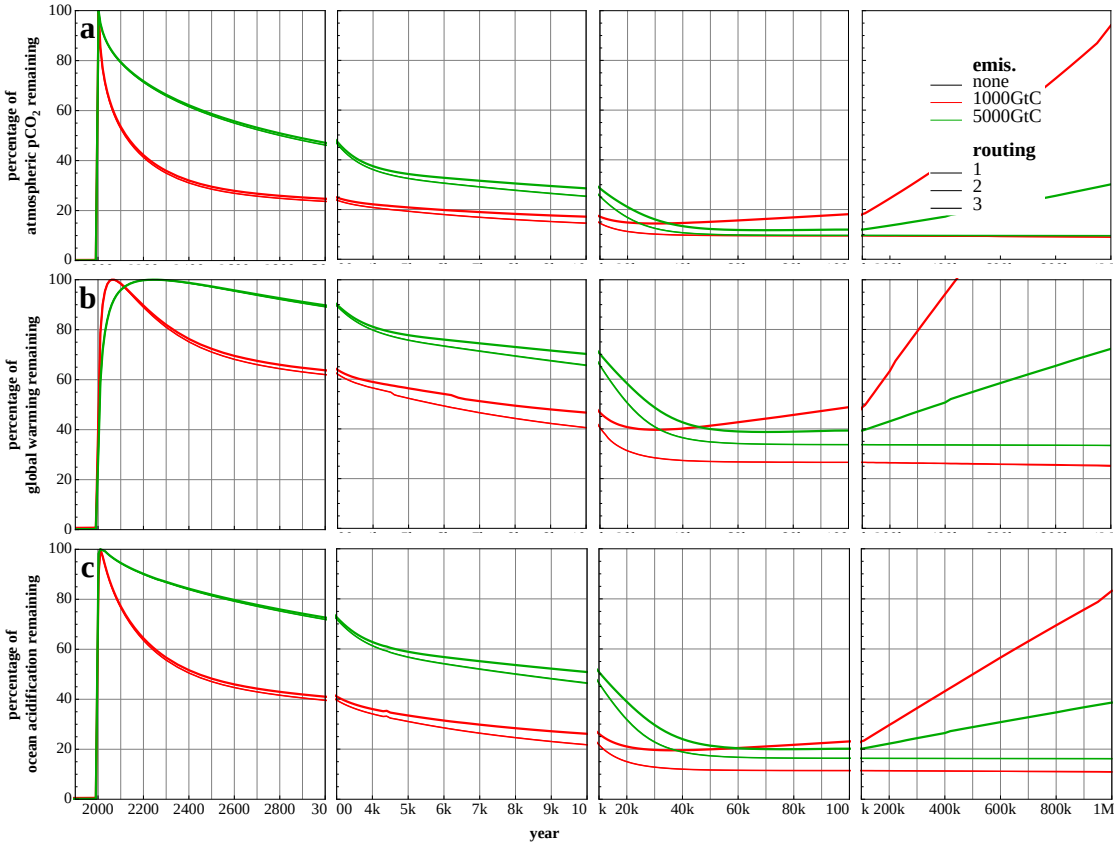

Figure 67: Percentages of key variables remaining for river routing schemes ensemble

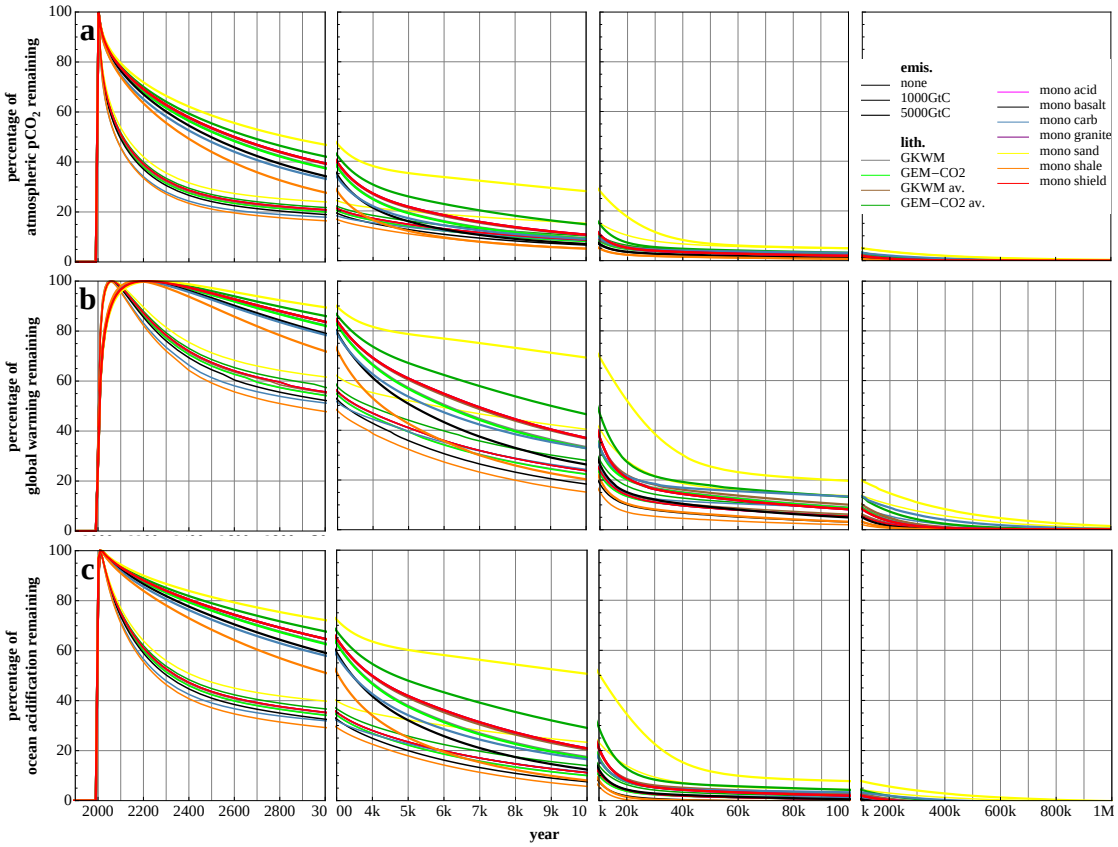

Figure 68: Percentages of key variables remaining for lithologies ensemble

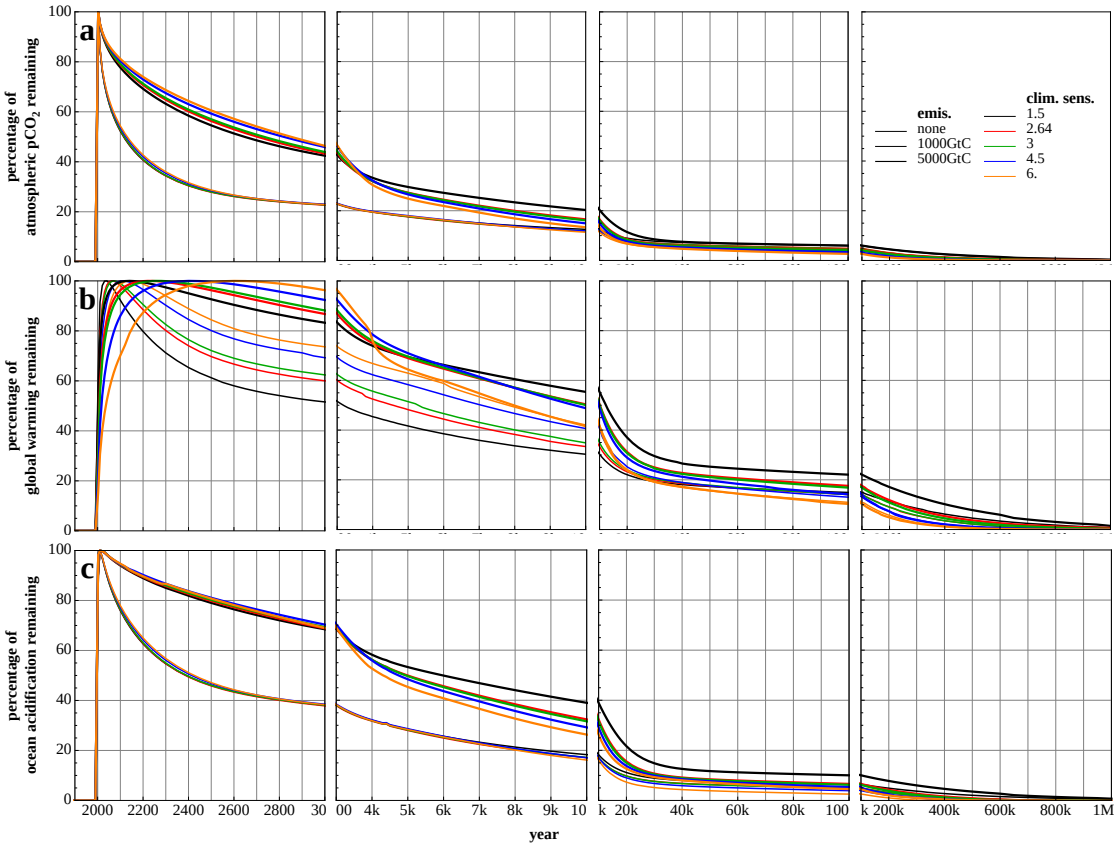

Figure 69: Percentages of key variables remaining for climate sensitivity ensemble

A.5 *e*-folding timescales of key variables remaining

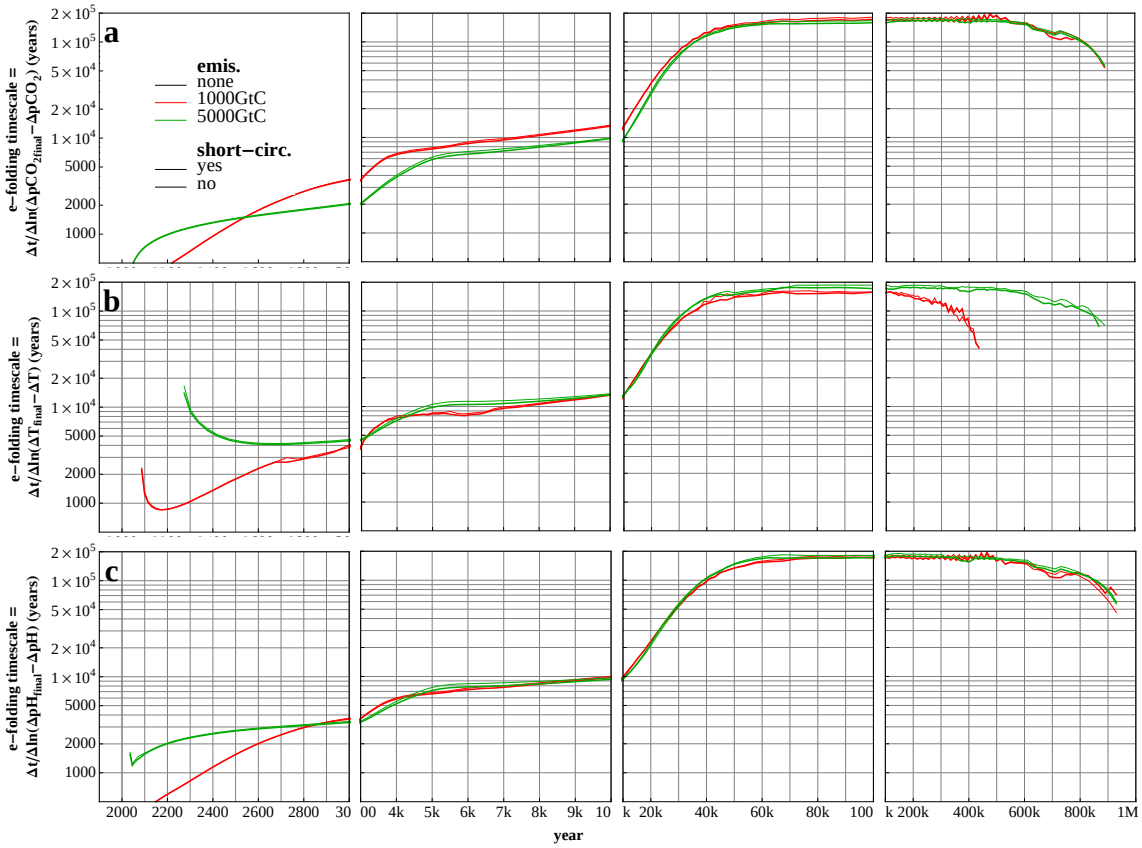

Figure 70: *e*-folding timescales of key variables for short-circuit test ensemble

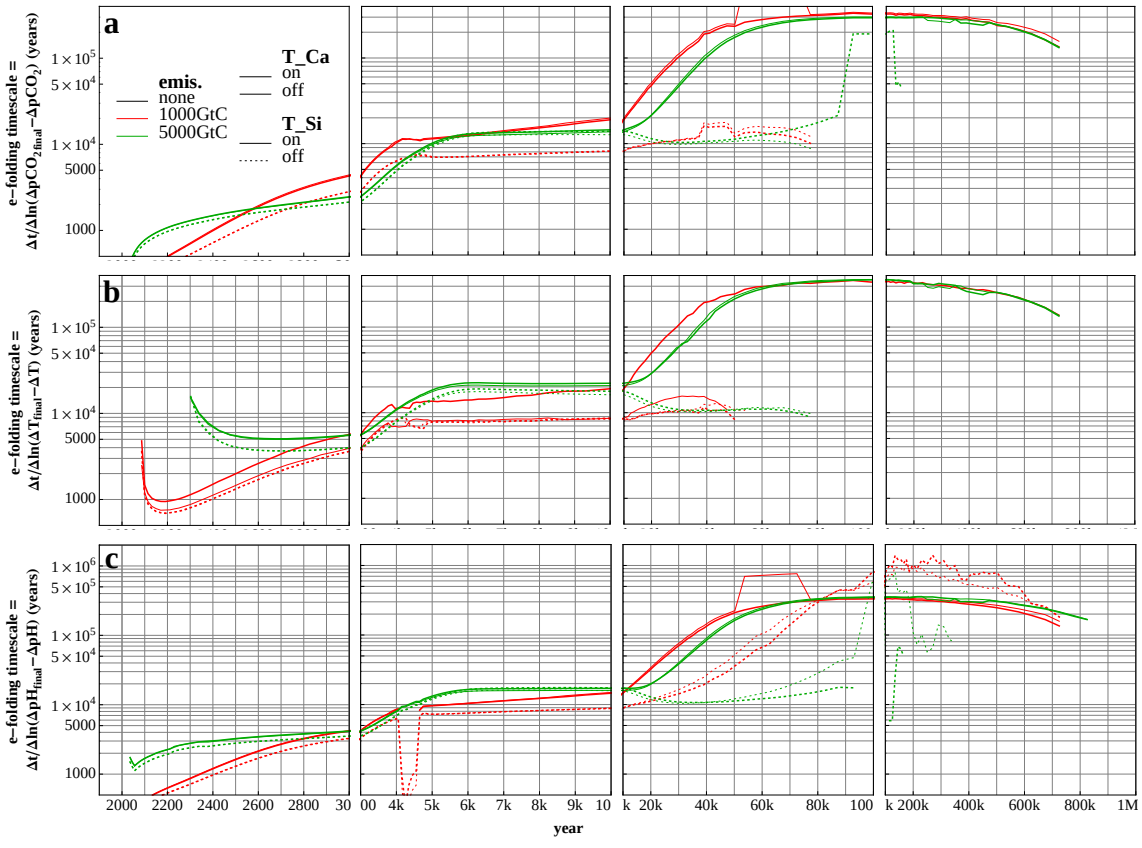

Figure 71: *e*-folding timescales of key variables for weathering-temperature feedbacks ensemble

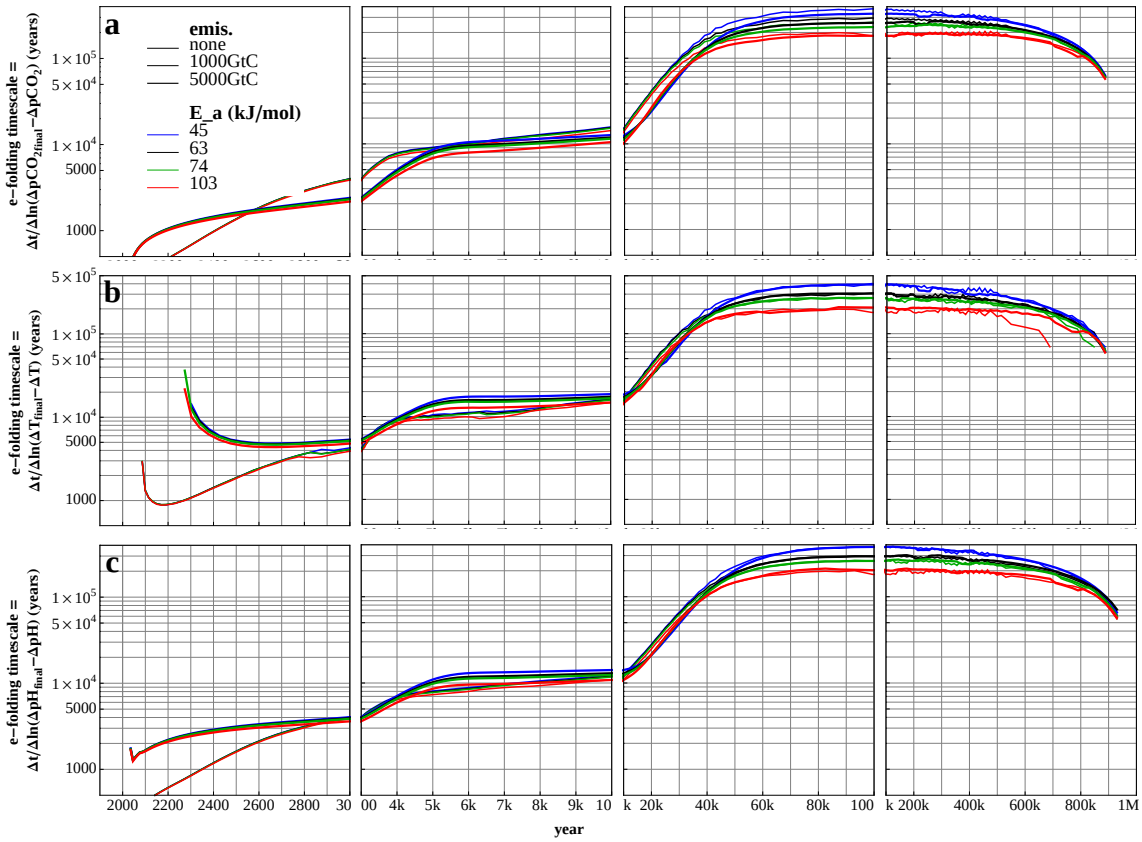

Figure 72: *e*-folding timescales of key variables for weathering activation energy ensemble

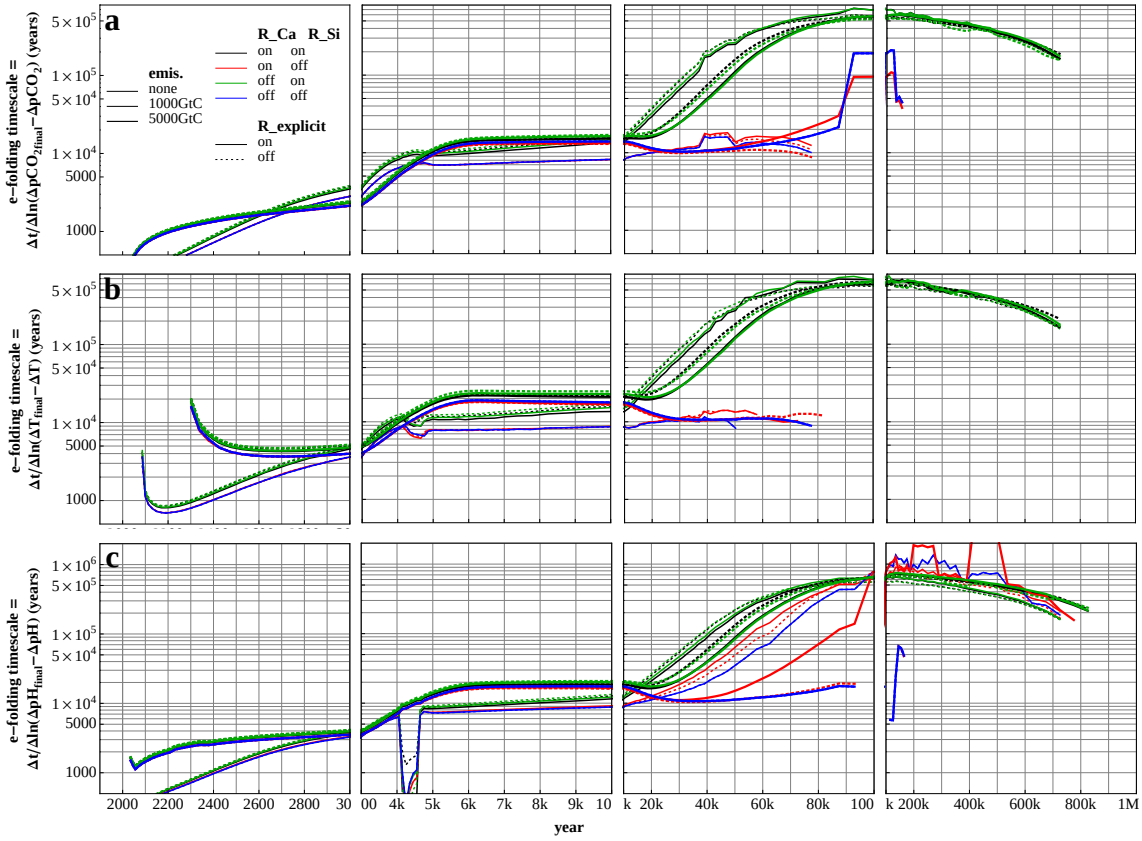

Figure 73: *e*-folding timescales of key variables for weathering-runoff feedbacks ensemble

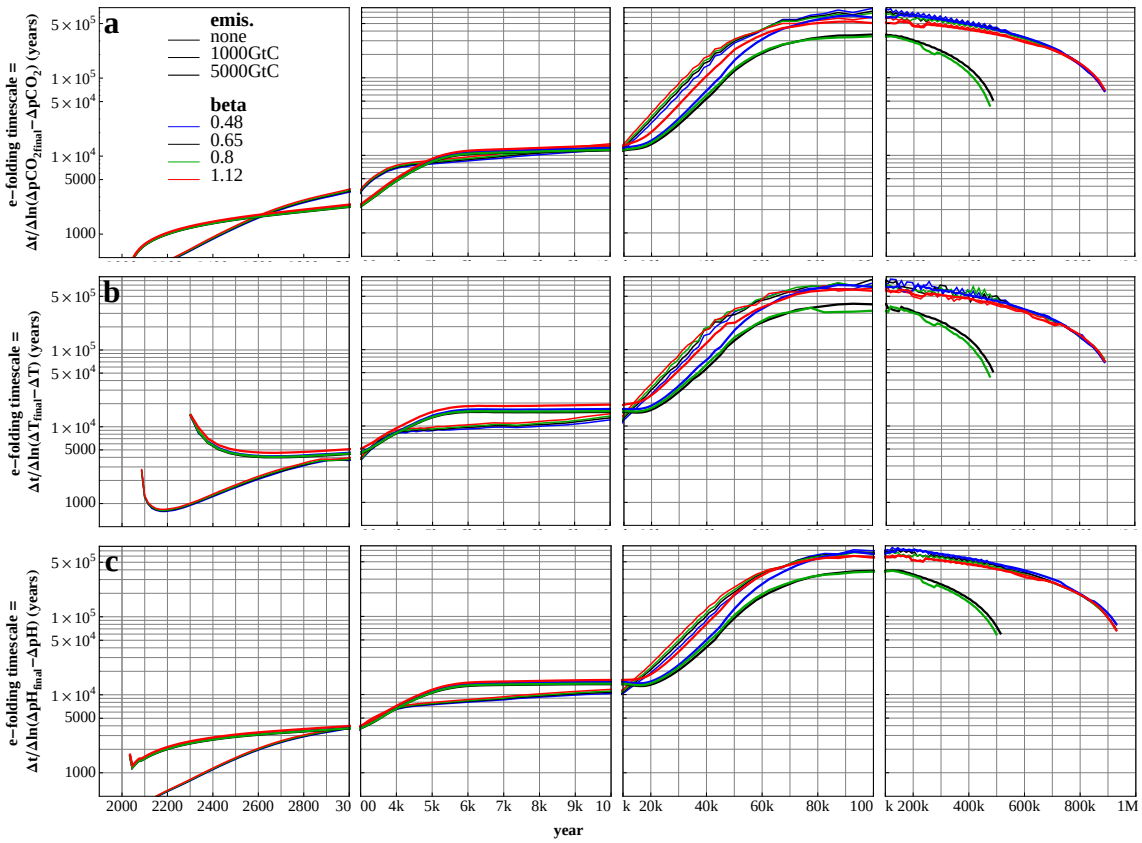

Figure 74: *e*-folding timescales of key variables for fractional power of explicit weathering-runoff dependence ensemble

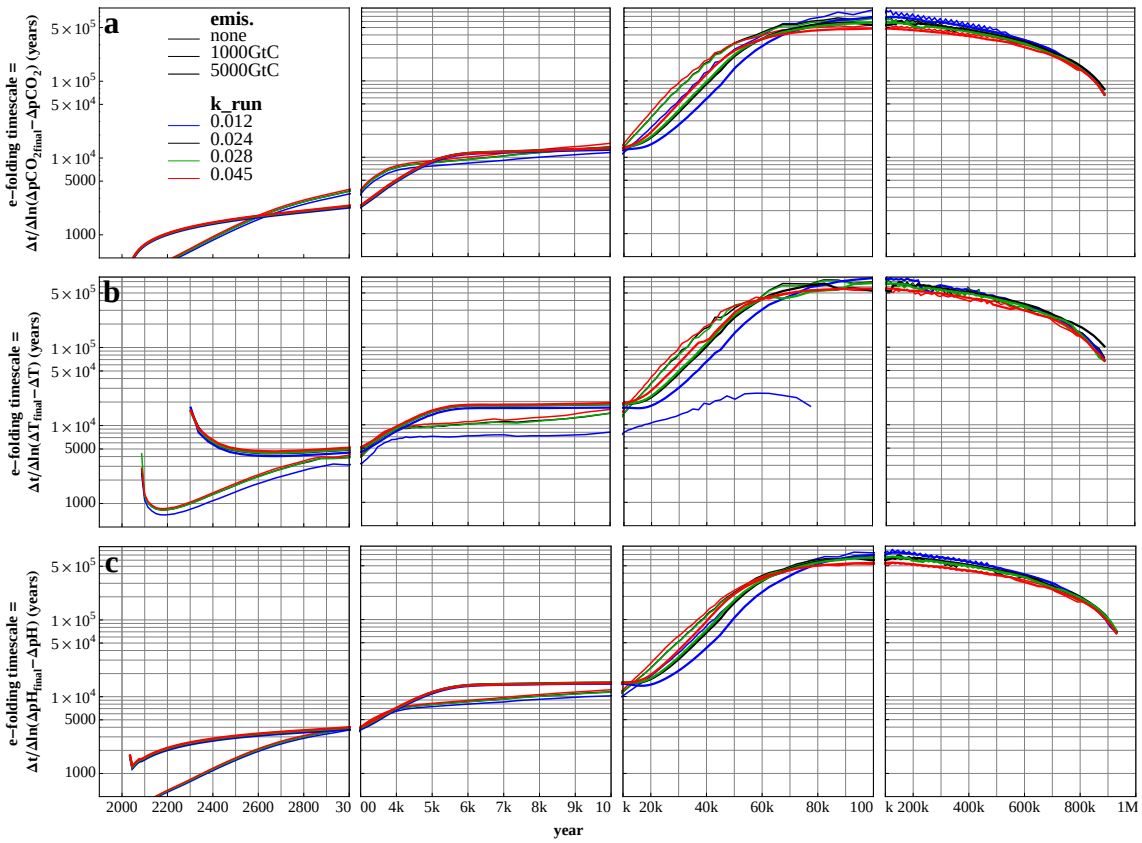

Figure 75: *e*-folding timescales of key variables for runoff-temperature correlation constant ensemble

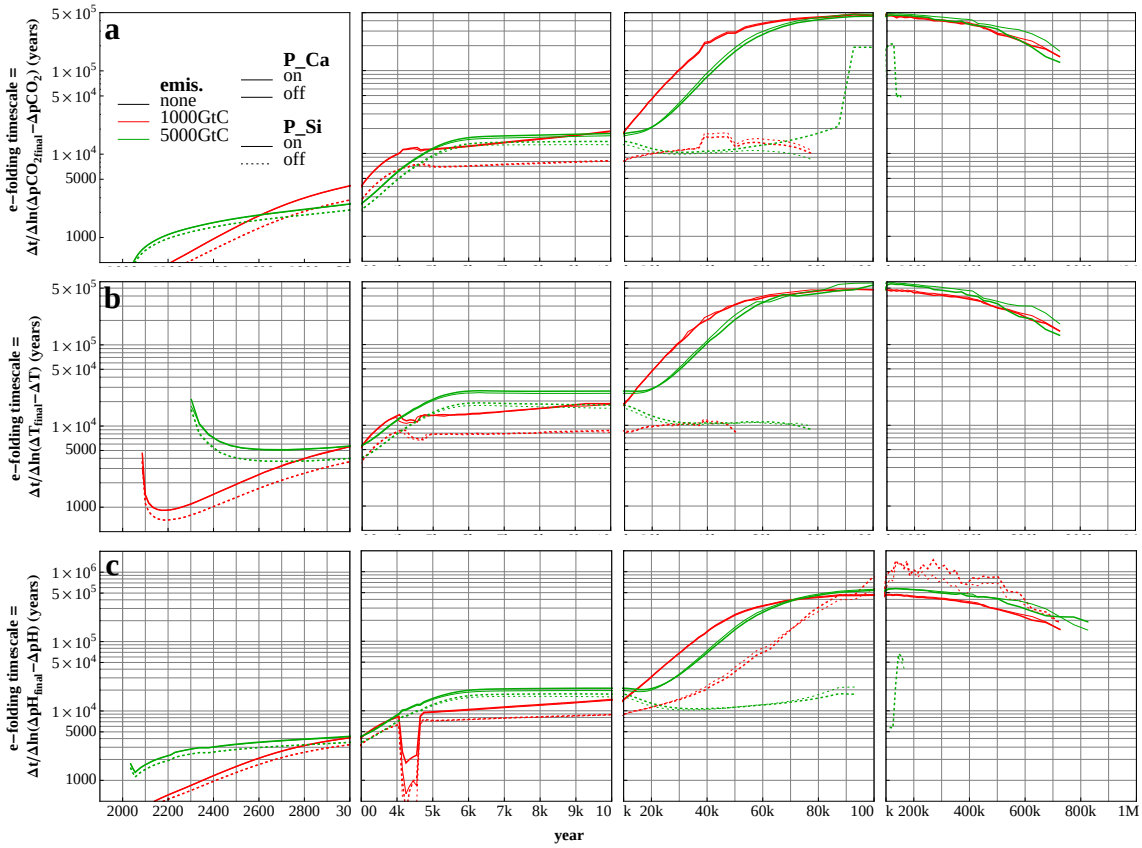

Figure 76: *e*-folding timescales of key variables for weathering-productivity feedbacks ensemble

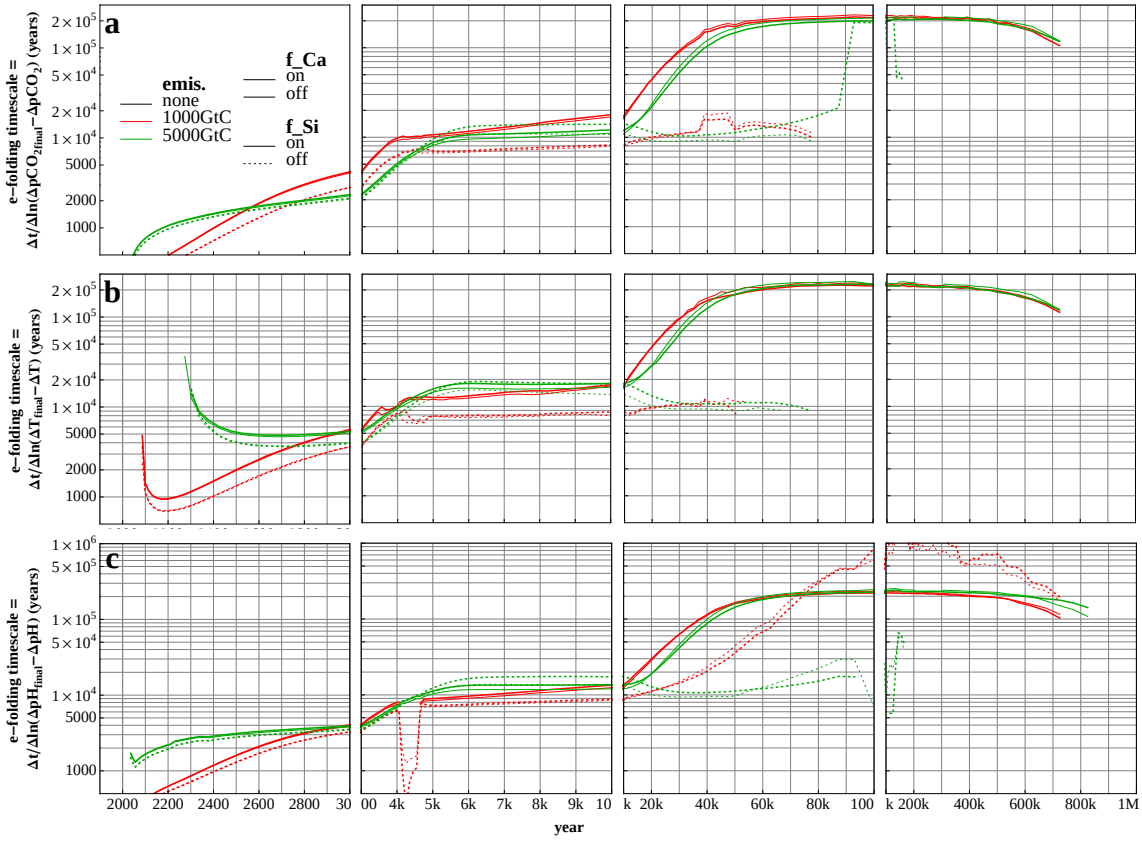

Figure 77: *e*-folding timescales of key variables for calcite and silicate weathering feedbacks ensemble

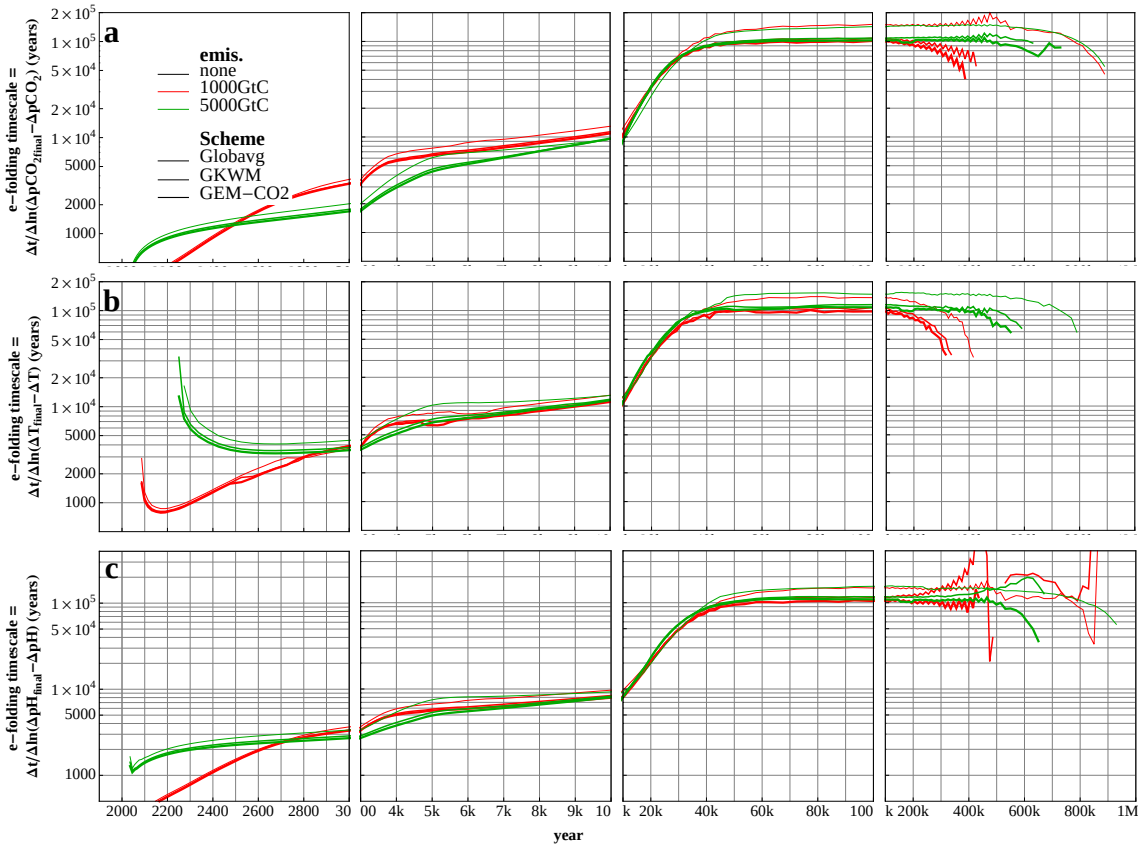

Figure 78: *e*-folding timescales of key variables for weathering schemes ensemble

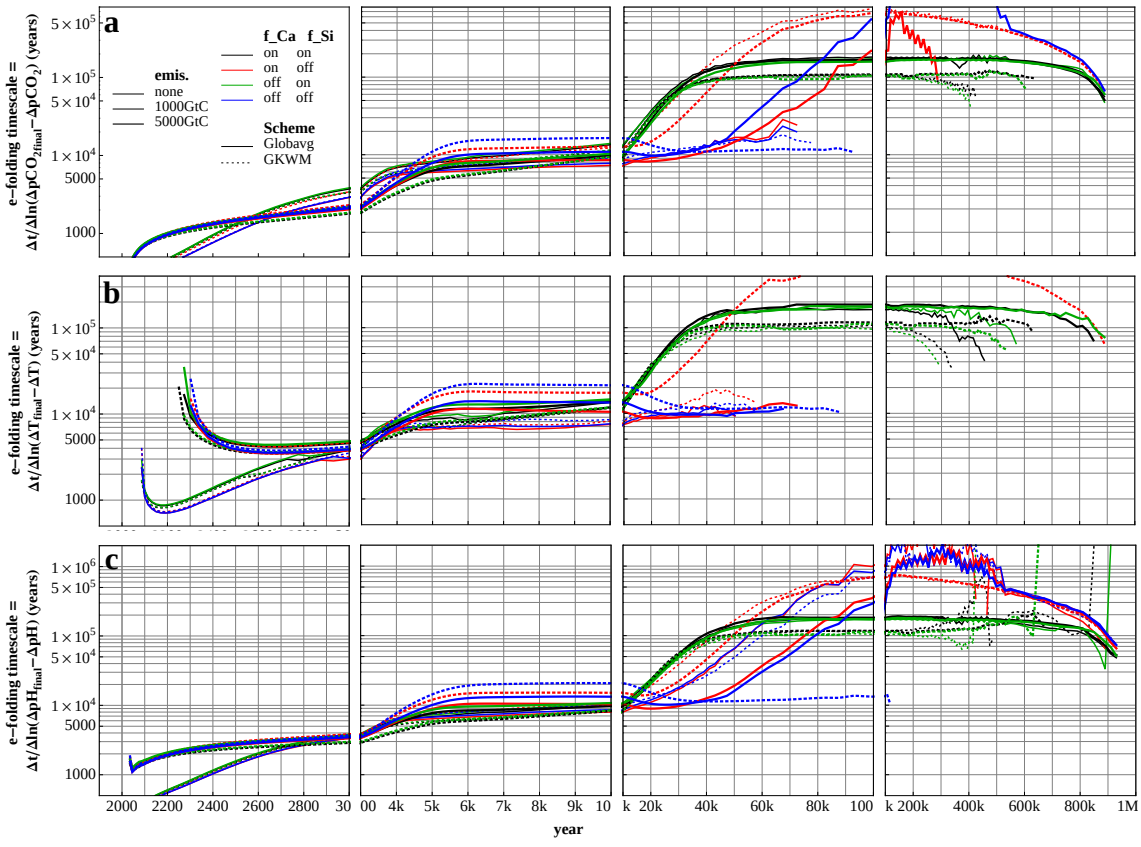

Figure 79: *e*-folding timescales of key variables for weathering schemes with f_Ca and f_Si on/off ensemble

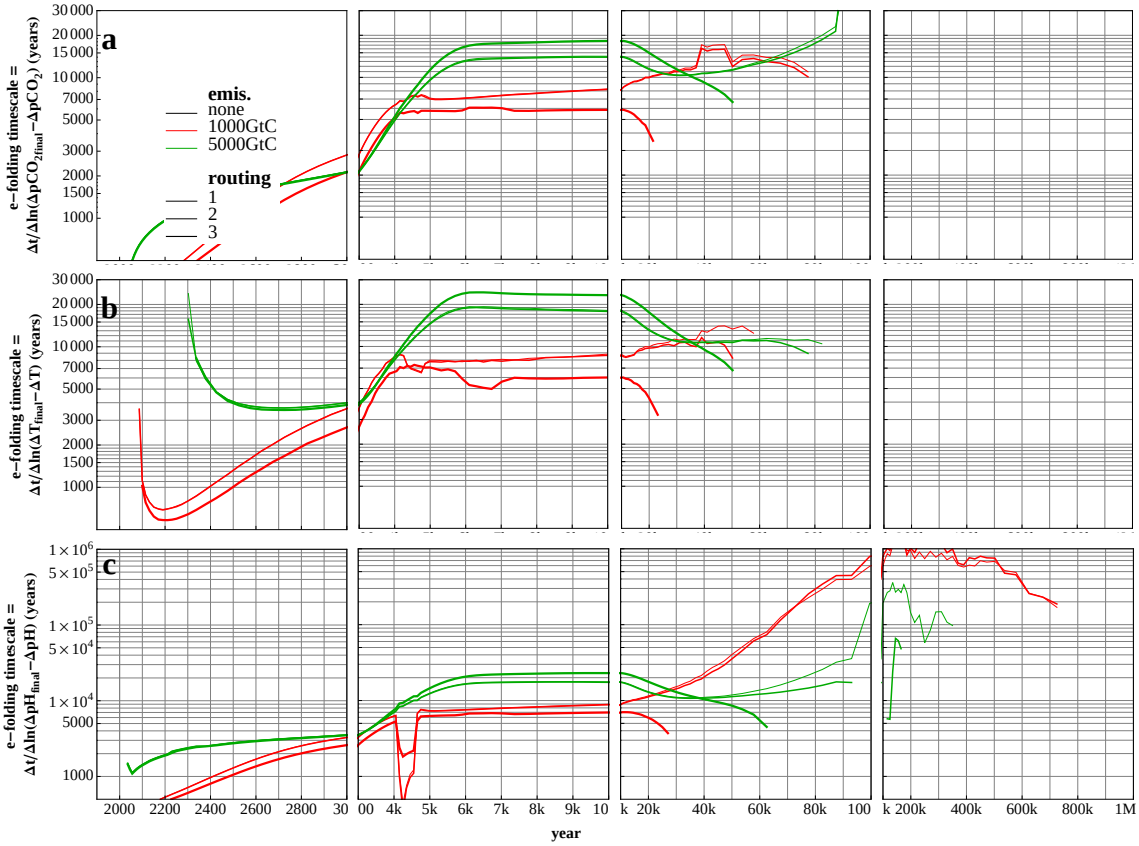

Figure 80: *e*-folding timescales of key variables for river routing schemes ensemble

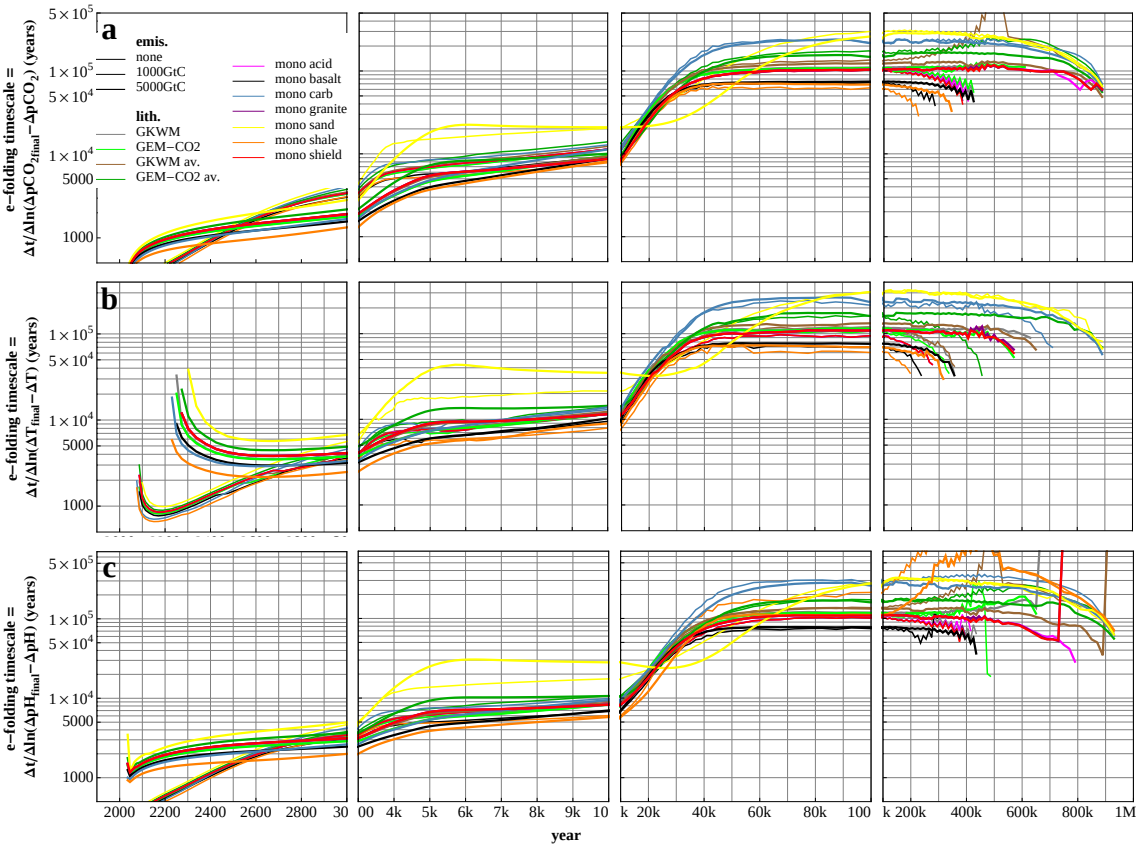

Figure 81: *e*-folding timescales of key variables for lithologies ensemble

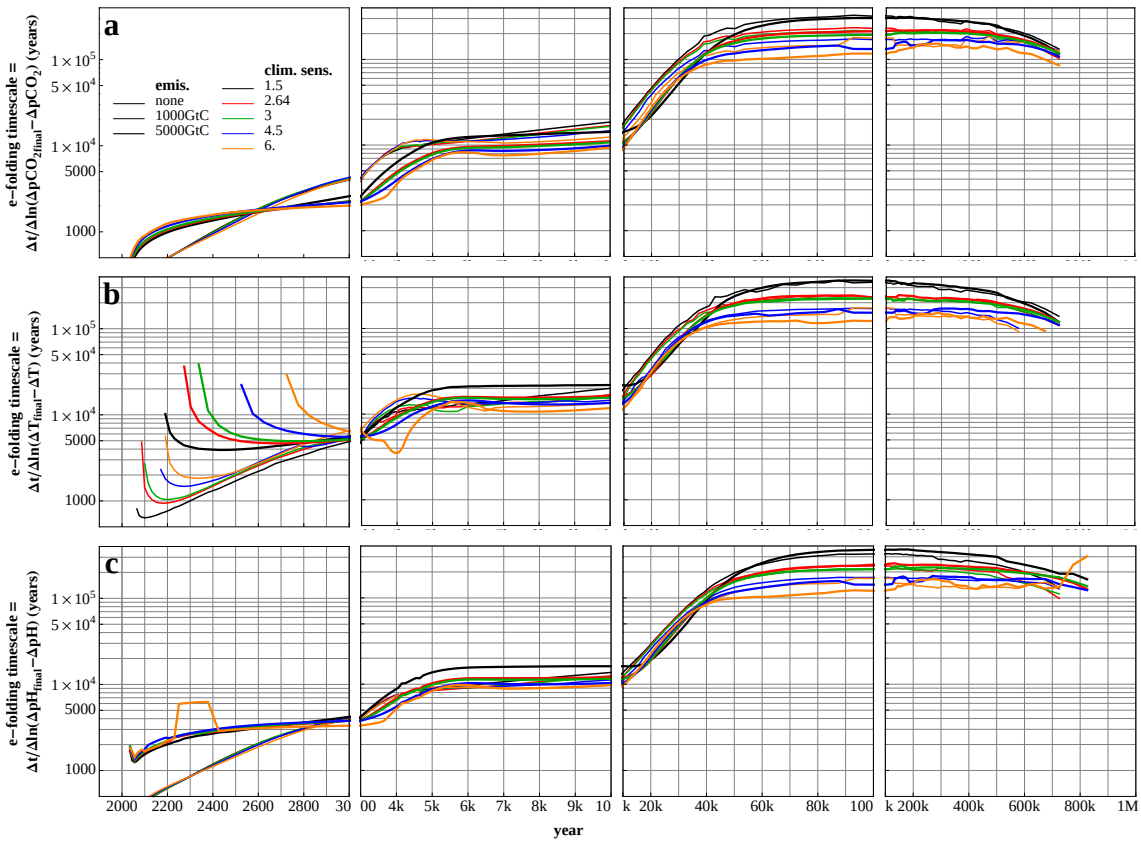

Figure 82: *e*-folding timescales of key variables for climate sensitivity ensemble

B Ensemble generation, model run and data visualisation scripts

B.1 README for run-scripts to chop GENIE runs into manageable pieces (useful for very long runs), and to generate ensembles and visualise their output using Mathematica

B.1.1 Pre-requisites

- The bash shell
- Grid Engine software (i.e. be on a cluster)
- Mathematica (for ensemble generation and data processing)

B.1.2 Automating splitting long runs with multiple stages into manageable pieces

1. Copy the contents of `genie-tools/genie_rootdirstuff` into your root directory (the directory where the genie directory resides). This contains the following:
   - `genie_output` [you should already have this].
   - `genie_configpatches` (where the config files with the user options to append to the base config are stored - AJR calls this genie_userconfigs now I think)
   - `genie_runlog` (to store the terminal output from script runs)
   - `genie_archive` (to store zipped archives of results) containing directories called `fresh`, `to_resub` and `to_clearout`
   - `results` (to store collated results from Mathematica output in - see below)
2. From the directory `genie-tools/runscripts` type:

   `/bin/bash qsub_genie_myr_multipart.sh $1 $2 $3 $4 $5 $6 $7 $8 $9`

   where
   - `$1` = MODELID: your config name, e.g `genie_eb_go_gs_ac_bg_sg_rg_el` (corresponding to `genie/genie-main/configs/genie_eb_go_gs_ac_bg_sg_rg_el.config`).
   - `$2` = BASELINE: your baseline config name - e.g. `worbe2_fullCC` (corresponding to `genie_configpatches/worbe2_fullCC`).
   - `$3` = RUNID: your run ID, e.g. `worbe2_preindustrial_1`.
   - `$4` = NPARTS: the number of parts to the experiment - e.g. `3` for a 2-stage spin-up, then a main emissions experiment.
   - `$5` = K: the experiment part counter, should be `1` (for spin-up 1).
   - `$6` = NEWPART: is it the start of a new part? 0=no; 1=yes (set to 1 initially)
   - `$7` = MAXYEARS: your individual job length in years, e.g. `4000`; means the job is broken into chunks of 4000 years each (this takes <5 hours on the UEA ESCluster).
   - `$8` = J: your start year, usually `0`, unless restarting a run. (the script `resub_genie_myr_multipart.sh` can automate restarts of ensembles - see below).
   - `$9` = MINJOBTIME: the crash tolerance - min number of seconds allowed between resubmits before job is killed (`10` is good for testing, `60` for actual runs).

   Our example looks like this:

   ```
   /bin/bash qsub_genie_myr_multipart.sh genie_eb_go_gs_ac_bg_sg_rg_el worbe2_fullCC ensemble_01_11
   3 1 1 4400 0 60
   ```

   For a more simple test, you might want to try something like:

   ```
   /bin/bash qsub_genie_myr_multipart.sh genie_eb_go_gs_ac_bg_sg_rg worbe2_fullCC rokgem_test 3
   1 1 40 0 10
   ```

   which will be quick to run, as by default the lengths of the runs for each stage are set to 6, 11 and 11. (Note that you will need to have the file rokgem_test in the genie_configpatches directory - there is an example file in the genie-tools/runscripts directory that you can use for this purpose).

   For your BioGeM, SedGeM and ENTS output not to be overwritten each time the model is restarted you need to set `bg_opt_append_data=.TRUE.`, `sg_ctrl_append_data=.TRUE.` and `ents_opt_append_data=.TRUE.` in your config file (as is set in `rokgem_test; rg_opt_append_data=.TRUE.` is set by default)

   Note that in `qsub_rungenie_test` there are pauses (`sleep 2`) in between job submits. These are just as a precaution so as not to overload the cluster. I put them in because I was finding that files weren't getting written in time and things were getting lost.

3. To run multiple experiments at once, edit the script `qsub_rungenie_test`, typing out lines of the above form for each run. Type `./qsub_rungenie_test` in the terminal to run the script.

   The way the scripting works is as follows: `qsub_genie_myr_multipart.sh` is used to submit a script `genie_myr_multipart.sh` to the job queue on the cluster. `genie_myr_multipart.sh` selects the appropriate parameters by loading them in from files `genie/genie-main/configs/$1`, `genie/genie-configpatches/$2_0` and `genie/genie-configpatches/$2_$5` (e.g.`genie/genie-main/configs/genie_eb_go_gs_ac_bg_sg_rg.config`, `genie_configpatches/worbe2_fullCC_0` and `genie_configpatches/worbe2_fullCC_2` for the second part of a full carbon cycle spin-up - see `genie-main/doc/genie-howto`: §5.1). `$2_0` contains parameters common to all parts of the experiment. The script `genie/genie-main/configs/$2_$5.sh` is also run, which automates tasks that need doing when progressing from one part of an experiment to the next (e.g. taking sediment burial from a spin-up and inputting it as weathering flux for an experiment); it is in this script that the length of the experiment part in years is set with RUNLENGTH. `genie_myr_multipart.sh` then calls `rungenie.sh`, which sets time-stepping and restart locations and launches the job with `genie-main/old_genie_example.job`. After the job has completed (following $7 years modelled time), `genie_myr_multipart.sh` updates the run year and/or part of experiment (and whether it is a new part or not) appropriately and resubmits itself to the job queue. It terminates when when all parts are finished, or if the time between job submissions is less than the crash tolerance (`$9`). Output is written to file in `genie_runlog`. When an experiment is completed, the script `qsub_sort_runlog.sh` is generated, which (via calling `sort_runlog_date.sh`) sorts files in `genie_runlog` into date order (this can be useful when thousands of files are being produced). `sort_runlog_date.sh` generates and runs the script `zz_sort_runlog_exe.sh` in place in the directory that it is sorting. The file `qsub_base.sh` is used as a basis for generating some of the `.sh` files that are run; it contains a header that specifies which queue to use on the cluster (medium), and where to direct output (`genie_runlog`).

   Note that in script `genie_myr_multipart.sh` requires that `sge`, `pgi` and `netcdf` modules are loaded onto the node being used. The lines

   ```
   ./etc/profile.d/modules.sh
   module add shared sge
   module add pgi/7.0.7
   module add netcdf-4.0
   ```

   will need to be edited to corresponding local equivalents if running elsewhere then UEA [the first two also used in `resub_genie_myr_multipart.sh`].

To automatically produce ensembles (using Mathematica), see §B.1.5 below.

B.1.3 Name shortening

The names for genie runs can get a bit unwieldy with all the `eb_go_gs_ac_bg_sg_rg_el` etc combined with the `configpatches`. This can especially be a problem when extracting from zip files. I've found that Mathematica won't do it if the path length to the `.tar.gz` file, including the name of the file, is more than 100 characters. Thus I try to reduce the names of the archive files, whilst preserving enough information to both describe and differentiate them. In the above scripts, the script `nameshortening.sh` is called, which contains a number of abbreviations implemented via `sed`. Add to these as you see fit. The first argument of `nameshortening.sh` is the name to be shortened, the second argument is the type of shortening (in `nameshortening.sh` there are two different versions of shortening, one for output directory names, and one for script names).

B.1.4 Restarting runs

1. Place the archive directories of the runs you want restarted (which will be in `genie_archive`) in `genie_archive/to_resub`.

2. From the directory genie-tools/runscripts type:

   ```
   /bin/bash resub_genie_myr_multipart.sh $1 $2 $3
   ```

   where `$1`, `$2`, `$3` are `$4`, `$7` and `$9` above i.e.

   - `$1` = NPARTS: the number of parts to the experiment - e.g. `3` for a 2-stage spin-up, then a main emissions experiment.
   - `$2` = MAXYEARS: your individual job length in years, e.g. `4000`; means the job is broken into chunks of 4000 years each (this takes <5 hours on the UEA ESCluster).

- $3 = MINJOBTIME: the crash tolerance - min number of seconds allowed between resubmits before job is killed (10 is good for testing, 60 for actual runs).

The other arguments for qsub_genie_myr_multipart.sh (see above), which is resubmitted by a script resub_genie_myr_multipart_exe.sh created by resub_genie_myr_multipart.sh, are obtained as follows: MODELID, BASELINE, and RUNID are worked out from the archive directory name; and K and J are worked out from the name of the last modified .tar.gz file in the archive directory.

This process of resubmission is automated for ensembles with the Mathematica script multi_ensemble_rgexpt.nb by checking the qstat. See part 4 below.

B.1.5 Ensemble generation and data visualisation (using Mathematica)

[Note: if you don't have access to Mathematica, you can get a free trial at www.wolfram.com/products/mathematica/experience/request.cgi. If you've not used mathematica before, execute cells by having the cursor within them (or highlighting the cell on the right) and pressing Enter or Shift-Return; double click the cells at the side to expand and contract them. Code generally consists of nested functions (Capitalised) using [ ] brackets, (* *) denote comments, { } lists, ( ) arithmetic brackets, and [[ ]] array parts. There is comprehensive documentation at http://reference.wolfram.com/mathematica/guide/Mathematica.html. Ideally, I'd like to re-do this in something open source, like SAGE, but probably won't get round to it.]

1. To automatically generate ensemble(s) (of non-xml config files), start by editing your base config .csv file(s) (which should be in genie_configpatches) - examples are given in genie/genie-tools/genie_rootdirstuff/genie_configpatches. Put commas between different values of parameters that you want to loop over in the ensemble (there should be no other commas), &s between parameters that you want to group together for the purposes of the ensemble, !s at the start of lines containing parameters not to be looped over and %s at the start of lines giving names for output (see multi_ensemble_params.nb, a facsimile of which is in Appendix B.2, for more details).

2. Edit the file multi_ensemble_params.nb (which can be run from anywhere, but you might want to save a renamed copy to the genie_configpatches folder). An explanation of the parameters is provided in the file.

3. Execute the contents of the above .nb file and then §"**Set-Up For Run:**" in multi_ensemble_rgexpt.nb. A file qsub_rungenie_expt_XXXXXXXXXX (where the Xs represent a date string, e.g. 201102150930 for 9.30 a.m. on the 15th of February 2011) should now be in the folder genie_runlog/expts. This is basically the same as qsub_rungenie_test as described in the part 3 of §B.1.2 above. Execute this file to set the ensemble(s) going (you'll probably need to chmod first - i.e. chmod 755 qsub_rungenie_expt_XXXXXXXXX at the terminal prompt. Then ./qsub_rungenie_expt_XXXXXXXXXX). If you accidentally set an ensemble going with lots of runs, you can use the script genie-tools/runscripts/qdel_ensemble.sh to stop them; supply it with an argument that is part of the ensemble name. i.e. type ./qdel_ensemble e01 (it uses grep, so this part should be unique otherwise other jobs may be killed - type qsub | grep e01 to test first - notice that this particular example picks up jobs running on nodes starting with 01!).

4. To check on your runs and resubmit those that have crashed, in multi_ensemble_params.nb set runmode to 2, then execute multi_ensemble_params.nb and "**Set-Up For Run:**" in multi_ensemble_rgexpt.nb (you'll also need to set qstat, qstatname, nrunlogstolookat and ncharsperrunlogtooutput - see multi_ensemble_params.nb for details). Hopefully, on screen in the Mathematica notebook will be displayed the bottom of the most recent run logs - which should give you an idea of why runs have crashed, if any have. If runs have crashed, a script will be generated in genie_runlog/expts called deadjobs_XXXXXXXXX (where the Xs represent a date string); run this script to automatically resubmit crashed runs. Note that if you want to start runs from completely afresh, it's best to delete their directories first in genie_output and genie_archive. Leaving these in place can interfere with the processing of this part of the script.

5. Once runs are finished, or on their way, execute "**Collate Results:**" to import data from time-series files and export to .xls files (i.e. collate the ensemble time-series into spreadsheets). Results (and any graphs created by setting saveallgraphs=1) will be saved in folders in the results folder corresponding to ensemble member names, experiment parts and date produced (if sameoutdir = 0 - see multi_ensemble_params.nb). Options (divisions, saveallgraphs, timescaleanalysis, timescalefitting, savenetcdfmovies - see multi_ensemble_params.nb) allow different combinations of runs to be collated, graphs to be plotted and saved, timescale analysis to be performed (specific to emissions runs where CO_2 is falling), tables to be created and exported along with graphs to LaTeX form, and animated gifs of various forms to be produced from netcdf output.

6. Execute sections "**a. Set-Up**" and "**b. Interactive time-series plotting**" in the section "**Interactive Plotting:**" to get an interactive time-series plotting widget with a fairly self-explanatory GUI. The tables displayed below the graph will be of use in picking which lines (ensemble members) to display (tab). To save a graph, check and then uncheck the "save graph" box (leaving it checked will produce a new file every minute). "**c. Interactive timescale analysis plotting**" is similar, but with timescale analysis (e-folding curves) for global average pCO_2 and surface temperature.

7. For interactive netcdf output, see section "**d. Net-CDF**". Execute section "**i. Set-up**" and then have a play with the other sub-sections, which get more complicated (and computer resource intensive) as they advance. Each one produces a GUI with geographic output that should be fairly intuitive. Note that if there are more (or less) than 2 ensemble variables, then the code needs to be altered where the grey commented out bits are. For example:

   ```
   {{v1, 1, vartitles[[vs[[1]]]]},Table[i -> varvalues[[vs[[1]], i]], {i, nvars[[vs[[1]]]]}]},
   (*{{v2,1,vartitles[[vs[[2]]]]},Table[i->varvalues[[vs[[2]],i]],{i,nvars[[vs[[2]]]]}]},
   {{v3,1,vartitles[[vs[[3]]]]},Table[i->varvalues[[vs[[3]],i]],{i,nvars[[vs[[3]]]]}]},*)
   ```

   would be adjusted to:

   ```
   {{v1, 1, vartitles[[vs[[1]]]]},Table[i -> varvalues[[vs[[1]], i]], {i, nvars[[vs[[1]]]]}]},
   {{v2,1,vartitles[[vs[[2]]]]},Table[i->varvalues[[vs[[2]],i]],{i,nvars[[vs[[2]]]]}]},
   (*{{v3,1,vartitles[[vs[[3]]]]},Table[i->varvalues[[vs[[3]],i]],{i,nvars[[vs[[3]]]]}]},*)
   ```

   in the case of there being 3 variables. This should really be automated as it is with the Do loops in the "**Collate Results:**" section, but I haven't managed to get it to work.

B.2 Mathematica parameters notebook

Parameters for use in generating GENIE ensembles and processing and visualising their output

Evaulate this notebook, then the corresponding secions of *multi_ensemble_rgexpt.nb*

KEY : black text - parameters that would not normally be changed unless the genie (or Mathematica) code is altered. [74]
blue text - parameters that should be edited (or at least checked) when making a first ensemble. [49]
magenta text - parameters that should be edited (or at least checked) when making an ensemble similar to a previous one, when checking on runs, or when re-processing output [14]
commented out parameters - those greyed out in between (*these brackets*) - are examples of useful selections.
text below blocks of parameters are used to explain their purpose (these can be hidden away by collapsing the cells to the right by double-clicking on them).

Set-Up For Run:

```
title = info = "worbe2 8 level weathering ensembles - ammendments to thesis";
titleshort = "rg8";
```

title - overall title to refer to all ensembles generated herein.
titleshort - short version of title.

```
ensembleroot = "ensemble_";
ensemblerootshort = "";
ensembles = {"01", "02a", "02a1", "02", "02b1", "02b2", "03", "04",
   "04a", "02e", "06", "07", "08r"}; liths = 12; nensem = Length[ensembles];
ensemoutnames = {"short-circuit test", "weathering-temperature feedbacks",
    "weathering activation energy", "weathering-runoff feedbacks",
    "fractional power of explicit weathering-runoff dependence",
    "runoff-temperature correlation constant", "weathering-productivity feedbacks",
    "calcite and silicate weathering feedbacks", "weathering schemes",
    "weathering schemes with f_Ca and f_Si on/off",
    "river routing schemes", "lithologies", "climate sensitivity"};
(*ensembles={"01"};nensem=Length[ensembles];
ensemoutnames={"Short circuit test"};*)
configs = Table["genie_eb_go_gs_ac_bg_sg_rg", {nensem}];
configshorts = Table["rg", {nensem}];
```

Ensembles are generated from files named *xy.csv* where *x* = *ensmebleroot* and *y* is a member of the list *ensembles*.
ensemblerootshort - a short version of the root of the ensemble name, for use in generating runid names (names of directories in genie_output referring to individual runs).
ensemoutnames - used for naming ensembles in output.
configs - a list of config names, one for each ensemble - corresponding to file *genie - main/configs/*.config*.
configshorts - short versions of the config names.
liths - refers to a special case for legends for the "lithologies" ensemble.

```
baseline = "worbe2_fullCC";
startexpt = 1;
nparts = 3;
partnames = {"1_spin1", "2_spin2", "3_expt"};
nyearss = {25 000, 75 000, 1 000 012};
startyears = {0, 0, 0};
saveblock = 4000;
(*nyearss={25,75,100};
startyears={0,0,0};
saveblock=40;*)
startyear = 0;
minjobtime = 20;
```

baseline - the baseline config used for each run (corresponding to $2 given to qsub_genie_myr_multipart.sh).
startexpt - the start value of the experiment counter (corresponding to $5 given to qsub_genie_myr_multipart.sh).
nparts - the number of parts to the experiment (3 is for a 2-stage spin-up followed by a main run).
partnames - the names of said parts.
nyearss - the number of years for each part of the experiment (i.e. 25,000 for the first stage of the spin-up, 100,000 for the second stage and 1,000,010 for the main experiment) These are copied into the files *baseline_0.sh-baseline_nparts.sh*.
saveblock - the individual job length in years, e.g. 4000 means the job is broken into chunks of 4000 years each (corresponding to $8 given to qsub_rungenie_2.sh). Note that due to sedgem giving funny results at start - up, make sure that saveblock doesn' t divide well into any of the nyearss and that the save sig files don' t have years in that are near restarts.
startyear - the start year for the first experiment (corresponding to $8 given to qsub_genie_myr_multipart.sh).
minjobtime - the crash tolerance of the model in seconds (If jobs resubmit in less time than this, they are cancelled; $9 in qsub_genie_myr_multipart.sh.

```
runmode = 2;
qstat = 1;
qstatname = "http://escluster.uea.ac.uk/qstat.php?userid=pvp06gzu&&sort=jobname";
(*qstatname="http://escluster.uea.ac.uk/qstat.php?userid=pvp06gzu&&sort=jobname";*)
nrunlogstolookat = 3;
ncharsperrunlogtooutput = 20 000;
```

runmode - set to 1 for new runs; 2 for restarting crashed runs (or to check whether runs have crashed and are in need of restart).
qstat - version of qstat to use for checking on runs: 1 for web-based; 2 for file genie_runlog/expts/qstat generated by terminal command "qstat | grep [username] > qstat".
qstatname - URL for web-based qstat.

```
inroot = "/Volumes/eslogin.uea.ac.uk/";
inroots = Table[If[e == 2 || e == 4 || e == 7 || e == 8 || e == 11 || e == 13,
     "/Users/Greg/Documents/PhD/", "/Volumes/eslogin.uea.ac.uk/"], {e, nensem}];
outroot = "/Users/Greg/Documents/PhD/";
clusterroot = "/esdata/env/pvp06gzu/";
geniename = "genie_dev9/";
genienames = {"genie_dev9/", "genie_dev6/", "genie_dev9/",
    "genie_dev6/", "genie_dev9/", "genie_dev9/", "genie_dev6/", "genie_dev6/",
    "genie_dev9/", "genie_dev9/", "genie_dev6/", "genie_dev9/", "genie_dev6/"};
genieversion = "genie";
genieroot = inroot ~~ geniename;
genieroots = Table[inroots[[e]] ~~ genienames[[e]], {e, nensem}];
scriptsroot = "genie/genie-tools/runscripts/";
runtimeroot = genieroot ~~ "genie_runlog/expts";
configroot = genieroot ~~ "genie_configpatches";
configroots = Table[genieroots[[e]] ~~ "genie_configpatches", {e, nensem}];
archiveroot = genieroot ~~ "genie_archive";
archiveroots = Table[genieroots[[e]] ~~ "genie_archive", {e, nensem}];
```

inroot - the directory where your genie folder is located, as viewed from where *Mathematica* is running.
inroots - separate *inroot* folders for each ensemble.
outroot - the directory where your results folders are located.
clusterroot - - the directory where your genie folder is located, as viewed from the remote system (i.e. the cluster where genie is run).
geniename - the name of your genie directory.
genieroot - the path to your genie directory.
genieroots - separate *genieroot* folders for each ensemble.
scriptsroot - the directory where all scripts for configuring and runnning the model are.
runtimeroot - the directory where scripts generated by multi_ensemble_rgexpt.nb are output to.
configroot - the directory where genie configpatches (or userconfigs) are kept.
configroots - separate *configroot* folders for each ensemble.
archiveroot - the directory where archived .tar.gz files of output from genie_output are kept.
archiveroots - separate *archiveroot* folders for each ensemble.

```
header = {"#!/bin/bash",
"#$-q short.q",
"#$-cwd",
"#$-j y",
"#$-o ../cgenie_log",
    "#",
    "cd ../../" <> scriptsroot};
```

header - the header to put in the .sh files to be submitted to the computer cluster.

```
comment = "#";
tagmarker = "%";
grouper = "&";
individual = "!";
```

Ensembles are specified by .csv files. See genie/genie-tools/genie_rootdirstuff/genie_configpatches/ensemble_*.csv for examples.
comment - the symbol used at the start of a line in the .csv config files to designate a comment.
tagmarker - the symbol used at the start of a line in the .csv config files to name the parameters being looped over in this form: %"variable name (long)","variable name (short)","value 1","value 2"... (e.g. %"short-circuit atmosphere","short-circ.","yes","no"). These names are used in output.
grouper - the symbol used to group together parameters to loop over in the .csv config files. e.g. with the line *rg_opt_weather_T_Ca=.TRUE.&rg_opt_weather_R_Ca=.TRUE.&rg_opt_weather_P_Ca=.TRUE.,rg_opt_weather_T_Ca=.FALSE.&rg_opt_weather_R_Ca=.FALSE.&rg_opt_weather_P_Ca=.FALSE*. An example of a .csv ensemble config file using this is genie/genie-tools/genie_rootdirstuff/genie_configpatches/ensemble_02d.csv.
{rg_opt_weather_T_Ca,rg_opt_weather_R_Ca,rg_opt_weather_P_Ca} are treated as one parameter when generating the ensemble so that only 2 combinations are created rather than 8.
individual - the symbol used at the start of a line in the .csv config files to refer to an individual ensemble member: the list of parameters on this line are not looped over. Each line started by *individual* refers to one ensemble member. An example of a .csv ensemble config file using this is genie/genie-tools/genie_rootdirstuff/genie_configpatches/ensemble_05.csv.

```
system = "Linux";
```

system - system run on (can be Linux or Windows; use "Linux" for Mac) - for purposes of path formatting. [Not fully implemented - only works with "Linux"]

Collate Results:

```
outputfolder = genieroot ~~ "genie_output";
outputfolders = Table[genieroots[[e]] ~~ "genie_output", {e, nensem}];
resultsfoldersuffix = outroot ~~ "results/";
finalresults = 1;
finalresultsfolder = outroot ~~ "results_final/";
writeuproot = "/Users/Greg/Dropbox/rokgem_manuscript/";
```

outputfolder - where GENIE output is kept.
outputfolders - separate *outputfolder* folders for each ensemble.
resultsfoldersuffix - the root directory for all output generated by multi_ensemble_rgexpt.nb.
finalresults - if set to 1, generates a script in *runtimeroot* (see above) that copies results from *resultsfoldersuffix* to *finalresultsfolder* for the sake of completion.
writeuproot - the directory that results for inclusion in LaTeX documentation are output to.

```
npartsoutput = 3;
dropvar = 1;
```

npartsoutput - the number of parts of the experiment output. This can be worked out by running the section "Set-Up For Run" in multi_ensemble_rgexpt.mb with *runmode*=2 if there is an appropiate way of reading in the qstat - see above.
dropvar - if set to 1, for parts of the experiment other than the last (i.e. spin-ups), the first variable (usually emissions and therefore redundant) is omitted from the results collation.

```
divisions = {0, 1, 1};
sameoutdir = 0;
saveallspreadsheets = 0;
saveallgraphs = 0;
timescaleanalysis = 1;
timescalefitting = 1;
screenoutputgraph = 1;
savenetcdfmovies = {0, 0, 0, 0, 0, 0};
```

divisions - 3 different types of output for spreadsheets and graphs; 0 = off, 1 = on. 1st is individual runs. 2nd is comparisons of runs with one free parameter. 3rd is all runs together.
sameoutdir - if set to 0 (or anything but 1), creates a new directory named by date in the folder resultsfoldersuffix/[ensemble_name]/[experiment_part] each time "Collate Results:" is run in *multi_ensemble _rgexpt.nb*; if set to 1, overwrites output data in folder resultsfoldersuffix/[ensemble_name]/[experiment_part]/9999999999.
saveallspreadsheets - if set to 1, saves all timeseries graphs (specified by *filenamenos* below) to resultsfoldersuffix/[ensemble_name]/[experiment_part]/[date]/graphs.
saveallgraphs - if set to 1, saves all timeseries graphs (specified by *filenamenos* below) to resultsfoldersuffix/[ensemble_name]/[experiment_part]/[date]/graphs.
timescaleanalysis - if set to 1, creates *e*-folding graphs and LaTeX tables for variables specified in *analysisvars* below, and graphs (and corresponding LaTeX code) for inclusion in write-ups specified by *plotfilenamenos*.
timescalefitting - if set to 1, fits a series of exponentials to outputs for variables specified in *analysisvars* below (requires that is *timescaleanalysis* on).
screenoutputgraph - outputs graphs generated in section 5 of "Collate Results:" in *multi_ensemble _rgexpt.nb* - e-folding and publication graphs - to screen.
savenetcdfmovies - represents 5 different types of netcdf movies generated in sections 6 *b* through *f* of *multi_ensemble _rgexpt.nb*. To save a type set the corresponding number to 1. Netcdf variables to save are set in *netcdfmodules* and *filenamenosnetcdf* below. The types are:

{i. Animations,
ii. Animations with averaging
iii. Animations with averaging and lat - time diagram
iv. Comparisons - single axis lat.plot
v. Comparisons}

Note that these can take a long time to output (e.g. from 16 seconds per .gif for Animations, up to 50 seconds for Comparisons on a 2009 laptop).

■ Part 3 - time-series spreadsheets

```
modules = {"biogem", "rokgem"}; nmodules = Length[modules];
columntitledividers = {"/ ", "/ "};
(*filenamenos={{3,6,7,8,9,33,34,35,36,38,46,47,48,50,51,54,55,56,58,59,64,
    65,66,67,69,73,74,75,76,77,78,79,80,81,82,83,85,89,91,92,93,95,96,97},
   {3,6,7,13,16,17,20,23,26,27,28,29}};*)
(*filenamenos={{3},{1}};*)
(*filenamenos={{3,6,79,97},{1,14,17,20}};*)
(*filenamenos={{3,6,56,65,79,97},{1,14,17,20,26,27}};*)
filenamenos = {{3, 6, 56, 65, 79, 97, 33, 36}, {17, 20, 26, 27}};
(*filenamenos={Delete[Table[i,{i,101}],{{37},{68},{84}}],Table[i,{i,29}]};*)
(*filenamenos={Delete[Table[i,{i,45,101}],{{68-44},{84-44}}],Table[i,{i,29}]}*)
```

modules - modules to collate time-series output for.
columntitledividers - dividers for titles in genie time-series output files - should be left unless changed in GENIE.
filenamenos - filename numbers for time-series output (the sub-lists correspond to the above modules). These are the numbers of the files *series* in the output folders genie_output/[config_name]/*gem. Depending on the platform used, they may be different as different operating systems have slightly different ways of sorting alphabetically (e.g. with names containing the same prefix but different numbers of characters). To help with picking the numbers, after running "Collate Results:" in multi_ensemble_rgexpt.nb, a list is generated in resultsfoldersuffix/[ensemble_name]/[experiment_part]/[date]/-time_series_output_list.xls (e.g. results/rg8_ensemble_01/1_spin1/9999999999/time_series_output_list.xls) that contains all the time series output files available (one sheet for each module) and their corresponding filename numbers. A version of this list - time_series_output_list.xls - correct for Mac OS X and up to date as of June 2010 is also included in genie-tools/runscripts; this may be used to start with.

■ Part 4 - time-series graphs

```
plotstartyears = {0, 0, 1750, 2010};
yearticks log = {{1, "1"}, {2, "2"}, {5, "5"}, {10, "10"}, {20, "20"}, {50, "50"},
    {100, "100"}, {200, "200"}, {500, "500"}, {1000, "1000"}, {2000, "2000"},
    {5000, "5000"}, {10 000, "10000"}, {20 000, "20000"}, {50 000, "50000"},
    {100 000, "100000"}, {200 000, "200000"}, {500 000, "500000"}, {1 000 000, "1M     "}};
yearticks lin = {
    {{2000, "2000"}, {2200, "2200"},
     {2400, "2400"}, {2600, "2600"}, {2800, "2800"}, {3000, "30    "}},
    {{3000, "     00"}, {4000, "4k"}, {5000, "5k"}, {6000, "6k"},
     {7000, "7k"}, {8000, "8k"}, {9000, "9k"}, {10 000, "10     "}},
    {{10 000, "   k"}, {20 000, "20k"}, {40 000, "40k"}, {60 000, "60k"},
     {80 000, "80k"}, {100 000, "100       "}}, {{100 000, "   k"}, {200 000, "200k"},
     {400 000, "400k"}, {600 000, "600k"}, {800 000, "800k"}, {1 000 000, "1M     "}}};
gridlines = Flatten[{Table[1900 + 100 * i, {i, 0, 11}], Table[j * 10^i, {i, 2, 6}, {j, 10}]}];
ranges = {{1900, 3000}, {3000, 10 000}, {10 000, 100 000}, {100 000, 1 000 000}};
nranges = Length[ranges];
```

plotstartyears - the year to start time-series plots at for each part of the experiment (e.g. 0 for spin-ups 1 and 2 and 1900 for main emissions experiment).
yearticks log - tickmark labels for years on logarithmic timescale plots (default is index notation, this avoids that).
yearticks lin - tickmark labels for years on broken-up linear timescale plots (default is index notation, this avoids that).
gridlines - gridlines on time axis (years).
ranges - ranges for each sub-plot in broken-up linear timescale plots.

```
coloursensem = Table[{Black, Red, Darker[Green], Blue, Orange, Purple, Pink, Yellow, Green,
     Brown, Gray, Darker[Blue], LightBlue, Magenta, Cyan, LightOrange}, {nensem}];
coloursensem[[3]] = coloursensem[[5]] = coloursensem[[6]] =
     {Blue, Black, Darker[Green], Red};
coloursensem[[12]] = {Gray, Green, Brown, Darker[Green], Magenta, Black,
    ColorData["Legacy", "SteelBlue"], Purple, Yellow, Orange, Red};
linethicknesses = {0.125, 0.00125, 0.003};
dashings = Flatten[Table[{{}, {0, Small}, {Small, Small}, {0, Small, Small, Small},
     {Small, Small, Small, Small, Large, Small}, {Tiny, Tiny, Large, Tiny},
     {Tiny, Tiny}, {Medium, Medium}, {Large, Large}, {Large, Small}}, {10}], 1];
(*Table[Graphics[{Dashing[dashings[[r]]],Line[{{0,0},{3,1}}]}],
 {r,Length[dashings]}]*)
combineland2 = 0;
saveformats = {"pdf"};
```

coloursensem - specifications for colours in time-series graphs for each ensemble: used progressively from first value as number of 1st variable in an ensemble increases (for cases where the 2nd variable has more than 4 values, colours are used for the 2nd variable and line thicknesses for the 1st). For ensembles with more variables than specified colours, colours are generated automatically when needed.
linethicknesses - thicknesses of lines on plots: first value is for legend, second for graphs, third for multi-part graphs. These are progressively multiplied by integers starting from 1 as the number of the 2nd variable in an ensemble increases (1st variable in the case of the 2nd variable having more than 4 values).
dashings - specifications for line-dashing in time-series graphs: used progressively from first value as number of 3rd variable in an ensemble increases.
combine1and2 - combine 1st and 2nd variables in plot legend (for when there are 4 variables).
saveformats - list of formats to save graphs to.

- **Parts 5a and 5c - timescale analysis and tables**

```
analysisfilenamenos = {3, 6, 79}; ndroptabvars = Length[analysisfilenamenos];
analysisvars = {"CO2", "temp", "pH"};
analysisvarslong =
  {"Atmospheric pCO2", "Surface warming", "Surface ocean acidification"};
deltas = {"ΔpCO2", "ΔT", "ΔpH"};
analysisunits = {2, 1, 1};
analysisunitnames = {"ppm", "oC", "pH units below 8.15 baseline"};
analysisshorts = {"pCO2 (ppm)", "warming (oC)", "acidification (pH)"};
analysisvshorts = {"pCO2", "T", "pH"};
analysisplotranges = {{200, 1600}, {0, 7}, {0, 0.8}};
nblips = {0, 0, 1};
peakposs = {5, 2, 5, 2, 5, 5, 2, 2, 5, 5, 2, 5, 2};
downcurvecutoff = 0.000001;
yefoldmax = 700 000;
efoldmovavg = 5;
```

analysisfilenamenos - analogous to *filenamenos;* filename numbers for timeseries analysis plots and tables - they must be included in the first part of *filenamenos* (i.e. are biogem output).
analysisvars - short names of the variables specified by *analysisfilenamenos*.
analysisvarslong - long names for the variables specified by *analysisfilenamenos*.
deltas - delta symbols for the variables specified by *analysisfilenamenos*.
analysisunits - units for the y-axis of graphs (the 2 is for pCO2 from biogem, as this is ppm; most other timeseries only have 1 unit type).
analysisunitnames - names of the above units.
analysisshorts - short titles for analysis variables (for use on timescale tables).
analysisvshorts - very short titles for analysis variables (for use on timescale tables).
analysisplotranges - y-axes ranges for the specified variables.
nblips - number of erroneous upward 'blips' to tolerate in decay curves output for each variable in *analysisvars*. (decay curves are calculated factoring in upward blips of this many time points).
peakposs- positions in timeseries output of main experiments where emissions are maximal (point before spike in analysis variables) for each ensemble.
downcurvecutoff - cutoff for depletion curves: when the difference of successive values in a time-series is less than this much in fractional terms, the final value is taken as reached.
yefoldmax - the upper limit of the y-axis scale for *e*-folding timescale plots.
efoldmovavg - moving average to apply to smooth *e*-folding timescale plots.

```
dropnames =
  {"value at year", "fraction at year", "value remaining", "fraction remaining"};
tabletypesshort = {"yearval", "yearfrac", "valyear", "fracyear", "fittab"};
ndrop = Length[dropnames];
analysiscaptions1 = {"",
   "\\textbf{Percentages} of remaining excess ",
   "\\textbf{Years} that specific values of ",
   "\\textbf{Years} that specific fractions of remaining excess "};
analysiscaptions2 =
  Table[{" (" ~~ analysisunitnames[[d]] ~~ ") reached at specific calendar years",
    " reached at specific calendar years",
    " are reached",
    " are reached"}, {d, ndroptabvars}];
maxcaptionlength = 110;
dropyears = {3000, 5000, 10 000, 20 000, 50 000, 100 000, 200 000, 500 000, 1 000 000};
ndropyears = Length[dropyears];
dropyearnames =
  {"3000", "5000", "10000", "20000", "50000", "100k", "200k", "500k", "1000k"};
dropvalues = {({1500, 1000, 750, 500, 400, 350, 300, 278} - 278) * 1. * 10^-6,
  {5, 4, 3, 2, 1.5, 1, 0.5, 0}, Table[i, {i, 0.7, 0.0, -0.1}]};
ndropvalues = Length[dropvalues[[1]]];
dropfracs = {0.9, 0.75, 0.5, 0.25, 0.1, E^-1, E^-2, E^-3, E^-4, E^-5};
ndropfracs = Length[dropfracs];
dropfracnames = {"90%", "75%", "50%", "25%", "10%", "e^-1", "e^-2", "e^-3", "e^-4", "e^-5"};
```

dropnames - names for tables displaying values and fractions remaining of variables specified by *analysisfilenamenos*.
tabletypesshort - short names for types of tables.
analysiscaptions1 - part 1 of captions for said tables.
analysiscaptions2 - part 2 of captions for said tables (*analysisvarslong* are sandwiched inbetween *analysiscaptions1* and *analysiscaptions2*).
maxcaptionlength - Maximum string length (number of characters) for caption, before it is split into 2 lines.
dropyears - years at which to output values and fractions remaining of *analysisvars* specified by *dropvalues* and *dropfracs*.
dropyearnames - names in text form for the *dropyears*.
dropvalues - lists of values to display for each of the *analysisvars*.
dropfracs - lists of fractions remaining to display for each of the *analysisvars*.
dropfracnames - names in text form for the *dropfracs*.

■ Part 5b - publication time-series plots

```
plotfilenamenos = {{3, 6, 79, 97, 33, 36}, {}};
nplotvars = Length[Flatten[plotfilenamenos]];
plotvars = {"CO2", "temp", "pH", "Seds", "ALK", "DIC"};
plotvaluenames = {"atmospheric pCO2", "global warming", "ocean acidification",
   "sediment CaCO3", "Weathering alkalinity flux", "Weathering DIC flux"};
plotunits = {2, 1, 1, 1, 1, 1};
plotunitnames =
  {"ppm", "°C", "pH units below 8.15 baseline", "weight %", "Tmol/yr", "Tmol/yr"};
autoplotranges = {0, 1};
plotranges = {{200, 1600}, {0, 7}, {0, 0.8}, {0, 40}, {20, 45}, {10, 15}};
plotranges2 = {{{200, 1600}, {260, 400}}, {{0, 2}, {0, 7}}, {{0, 0.3}, {0, 0.8}},
   {{20, 40}, {0, 40}}, {{20, 27}, {20, 45}}, {{10, 12}, {10, 15}}};
unitschange = {10^6, 1, 1, 1, 10^-12, 10^-12};
latexscale = 0.49;
```

plotfilenamenos - analogous to *filenamenos;* filename numbers for publication plots to output - they must be included in *filenamenos*.
plotvars - short names of the variables specified by *plotfilenamenos* (note that the list - and those subsequent - is/are flattened so not to explicity consider sub-lists pertaining to different modules).
plotvaluenames - long names for the variables specified by *plotfilenamenos*.
plotunits - units for the y-axis of graphs (the 2 is for pCO2 from biogem, as this is ppm; most other timeseries only have 1 unit type).
plotunitnames - names of the above units.
autoplotranges - switch to turn automatic *y*-axes ranges on (1) or off (0) for main body plots (first number) and appendix plots (second number).
plotranges - If *autoplotranges*=0, *y*-axes ranges for the specified variables.
plotranges2 - multiple *y*-axis ranges for 2 emissions scenarios.
unitschange - factors to multiply *plotvars* by for output (e.g. atm -> ppm for pCO2.
latexscale - scale for latex plots (set so fit neatly on the page).

■ Part 5d - timescale analysis fitting

```
fitbase = E;
commentary = 0;
graphoutput = 0;
confidence = 0.95;
maxiterations = 1000;
threshold = 10^7;
paramrelerrorthreshold = 2;
biccutoff = 0;
maxnexpfits = 7;
maxtableportraitrows = 64;
```

fitbase - the base for the timescales; E gives e-folding timescales, 2 gives half-lives.
commentary - if set to 1 outputs to screen the progress of the fitting; if set to >1 shows the fitting in detail.
graphoutput - if set to 1, shows graphs of the fits.
confidence - the confidence interval given to the fits.
maxiterations - the maximum number of iterations to perform when doing the fitting (it was found that no fits that could not be completed after 1,000 iterations could be after 20,000).
threshold - the maximum value of parameters permitted.
paramrelerrorthreshold - the maximum relative error permitted for parameters.
biccutoff - if set to 1, the fitting automatically stops when the BIC (Bayesian Information Criterion) increases, indicating a worse fit (not recommended as it was found that for the early fits (low numbers of exponentials), BICs fluctuated).
maxnexpfits - the maximum number of exponentials to include in the fit (up to 10 has been tried, but no fits with *maxnexpfits*>7 have been found to be optimal).
maxtableportraitrows - maximum number of rows in a portrait table (this is equivalent to 21 lots of 2 rows each for a landscape table of timescale fitting); tables are broken up they exceed this maximum size.

Part 6 - Netcdf movies

```
netcdfmodules = {"biogem", "sedgem", "rokgem", "ents"};
nnetcdfmodules = Length[netcdfmodules];
dimensions = {{2, 3}, {2}, {2}, {2}};
nhousekeepingdata = {22, 13, 17, 3};
netcdfstartyearnos = {1, 1, 1, 1};
(*netcdfmodules={"rokgem"(*,"ents"*)};nnetcdfmodules=Length[netcdfmodules];
dimensions={{2}(*,{2}*)};
nhousekeepingdata={17(*,3*)};
netcdfstartyearnos={1(*,1*)};
filenamenosnetcdf={{{3}}(*,{Table[i,{i,17}]}*)};*)
filenamenosnetcdf = {{{47}, {1}}, {1}, {1, 3}, {1}};
(*filenamenosnetcdf[[1,1]]=Delete[filenamenosnetcdf[[1,1]],{{5},{6}}];*)
nlevels = 8;
depths = {87, 290, 564, 934, 1433, 2106, 3105, 4241};
genielat = 36;
genielon = 36;
```

netcdfmodules - modules to collate netcdf output for (the below lists with {} need to be edited to reflect this if changed).
dimensions - dimensions of netcdf data for each module.
nhousekeepingdata - amount of housekeeping data in each netcdf file, by module (to be skipped).
netcdfstartyearnos - the position in the list of output years to start at, by module.
nlevels - no. of ocean levels for 3D data.
depths - depths of ocean levels.
genielat - latitudinal resolution of genie (in gridcells).
genielon - longitudinal resolution of genie (in gridcells).

```
landmaskfile = genieroot ~~ "genie/genie-rokgem/data/input/worbe2.k1";
bignumber = 10^30;
maxmem = 2 000 000 000;
maxnetcdftitlestringlength = 33;
maxnetcdfsubtitlestringlength = 20;
netcdfimagesize = 800;
netcdfoutliers = 1;
nodatacolour = White;
```

landmaskfile - path of a landmask file used.
bignumber - a number lower then the default value given to NaNs in the netcdf data, but higher than all data values.
maxmem - maximum memory (RAM) to use up doing netcdf stuff (of memory exceeds this amount then the process is aborted, rather than crashing the compute by filling up memory).
maxnetcdftitlestringlength - Maximum string length (number of characters) for titles of netcdf plots, before they are split into 2 lines.
maxnetcdfsubtitlestringlength - Maximum string length (number of characters) for sub titles of netcdf plots, before they are split into 2 lines.
netcdfimagesize - size of image files of netcdf output produced (in printer points).
netcdfoutliers -number of outliers at minimum and maximum range of data to exclude from coloured plot scale.
nodatacolour - colour for areas on plots with no data.

C Accompanying digital media

Digital media accompanying this thesis contains full model output, as generated by the scripts in Appendix B above, including spreadsheets and graphs of time-series data, timescale analysis, and animations of 2D and 3D spatial output. Also include are all the files used in producing this PhD.

Key things to look out for are the .gif animations for Figures 32 and 37 (in the top level), and the complete GENIE codebase for my branch of the svn repository (Greg's branch; see §2.1), that I have used in the development of RokGeM and the accompanying processing scripts. Code that I have written is contained in the directories genie/genie-rokgem and genie/genie-tools.

A fully-hyperlinked .pdf version of this thesis document is also included, as well a directory full of all the files used to create it.